Anna Eskes

Connecting Glass to Glass with Glass

A Master Thesis on Heat Bonded Glass Connections

Connecting Glass to Glass with Glass

A Master Thesis on Heat Bonded Glass Connections

Anna Eskes

September 2018

This is a master thesis in partial fulfillment of the requirements for the degree of Master of Science in Civil Engineering, Building Engineering

Author:
Anna Eskes
+31 6 533 96 122
annaeskes@live.nl

Thesis Assesment Comittee:
Prof. Ir. Rob Nijsse, chair (TU Delft, professor of Structural Design)
Ir. Diana de Krom (ABT bv)
Ir. Telesilla Bristogianni (TU Delft, department of Structural Design)
Ir. Lisa Rammig (TU Delft, department of Building Technology)
Dr. Ir. Fred Veer (TU Delft, department of Architectural Engineering and Technology)

Abstract

Glass is a fascinating material which has been used for load bearing structures in the past decades. The development of structural glass has been moving towards more transparent structures.
The thermal properties of glass can be used to create heat bonds. Heat bonds can be produced in two ways: welding and fusing. With welding, the regions that are to be connected are locally heated. With kiln formed fusing, the elements to be bonded will be globally heated in an oven. This results in the research question: What is the best method, among glass welding and kiln formed glass fusing, to produce heat bonded systems for applications in glass structures?

In theory, safety measures consist of three basic strategies: creating secondary load transfer mechanisms, protectioning and overdimensioning.
These strategies can be used on the scale of the system and the structure. The heat bonded system could theoretically be laminated, reinforced and tempered. On a structural level, safety can be ensured by a combination of the strategies.

To produce glass welds, the glass is preheated in an oven. A small opening in the oven is made and a line burner is used to heat the to be welded area from both sides. One element is pressed down on the other to make the connection. The oven is closed and the specimen is annealed.
Finite element models have been used to analyze thermal shock failure during the weld production process. The recommendations for production were to use an additional flame on the bottom of the specimen or to maintain the surroundings at elevated temperature. The latter option is applied in the experiments.
The results were three transparent, all-glass, soda lime T-shaped objects. Little residual stress remained in the products.

The fused objects were globally heated in an oven. The glass was fused in moulds, made of a gypsum plaster. The products were translucent, all-glass, soda lime, T-shaped objects. The objects deformed significantly during production. Little residual stress remained in the products.
Throughout the experiments, factors have changed. An aspect with no direct influence on the product was quenching after maximum temperature. Adapting the mould and polishing the glass edges prior to fusing had an influence on the objects' shape or texture. None of the factors influenced the order of magnitude of the deformation or the seam between the elements.

A structural test has been performed to compare the specimens with a glass T-shape bonded with transparent UV-curing adhesive. The connections were loaded in shear. The results of the failure loads and stress at failure are of the same order of magnitude. The largest spread was among the fused specimens, the smallest among the welded.
The cause of failure is most probably a combination of elevated stress due to the stiffness and support of the test set-up and peak stress due to irregularities on the glass surface. Other causes could have contributed to failure.
The welded glass product requires most time, energy, skill and money. The adhesive product requires least time and energy. The welded and fused objects had neither acceptable dimensional accuracy, nor a smooth fillet in the joint.

In the current state of development, glass fusion results in less residual stress, requires less skill and is cheaper to produce. Glass welding results in a transparent glass to glass connection and its structural performance is promising. Further research is encouraged into the heat bonded and adhesive connections to create fully transparent connections for structural glass.

Preface

Delft, 2018

There are many stories about the beauty of glass structures, but for me personally, the story around this picture tells it best. This is my sister and me, seven years ago, at, in my humble opinion, the most iconic building of the most fascinating material. The picture makes me think of my ignorance at that time, before I went to Delft, which made me visit the Apple Cube without realizing what it was or knowing how I was to be intrigued by this world of engineering beauty.

As this picture was posted on Facebook, a comment came from our other sister, exclaiming: 'Your hands!' It looks like we are holding them up. Upon close inspection, one can discover that our hands rest on the balustrade. With that in mind, our pose changes from excited to relaxed. This is exactly the mesmerizing effect of glass structures. The dematerialization warps observations, alters perception, creates illusions. At the TU Delft, this was combined with its need for detailed and sophisticated engineering, and my fascination was born.

I would like to thank the members of the committee for their guidance, support and enthusiasm. I would like to thank Kees, for his practical approach and availability at all times. I would like to thank Frans Folst and Tom Jansen, who invested more time than they should have out of interest and kindness. I thank all colleagues at ABT for their interest and help and for allowing me to use the knowledge, funding and facilities of ABT.

Finally, I would like to thank my friends and family for their support and their presence, not just during my thesis but for all past years in Delft. I thank Han for being my companion and foundation. I thank my parents, who have taught me to get as much as I can out of my talents and gave me the best start in life imaginable.

Anna Eskes

Contents

Part I

Introduction

This part introduces the subject. It opens with an overview of glass in buildings and its development from a filling to a structural material. Then, the heat bond is introduced and the difference between glass welding and glass fusion is explained. A chapter is devoted to the possible applications of the heat bond in the building industry. The part finishes with the research questions, scope, hypothesis and method.

1 Glass in the Building Industry

Glass has been a fascination for centuries. It is a material for decorative items and art. But glass is not just aesthetic, it is also used for functional reasons, for example in laboratories or vehicles. In everyday life, glass is present in many shapes, sizes and functions, from drinking cups to windows.

With the industrialization of the glass production process, glass windows were more frequently applied and in larger sizes than before (Nijsse 2003). In the past few decades, a new function of glass in buildings has been created: load bearing. Structural glass has developed and is applied in several interesting projects.

1.1 Glass as a Filling Material

Glass in buildings is mostly used to visually connect the inside to the outside. Humans need this connection, as they are healthier and more productive in a space with natural light (Schipper 2011). Glass offers this visual connection, while keeping harsh elements like wind and water out.

The first evidence of glass in a building envelope was found in the Roman ruins of Pompeii and Hercunaleum (Schittig et al. 1999). The panes were small, three hundred by five hundred millimeter, and a few centimeters thick. They were occasionally installed without framing. This glass was green and not very transparent.

The glass elements in buildings have been governed by the production method. When the only known technique was the blow pipe, small window panels could be produced (Nijsse 2003). This is visible in the architecture of the Gothic churches, where the coloured panels are small. The lead in between the glass panels was too weak to ensure large spans. The loads act on the stone arches around the glass.

As production techniques improved, the sizes increased. In most of the modern buildings, glass has only a function in the building envelope. It has to ensure that wind and water stay out, and heat remains inside. It should let the light from outside in. Loads are born by window frames and surrounding walls.

1.2 Glass as a Strengthening Material

As the desire increased to create more transparency in buildings, the strength of glass has been used to support the building envelope structurally. This was also supported by the development of iron as a structural material (Schittig et al. 1999). The load bearing function could be located inside the building and the building envelope was released from its structural duties.

A remarkable and daring example is the Crystal Palace, designed by Joseph Paxton in 1851 (Figure 1) (Schittig et al. 1999). He extrapolated green house design to a 560 meter long and 40 meter high pavilion in iron and glass. Due to prefabrication, the construction time was revolutionarily short. It resulted in the first large, open and light space, where the borders between inside and out were blurred.

Many buildings with glass facades have been erected in the 20^{th} century. These facades are developing towards all glass envelopes and are continually growing in size and span. This requires innovations for the glass elements spanning the facade and bearing the loads on this facade.

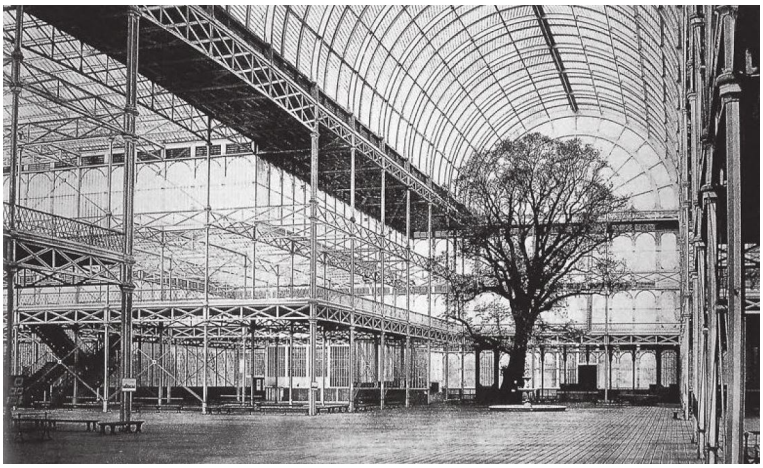

Figure 1: The Crystal Palace, by Joseph Paxton for the World Expo in 1851 (Schittig et al. 1999)

The development has resulted in innovations that minimized the connections. The well known window frames became slimmer and eventually obsolete. An early example of this is La Cité des Sciences et de l'Industrie in Paris, France in 1986, engineered by Peter Rice (Figure 2) (Schittig et al. 1999). Here, a spider is used to connect adjacent glass panels to a load bearing structure. A sealant is used between the panels to make it air- and watertight.

The modern challenges for the facade industry are to be found in the sustainability of the design and complexity of the shape (Blandini 2016). The heat loss in winter and solar gain in summer must be minimized and the material used must be minimum and recyclable. Contemporary architecture requires complex geometry, which challenges engineers to deal with the detailing, producing and erecting these facades. An example of the latter is the facade of the Enzo Ferrari museum in Modena, Italy, which is shaped with two conical surfaces under an inclination (Figure 3).

An interesting development to increase the structural capacity of facade panels is the innovation of a corrugated panel, as applied in the Casa da Musica in Porto, Portugal (Figure 4) (Nijsse 2003). In this project, the modulus of inertia of the cross-section of the panel is increased by curving the panels. This makes it possible for the panels to span a larger height. When this system was applied in the Museum aan de Stroom in Antwerp, Belgium, spans of 5,5 meter were realized with one panel (Nijsse 2008).

Figure 2: Facade of La Cité des Sciences et de l'Industrie, engineered by Peter Rice (Solla 2011)

Figure 3: Enzo Ferrari Museum (Blandini 2016)

Figure 4: Corrugated facade in Casa da Musica (Nijsse 2008)

1.3 Structural Glass

With the mentioned developments, windows grew from small openings in massive walls to the whole building envelope. This increase in transparency was taken a step further at the end of the 20th century. Relatively small projects were designed to be fully transparent, challenging the structural engineers to apply glass as a load bearing material.

An early application of structural float glass is an all glass pavilion for the Sonsbeek Art Exhibition in Arnhem, 1986 (Figure 5) (Nijsse 2003). The design is a transparent tunnel with glass walls and roof, supported by glass fins as columns and a slender steel truss as beams.
The tunnel was a temporary building, allowing the engineers to work around the strict building regulations. The other consequence is that the tunnel no longer exists.

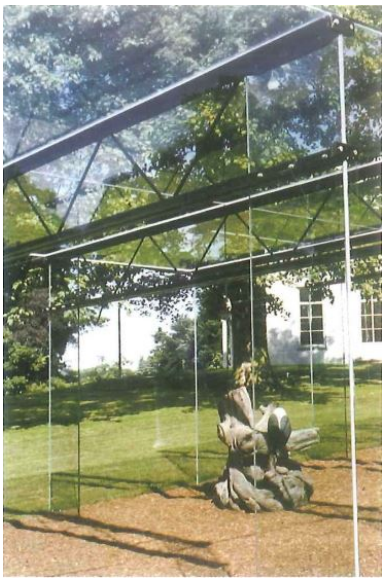

Figure 5: View through the tunnel at the Sonsbeek Art Exhibition (Nijsse 2003)

As the development continued, glass beams were introduced. The design for an extension in London, the United Kingdom, designed by Rick Mather and engineered by Dewhurst MacFarlane, included a laminated, glass portal (Figure 6) (Nijsse 2003). This type of portal has been applied in many structural float glass buildings since.

One of the most iconic glass buildings is the Apple Store in Manhattan, New York, United States of America. The cube is engineered by Eckersley O'Callaghan in 2006 (Figure 7) (O'Callaghan and Bostick 2012). Five years later, the original client, engineer and producer decided to rebuild the Apple Cube to show the progress made in the structural glass industry (Figure 8). The development involved the possibility to temper and laminate larger panels and to laminate embedded steel connection elements.

Figure 6: All glass extension designed by Rick Mather (Rick Mather Architects n.d.)

Figure 7: The Apple Cube from 2006 (O'Callaghan 2008)

Figure 8: The Apple Cube 2.0 from 2011 (O'Callaghan and Bostick 2012)

A different approach towards glass structures has been realized in the Crystal House in Amsterdam (Figure 9). This monumental facade has been partially replaced with glass bricks (Oikonomopoulou, T. Bristogianni, et al. 2016). The facade is self-supporting. Lateral stability is guaranteed by buttresses.
The bricks are produced by casting molten glass in a mould. This process requires a high level of temperature control to create a smooth surface and little residual stress. The construction of the facade was possible by overcoming many challenges. The environment had to be strictly controlled to prevent dust inclusion and a high accuracy was necessary for success.

Figure 9: An impression of the Crystal House glass brick facade (Oikonomopoulou, T. Bristogianni, et al. 2016)

2 Connecting Glass to Glass with Glass

Structural connections in glass are challenging. The transparency of the element can be less apparent if the connection is distracting. A big, opaque, eye catching joint draws the attention away from the transparent beam or fin. On the road towards fully transparent structures, connections have been minimized. For example, this minimization is not just visible in, but also a reason for the rebuilding of the Apple Cube (O'Callaghan and Bostick 2012).

Glass is a material that is produced by melting it (Section 5). Melting can also be a way to make a connection. This is called *heat bonding* and is the topic of this thesis. This process has potential, as it allows to design beyond the sheet geometry in which glass is produced. The connection is in an early state of development.
In this section, the properties of a heat bonded joint are discussed. Then, two methods of heat bonding will be explained. The first is the glass weld, the second is glass fusion. For both methods, the current state of development is discussed.

In this thesis, the term *element* or *component* is used to describe a body that is connected to another body by a *connection* or *joint*. The term *system* is used to describe the connected product, consisting of multiple elements and a connection.

2.1 Heat Bonding

Glass has interesting thermal properties, one of them is that is has no discrete melting point, but a transition range of temperatures (Section 5). It can be shaped by using its ability to be manipulated while hot and viscous and solidified in the correct shape by cooling. This ability has been used by glass blowers for centuries and can be used to create heat bonds.

Heat bonding results in a monolithic glass connection. This means that the properties of the joint are the same as the parent material, in this case glass, provided the connection is manufactured well. If one assumes the heat bonded connection is monolithic, predicting its behaviour is the same as predicting behaviour of glass. The bonded system is structurally less complicated than a system consisting of multiple materials, especially when these do not behave linear elastically.

Glass is a very durable material (Section 5). The connection does not corrode and its behaviour is time independent. The heat bonded joint will have the same durability.

Furthermore, glass is highly recyclable (Section 5). The heat bonded system can be molten and re-shaped and is just as recyclable as a bottle or jar.

But those are just the structural, environmental and functional benefits of a monolithic system. Aesthetically, the connection has an important benefit. The connection is no visual obstruction at all. The joint is only visible due to the reflecting and refracting rays of light. Because this behaviour is the same as for the parent material, it is in full compliance with the rest of the structure.

The brittle character of structural glass will cause a brittle failure of heat bonded joints. An important downside is that if a heat bonded system fails, the bond will not stop the crack from propagating. Not only is the failure of the joint brittle, but every element which is part of the heat bonded system will fail.

When a material is heated, it expands. When a glass element is heated and cooled, differences in temperature cause differences in strain and therefore stress within the glass (Section 10). This is called residual stress and is a key parameter when researching heat bonded elements.
Residual stress is an undesired side effect, because it causes unpredictability. With residual stress, the (tensile) limit of the material can be reached at a lower load than predicted based on a stress free material. Only when the residual stress is introduced with a purpose and in a controlled way, simlar to when glass is tempered , it can be advantageous (Section 5).

2.2 Welding Glass

The glass weld has been and is being researched for structural application. In 2008, research is performed by dr. Freek Bos, dr. Fred Veer and ir. Cecile Giezen (Bos, Giezen, and Veer 2008) (Giezen 2008). At the time of writing, it is researched by ir. Lisa Rammig, who is analyzing welded flat glass to make way for the use of additive manufacturing (3D printing) in structural glass (Rammig 2012) (Rammig 2016). This section is based on these publications, unless mentioned otherwise.

Welding glass is locally heating pieces of glass and bonding them. Welding glass has been used for many years outside the building industry. It's application on a relatively large scale is found in the production of laboratory equipment. Similar to the procedure in steel, the glass is heated to a level where it is workable.

Ir. Giezen has researched welded glass tubes for a facade support structure. The main, welded joint was a star of perpendicular tubes (Figure 10). Welded tubes were manufactured and tested under different loading conditions. In this thesis and other publications of this research articles, it has been stated that the weld is not normally weaker than the parent material.

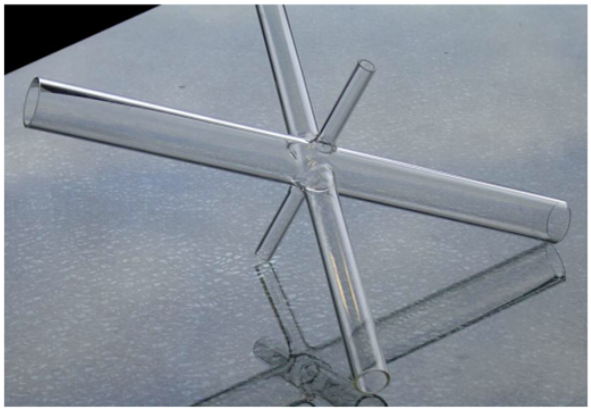

Figure 10: Scale model of a star shaped welded connection of glass tubes (Giezen 2008)

Ir. Rammig is researching the application of additive manufacturing, commonly called 3D printing, in glass. Her vision is to combine the advantages of additive manufacturing with glass architecture.
A method has been developed to create glass objects with additive manufacturing (Klein and Oxman 2015). A kiln with molten glass, with an opening at the bottom, deposits a string of viscous glass on a tray and creates layers of glass. The environment is kept at elevated temperature to prevent thermal shock. According to the definitions in this thesis, the connections between the layers are fused, as the

chamber heats the whole object. To research this connection, Rammig has made and analyzed welded glass connections.

To develop this method, the annealing of welded plates is researched. The results are optimistic: with a proper annealing process, residual stress can be reduced to a level at which the glass can be considered annealed glass.

The welded flat glass specimens have been tested to destruction, but the results have not been published at the time of writing.

The importance of annealing emphasizes an important boundary condition: the welded system is limited by the size of the oven in which it is annealed. Furthermore, the need for an annealing oven dictates that either the system is produced off-site, or that an annealing facility is made on the construction site.

In both research series, the used material is borosilicate. This type is preferred over soda lime glass, because it has a lower coefficient of thermal expansion. Practically, the thermal stress during production and annealing is lower, and thermal shock failure is less likely to occur in borosilicate (Section 8).
The downside is that the borosilicate glass is significantly more expensive than soda-lime glass. This results in a relatively high price for a welded glass structure.

In 2006, an exploratory, experimental research has been performed into soda lime glass welding by prof. Dr. Ir. Jan Belis and others (Belis et al. 2006). They welded soda lime plates in several production techniques and tested the samples mechanically. They concluded that welding soda lime float glass is possible. Specimens failed during production due to thermal shock failure. Heating the glass from both sides with a double torch and preheating the glass proved successful measures to prevent thermal shock failure. The structural performance of the welded, products was poor. The authors state residual stress was not the cause because the specimens were annealed. The imperfections in the joint are likely to have caused the low capacity.

2.3 Fusing Glass

Heat bonded joints can also be made with kiln formed fusion. In some literature, the term fusion is used for any kind of heat bonding, including the welding process. In this report, the term *fusion* will be used only if the method of kiln formed fusion is considered.

Fusing is a method mainly used by glass artists to produce their work. There are documentations in the glass art community published to help artist with their kiln forming. These are the TechNotes, manuals provided by Bullseye Glass Co. on how to deal with the technical aspects in kiln forming their glass products (Bullseye Glass Co. 2009).
Dr. Joanne Mitchell promoted on fusing soda-lime float glass with air entrapment (J. Mitchell 2015). The aim was to create art with hollow air pockets that shape a figurine or text.
This section is based on these publications, unless mentioned otherwise.

When glass is positioned in a certain configuration, placed in a kiln and heated, the glass will bond at a certain temperature. Like the process of welding, heat is used to form the connection. The difference is that with welding, local heating is applied, and with fusing, the whole system is heated.

The technical manuals are used as a source to get a grip on what temperatures and amount of time are required to fuse glass. It is important to mention that this knowledge is applicable to Bullseye glass. This glass is a collection of products in many colors which are compatible with one another. It is necessary to determine to what extend the information can be applied to soda-lime float glass.

Dr. Mitchell's art show the transparency that can be achieved with this method (Figure 11). She used several slabs of glass and cut out the figurine she wanted to trap. With a fusing method she developed, she successfully sealed the system, with the wanted and without the unwanted air bubbles.

Figure 11: Glass art produced with kiln formed fusion and air entrapment (J. Mitchell 2015)

Because the heat bond is produced in a kiln, fused systems are limited by the size of the oven. The system has to be cooled gradually to prevent residual stress, which is done in the same oven. Similarly to the welding process, the possibility to properly anneal the system is an important aspect of the method to make it fit for structural use.

The temperature of the oven influences the product. The higher the temperature, the lower the viscosity of the material and the stronger the fuse.
At a relatively low temperature, tack fusing can be achieved. In this state, the glass sticks together while remaining its original shape, though the edges are rounded.
At higher temperatures, full fuse will occur. At a temperature just above the fusing temperature, the Bullseye glass follows a 'six millimeter rule': thicker systems will flatten to a thickness of six millimeter and thinner systems get thickened perimeters and smaller footprints. Dams and moulds can be used to limit deformations.

Practically, one of the challenges in fused systems for structural components will be the control of the shape of the product. The final dimensions must be predictable in order to design adjacent elements and to implement the system. This can be done by influencing the shape in the kiln by using dams and moulds and/or post processing, grinding and polishing, the product to a desired shape and size.

3 Applications of the Heat bonded Glass Joint

It has been stated that the heat bond has great potential. This section will address that potential.

Heat bonded systems, welded and fused, are limited to the size of the annealing oven. This is a boundary condition that is unavoidable. In 2008, the maximum oven used in industrial glass production processes has an order of magnitude of 2,5 by 1,5 by 2 meter (Giezen 2008). If heat bonded systems are to be used in the building industry, larger systems could be desired. If production demands it, it is likely to assume that oven sizes will increase in the future. If a heat bond will be made on site in a special facility with a large annealing oven, transport would not limit the size.

With that in mind, it is logical to display the potential application of the heat bond as if it is unlimited in size. To keep the reality from today in the picture, other ideas are presented which are limited by oven sizes.

Following applications are not all created by the author. Many have been suggested in informal conversations with tutors, peers and colleagues. The collection is not complete. The applications should be considered as suggestions. It is encouraged to generate applications different from the ones mentioned below.

3.1 Heat Bonded Systems in the Future

When the limits imposed by the annealing oven are ignored, heat bonding is a way to create systems of larger sizes. Beams can be connected, to be as long as imaginable. Facades can be constructed with one panel, removing the need for frames or spiders.

Secondly, the motivation for Lisa Rammig's research should be mentioned: additive manufacturing of structural glass elements.

With heat bonding, structures can also consist profiled glass members. For example, the flanges in a steel H-profile have a structural benefit which can be achieved in glass, heat bonded H-profiles.

There are more structural concepts to mimic in glass. With heat bonding, trusses, spaceframes and vierendeel frames become a fully transparent possibility.

Plate members can also be adapted to benefit from a non-flat shape. Glass stiffeners can be bonded upon wall or floor members, to increase out-of-plane bending resistance (Figure 12). This can help to overcome complex detailing currently necessary to design load bearing glass walls.

The cross section of the glass can be increased where-ever necessary to reduce stress where peak stress occurs. Examples in steel are local stiffeners in connections. Heat bonding glass where it is needed will reduce material use, when compared to increasing the total cross section of the member.

Another idea, inspired by the earlier mentioned research of Lisa Rammig, is to create glass connection elements. These are ssimilar to consoles that are heat bonded to a structural member (Figure 13). On site, the glass connection elements can be connected through an interlocking interface.

There are also non-structural applications imaginable. Heat bonding can be a way to make glass

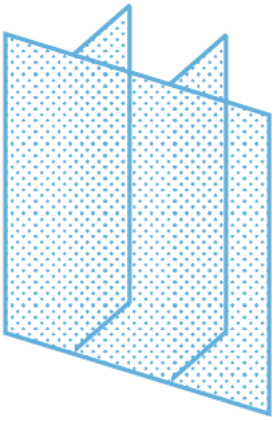

Figure 12: Heat bonds connecting plates to increase out of plane bending stiffness

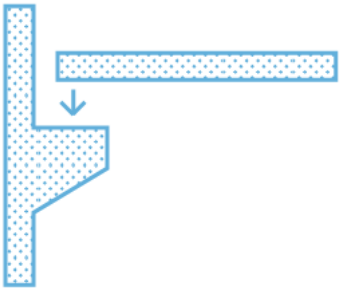

Figure 13: Heat bond connecting a console to a member

elements air- and watertight transparently. This can be applied in a glass facade that is shaped like a part of a box (Figure 14). The edges and corners can be sealed by heat bonding.

3.2 Heat Bonded Systems on a Smaller Scale

As has been said before, the oven imposes size limit in the current state of development. What are the possible applications for the heat bond when the maximum system size is 2,5 by 1,5 by 2 meter?

Almost all of the above mentioned applications are still possible in this size. This is the case for the profiled glass beams and columns, trusses, spaceframes and vierendeel frames, stiffened plates and other elements where additional glass resists peak stress. The glass connection element can be fused on smaller structural members. Smaller, non-flat, glass envelope designs can be sealed transparently.

A combination is possible: a profiled glass beam with glass connection elements bonded to its ends, making it possible to install the all glass element on site.

There are also new applications surfacing when considering this system size. One is a glass hollow core slab (Figure 15). The structural advantage of a high thickness is achieved without adding weight. This could be applied in a glass stair step.

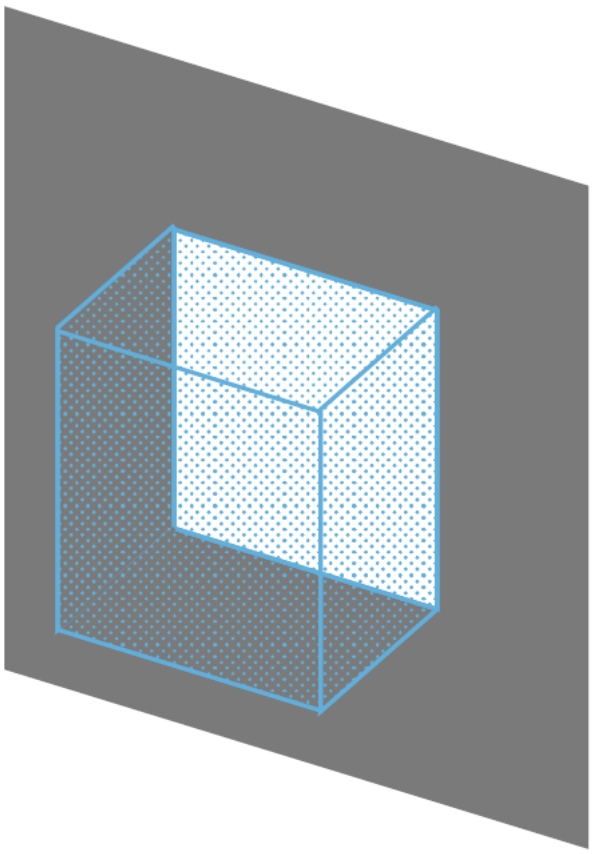

Figure 14: Heat bonded glass box on facade

The same is possible with glass bricks. In masonry, hollow bricks are used to reduce weight. Hollow glass bricks can reduce the weight of glass masonry.

A promising application is the non-flat glass connection piece (Figure 16). Large glass members can be joined by laminating a connecting piece of glass in between the layers of the members. This has only been possible if the members were parallel. When the connecting glass is heat bonded with an angle, the joint can be of any angle. The element can be produced in a work shop off site and the lamination can be done on site.

3.3 Structural Safety

When considering applications, an engineer should be aware of practical challenges and risks. Common structural materials, like steel, are designed with the use of a probabilistic approach. Glass structures are not suited for this for several reasons (Section 12)(Bos 2009).

Professionals designing with glass as a structural material, adopt several approaches to ensure the structural safety with different methods (Bos 2009). The consensus is that it should always be taken into account that the glass element fails. If this happens, for whatever reason, injury should be prevented, the remaining structure has to be able to withstand a reasonable load and the element should

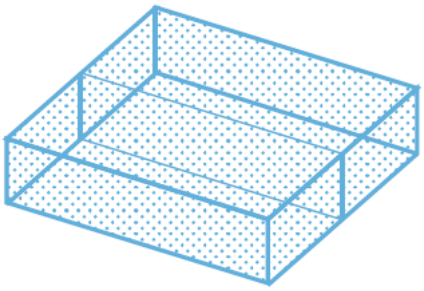

Figure 15: Heat bonded glass box on facade

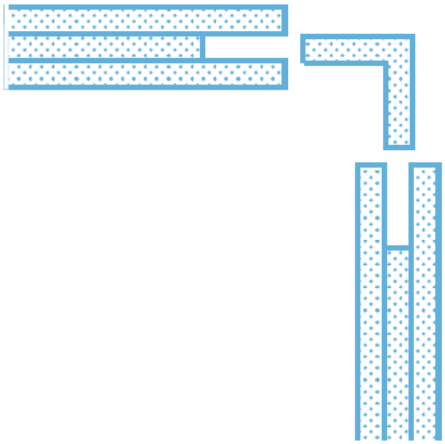

Figure 16: Heat bonded connection piece: installed on site, fully transparent

be replaced without bankrupting the owner.

Heat bonds challenge these failure scenario's. A heat bonded system must be considered as one glass element that collapses at failure. This challenge is of major importance for any structural implementation of heat bonded systems.

4 Research Questions

What is the best method, among glass welding and kiln formed glass fusing, to produce heat bonded systems for applications in glass structures?

To be able to answer the question objectively, a set of sub-questions is presented:

- How can the structural safety of a heat bond be ensured?
- Which method results in a system with the least residual stress?
- How can thermal shock failure be prevented during the welding process?
- How can the tolerances of the fused product be limited, to make the product applicable in structures?
- Which method, among heat bonded joints and suitable alternatives, has the best structural performance?
- How do the methods, heat bonded joints and suitable alternatives, compare on qualitative aspects?

4.1 Scope

The scope of the research is soda lime float glass systems of a few hundred millimeter in size. One material is chosen to unify the material in all experiments. Soda lime glass is chosen because of its price and availability, both useful in the thesis but also in future application.
The size limit is because both methods require an oven for annealing, limiting the size of the product.

Additionally, the thickness of the object is $10\ mm$. This thickness is 'structurally relevant': it is a thickness of the order of magnitude applied in glass structures.

The shape of the element consists of flat plates assembled in a T-shape. The flat shape is chosen because the systems are composed of commonly produced elements, like float glass sheets. The T-shape is chosen, because when the glass is under an angle, the system is topologically different from the glass sheets.
It has been decided not to connect parallel plates, because this would not result in a new object. The size limitation of the oven is smaller than the limit of float glass production. Creating a bigger sheet should not be done by welding or fusing, but by cutting a bigger sheet from the float process.

The T-shape is a topology for glass sheets under perpendicular angles. The method to create a T-shape can be applied to make an L-shape as well. The L-shape is outside the scope of this thesis, but it is considered that when the T-shape is researched, the L-shape is a small step further.

The suitable alternatives are transparent glass connections. These are cast glass and adhesive joints, with the adhesive used in the Crystal Houses project. However, casting soda lime glass requires high temperatures. Special moulds of a different material would be required. Time would be spent on producing cast soda lime glass. Because this is not the main part of the research, the cast glass is not in the scope of the research.

The only researched suitable alternative connection method is the adhesive joint.

4.2 Hypothesis

The structural safety of the heat bond can be ensured, if multiple heat bonds are used and/or if it is combined with other connection methods. A design can be made in which the bond is sufficiently protected.

It is predicted that both methods result in glass to glass bonds. It is possible that air inclusions will occur. For the fused object, this will probably depend on the state of the edges before fusing. In the welding process, it will depend on the skill of the welder.

It is predicted that residual stress can be sufficiently prevented, if the product is properly annealed after connection.

The ability to resist thermal shock sufficiently will determine whether the weld can be produced or not.

It is predicted that it will be possible to create a fused specimen with a monolithic bond, but that its other regions are reshaped by the process. It is predicted that the quality of the product's shape is directly linked to the quality of the mould during production.

To be able to compare alternatives, the structural performance will be compared to suitable alternatives, which is the adhesive joint.
Provided that the connection is monolithic and the specimen is well annealed, the fused and welded specimens should be as strong as the theoretical calculations predict. It is expected that production flaws will result in lower failure loads in the experiments. The adhesive specimen is predicted to have a lower strength than the theoretical monolithic element.

If all products are made successfully, it is predicted that the fused product requires least time, energy and money because it can be produced at relatively low temperatures and with little skill. The welded specimen requires more time, energy and skill. The bonded specimen requires more skill but less energy than fusing.

4.3 Method

The research will be conducted with a theoretical and practical approach. There will be a balance between gaining and applying knowledge and trial and error.

The structural safety will be researched theoretically. By analyzing project cases, general methods for structural safety will be stated. These methods will be analyzed for their suitability in applying heat bonds. Then, recommendations will be made for the safe design and safety limits of heat bonded joints. Two scales are considered: solutions within the heat bonded system and solutions in the structure with heat bonded systems.

The sensitivity to thermal shock of the weld production process will be researched theoretically. This will be done with finite element models. The aim of the model is to predict the temperature distribution in the specimen for different production conditions.
Using the temperature difference, the thermal stress in the element can be computed. This will be compared to a defined stress limit to predict whether thermal shock failure would occur. The conclusions

consist of recommendations for the weld production process.

The production process of the weld will be designed in collaboration with professional glass blowers and based on the recommendations of the theoretical analysis.

The fused specimen will be researched more practically. Knowledge gained from literature will be applied in a first fusing experiment. The product will be analyzed, after which points of attention are determined. Solutions will be created and implemented in a new experiment.

The structural performance will be researched both theoretically and practically. The theoretical approach consists of finite element analyses, predicting the strength of a monolithic glass element without imperfections.
The practical approach is to perform structural tests on the fused and welded specimens and on specimens of suitable alternatives. The results can be analyzed and compared to the results of the models.

The presence of residual stress will be reduced by annealing the specimens. Afterwards, this will be analyzed qualitatively by using polarization filters to assess the stressed areas in the specimens.

The comparison of practicality of the joints will be theoretical and qualitative. Based on results from this research and literature, conclusions will be drawn on the use of time, energy and money for the fused, welded, and adhered products.

Part II

Literature Review

This part contains the theoretical background gathered for this research. It opens with a brief history of the material, the production process and the products.
To position the heat bond among other glass to glass connections, the most common connection methods are listed and described. In the following section, they are compared on transparency, structural behaviour, sustainability, durability and other aspects.
Heat bonds are formed by raising the glass temperature. Therefore, it is researched what happens in a material when it is heated. A section is devoted to explaining the mechanisms of heat transfer and thermoelasticity, the relations between temperature and stress.
The next section describes what the behaviour of glass is at elevated temperatures. Glass has no discrete melting point and the continuous change from solid to liquid as temperature rises is explained. The effect on the development and relaxation of elastic stress is described.
The final section describes residual stress, a permanent type of thermal stress. In this section, it is described what causes residual stress and how it is prevented and analyzed in glass.

5 The Material Glass

Glass is a material touched, seen and used on a daily basis. Its use is common, but its characteristics are unique.

Most literature on structural glass of considerable size contains a chapter on the material history, properties and products. This thesis is no exception. The sources containing information are numerous and a few have been selected. This section is based on the works of Nijsse 2003, Schittig et al. 1999, Bos 2009 and Louter 2011.

5.1 History

It is unknown how and where glass has been invented, though the first evidence of an ash to glaze ceramics were found in Mesopotanian articles in the fifth century BC. When tombs of pharaohs were discovered, glass beads dating from around 3500 BC were found. The most influential developed technique in this early stage was the blow pipe, which was invented in Syria in the first century. With this technique, still applied today, the shaping of hollow vessels like cups, bottles and vases was possible.

In the Middle Ages, production of vessels continued. There were techniques to use the blowpipe to create flat panels, but the sizes were limited. The glass blowing technique has developed in Venice, the major glass producer of that time.

In 1687, a cast glass process was developed in France. This technique could be used to make larger panes, 1,2 by 2 meter, with less manpower and of better quality. Around 1900, Belgians developed the process of industrially pulling glass sheets form a bath of molten glass. A steel bar was lifted from the bath, followed by a sheet of glass that hardened during he drawing. Theoretically infinite sheets could be produced with this method.

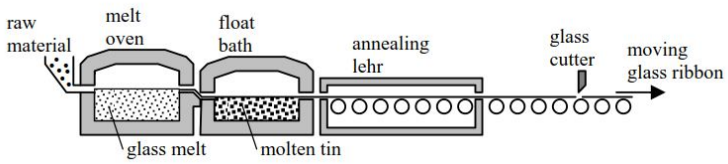

Figure 17: Simplified process of the production of float glass (Bos 2009)

In the 1950's, Alistair Pilkington developed the float-glass process (Figure 17). Here, the molten glass is poured on a bath of molten tin, resulting in a glass sheet with smooth and flat surfaces on both sides. The product, float glass, is still the most common glass product in the building industry. The width of the production chain determines the width of the product, which is generally 3,21 m. The panels can be as long as possible, for one can choose to cut the glass at any length, but lengths up to 6 meter are common. For larger elements, the production equipment will be different from the standard equipment.

5.2 Properties

Glass is an inorganic material which is cooled to a rigid condition without crystallization. Many solid materials have a molecular or atomic structure that has a regular pattern. Glass molecules are not ordered and therefore resemble the microstructure of a liquid (Figure 18). Contrary to urban legend, glass at room temperature is not a liquid, because the molecules cannot flow.

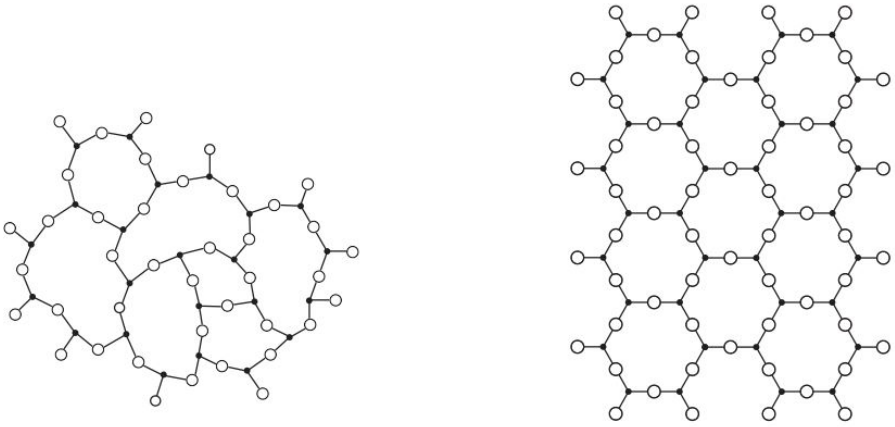

Figure 18: Amorphous glass molecular structure (left) as opposed to a crystalline structure (right) (Bullseye Glass Co. 2009)

Glass molecules do not form a crystalline structure, because they cool down and stop moving before they crystallize, contrary to most solids. This description of glass does not limit itself to the transparent silica based material commonly called glass. Theoretically, every material can form glass if it is cooled from liquid to solid state at such a high rate that it does not crystallize.

Glass has a transformation range, a temperature range on which it changes from a liquid to a frozen solid. Materials that crystallize have a melting point, a temperature at which the material remains until the phase change is complete, like when water changes to ice (Figure 19).

The transformation range of glass makes it fit for production methods like glass blowing. By using the gradually changing viscosity over a temperature range, the shape of the glass in which it solidifies can be controlled.

Physically, a glass can be made from any material. However, the term glass is widely reserved for the silicate based material. The major ingredient is siliciumdioxode (SiO_2), assembled in tetrahedral configuration. The oxigen atoms are connected to four silicone atoms, linking all tetrahedrons. The irregularity that results in amorphous structures is caused by different bond angles and rotations.

Glass consisting mainly out of these tetrahedras are quartz glasses. Other types of glass materials contain siliciumdioxide and other salts.
Borosilicate glass contains borontrioxide (B_2O_3). This material is used for its high resistance to thermal shock. It is applied in laboratory equipment and oven dishes.
The most commonly produced glass is soda lime glass. This material, contains soda (Na_2O) and lime (CaO). This is the material used in cars, bottles, lamps, vases and, last but not least, buildings. Soda lime glass is cheap, among other reasons because the Pilkington float glass production method has

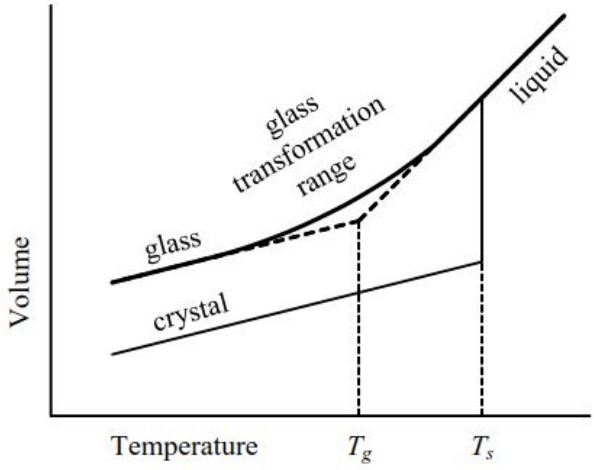

Figure 19: Schematic representation of the relation between temperature and volume of a glass and a crystal (Louter 2011)

been well developed for this material. This product, soda lime float glass, is also of a high quallity, with flat, parallel and smooth surfaces.

Glass does not corrode, making it a durable material. Furthermore, because the glass is a homogeneous material which can be molten and reshaped, glass is highly recyclable and therefore sustainable.

5.3 Strength

Theoretically, glass is stronger than any common structural material. Based on the stress required to break the atomic bond, its strength would be 32 GPa. This is a hundred times stronger than steel.
But, in practice, the capacity is much lower. According to the Eurocode, its characteristic bending tensile strength is 45 MPa (Het Nederlandse Normalisatie-instituut 2014). This difference is due to the high sensitivity of glass to flaws on its surface. These flaws are microscopic and randomly distributed and cause stress concentrations, peak stress.

Other materials redistribute peak stresses. The stress can be reduced because it is compensated with plastic strain. Glass is known for its fragile and brittle nature, because it does not deform plastically. Therefore, glass cannot redistribute peak stress, making its strength is highly dependant of the flaws on the product.

Due to cutting and machining processes, more and larger flaws are present at the edge of a glass panel. To ensure the panel's strength, the edge finishing, grinding and polishing, has to be done properly.

Experiments showed a large scatter in the strength of glass. Often, the Weibull distribution is used as statistical distribution. However, this description of the statistical strength of glass is argued by several authors.
The practical consequence of the large scatter is that it is probable that a glass member fails at a much lower stress than its characteristic strength. The consensus among structural glass engineers is that it should always be taken into account that the glass element fails.

Glass can be thermally treated to improve its stress capacity. This process is called tempering. Glass is heated and rapidly cooled. When something cools, it shrinks (Figure 19). When glass is cooled rapidly, the outer surface is cooler and shrinks more than the inside of the panel. When the inside cools afterwards, the outer surface of the panel is compressed. There is a compressive prestress at the surface of heat treated glass (Figure 20).
Small flaws on the glass grow into cracks when the glass is under an effective tensile stress. By thermally prestressing the glass, this is achieved at a larger load, making the glass stronger.

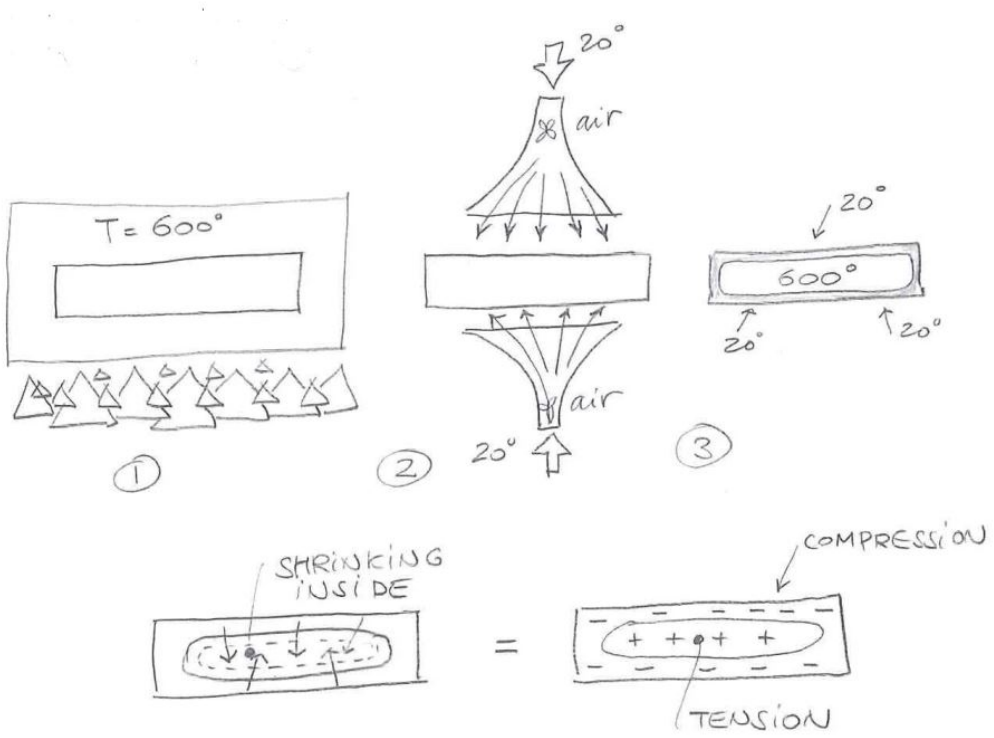

Figure 20: Visual representation of the tempering process and effect (Nijsse 2003)

There is an energy balance between the tension in the core and the compression in the outer surface. When the glass is cracked, this balance is disrupted, causing the panel to shatter. Annealed glass, glass that is cooled at a rate slow enough to prevent this prestress, breaks in large fragments. This disruption of balance is the reason why tempered glass shatters when it is cut or drilled. Mechanical processing should occur before heat treating.

There are more ways to deal with the brittle behaviour of glass. A commonly applied solution is laminating glass. Two, or more, panels are laminated with a transparent, plastic interlayer. If one of the panels fails, the fragments remain in place. This way, there is a small residual load the broken panel can bear and no injury is caused by falling shards of glass.

6 Structural Glass Connections

To position the heat bond in the field of structural glass connections, alternative methods for connecting structural glass are assessed and compared. The assessment is presented in this section.

In Table 1, the connection between different element types have been gathered. To make the table fit the page, letters are used to indicate the connection. The letters correspond to the following list:

- a: Point fixed metal connection elements
- b: Line fixed metal connection elements
- c: Laminated overlap
- d: Heat bond
- e: Silicone
- f: Thin layer adhesive
- -: Irrelevant due to symmetry of the table

	Beam	Column	Rod	Floor/Roof	Wall	Brick
Beam	a, b, c	a, c		a,b, e		
Column	-	a, c			a, e	
Rod	-	-	a, d		a	
Floor/Roof	-	-	-	a, b, e	a, b, e	
Wall	-	-	-	-	a, e	
Brick	-	-	-	-	-	f

Table 1: Connection type inventory. The rows correspond to connected glass element 1, the columns to connected glass element 2. (Nijsse 2003) (Teeuwen 2016) (O'Callaghan and Bostick 2012) (O'Callaghan 2008) (Bos, Giezen, and Veer 2008) (Takeuchi, Sugizaki, and Yasuda 2012) (Oikonomopoulou, T. Bristogianni, et al. 2016)

Table 1 shows there are many ways to connect glass to glass. It also shows some blank spaces. These connections are either not found or do not transfer loads. Some of the mentioned connections have been developed but not applied in projects, like the heat bond or the beam to beam connection of type b (Bos, Giezen, and Veer 2008) (Teeuwen 2016).

Heat bonding has been explained in section 2. The other methods are explained in this section and examples are provided. In section 7, they are compared on several criteria.

6.1 Point Fixed Metal Connection Elements

One of the most common methods to connect glass is inspired by connections in steel. Holes are drilled in the glass and connected to another element with steel bolts. When holes are undesired, bonded point fixings are a possibility. Here, a steel element is glued on the face of a glass panel.

There are many examples of the application of this method. For facades, it has often been applied in the shape of spiders, like La Cité des Sciences et de l'Industrie (Figure 2)
Another example worth mentioning is the connection in the facade of the Hogeschool Limburg in

Heerlen (Nijsse 2003). Here, a glass facade has been realized with a profiled glass fin (Figure 21). The connections are made with steel plates and bolts.
This category also contains embedded point fixings, which are for example applied in the second Apple Cube (O'Callaghan and Bostick 2012).

Figure 21: Facade of the Hogeschool Limburg in Heerlen (Nijsse 2003)

If bolts are applied, this connection behaves like similar connections in steel. Provided that the glass is not the limiting factor, the connection is as strong and ductile as steel. The bolts are easily installed and removed, which makes replacement of glass elements convenient.

In reality, glass usually is the limiting factor for these connections. Bolting glass requires drilling holes in the panels. The drilling process weakens the glass significantly by introducing flaws (Dispersyn and Belis 2016). High peak stress can occur due to the contact between metal and glass. These disadvantages have been the cause for the increased popularity of laminated point fixings.

The bonded point fixings introduce a new ingredient to the connection: the adhesive. For the (embedded) bonding of metal to glass, SentryGlas, an ionomere interlayer by DuPont, is often used (Stelzer 2010) (Veer 2016). The material properties of this product depend on load duration, temperature and are sensitive to fatigue. These properties make the design with this material more complex. SentryGlas can withstand its highest stress at a relatively large strain, making the material ductile. Its tensile capacity in the elastic region is in the order of magnitude of that of annealed glass.

Another bonding agent is Transparent Structural Silicone Adhesive, also known as TSSA (Hagl 2012). This is a heat cured adhesive, usually cured in an autoclave. This material is less strong and stiff than SentryGlas. Its high strain at failure results in a ductile connection. An interesting phenomenon of this material is that the transparency is lost under high stress. This is called stress whitening.

Though the bonding procedure has to occur in controlled conditions, connecting a glass element with pre-bonded metal on site is not a complex operation. This can simply be done by bolting metal to metal. The glass element can also be easily disconnected and replaced, though the replaced glass cannot always be recycled easily since the adhesive has to be removed.

6.2 Line Fixed Metal Connection Elements

This type of connection resembles a common window frame. The scope of the presented connections is those connecting structural glass. This type is therefore dubious, because in many cases, frames are the load bearing elements. The essence of this type is that the loads from the structural glass are transferred via metal elements, but the fixation to the glass is a linear typology instead of a point. Because of their load bearing function and poor transparency, clamped connections are not included.

The line fixed connection element is applied in a renovated office of the Nationale Nederlanden ING Bank in Budapest, Hungary (Nijsse 2003). The steel element is hidden in the detail in this example (Figure 22). A second noteworthy example is a connection between beam segments with embedded bonded aluminum profiles, see figure 23 (Teeuwen 2016).

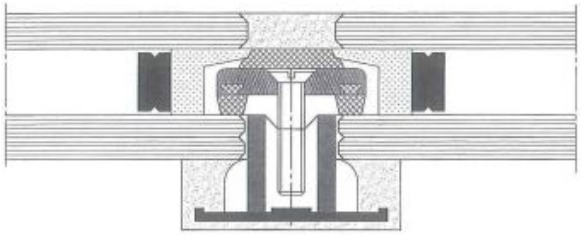

Figure 22: Detail of the roof plate joint in the renovated office in Budapest. The mechanical element is only present at the bottom, the top is sealed with silicone (Nijsse 2003)

This type of connection also uses an adhesive to connect metal to glass. The metal components make installing and dismounting on site a simple operation.

6.3 Laminated Overlap

Lamination is used to provide safety in structures (Section 5). This application of lamination is not a method to connect structural members and therefore outside the scope of this collection.

However, lamination has also been used to make longer elements than production allows. Creating larger beams or columns through lamination has been done in many buildings, like the Apple Cubes and the extension in London by Dewhurst MacFarlane (Figures 6, 7 and 8).

In these examples, another application of this connection is present: the corner connection of a glass portal by laminating the column and beam. This connection is slightly different, as it can be produced on site (Nijsse 2003).

An important aspect of this connection, is that overlapping panels are connected. This limits the

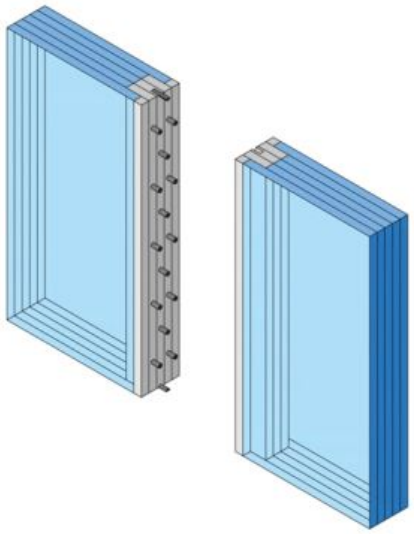

Figure 23: Connection between two beam segments with embedded aluminum and bolts (Teeuwen 2016)

shapes of the connection, because the elements have to be in plane of each other. A perpendicular connection, like a fin to a wall, cannot be made with this kind of connection.
The scope of this report contains connections to create elements that are not bound by the flat shape in which glass is produced. This connection method does not escape that constrain and is therefore not considered a relevant solution.
However, laminated connections are present in the most iconic glass structures. To get a proper view on the connection types known in structural glass, laminated joints are included in the collection and comparison.

A laminated joint has the significant advantage of being transparent. Many adhesives can be used to obtain laminated joints. For safety glass, SentryGlas has been widely recognized as the best interlayer (Veer 2016).

The connection is formed by assembling the panels and interlayer, heating the assembly and adding pressure to create a bond. This connection is not easily undone, which results in a large amounts of laminates being discarded (Anderson 2012). This is not just a waste of materials, but also harmful to the environment, because the toxic chemicals of the interlayer are released.

Delamination is possible (Anderson 2012). This is done by heating the laminate, softening the adhesive and pulling the glass panels apart. When done properly, the glass can be recycled. The adhesive can be recycled as well, but the (chemical) characteristics of the adhesive determine whether it can be re-used as adhesive. It is safe to assume that delamination is a process that requires investment. Therefore, laminated glass is not well recyclable.

6.4 Silicone

Silicone is often applied in glass structures. They do not only transfer loads, but are also a filling and sealing material. In the all float glass structures of the Apple Cubes and the extension in London, this typical joint is present. Here, silicone is applied to connect the edges of the panels. It is used to connect roof to roof, roof to wall, beam to roof et cetera.

Silicone has a low material stiffness and allows high strains (Hagl 2016). The flexibility of the material makes it very suitable to apply when a large tolerance is required or to compensate thermal expansion. It is a hyper-elastic material, allowing large strains in tension and almost perfect incompressibility in compression. Silicone has reasonable resistance against age and weather.

Silicone is a rubbery material with similar properties, like its softening after loading and visco-elasticity (Hagl 2016). Many of its properties do not behave linearly, complicating the predictability of the silicone. Special and complex material models need to be developed to understand and implement the material optimally.

Aesthetically, silicone is not ideal. Many types of silicone are opaque (Dow Corning 2014a) (Dow Corning 2014b). Transparent silicone is under development.

Furthermore, silicone is not very strong. Its strength is roughly 20% of the strength of TSSA and 10% of the strength of SentryGlas (Dow Corning 2014a) (Hagl 2012) (Stelzer 2010). The strength of about 2 MPa is significantly weaker than the design tensile strength of glass. If the silicone is loaded in tension, its strength imposes a limit.

6.5 Thin Layer Adhesive

This connection is similar to the laminated overlap and the silicone joint. That is because it uses an adhesive material to connect glass directly. When considering the application in the Crystal House, as visible in figure 24, it deserves its own category. Here, there is no overlap of panels, but faces are directly glued together. It is also different from a silicone joint, because the interlayer has a thickness of 0,3 millimeter and demands a high precision of the dimensions of the glass (Oikonomopoulou, T. Bristogianni, et al. 2016).

The adhesive in the crystal house project is a transparent, UV-curing acrylate (Oikonomopoulou, Veer, et al. 2014). The connection has many advantages. It is transparent, has adequate compressive behaviour and has a high bond strength with glass.

The construction of the Crystal House came with challenges difficult to overcome. To ensure good adhesion and prevent offsets in height or width of the structure, the tolerances for the dimensions and flatness of the brick was limited to 0,25 mm (Oikonomopoulou, Veer, et al. 2014).
Applying the adhesive came with unusual procedures. The building site had to be covered in a UV-filtering tent to prevent the sun from curing the adhesive prematurely (Oikonomopoulou, T. Bristogianni, et al. 2016). Temperature and humidity had to be controlled. After proper cleaning of the glass surfaces, the adhesive was applied with use of a mould and the block positioned. In this process, air bubbles and dust intrusion had to be prevented. The adhesive was cured shortly to fixate the block in position, excess adhesive was removed and the joint was fully cured.
The adhesive has a very low viscosity, so it can only be applied on horizontal surfaces. As a result,

Figure 24: Close-up of the executed facade of the Crystal House in Amsterdam (Oikonomopoulou, T. Bristogianni, et al. 2016)

the vertical joints in the masonry are not bonded (Oikonomopoulou, T. Bristogianni, et al. 2016). To construct the architraves, a rotating mould was used to keep the to be bonded surface horizontal.

Unbinding the adhesive is possible (Oikonomopoulou, Veer, et al. 2014). The adhesive must be heated to 120 $°C$ to soften, allowing the removal of the glass.

The overlapping laminated joint is limited, because connections are only possible in plane of the element. Using adhesives could be a way to connect glass edges, creating possibilities for other typologies.

7 Comparison of Structural Glass Connections

In section 6, several ways of connecting glass to glass are presented. To be able to place the heat bond among them, the methods are compared. The comparison is made based on several criteria. The aim is not to find the best connection method, but to show the differences and to determine the added value and focus points of the heat bonded joint.

In the comparison, it is assumed that the connection is perfectly well executed. Every glass structure is weakened if the connection is not properly formed, because the material is highly sensitive to stress peaks. The adhesives are assumed to have no air bubbles or dust intrusion. The heat bonded systems are assumed to be perfectly monolithic and annealed.
Obviously, this might not be the case in practice. The presented comparison has to be interpreted as a theoretical view on the connections.

In section 6, the metal point fixing has been considered as one connection type, because of its appearance. It is not always visible whether it is a bolt or two bonded metal element on each side of the panel. However, the presence of a hole in the glass panel and the differences in the processes of bolting and bonding demand that in this chapter, this connection type is split.

The comparison is made by different criteria. In the following sections, the criteria are first described and then the connections are judged related to these criteria.
Many characteristics and properties of the methods and materials have been discussed in section 6. In this section, these are often compared to the characteristics and properties of glass, which are discussed in section 5.

The results of the comparison, for most criteria expressed in advantageous and disadvantageous properties, are shown in table 2.

7.1 Strength

From an aesthetic point of view, strength is relevant. If the connection medium is stronger, less material is needed to create it. If the connection is opaque, this adds to the transparent character of the connection.
Form a structural engineering point of view, the strength of the connection is an important parameter. If the connection is stronger than the member, the member will be the first element to fail and vice versa. It's the engineers task to balance these phenomena by design.
The strength of the connection, defined as its load capacity, is not defined by the strength of the material, defined as its stress capacity. A weaker material is not necessarily worse to design with, it requires a different approach. This criterion is therefore not judged as advantage or disadvantage in table 2.
However, to get a grip on the relative strength of the connection methods, the strength will be a criterion for comparison. The most objective parameter is the stress capacity of the material, because the load capacity of the connection depends on design.

Steel is stronger in tension than glass. Adhesives like SentryGlas, TSSA are weaker (Stelzer 2010) (Hagl 2012). Silicone is weaker than these adhesives (Dow Corning 2014a) (Dow Corning 2014b). Heat bonded connections are relatively strong, because they have the strength of glass. With this knowledge, the mono-material connections are easily categorized.

	Bolted Point Fixed Metal Element	Bonded Point Fixed Metal Element	Line Fixed Metal Element	Lami-nated Overlap	Sili-cone	Thin Layer Adhe-sive	Heat Bond
Strength	v.high	low	low	low	v.low	low	high
Stiffness	v.high	low	low	low	v.low	high	high
Transparency	- -	- -	- -	+	-	+	++
Ductility	++	+	+	+	++	- -	- -
No Failure Introduction	- -	+	++	++	++	++	+
Durability	+	-	-	+	- -	- -	++
Demount-ability	++	++	++	- -	+	-	- -
Recycl-ability	+	-	-	-	-	- -	++
Simple Process	++	+	+	+	++	- -	- -
Low Price	++	+	+	-	++	- -	- -

Table 2: Schematic comparison of the methods to connect structural glass, *v.* stands for *very*. All criteria are discussed in section 7

The bonded metal point and line fixings contain multiple materials: a metal and an adhesive. Because a chain's strength is defined by its weakest link, the property of the adhesive is dominant. Therefore, these connections are considered to have a low strength.

The strength of the thin layer adhesive as applied in the Crystal Palace is difficult to determine. The adhesive is mainly loaded in compression. Experiments showed that load concentrations on the bricks caused the failure mechanism and not the adhesive's limits (Oikonomopoulou, Veer, et al. 2014).
Tensile tests have not been performed, though an out of plane bending test did load the adhesive in tension (Oikonomopoulou, Veer, et al. 2014). In this test, a maximum stress of 9 MPa was reached. It has not been indicated whether failure occurred in the bricks or the joint.
It is therefore unknown what the limit to the thin layer adhesive is. Conservatively, the tensile limit of 9 MPa is assumed. This is a strength level similar to TSSA. Therefore, the strength is considered to be low.

It should be noted that adhesives are often loaded in shear. Also, in this report, the strength of adhesives is judged by its cohesion, its ability to stick to itself. Another aspect is adhesion, its ability to stick to another material, like glass.

7.2 Stiffness

To be able to predict and control deformations in the structure, stiffness is the key parameter. As for strength, the stiffness of the material does not define the stiffness of the connection. It is included as a criterion to indicate relative differences. A stiff material can be advantageous because it will minimize deformations in the structure. A more flexible material can be advantageous because before collapse,

large deformations will act as a warning sign. Comparable to the criterion of strength, a high or low stiffness is not presented as a (dis)advantage in table 2.

Similar to strength, the stiff properties of steel and flexible properties of adhesives can be directly extrapolated to the mono-material connections. Silicone is hyper-elastic and often applied because of its ability to compensate for thermal deformations. Its stiffness is therefore very low.

The bonded point fixing is for this criterion judged by its weakest link: the lower stiffness of the adhesive.

It is unknown what the deformations were in the Crystal House experiments (Oikonomopoulou, Veer, et al. 2014). Because of the thin layer, it is probable that deformations of the interlayer are not large, even if the strains are large, and do not govern the deformation of the specimen. To make a conservative assumption from a structural point of view, brittle failure is assumed. In that case, the stiffness of the material is too high to provide warning before failure.
It should be noted that the presence of a visible warning sign does not depend on stiffness, but on deformation, which is also related to the thickness of the joint. In the case of a thin interlayer, even with a very flexible adhesive, the deformations might be too small to see.

7.3 Transparency

The fascination for the material glass is largely founded in its transparent character (Section 5). Considering glass connections, transparency has been the drive for many innovations, for example embedded fittings and adhesives (Section 1). Transparency is an important characteristic, if not a requirement, for this report.

Metal point or line fixings are opaque. Silicone connections perform slightly better, because transparent silicone is a probable option in the near future. Still, these transparent rubbery joints will reflect and refract light differently and are therefore clearly visible.

The transparent connections have been realized with transparent adhesives. This is the case for the laminated overlap and the thin layer adhesive. The joint is visible due to the reflection and refraction of the glass faces in the joint, see figure 24.

Transparency is one of the main benefits of the heat bonded joints. Not only does the monolithic glass show the same reflection and refraction, but there are also no glass faces within the joint. The molecular bond allows light to travel undisturbedly.

7.4 Ductility

Structural glass is notorious for its brittle failure behaviour. Ductility is desired in connections, because it results in warning signs before ultimate failure. The possibility to create ductile connections with each method is considered in this criterion.

The ductile behaviour of steel and silicone result in very ductile behaviour for these connections. The ultimate strain of SentryGlas is lower than of silicone and TSSA (Stelzer 2010) (Hagl 2012) (Dow Corning 2014a) (Dow Corning 2014b). The laminates and bonded metal connections are considered

ductile, though it depends on which adhesive is used.

As mentioned before, the thin layer adhesive is assumed to have a brittle character, not only to be conservative, but also because large strains in thin interlayers do not cause visible deformations.

For heat bonded systems, it has been stated that in case of failure, the whole system fails (Section 2). This is a very negative property in this criterion.

7.5 Unlikely to induce glass failure

The type of connection can weaken the glass elements. This is mainly the case for bolted joints. The bonded point fixed joints also score positively, because no holes are drilled in the panels. The point introduction of forces does limit the strength of the system. Other methods with adhesive materials do not interfere with the structural integrity of the glass elements.

Heat bonding introduces residual stress. These can be removed with proper annealing, removing the risk of inducing failure. If it is assumed the connection is perfectly well executed, it can be concluded that this connection is not very likely to induce failure.

7.6 Durability

This characteristic is related to the ability of the connection to withstand time and exposure to several different environments. Glass is a durable material, because it does not change when exposed to light or to a humid environment. Glass does not corrode (Section 5). Structural glass members have a relatively long life span.
It is a disadvantage when connections have time dependent properties, because then, the initial quality can not be guaranteed for a long time. It would be a waste if the life span of a glass structure is determined by the life span of the connection.

Adhesives have properties dependent on time, temperature and radiation. These materials are considered not durable. This affects all connection types with adhesives.

Steel is relatively durable when it is treated properly. Coating is required to prevent corrosion.

The heat bonded joints are as durable as glass.

7.7 Demountability

In structural glass design, the engineer always has to keep in mind that every element can fail. This can be unexpected failure, for example because of invisible flaws on the glass surface, but also because of acts of vandalism.
When a glass member has failed, it needs to be replaced. For this, the ability to demount the connection is key.
Another advantage of demountability is the possibility to deconstruct the structure and re-use its components.

Bolted structures are most easily demounted. The bonded point and line fixings are easily demounted if the steel is easily disconnected. Then, the glass elements, including laminated or embedded fixings, can be replaced. Silicone can be cut up and replaced.

Delamination is a more complex procedure. It generally requires heat and force. For the connections where glass is bonded to glass, this results in possible, but difficult demountability on site.

Heat bonded connections can theoretically be demounted. Practically, this will not be possible. The required temperature is very high. Furthermore, it will be complicated to control the shape and dimensions of the remaining edge.
However, the most important motivation to demount, removing and replacing a glass element, will not be relevant. If an element fails, the joint and other glass element are also broken.

7.8 Recyclability

The building industry has a responsibility to reduce waste of material. Sustainability is and has to be an important theme for innovations in this industry.
Waste of materials can be reduced by re-using building components. This ability is judged in the previous criterion of demountability. If re-use is not possible, recycling is another method.
Glass can be recycled very easily. It can be molten and reshaped, for example by adding used glass to the melting kiln at the start of the float glass production line.
Recycling glass is only possible if the glass can be separated from the other material. This criterion concerns the possibility to separate the different materials to make the components recyclable.

Heat bonded systems already consist of one material. They are easily recyclable.

As mentioned before, delamination is possible, but complex. It is possible to separate bonded elements and remove the adhesives to create clean panels, but this requires effort and investment. Furthermore, not all adhesive materials can be well recycled. The connections containing adhesives are considered not easily recyclable. The thin layer adhesive will be more difficult to remove, because of its thickness.

It is relatively easy to disconnect the glass from the other material if bolts are applied.

It should be noted that both criteria on demountability and recyclability concern the possibility to undo the connections. Nevertheless, it is argued that these criteria should both be included. There is a difference among them regarding connections with multiple links, the bonded point and line fixed metal elements. These joints contain easily disconnectable steel-to-steel connections and more complex bonded steel-to-glass joints. Replacement and re-use is simple in this case, because then, the steel has to be disconnected from the steel. When recycling is considered, the steel has to be disconnected from glass as well, which is a more complex process.

7.9 Simple Connection Process

Complex connections require knowledge, experience, craftsmanship, rare machinery and/or time. The larger the simplicity, the lower the threshold to implement it in a structure.
Complex connections are not only more expensive, they also bring along risks. However, this should not be taken too strictly, because projects with structural glass contain more risks than 'regular' con-

struction projects, regardless of the connection method.

It has been stated before that the metal joints are common and will be easily installed.

The bonding procedure under controlled conditions of glass to glass or glass to metal has been developed relatively well. It requires precision, but has been performed relatively often and is therefore considered relatively simple.

Silicone joints can be installed on site. Because of the flexibility of the material, the connection has relatively high simplicity.

The thin adhesive comes with a complex construction process. This is due to the low tolerances and controlled conditions it requires.

The heat bonded systems require knowledge, and in the case of welding, skilled labour. Currently, it is a challenging process, because it is not well developed. It is unknown if the simplicity of the method increases with development.

7.10 Low Price

Even though glass structures are reserved for prestigious projects, costs are still important. With most glass structures, the limits of the industry are pushed further, requiring innovation, research and experiments and therefore investments. However, the choice for the method of connection has a large influence on the final bill.
The price of a connection is high if the connection requires specific professionals and if it's not often applied. It is also determined by material costs.

The often used metal and silicone connections are considered simple and therefore cheap. However, for embedded bonded point fixings, this is not the case.

Lamination is more expensive, because it has to be done off site with special machinery, but well developed and often applied. Therefore it is considered relatively cheap.

The thin layer adhesive requires craftsmanship and time, which determines many properties including the price. The mentioned labour intensive processes of heat bonding also result in a high price. Furthermore, the glass weld has only been researched in borosilicate, which adds to the material costs significantly.

It should be noted that the most expensive methods are least developed and applied. Further research in heat bonding and thin layer adhesion will eventually result in a faster, better and cheaper approach.

7.11 Conclusion

The comparison in table 2 shows the points to focus on in the development of the heat bond. The aspect that requires attention is the annealing of the system. If this is well researched and possibly even standardized, the joint is less likely to introduce failure, the process is simplified and the cost reduced.

When comparing heat bonding to current conventional connection methods, the heat bond is not the method to have the most positively scored criteria. This rises the question why to research heat bonding at all. Why is it relevant to consider a method that seems worse than others?
The answer lies in the importance of criteria. One can be of more influence than the other. This can be assessed by assigning scores and percentages and finding a final grade expressed in objective, comparable numbers. There is a risk, that in doing so, false objectivity is introduced by subjectively choosing influence and presenting it as objective numbers. Therefore, it is chosen not to use this approach. In this thesis, it is stated that the transparency of the joint is the reason for the pursuit of the heat bond.
It is not that the other criteria, positive or negative, do not matter. These can be seen as additional benefits or challenges to overcome.

As has been stated in this chapter, the heat bond is as transparent as glass. It is even more transparent than connection with clear adhesives, because the glass face in the connection is not there.
It is widely recognized in the field of structural glass, that transparency is the main motivation for applying it. It is also the main motivation for innovation in structural glass. Why use a glass fin if a steel one performs better, if not for the transparency? Why bother researching glass bricks and executing a complex construction process if the main desire is not to construct a transparent, shimmering facade? The core of structural glass is to achieve transparency.

In some architecture, connection elements are used to visibly mark the design. Even still, the trend of connections becoming smaller or shifting from metal to other, transparent materials, shows the desire of architects and engineers to not allow connections to reduce the transparency of the structure. This thesis proposes a currently unconventional way to reach that goal.

The heat bond is not a perfect connection method. In many ways it is not even the best connection method. If engineering was led by the philosophy that this would be a reason to stop development, innovation is impossible. Luckily, this is not the case, creating the possibility to study the ways to make heat bonds for structural applications.

8 Temperature and Stress in Materials

In this section, theoretic background is provided, which describes what happens during the production of heat bonds. Specifically, this theory is applied in the finite element analysis of thermal shock failure during the welding process.

First, the heat transfer mechanisms are described. Then, the scope shifts to what this does to the material. Afterwards, the temperature change in the material is related to elastic stress in the material. The section ends with a criterion to be applied as a failure criterion for thermal shock failure.

8.1 Heat Transfer Theory

There are three mechanisms that transfer heat: conduction, convection and radiation. Conduction is the ability of a material to transfer heat through it. The conductivity is a material property.

Heat transfer at boundaries occurs through the remaining mechanisms of convection and radiation. The amount of power P through convection is described as (Het Nederlandse Normalisatie-instituut 2011):

$$P_c = h_c(T_1 - T_2)$$

Here, $T_1 - T_2$ is the temperature difference between the material, glass, and the surrounding air. The convection coefficient, h_c, is a measure of the amount of energy transferred on a unit surface for a unit temperature difference and is expressed in $\frac{W}{m^2°C}$.

The power a material radiates to its surroundings is described as following:

$$P = \iota\kappa T^4$$

Here, ι is the emissivity of the material, a value between 0 and 1 without a unit, 1 indicating black body radiation. The constant κ is the Stephan Boltzmann constant, which is $5,67 \cdot 10^{-8} \frac{W}{m2K^4}$ (Het Nederlandse Normalisatie-instituut 2011). In most literature, these are indicated with the symbols ϵ and σ respectively. However, because these symbols represent strain and stress in this thesis, other symbols are used.
In this formula it is essential to use Kelvin as a unit of temperature.

Radiation loss is a result of two nonlinear radiated emissions: form material 1 to material 2 and from material 2 to material 1. The netto energy transfer can be described as the following (Het Nederlandse Normalisatie-instituut 2011):

$$P_r = \psi\iota_1\iota_2\kappa(T_1^4 - T_2^4)$$

The ψ is the view factor. This factor, varying from 0 to 1, indicates the portion of the hemispherical environment of surface 1, that surface 2 occupies and vice versa. If all radiative heat transfer of surface 1 is exchanged with surface 2, the factor is equal to 1.
Due to the nonlinear relation, it is essential to use Kelvin as a unit of temperature.

8.2 Temperature Changes

The theory behind the actual change of temperature is not very complex. Before, it was described how energy from a heat source transfers to a material. Here, it will be discussed what this change of energy does to the material.

The heat introduction in the material changes the enthalpy of the material through a property called specific heat capacity (Richet et al. 1997). It is considered unnecessarily elaborate to discuss enthalpy in this thesis. The specific heat capacity, expressed in $\frac{J}{g^\circ C}$ or $\frac{J}{m^3 \circ C}$, is a measure for the amount of energy required to raise the temperature of a unit weight or mass of the material with a unit temperature (Nodehi 2016).

8.3 Thermoelasticity

The theory of thermoelasticity will be discussed. This section is based on the work of Shorr 2015.

If a material is heated, it expands. If this expansion is limited by constrains, this causes stress In the material. The theory is based on the following assumtions:

- The temperature distribution is known and not influenced by the stress in the material.
- The thermal strain (ϵ_T) and elastic strain (ϵ_σ) may be summarized to result in a total strain.

These assumptions result in the following basic equations:

$$\begin{aligned} \epsilon_\sigma &= \frac{\sigma}{E} \\ \epsilon_T &= \alpha_T \Delta T \\ \epsilon_{total} &= \epsilon_T + \epsilon_\sigma = \frac{\sigma}{E} + \alpha_T \Delta T \end{aligned}$$

The thermal strain depends on the temperature difference ΔT and coefficient of linear thermal expansion α_T.

The effect of a change in temperature on stress is most easily explained by an example of a rod. Suppose an elastic rod of length L and cross-section A, heated in ΔT. If the rod is not constrained, its length would increase with $\Delta L = \epsilon_T L = \alpha_T \Delta T L$. However, if both ends of the rod are constrained, a reaction force causes a compression according to $\Delta L = \frac{FL}{EA}$. Equalizing the length differentials results in the following:

$$\begin{aligned} F &= E \alpha_T \Delta T A \\ \sigma &= \frac{F}{A} = -E \alpha_T \Delta T \\ \epsilon_{total} &= \epsilon_T + \frac{\sigma}{E} = 0 \end{aligned}$$

Here, the negative sign indicates compression in the rod.

When considering thermoelasticity in a three dimensional situation, these basic equations essentially hold up, though the Poisson's ratio ν is used to adapt for changes in volume instead of one dimensional

length. For the interchangeable principal directions i, j and k, the strain is $\epsilon_i = (\sigma_i - \nu(\sigma_j + \sigma_k)/E + \epsilon_T$.
For example, the stress in a volume which is heated in ΔT and constrained in all directions, resulting in no change of total volume ($\theta = 0$), is described in the following manner:

$$\begin{aligned}
\theta &= \epsilon_1 + \epsilon_2 + \epsilon_3 = 0 \\
\epsilon_1 &= \epsilon_2 = \epsilon_3 = \epsilon = 0 \\
\sigma_1 &= \sigma_2 = \sigma_3 = \sigma \\
\epsilon &= \frac{\sigma(1-2\nu)}{E} + \epsilon_T = 0 \\
\sigma &= \frac{\epsilon_T E}{1-2\nu} = \frac{\alpha_t \Delta T E}{1-2\nu}
\end{aligned}$$

Similarly, in the case of a segment of a plate heated in ΔT, this returns:

$$\begin{aligned}
\sigma_1 = \sigma_2 = \sigma,\ \sigma_3 &= 0 \\
\epsilon &= \frac{\sigma(1-\nu)}{E} + \epsilon_T = 0 \\
\sigma &= \frac{\alpha_t \Delta T E}{1-\nu}
\end{aligned}$$

The latter situation could represent a glass panel constrained in a frame, but free to expand by an increase in thickness. Using the properties of glass (Section 18), it is calculated that the temperature decrease required to obtain the tensile limit of 45 MPa, is a cooling of $59°C$.

8.4 Thermal Shock

Thermal shock failure is a name for failure as a result of a (sudden) change in temperature. There are theories developed to predict it (Hasselman 1969). This theory is based on an energy balance: the amount of elastic energy stored in the material should exceed the energy required for crack propagation for thermal shock to occur. The stored elastic energy is increased by raised stress as a consequence of a temperature change. The crack propagation energy is computed with the properties of initial flaws on the material: their density on the surface and their size. The theory shows a dominant influence of initial flaws on the strength of the material in case of thermal shock failure.

Because these parameters were not known or found for glass panels which are to be used in the experiments, this theory is not applied in this thesis.

9 Glass at Elevated Temperature Levels

In section 8, theoretic background is provided. However, this is not the complete story, required to grasp what glass does when temperature rises. This is because glass has no discrete melting point (Section 5). This property is the cause of the possibilities of glass blowing and has been used to an advantage throughout this research. To benefit from this property, one needs to know the behaviour of this property. This section is about the behaviour of glass in its transition range, the state between solid and liquid.

The mentioned values are not the same in every literature source and should not be taken as strict definitions. They are considered as guide lines, functioning as a starting point for this research.

9.1 Viscosity

The viscosity of a material states its level of liquidity (Leidse Instrumentmakersschool n.d.). It is a measure of its resistance to shear deformation (Brow n.d.). The viscosity of glass continuously decreases as temperature increases, determining the transition phase. As the glass becomes hotter and less viscous, it will behave more like a liquid.

The relation of temperature and viscosity for soda lime glass is plotted in figure 25. In this graph, several levels of viscosity are plotted. These levels are defined below (Brow n.d.) (Leidse Instrumentmakersschool n.d.). The temperatures for the viscosity points are the properties of soda lime float glass. In this research, the temperature values as published for Pilkington float glass are applied (NSG Group 2013). Therefore, the values below do not match figure 25.

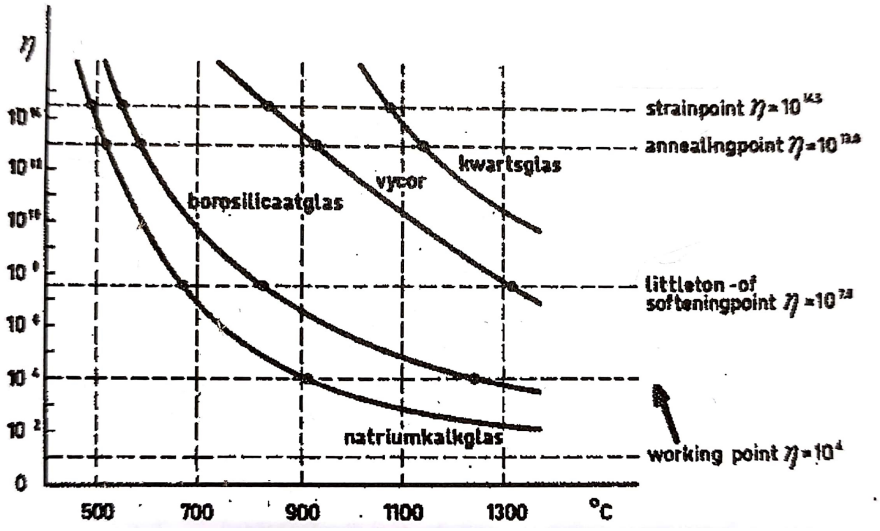

Figure 25: Relation between viscosity and temperature for several types of glass. *Natriumkalkglas* translates to soda lime glass. The unit of viscosity is poise, $1P = 0,1\frac{Ns}{m}$ (Leidse Instrumentmakersschool n.d.)

Strain Point, $\eta = 10^{13,5}\ \frac{Ns}{m}$, $T_{strain} = 511\ °C$.
This point is defined as the viscosity at which stress is substantially relieved in several hours.

Annealing Point, $\eta = 10^{12,8}\ \frac{Ns}{m}$, $T_{anneal} = 548\ °C$.
This is defined as the viscosity at which stress is substantially relieved in several minutes.
Another term often found in literature is the transformation temperature, T_g. This temperature corresponds to a viscosity around the annealing point.

Softening Point, $\eta = 10^{6,8}\ \frac{Ns}{m}$, $T_{soft} = 715\ °C$.
At this viscosity, the self-weight of the glass causes deformation.

Working Point, $\eta = 10^{3}\ \frac{Ns}{m}$.
This level of viscosity allows the glass to be formed and manipulated.

Paradoxically, the ideal viscosity for glass blowers to manipulate the material is between 10^5 and $10^9\ \frac{Ns}{m}$ (Leidse Instrumentmakersschool n.d.). This is a region around the softening point.

In some situations, it is required to know the viscosity of any given temperature or vice versa. In this thesis, the relation of temperature and viscosity is interpolated linearly, with the viscosity on a logarithmic scale between the points mentioned above (Figure 26). This interpolation will provide higher viscosity for any temperature than the relation in figure 25. A higher viscosity causes more stress to remain in the glass, this will be elaborated on further in this section. If an assumption results in more stress, it is conservative. This linear interpolation is considered conservative.

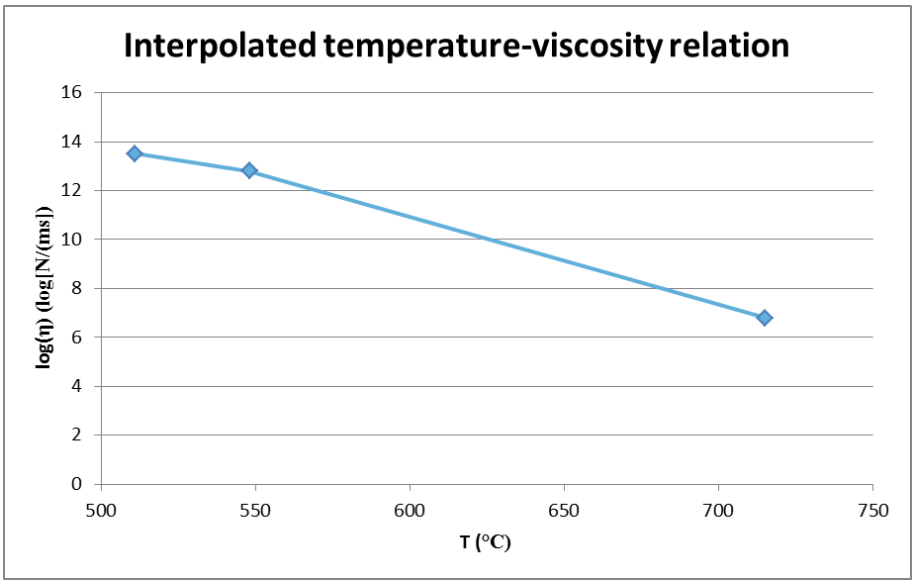

Figure 26: Interpolated relation between viscosity and temperature, as used in this thesis.

9.2 Stress and Relaxation Time

At low temperatures, glass behaves like a solid, elastic material and deformations are instantaneous (Brow n.d.). At high temperatures, glass is a liquid and deformations are time dependent. At intermediate temperatures, glass is a viscoelastic material (Figure 27).

The viscoelastic behaviour is described by the Maxwell element (Figure 28). This is a series of a spring and dashpot, representing the elastic and viscous behaviour respectively. Because viscosity is

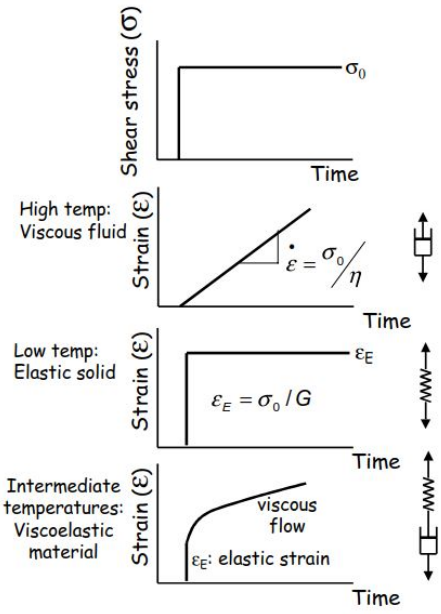

Figure 27: For the same instantaneously applied shear stress (top), the stress is plotted over time for a viscous fluid, elastic solid and a viscoelastic material (bottom) (Brow n.d.)

related to shear deformation, the shear modulus G is the elastic constant.

If this element is strained, the instantaneous strain is provided by elongation of the spring. This results in stress in this spring. As time continues, the dashpot elongates. This reduces the elongation of the spring and corresponding stress. This process is called stress relaxation: with time, the stress in the material is relieved by viscous behaviour.

This process knows the following formulae.

$$\sigma_t = \sigma_0 \, e^{\left(\frac{-t}{\tau}\right)}$$

$$\tau = \frac{\eta}{G}$$

$$G = \frac{E}{2(1+\nu)}$$

Here, τ is the relaxation time. This value determined how fast the stress is relieved form the material. The shear modulus G can be obtained from the Young's modulus E and the Poisson's ratio ν. From this formulae it follows, that a time of $t = 3\tau$ is sufficient to relieve 95 % of the stress in the material

In this research, the values provided in the national code are used, $E = 70.000 \; MPa$ at room temperature and $\nu = 0,23$, returning a shear modulus of $G = 29.000 \; MPa$ (Het Nederlandse Normalisatie-instituut 2014).

With this process, one can relate the viscosity to the stress in the material. In table 3, values are provided for the relaxation time of glass at the viscoisty points. Now, it is possible to relate load speed to stress in the material.

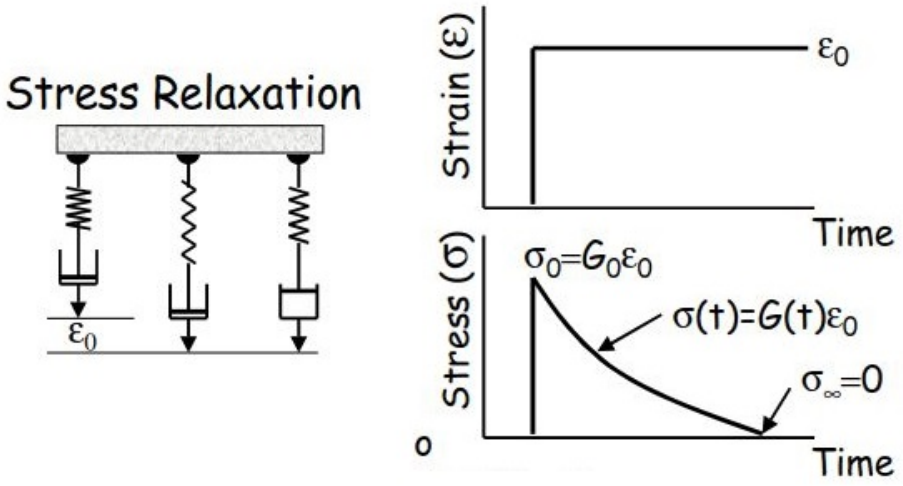

Figure 28: Viscoelastic behaviour explained with the Maxwell element (Brow n.d.)

Point	$T(°C)$	$\eta\ \left(\frac{Ns}{m}\right)$	τ (s)
Strain Point	511	$10^{13,5}$	1090 (18 minutes)
Annealing Point	548	$10^{12,8}$	217 (4 minutes)
Softening Point	715	$10^{6,8}$	$2,18 \cdot 10^{-4}$
Working Point		10^{3}	$3,45 \cdot 10^{-8}$

Table 3: Relaxation time corresponding to viscosity points

If a moderate load speed is considered, in the order of magnitude of 10 MPa per second, it can be concluded that this will cause elastic stress at the annealing point, where 12 minutes are required to relieve 95 % of stress. However, at the softening point, the stress is relieved virtually immediately, leaving no time to build up any stress in the material. Note that stress can build up in glass at the softening point in case of high load speeds, for example in case of impact.

At a temperature below the annealing point, the glass is mechanically a solid. Above the softening point, at moderate load speeds, glass is mechanically a liquid.

10 Residual Stress

The combination of the glass transition from liquid to solid and thermoelasticity, results in temporary and permanent stress when glass is cooled from temperatures beyond annealing point to room temperature.

10.1 Cause and Prevention

Thermal stress in unconstrained glass can be divided in two categories (Borom 1980). The first is temporary stress. This is caused by a temperature gradient in the material.
The gradient is essential: if the temperature is uniform and the glass is unconstrained, thermal expansion prevents stress. If there is a gradient in the material, the thermal strain in the colder area is lower than the thermal strain in the warm area. The strain differential causes stress.
If the temperature gradient is removed, the stress is relieved as well.

This type of thermal stress is illustrated by an example. Consider a plate is constrained in plane and heated over a temperature difference of ΔT. The thermal difference causes a thermal expansion of $\epsilon = \alpha \Delta T$ (Section 8). Due to the constrained at the edges, this causes a stress of $\sigma = \alpha \Delta T E$. This process is reversible: removing the gradient reduces the stress back to zero, because the thermal strain becomes zero again.
Now suppose that this plate is not constrained at the edges, but that center is heated and the edges are not. The thermal difference over the material is ΔT. The thermal strain at the edge of the plate is zero. The edges will not deform or displace. The center however has a thermal strain of $\epsilon = \alpha \Delta T$, and its expansion is hindered by the cooler edge. The difference in strain causes elastic stress of $\sigma = \alpha \Delta T E$.
If the center of the plate is cooled to original temperature, the thermal gradient and difference in strain are reduced to zero, and the stress is zero again.

The second type of thermal stress is permanent, also called residual stress (Borom 1980). With this type, the theory on thermal stress is combined with viscosity and glass transition (Section 9).
Consider a glass at a temperature substantially above the annealing point, which ensures the possibility of viscous flow of particles. When this glass is cooled, a temperature gradient will be enforced, where the core of the glass is hotter than the edge. Due to viscous flow, particles can rearrange, which relieves temporary stress. The rearrangement results in densely packed particles at the cool edge and a lower particle density in the warmer core. As the glass cools, it passes the transition range of temperature, and the particles freeze in position. There is no stress in the glass at this point.
The glass is continuously cooled to room temperature. The temperature gradient is relieved when both core and edge of the glass are at room temperature. However, the frozen particle structure with relatively more particles at the edge of the object, causes compression at the edge. This internal stress is balanced by tensile stress in the core.

The magnitude of the residual stress is related to the magnitude of the temperature difference at the moment the particle structure freezes in position (Borom 1980). This means that the thermal gradient in the transition zone should be as small as possible. For large three dimensional objects, like glass bricks, the thermal gradient within the object is likely to be larger than for smaller and thinner objects. It is complex to predict the thermal gradient. It depends on the shape of the object, the exposure to cooling, the surrounding thermal masses and the properties of the oven in which it is placed (Oikonomopoulou, T. Bristogianni, et al. 2017). Annealing schedules are therefore mainly based

on experience. In practice, the temperature gradient in the object is decreased by controlled cooling of the glass. The glass is kept at a temperature above annealing point, to create a homogeneous temperature. As the glass is cooled further slowly, a minimal gradient is present in the material as the particles freeze in position.
If the glass has cooled to room temperature and residual stress is present, reheating the glass to a level above annealing point, and cooling it slowly has proven to substantially reduce residual stress (Rammig 2016). This means that it is not necessary to limit residual stress development in the first cooling.

The cooling of the glass is also controlled, to prevent fatal temporary stress, thermal shock (Borom 1980). When the glass has passed the temperature at which viscous flow does practically not occur, prevention of thermal shock failure governs the cooling rate. (Oikonomopoulou, T. Bristogianni, et al. 2017).

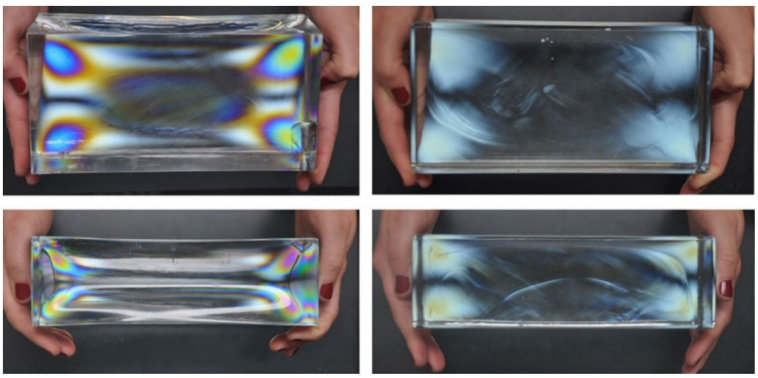

Figure 29: Results of the qualitative Polarization Test for the glass bricks of the Crystal Houses Structure (Oikonomopoulou, T. Bristogianni, et al. 2017)

10.2 Polarization Test

If residual stress is present in a material, this can be measured with polarized light (Oikonomopoulou, T. Bristogianni, et al. 2017). A qualitative analysis can be performed by using a polarized light source and a crossed polarized film as a filter. Stressed glass shows optical anisotropy. The following explanation is based on Aurik 2017 (Figure 30).

Light travels in a wave. Natural light contains light which oscillates in all directions. Polarized light oscillates in one direction. LCD screens emit polarized light and a polarization filter can be used to polarize natural light as well.
Birefringe materials refract light differently, depending on the polarization of the light. If glass is stressed, it develops birefringe. If a polarized light beam travels through stressed glass, it splits in two components with different oscillation orientations and different speeds through the glass, depending on the differences in the directions and levels of the principle stress. After passing through the glass, the waves have a phase difference.
A second polarization filter combines the waves in one oscillation direction. Due to the phase difference, interference occurs. Colors are amplified and extinguished, and these colours are visible.
Coloured patterns will occur when polarized light passes through the component. The colour depends

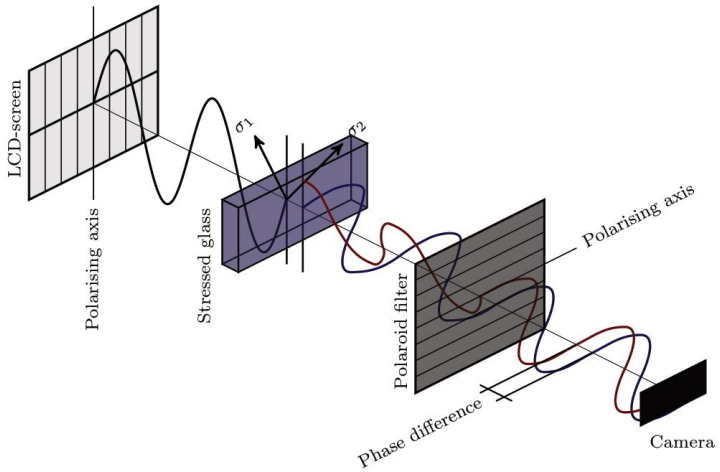

Figure 30: Set up of a polarization test (Aurik 2017).

on the difference in principle stress levels.
Glass without stress will appear black. If it shows patterns with black and grey colours, the present residual stress is low. If the pattern has a coloured spectrum, the stress is higher.

With this method, the stress cannot be quantified. Only the difference in principle stress is measured and not its absolute values. However, this qualitative method distinguishes high and low stress levels and was sufficient for analyzing the bricks for the Crystal Houses structure (Oikonomopoulou, T. Bristogianni, et al. 2017). In figure 29, such an analysis is shown. The brick on the left shows coloured patterns and such a brick was therefore discarded. The brick on the right shows only black and gray areas and was accepted to be used in the facade.

10.3 SCALP

Quantitative measurements of residual stress can be performed. This can be done with a scattered light polariscope, SCALP (Aben et al. 2010). A SCALP emits a laser beam under an angle through the glass. Birefringence influences the polarization of the beam, which is recorded with a camera. Along the beam, the variation and intensity is measured. Software compiles this data to a stress profile.

Part III

Structural Safety

Many glass structures contain measurements to increase the structural safety of the glass elements. Because of the brittle nature of glass, the heat bond will have a brittle nature as well. Therefore, attention should be paid to the structural safety of the heat bonded connections. The all-glass connections can be improved by applying the safety philosophy for glass elements.

In this part, the methods to improve the structural safety of the heat bond are analyzed. This is done by presenting cases and applied measurements for structural safety in glass engineering. Then, the integral safety approach, formulated by dr. ir. F. Bos, is explained to offer a philosophy for safety in structural glass in general. In the following section, these general solutions are applied on a system level. Also, measurements to increase safety are presented on a structural level. The latter is done for several examples in which heat bonded systems can be applied.

11 Case Studies

To research the measures to increase the structural safety of heat bonded joints, one could use the measures applied on structural glass element. The goal is to prevent collapse without warning and/or with the consequence of injury, fatality or unbearable economical loss.

What is being done to increase the safety of glass structures? In this section, realized glass structures are analyzed to gain an overview of common current methods to achieve this goal.

The first example considered is the Glass Conservatory in Leiden, constructed in 2002 (Nijsse 2003). This glass extension, like the extension in London presented in section 1, consists of glass fins and beams to support a roof and a facade. The structural engineer, Rob Nijsse, at the time connected to

Figure 31: Glass Conservatory, Leiden 2002 (Nijsse 2003)

ABT, applies multiple layers of laminated glass to provide redundancy (Bos 2009). He considers failure of one sheet at any time, or two outer sheets if there is risk of vandalism.
This philosophy is present in the conservatory in the multiple aspects. In the conservatory, the insulated roof panel is laminated with a PVB foil (Nijsse 2003). The polyvinyl butyral interlayer have been the dominating interlayer before SentryGlas gained popularity (Stelzer 2010).
The beams and fins in the structure were bonded with resin.

Another case is the roof of the ING bank in Budapest, engineered by Nijsse in 1994 (Nijsse 2003). The glass beams consist of four layers: two thermally toughened which were load bearing and two annealed on the outside (Bos 2009). The outer panels can take impact, for example from acts of vandalism, and protect the inner panels. The thermal treatment is applied to strengthen the glass.

The third example that is to be presented is the addition to a monumental building in Ruurlo. This structure, engineered by Erwin ten Brincke and Diana de Krom, ABT, shows a similar approach (Krom 2014). The structure consists of insulated and laminated roof and facade panels. The roof panels are tempered, the facade panels heat strengthened. The beams and fins consist of three layers of laminated and tempered glass.
All elements are designed for the situation of lateral failure. This is the case when impact on the surface of the glass element had caused the outer sheet to fail. All elements are therefore calculated for the case in which one outer sheet is missing. It has not been taken into account that the thick sheet

Figure 32: ING office, Budapest (Nijsse 2003)

will fail, because it is protected from impact by the outer two.

Figure 33: Glass extension to the Castle of Ruurlo (ABT Ingenieurs in Bouwtechniek n.d.)

For the structure of the Crystal Palace, it might seem no measures have been taken to provide safety. However, the safety philosophy is embedded in the design of a brick wall, by using of multiple elements. If a brick fails, the load will be redistributed to and beared by the remaining bricks in the row. This redundancy allows removal and replacement of the failed brick (Oikonomopoulou, T. Bristogianni, et al. 2016).

The current version of the Apple Cube (Figure 8) consists of 35 glass units, all laminated with SentryGlas (O'Callaghan and Bostick 2012). To increase structural strength, necessary for larger spans, and limit the added weight on the original Apple Cube's foundation, the heat strengthened glass was replaced with fully tempered glass.

An important engineer behind the Apple Store staircases is Tim McFarlane, Dewhurst MacFarlane and GLaSS (Bos 2009). He has engineered glass structures since the 1980's. His philosophy to provide safety is to make many calculations and to consider what can go wrong and adapt the design accordingly. His basic attitude is to assume that every piece of glass may break. If this happens, the structure should not collapse and replacement should not bankrupt the owner. He does not specify safety requirements beforehand, to ensure the measures are fit for the project.

12 Safety Philosophy

In his thesis, Freek Bos presents the Integrated Approach, a general method to assess the structural safety of a glass element (Bos 2009). Structural safety can be improved by improving four aspects of the element. This section explains the Integrated Approach and is therefore based on this thesis.

Other structural materials are described by probabilistic analyses of failure based on the element's strength and the actions on this element. This approach is ill-fitted in glass design, because of several reasons.
One of them is that failure hardly happens due to the loads of expected actions. Glass is very sensitive to the unexpected impacts that cause failure.
Another reason is that the strength of glass and its probabilistic distribution is still a subject for discussion in the scientific community. This reduces the validity of the probabilistic approach.
Third, glass element failure and collapse are often coinciding. This removes a hidden, additional safety margin other materials know.
Furthermore, deformations before collapse may allow a redistribution of loads. The brittle nature of glass results in limited deformation and therefore no redistribution.
And finally, the risk of injury is higher in the case of glass failure, because of the sharp shards in which the glass remains.

The scope of this approach is limited to the design, and not manufacturing or execution. Furthermore, it is limited to glass elements, not to glass structures.

12.1 Damage Sensitivity

The damage sensitivity of a glass element describes how likely an unconsidered cause will result in damage or failure. I can be assessed by listing possible impacts. However, because impacts can be unknown, even by definition, this list is ever exhausting. The damage sensitivity can therefore only be assessed partially.

The list of impacts can contain: soft body impact, hard body impact, thermal impact, vehicle collision, peak stress due to execution error, and more.

An example for damage sensitivity is the amount of damage resulting from different cases of hard body impact, like a thrown rock, on two different glass beam designs. The first contains three sheets of 8 mm thickness, the second two outer of 6 mm and an inner panel of 12 mm. If the impact of the rock results in glass sheet failure, the first will be relatively more damaged by the impact, for only two thirds of its strength remains. The second beam is left with three quarters of its strength after impact. The damage sensitivity of the first is higher.

Assessing this parameter affects design. First of all, a list is made assessing possible impacts, which reduces the amount of unknown impacts. Mind that the amount unknown impacts can never be reduced to zero. Also, it shows that dividing the material in smartly can reduce the consequence of impact.

12.2 Relative Resistance

The relative resistance is the ratio of the resistance of an element and the loads that act on it in ultimate limit state. It is the inverse of the Unity Check. If an element is designed to satisfy the unity check, the relative resistance shows the safety margin beyond that.

The unity check is used as a pass/fail criterion. The relative resistance is a method to compare two designs that pass the unity check to assess which one is more safe.

If the relative resistance is large enough, the probability of damage due to exceeded calculated loads on the structure becomes irrelevantly small.

12.3 Redundancy

This property describes the element's behaviour at different stages of damage.The redundancy is the residual strength over increasing damage levels.

In a laminated glass element, damage occurs in discrete steps, as the damage is suddenly increased when a glass sheet breaks. For each level of damage, the residual strength of the element can be assessed, returning the redundancy of the element at that damage mode.

12.4 Fracture Mode

The fracture mode describes the possibility of injury in case of glass failure. It can be divided in three categories:

- A: several cracks and fragments with sharp edges (annealed glass)
- B: several cracks, but the glass remains in postition (laminated glass)
- C: disintegration resulting in a large number of frangments that are relatively harmless (tempered glass)

Every glass element can be categorized in this system. In some cases, an element can be part of multiple categories. Two obvious cases are the one of an annealed laminated beam and a tempered laminated beam. Both beams would be part of category B. The property that the glass remains in position has more influence on the probability of injury than the quality of the edges of the fragments.

12.5 Thermal Prestressing and Safety

An interesting safety measure is thermally treatment of the glass. This is because it affects many safety parameters, but not all positively. This is because tempered glass fails differently from annealed glass.

Thermally treated glass has a internal stress equilibrium: prestressing compression on the surface, tension on the inside. This results in a higher failure load. However, if a crack propagates through the glass, this equilibrium is lost and many cracks propagate, resulting in many fragments. These are too

small to transfer loads in a laminated element.
Tempered glass has an reduced damage sensitivity. The parameter is reduced, because tempered glass is stronger than annealed glass, requiring a larger impact load.

Also, the fracture mode is more beneficial. Failed tempered glass contains less harming fragments.

However, when the redundancy is considered, tempered glass performs poorly. The load which a failed element can transfer, is zero, as the failed tempered glass sheet cannot transfer loads.

Therefore, single sheets of tempered glass is could be considered as a flawed idea of safety and should not be relied upon.

12.6 Structural Safety Strategies

To increase the structural safety of the element, one can decrease damage sensitivity, increase relative resistance, increase redundancy and improve the fracture mode. How do these changes materialize in design? Using the theory presented above, the following strategies are suggested.

The damage sensitivity can be reduced by protecting vital glass elements from any kind of impact. This can be done by adding glass layers at exposed sides of the structure. This could be combined with measurements to keep people away from the structure, like fences, railings or markings.

The relative resistance can be increased by overdimensioning. It is defined by the ratio of expected load and capacity, so increasing its capacity by overdimensioning will increase this property.

The redundancy can only be valid if there is a second load transfering mechanism. If the first origination of damage or sheet failure coincides with collapse, there is no residual strength to consider. This parameter is influenced by creating a second load transferring mechanism or more, and increasing the residual capacity by overdimensioning.

The final parameter, fracture mode, can be influenced by thermal treatment or lamination. With thermal treatment, the mode can be upgraded from A to C. With lamination, mode B can be achieved. These measures influence the other parameters as well.

These measures are considered strategies: protecting, overdimensioning, creating secondary load transfer mechanisms and reducing the risk of injury. For the heat bonded system in the scope of this thesis, the focus will be on the first three strategies.

13 Safety Measures for the Heat Bonded System

In this section, the theory discussed in section 12 will be put into practice for heat bonded joints in general. Regardless of any application, the T-shape typology will be made redundant and safe. Only the heat bonded system is considered

A basic assumption in these designs, is that in case of glass failure in the heat bonded system, coincides with collapse of that system. The system has no capacity to stop cracks from propagating, and should therefore be dealt with in the same manner as a glass sheet.

13.1 Secondary Load Transfer Mechanism

The system itself can only be made safe if there is any redundancy. The system must be able to transfer load in case of damage. When you consider a failed glass panel unable to transfer loads, other panels or materials need to provide residual strength. As dr. Bos wrote in his PhD thesis, "[...] any glass element with post-failure resistance will have to be a composite."(Bos 2009).
These composites can be formed by laminating and reinforcing glass. An example of a laminated heat bonded system is shown in figure 34, an example of reinforcement in figure 35

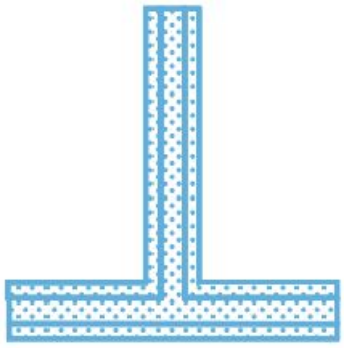

Figure 34: Laminated heat bonded system

In the case of a laminated heat bonded system, the original T-shape is laminated to panels, which are optionally heat bonded as well. In case of failure, there is another intact glass element transferring the load.

When the heat bonded system is reinforced, the post-failure capacity is provided by a metal bar, that remains intact after failure of the glass.
This bar is not used structurally before failure, because the deformation of the glass is not large enough to create significant stress in the metal (Bos 2009). If the glass fails and the deformations of the system become larger, the stiffness of the metal ensures stress in the metal, resisting the load on the system.

An interesting method to reinforce heat bonded glass, is by fusing two plates with a steel reinforcement net between them. This is similar to laminating, but the reinforced glass can resist heat treatment. After the plates are fused, a heat bonded joint can be made. Similar to in-situ cast concrete, reinforcement can protrude the glass body to be able to make a redundant connection.

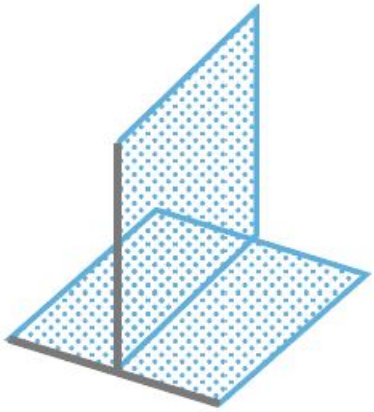

Figure 35: Reinforced heat bonded system

13.2 Protect

The current design code for structural glass dictates that annealed glass can fail due to impact, but that impact is very unlikely to result in failure in the layer behind the glass panel that was impacted (Het Nederlandse Normalisatie-instituut 2014). Only in tempered glass, spontaneous failure can occur due to entrapped nickel sulfides. Since the scope of this research is annealed heat bonded systems, this will not occur. The conclusion is that only spontaneous failure of the outer sheets has to be considered. In the system of figure 34, the T-shape system can be assumed to remain intact, even in case of failure. Laminating the system is a good way to protect the glass from impact, increase damage sensitivity and improve safety.

More innovative protection is also imaginable. One could consider a nano coating, which strengthens the glass because it closes gaps on the surface. Or a coating which is able to keep the glass in position after failure, preventing injury.

13.3 Overdimension

If the glass layers have an increased thickness compared to what is necessary to withstand the ultimate loads, the post failure resistance will be more likely to be sufficient. In the case of laminated systems, using multiple and larger systems is a way to achieve this (Figure 36).

For the T-shape typology, a solution similar to figure 36, by laminating three heat bonded systems, is theoretically possible. One could create three different shapes that can all individually connect the three ends necessary for the T-shape and are present in the same cross-section (Figure 37). This requires a more complex combination of three-dimensional systems. It can be considered that, though it is possible, it might be easier and cheaper to solve this differently, on a structural level (Section 14). The solution provided in figure 38, stacking the systems on top of each other, might be preferable.

Figure 36: Example of overdimensioned heat bonded systems: three elements are used though two would provide the required capacity.

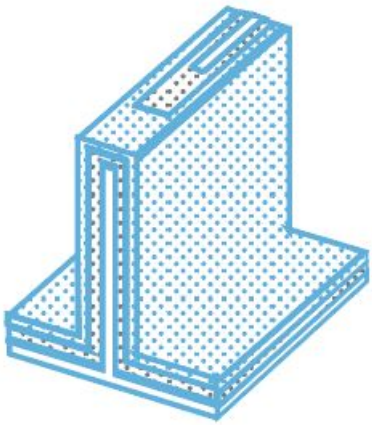

Figure 37: Overdimensioned T-shape. All elements are at the end of the three branches, and all elements are present in all cross-sections of the system

13.4 Thermal Prestressing

Tempering the heat bonded system can become an option. In theory, the system should be cooled more quickly to create internal stress equilibrium and compression at the surface. This procedure is well-known for flat glass and could be extrapolated for non-flat shapes as well.
It should be noted that tempered glass is only considered safe in combination with lamination, and that failure due to entrapped nickel sulfides are a possibility in tempered glass (Bos 2009).

13.5 Future Research

The measurements presented here are applications of known techniques on heat bonded systems. To do this, further research is required, for the following reasons.

If heat bonded systems are to be laminated, the current practice is not suited yet. Autoclaves are currently build to laminate glass sheets. The varying shapes of heat bonded systems require different machinery.
Considering that pressure and heat are required for lamination, it should be possible to make this machinery. Also, the surfaces of the system need to be very flat.

It is also possible to reinforce heat bonds. With clever design this can be a safe solution. However, it should be considered if the transparency, achieved by heat bonding, is undone with reinforcement. The measurement should not harm the transparency, for then the main reason to apply heat bonds is lost.

Thermally prestressing heat bonded systems is theoretically possible. Due to the different geometry, it is yet unknown what cooling rate would be required at what surface to obtain a certain level of increased capacity. Further research would be required to develop this application.

It is concluded that though these measures are all possible, they require additional research. This is not odd, because the heat bond itself requires additional research, before it is allowed to be applied in structures. However, the additional research would postpone the application. It is not likely that the redundancy is to be provided on a system level in the near future.
Luckily, the safety can also be ensured on a structural level.

14 Safety Measures for the Structure with Heat Bonded Systems

Measurements on a structural level can also be considered. The measurements are the same: create secondary load transfer mechanisms, protect and overdimension. To show how they materialize, the subject is pulled slightly out of the scope of this thesis: to consider safety measures on a structural level, applications have to be considered.

This section presents several methods to increase and improve structural safety for some of the applications presented in section 3. These are the connection piece, the sandwichpanel and the glass console.

The measurements are presented as individual options. However, it is strongly advised to use a combination of these measures in design.

14.1 Overdimensioning and second load transfer mechanisms

The basis of this measurement is the same for all examples: use three heat bonded systems when two provide the calculated capacity. This measure combines two strategies. A second load transfer mechanism is introduced by using multiple systems. The structure is overdimensioned by using one more system than required for the calculated capacity. With these measures, a system can fail and collapse, without resulting in structural collapse.

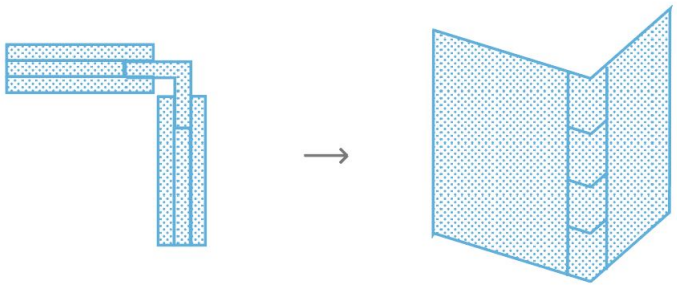

Figure 38: Design Example of the connection piece with overdimensioning and secondary load transfer mechanisms

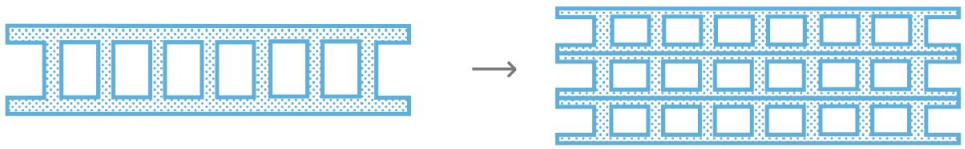

Figure 39: Design Example of the sandwichpanel with overdimensioning and secondary load transfer mechanisms

This safety measurement is only sufficient if both overdimensioning and multiple systems are used. A second load transferring mechanism can be introduced by making two systems of half the size of the original. However, if one of these systems fail, the other would have too little capacity to prevent

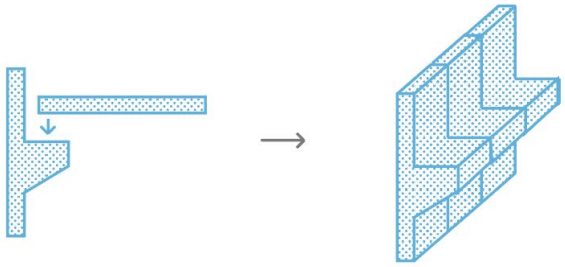

Figure 40: Design Example of the glass console with overdimensioning and secondary load transfer mechanisms

consecutive collapse.
The system can also be overdimensioned by making the system larger. This will not provide sufficient safety, because in glass engineering, one should always consider a scenario of glass failure. Furthermore, the system is assumed to collapse at failure. One system with a larger capacity results in zero residual strength after failure and is therefore not safe.

14.2 Protect

The heat bonded systems can be protected in many ways. The basis of this measurements is to bond glass to the outer surfaces of the system.

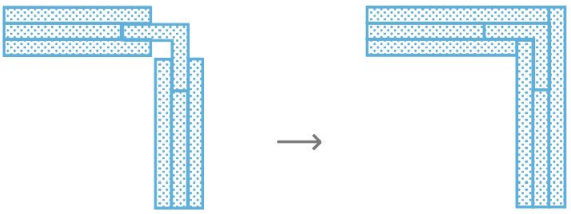

Figure 41: Design Example of the connection piece with protection

Figure 42: Design Example of the sandwichpanel with protection

Figure 43: Design Example of the glass console with protection

The scope of this thesis is annealed heat bonded systems. Apart from overloading, annealed systems fail due to impact (Het Nederlandse Normalisatie-instituut 2014). They do not have to be considered to fail spontaneously due to entrapped nickel sulfide. Therefore, if the system is protected from impact by an outer glass layer, the glass very unlikely to fail.
Practically, this means that protection will ensure the safety if the glass is annealed. If this is not the case, a combination with the previously mentioned measures is necessary.

15 Conclusions on Structural Safety

Structural safety of heat bonded systems is an interesting aspect. The joint has no capacity to stop crack propagation. Failure in the system immediately results in collapse of the system.

In this part, it has been shown that there are many ways to ensure the structural safety of heat bonded glass structures. The measurements are the same as those currently applied for structural glass sheets.

In practice, glass engineers assume a scenario in which the glass has failed. Multiple elements, lamination and sacrificial panels are used to create redundancy.

In theory, safety measures for glass elements focus on four properties: damage sensitivity, relative resistance, redundancy and fracture mode. These can be influenced by three basic strategies: creating secondary load transfer mechanisms, protection and overdimensioning.

These strategies can be used on the scale of the system and the structure. Future solutions for the heat bonded systems are lamination, reinforcing and tempering.

On a structural level, safety can be ensured by a combination of creating a secondary load transfer mechanism and overdimensioning. In some cases, protection is sufficient. It is advised to use a combination of all three in structural glass design with heat bonded systems. With the use of three applications, sketch designs have been made for several applications of the heat bond.

15.1 Recommendations

Further research is required into these measures. Especially the solutions within the system are currently not available. It should be researched if and how the systems can be laminated, tempered or reinforced.

In the near future, it is recommended to apply safety measures within the structure, for these are readily available.

It is recommended to fit the safety measurements to the situation of the application.

Part IV

Glass Weld

This part is about the production process of the glass welds.

First, the welding production method is presented. Then, it is the aim to predict whether thermal shock failure will occur during production, by making and analyzing finite element models. The model is explained by describing the geometry and the type of performed analyses. The criteria for the results are presented and it is described how the results are interpreted. An important aspect of the model is that solid elements are used to model liquid material.

For the model, theory has to be translated in factual numbers, values, constants, variables and other parameters. An important aspect in this section is the definition of the transition range.
All used parameters and the considerations behind them are presented. This section is concluded with a list of the assumptions and simplifications made for the finite element model and analysis.

The next section is a summary of the results, which are all gathered in Appendix A. A section is about the conclusions, discussion and recommendations of the finite element analysis. It ends with recommendations for the weld production process.

Then, the practice is introduced, describing the production as it materialized in the experiments performed for this thesis. The products of the weld experiments are presented and described.

With the knowledge gained in the experiment, the finite element model is reviewed critically. The model is adapted for the situation as it has occurred, and a small validation of the model is described.

The final section of this part contains the conclusions, discussion and recommendations of the glass weld experiments.

16 Method of the Glass Weld Experiments

This section explains how the glass weld is to be produced. In previous research, several approaches were found. The knowledge is used to design a process specific for the purpose of welding T-shaped ten millimeter soda lime glass.

16.1 Previously Applied Methods

Lisa Rammig's production method has been explained in conversation with the author. Her team produced welds in borosilicate float glass, by having the glass mounted on a jig. All glass was heated with a so-called 'cold' flame. When the temperature was right, a moment decided through the experience of the glass blower handling the torch, the flame was changed to a 'hot' flame, emitting more heat, and the glass was locally heated to create the welded joint. The jig allowed the possibility to position the glass and introduce the heat exactly where needed. Also, the jig allowed for a very precise movement of the glass segments towards each other. This made it possible to create welds which were invisible afterwards.

After the weld was produced, the flame was made 'cold' again and all glass was gradually cooled to room temperature. Based on her experience, Rammig stated that this stage was most sensitive to thermal shock failure. Afterwards, the welded glass was placed in an oven for an annealing cycle.

In the thesis of Cecile Giezen, a similar welding process is described (Giezen 2008). The borosilicate glass tubes are mounted on a jig. After heating, when the glass is viscous enough, the joint is made. With graphite tools and a blow hose, the weld is formed and shaped. Cooling is controlled and the specimens are annealed afterwards. No mention is made of preheating all glass before welding.

A third source describes a welding process for soda lime glass (Belis et al. 2006). After experimenting with several set-ups, key parameters were detected. These were the temperature of the welding torch, the glass temperature during the process and the temperature gradient along the specimen. To reduce the risk of thermal shock failure and to control the temperature of the glass specimen, welding inside an oven was introduced. The glass was preheated, the oven door was opened and the weld was made with a welding torch.
When the oven door was open, the air in the room cooled the glass, increasing the temperature difference and risk of thermal shock failure. To reduce the exposure to the cooler environment, a symmetrical torch was introduced. This allowed the weld to be made on both sides simultaneously, shortening production time.
Another conclusion was not to use a too high temperature for the oven, to prevent the glass object from becoming too soft. In the case of T-shaped joints, the glass lost its shape due to self-weight and loss of viscosity in cases with a too high oven temperature.

16.2 Proposed Production Method

The welds for this thesis have been produced by Frans Folst and Tom Jansen. They are professional glass blowers, working as teachers at the glass blowers education of the Leidse Instrumentmakersschool, LiS. The welds are produced at the LiS.

In collaboration with Folst and Jansen, a proposal is made for the weld production method for the T-shaped system of 10 mm thick soda lime glass. This process is illustrated in figure 44 and follows the following steps:

- Step 0: A line burner is produced. This is a rod in which holes are drilled, connected to a gas supply. When ignited, a flame in the shape of a line will occur. The glass is prepared. It has to be cut, ground and polished. The edge of the web that is to be welded will be faceted.
- Step 1: The glass is positioned in the oven. in the desired T-shape. The web has to be held up by a support.
- Step 2: The oven is closed by lowering the box. The specimen is slowly heated up to a temperature of $500°C$.
- Step 3: The oven is opened by lifting the box. The line burner is positioned at both sides of the welding zone.
- Step 4: This is the cross section of the welding zone. Note the faceted edge of the web. This is to prevent air inclusions in the joint, as the joint will be made in the center first, pushing the air outward instead of trapping it.
- Step 5: The line burner heats the welding zone equally over the length of the weld.
- Step 6: The glass in the welding zone becomes less viscous.
- Step 7: When the viscosity of the glass is low enough, the web is lowered on the flange.
- Step 8: The web is slightly lifted to shape the glass in the welding zone. This will cause the excess glass in the zone to form a smooth fillet weld.
- Step 9: The burner is removed.
- Step 10: The oven is closed. The welded product will reach a homogeneous temperature and be annealed. This process will take several hours.
- Step 11: When the specimen is gradually cooled to room temperature in the oven, the oven can be opened and the welded system can be taken out.

Though the weld is produced manually, the proposed production method offers a possibility to control temperature. Most temperature control is provided during preheating and cooling after the production of the weld. By cooling the glass in the oven immediately after production, the risk thermal shock failure due to manual cooling with a flame is reduced.

The preheating temperature is set to $500°C$, because this is below the strain point of glass (Section 9). Below this temperature, the glass will not deform. This reduces the risk of deformations in the glass outside the welding zone.

Most risk of thermal shock failure is when the glass is exposed to the cooler surroundings when the oven is open.

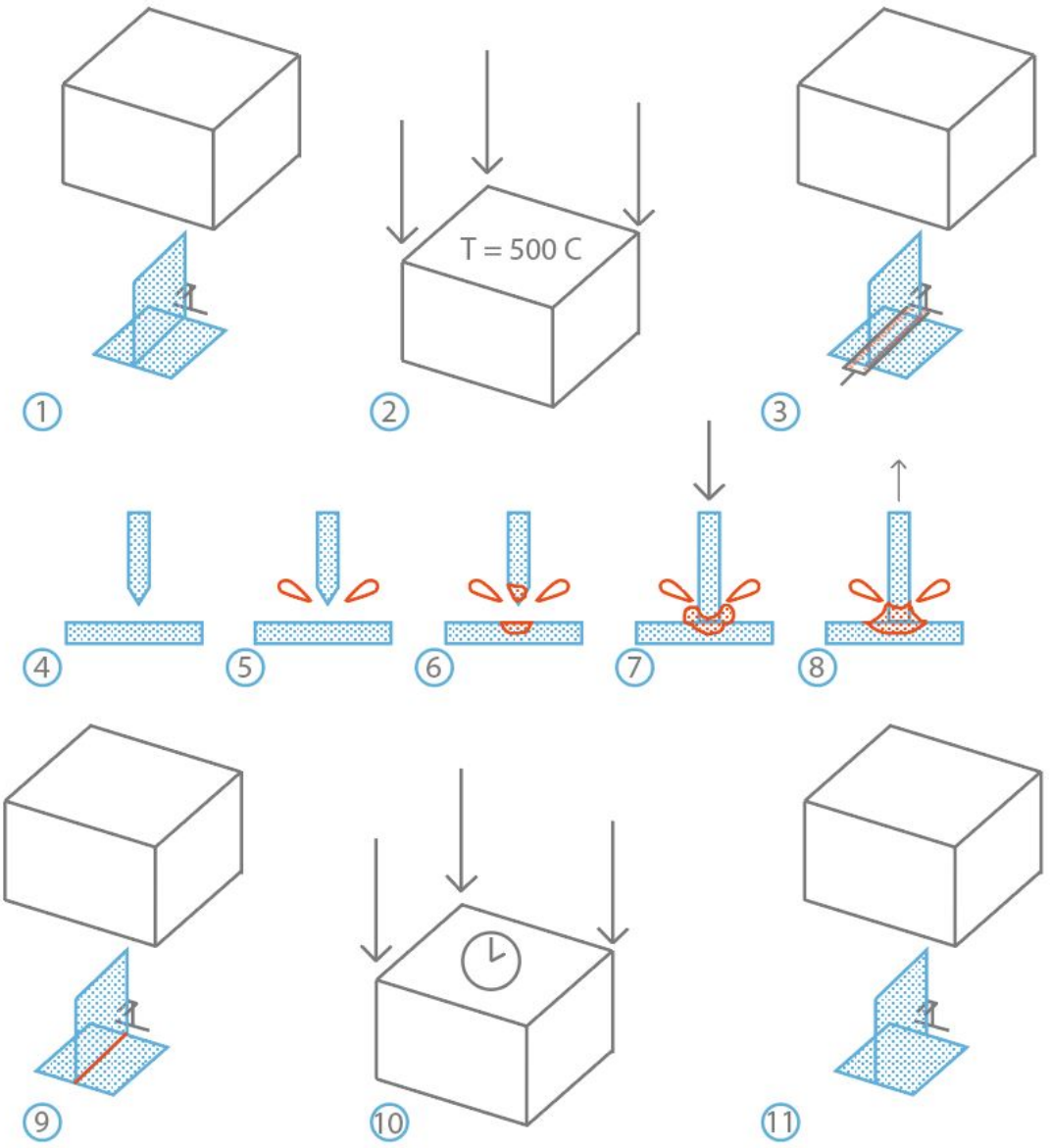

Figure 44: Welding process for the T-shaped system. Explanation provided in section 16

17 Finite Element Model

The risk of thermal shock failure during production is high if there are unsuitable temperature gradients in the glass (Belis et al. 2006). The highest temperature difference in the glass specimen is between step 3 and 10, when the oven is open. To aid the production process, this time window is researched with thermal finite element models. The used software is Diana FEA, educational version 10.1.

The aim of the model is to determine if the specimen fails due to thermal shock failure in the time window in which the oven is opened. Additionally, the aim is to find the ideal circumstances for the production process. This is done by modelling the glass thermally and mechanically.

The glass is virtually exposed to heat gain on the surface close to the line burner and heat loss at the other outer surfaces of the glass. This will cause a change in temperature over time and a temperature gradient in the glass.

When the temperature distribution is known, the stress in the material is computed in the model. This stress is analyzed and it is determined whether the specimen will fail or not. The movements in step 7 and 8 are not modelled. The manipulated glass will not be viscous enough to build up stress due to these movements (Section 9).

It is analyzed what the required time is to heat the welding zone to an appropriate temperature and whether the specimen is prone to thermal shock failure. Conclusions will be drawn on whether the weld can be produced and if so, whether there is enough time to make the weld (steps 7 and 8).

17.1 Geometry

The model consists of two solids, representing the glass bodies. Two axes of symmetry are used, one along the x-axis and one along the y-axis (Figure 45). The solids are not attached, $0,5\ mm$ space is left between then, to prevent heat transfer through conduction and to prevent stress due to hindered displacement.
The bottom edge of the web is faceted. The angle is $45°$. This edge and the area of the flange near it are called the *welding zone*.

The solids are equipped with the material 'Glass', which has thermal and structural properties (Section 18).
The supports are shown in figure 46. The symmetry axes contain supports normal to the symmetry plane. The vertical support is the bottom of the glass solid flange. The glass web is suspended in position, which is modeled with small line supports in z-direction at the top of the web. This support is not a correct representation of reality, but is inserted to make the model kinematically determined. The distance from the welding zone to these supports is large enough to make them irrelevant for the structural analysis, especially because loads due to self-weight are not calculated.

On the surface of the solids, two different boundary surfaces are applied. The first is the flame boundary surface, which models heat gain due to the flame. The second is the surroundings boundary surface, which represents heat loss to the surroundings. A surface can have only one boundary assigned to it.

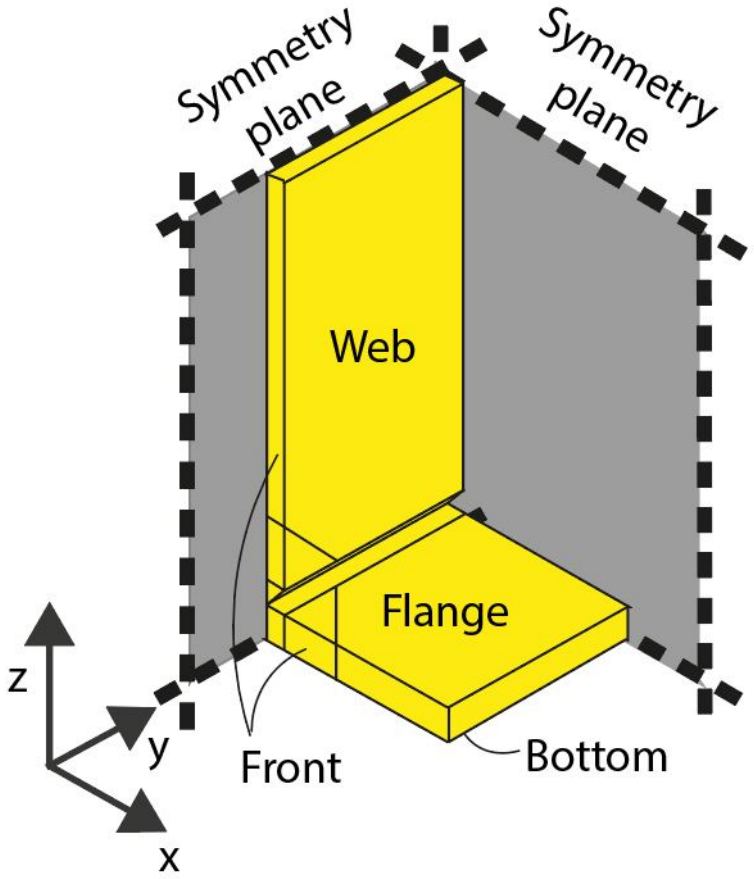

Figure 45: Geometry of the finite element model. Symmetry planes and names for locations are indicated

The flame boundary surfaces are attached to the surfaces at the welding zone: along the side of the web, the top of the flange and at the front of both (Figure 47).
The bottom surface has no heat transfer boundary assigned. In the experiment, this surface is positioned on the floor of the oven. This floor is not heated, but consists of soft, granular insulating material. It is assumed no heat is transferred at this surface.
All other surfaces are heat transfer boundaries to the surroundings.
The heat transfer mechanisms are described in section 8, the heat transfer properties are discussed in section 18.

The boundary surfaces are equipped with boundary conditions. The boundary surfaces of the flame contain one condition on conduction, with an external temperature equal to the flame temperature. Radiation of the flame is insignificant (Section 18).
The surrounding boundary surface has a condition for convection and radiation. The external and radiative temperatures are the temperature of the surroundings (Section 18).
All boundary conditions start at $t = 0$ and are constant for a time of $600\ s$. All analyses have a shorter duration, so the boundary conditions are present at all times.

The solids are equipped with an initial temperature. This temperature is homogeneous.

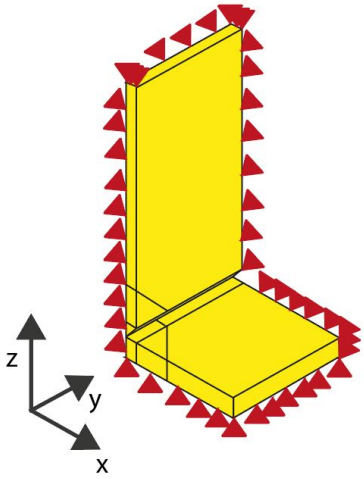

Figure 46: Structural supports of the finite element model.

The mesh size of the analysis is found by experiment. This is described in appendix A. The aim was to use a mesh which is accurate but does not require too much time in the analysis.

17.2 Analysis

The analysis is performed in two steps. The first is a transient heat analysis. Here, the software uses initial conditions and time dependent boundary conditions to calculate the heat flow in the model. The output is the temperature distributions over time.
It is important to perform a non-linear analysis, because radiation is a non-linear process. In general, convergence was reached within one iteration.

The second part of the analysis is the mechanical analysis, which is non-linear as well, due to the material properties of glass. (Section 18). In this step, the temperature distribution computed in the previous one, is used as an input value. The thermal strains are calculated and the stiffness matrix is used to compute a stress distribution in the glass. Again, in general, convergence was reached in one iteration.
The structural analysis is performed in time steps as well, but time is of no influence. The time steps are to link the thermal output to the structural input. Time steps of any size are possible, provided it is a multiplication of the time step of the thermal analysis.
The structural analysis should not be computed for any time step later than the thermal analysis, for the thermal distribution would be incorrect for these moments.

17.3 Result Definitions, Criteria and Interpretation

There are a few definitions for the interpretation of the results, which require further explanation. The first is the weld time, t_{weld}, which is the time required to locally heat the glass to a temperature at which the glass can be manipulated to form the weld. This is defined as the earliest time at which the core of the welding zone has a temperature of 650 $°C$ or higher. At this temperature, the viscosity of the glass, based on the linearly interpolated relation between temperature and viscosity (Figure 26)

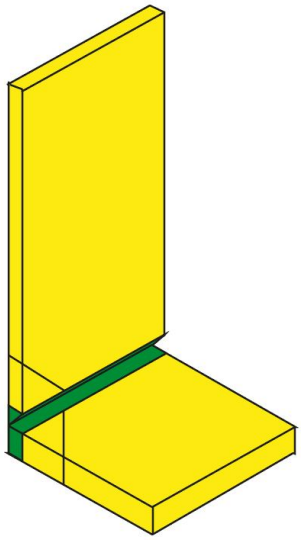

Figure 47: Finite element model with the flame boundary surfaces indicated in green.

is $10^5 \frac{Ns}{m}$, the viscosity at which the glass can be manipulated with glass blowing techniques (Leidse Instrumentmakersschool n.d.). At the weld temperature, the manufacturing of the weld can start: the web can be lowered on the flange.
The point at which the temperature is measured, the core of the welding zone, is indicated in figure 48.

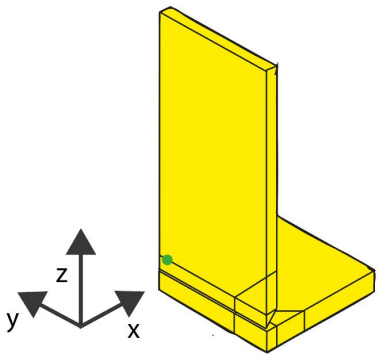

Figure 48: Location of the measuring point of the temperature in the core of the welding zone.

After weld time, the weld should be produced. It is estimated that 30 s is enough to manipulate the glass and form the weld, before the oven is to be closed again. If the stress is not critical up to thirty seconds after weld time, it is predicted that the weld can be produced without thermal shock failure.

The second phenomenon that needs to be explained for result interpretation, is the thermal shock criterion. When will the results show that the specimen is predicted to fail of thermal shock failure? In section 8, the theory of Hasselman is suggested. Here, the flaw properties of the glass result a criterion for thermal shock failure. However, these parameters are unknown for the glass that is to be welded in the experiment.

In this thesis, the tensile capacity of glass is used as a failure criterion. The tensile stress of glass is a common point of discussion, because the inability of glass to redistribute forces results in peak stresses and unpredictable failure loads (Section 5).

In glass engineering, the tensile strength of a glass beam loaded in bending has a characteristic capacity of $45MPa$ (Het Nederlandse Normalisatie-instituut 2014).
The value of $45\ MPa$ is a characteristic failure load, not a design capacity. The value is considered acceptable in this thesis, because the number of specimens produced is small. It is decided to be over-conservative to handle a 1 in 10.000 chance of failure. If this model and method are to be applied on a large scale production process, this capacity value should be re-evaluated with material factors.

The thermal shock criterion becomes the following: if the principle stress in the material is higher than this critical level, the glass is predicted to fail from thermal shock.

Because both the thermal shock theory found in literature and the tensile stress capacity of glass depend on the amount and size of flaws on the glass, it is stated that the tensile capacity of glass is a proper criterion for thermal shock failure.

17.4 Limitations of the Solid Model

The finite element model uses solid elements. The nodes connect the same elements in every result. The nodes can displace. This causes a displacement and/or a strain in the adjacent elements.

In section 8, it is shown how temperature difference can cause stress in a solid material. A relation is presented through two properties, the coefficient of linear thermal expansion and the Young's modulus. This theory will be applied by the software on all elements at all temperatures.

In a liquid material, the theory is not applicable. Thermal differences only cause stress if the material is constrained. In a liquid, the possibility for particles to flow means it is not constrained. Thermal stress will not develop.

This model covers glass at temperatures when it can be considered a solid, a liquid, and in the transition phase in between. It has been decided not to model flow of elements. To facilitate this, the elements must be very small, for example the scale of atoms. (Veer, Bristogianni, and Justino de Lima 2018) This requires computational capacity beyond the reasonably available resources. Therefore, the limitations of a solid model are accepted for this thesis.

This does not alter the fact that no thermal stress should be present in a liquid material. Therefore, the software has to be manipulated, to return liquid results for a solid model. The behaviour of liquid glass is mimicked by adapting the properties influencing the thermal stress. These are the coefficient of linear thermal expansion and the Young's Modulus. Considering the mathematical relation, these parameters need to be reduced to insignificant values to reduce stress for any given temperature gradient.

In section 18 it is explained how this is put into practice. The theory of viscoelastic behaviour and stress relaxation presented in section 9 will be applied to define temperature ranges for material phases and parameters are adapted for these phases, by making them temperature dependent.

18 Parameters for the Model

To model any situation, properties need to be translated to numerical parameters. In sections 8, the theory behind these properties has been provided, explaining their influence. In this section, values for the parameters will be presented. Some assumptions and simplifications have to be made, these are collected in a list at the end of this section.

18.1 Solid, Transition and Liquid Temperature Ranges

In section 17.4, it is explained that limitations to the model require the adaptation of properties to mimic liquid behaviour. This is done by making them temperature dependent.
In a certain range of temperatures, the glass is considered solid, and the behaviour of the glass is accordingly. Above another temperature level, the material is considered liquid and without thermal stress. This is done by making the Young's modulus and coefficient of linear thermal expansion insignificantly low for temperatures at which the material is considered liquid.
In section 5 and 9, it is explained that glass has no melting point. It has a transition range in which the material is mechanically solid nor liquid. Its behaviour is viscoelastic. Stress relaxation over time occurs.

Now, three temperature ranges will be defined: the solid range, the transition range and the liquid range. These definitions will be based on the ability of glass to relax stress at certain temperatures. In section 9, relations are presented between the glass temperature and viscosity and between viscosity and relaxation time. With the relaxation time, one can find the decrease of initial stress over time. Combining all relations returns for a certain temperature what the relative stress level is after a certain time frame.

In this thesis, the solid, transition and liquid temperature ranges are marked by the following definitions:
The upper limit of the solid state is defined as the temperature at which 5 % of the stress is relaxed in a time frame of one second. This temperature is $585°C$.
Similarly, the lower bound of the liquid range is defined as the temperature at which 95 % of stress is relaxed in a time frame of one second, corresponding to a temperature of $630°C$.
The temperatures between these limits are in the transition range. Here, 5 to 95% of stress is relaxed in a time frame of one second.

These definitions contain two values, the percentage and the time frame, which seem arbitrary, but are elaborately defended in the analysis of the model's sensitivity to the transition range (Appendix A.12).

The time frame is the time in which the liquid material is able to relax almost all stress. The magnitude of the time frame should be related to the load speed to obtain a value that is fit for the modelled situation. This relation should make sure that stress is not underestimated.
The magnitude of the time frame will not be based on the total stress in the material, because both the loading and the relaxation happen at the same time and because the relaxation continuously depends on the total stress. To be able to get a magnitude of the time frame, the load increase and relaxation are considered as two separate mechanisms and treated conservatively to make up for the simplification.
A very conservative approach is chosen: the time frame for the liquid material to relax should be

smaller than the time frame for a load to develop from zero to critical level. In such a case, the stress relaxation has the same speed as critical stress development, so the summation of the two cannot result in critical stress levels.
The critical level is $45\ MPa$. The corresponding temperature increase in a constrained plate is $60\ °C$ (Section 8). Thus, the limit to the load speed is that it must be lower than $60\ °C$ in the relaxation time frame. For a time frame of one second, the maximum temperature increase rate is $60\ \frac{°C}{s}$.
The $60\ °C$ limit is based on a plate, constrained in plane. During the welding process, the plates will not be fully constrained, making the limit conservative.

In conclusion, the solid range of the glass in this analysis is any temperature below $585\ °C$. The transition range is between $585\ °C$ and $630\ °C$. The liquid range contains all temperatures above $630\ °C$.

18.2 Heat Transfer from Flame

For the flame, a gas flame comparable to a bunsen flame, convection is dominant. Large, turbulant fires radiate signifcantly, but a bunsen flame is nonluminous (Wang et al. 2009). This is supported by the Eurocode, where a formula to calculate the emissivity (ι in secton 8) of a flame is provided. For a one centimeter wide flame, this emissivity would be $0,003$. This value reduces the radiated power to an insignifcant contribution. Therefore, the radiation of the flame is neglected.

The heat transfer through convection requires a convection coefficient and the temperature of the air at the glass surface near or in the flame. Literature describing heat transfer of a bunsen gas burner provides a convection coefficient of $50\frac{W}{m^2K}$ and a flame temperature of $1730°C$ (Wang et al. 2009). These values can be adopted in case of a laminar flame.

18.3 Heat Transfer to Surroundings

The Eurocode provides data to be adopted for heat transfer under regular conditions indoors. This transfer knows both radiation and convection.

Radiation is calculated with absolute temperatures (Section 8). The software requires input that represents the interaction between two radiating bodies, the radiation from body 1 to body 2 substracted with the radiation from 2 to 1. If both emissivities are equal, a multiplication of the emissivity facors suffices to calculate this interaction (Het Nederlandse Normalisatie-instituut 2011).
The emissivity of both room and glass are $0,8$ (Het Nederlandse Normalisatie-instituut 2011). This results in a netto emissivity $\iota_1\iota_2$ of $0,64$. The temperature or the surroundings is room temperature, $20°C$. It is assumed that when the oven is opened, the surrounding temperature will immediately become room temperature.

It should be noted that there is literature explaining that the emissivity of optically transparent materials is more complex (Gardon 1956). It depends on the temperature and the thickness of the material. However, it is considered unnecessarily complex to take this effect into account. The emissivity of 10 mm thick soda lime glass varies from 0,9 to 0,7 at the temperatures of interest (Gardon 1956). The average of 0,8 is considered an appropriate approximation.

In the Eurocode on fire loads on structures, the convection coefficient of an unexposed side of a sep-

arating element is $4\frac{W}{m^2°C}$ (Het Nederlandse Normalisatie-instituut 2011). Essentially, this represents heat loss of a surface in a standard indoor space and is therefore applicable in this model. The temperature is $20°C$.

18.4 Specific Heat Capacity

The specific heat capacity of the material is the amount of energy per unit time required to heat or cool the material with a unit temperature (Nodehi 2016). The value depends on glass temerature and varies between $0,84$ to $1,5\frac{J}{g°C}$ (Richet et al. 1997) (The Engineering ToolBox n.d.).

In his publication, Richet demonstrates a sudden jump in the specific heat around a temperature of $600°C$, even though a range of $100°C$ is described between the solid and liquid state. In this thesis, a discrete change from solid to liquid is not accepted. It is preferred to apply the solid and liquid definitions of this model. Therefore, the increase of the specific heat is spread linearly over the transition range. The resulting relation of specific heat capacity and temperature is provided in figure 49.

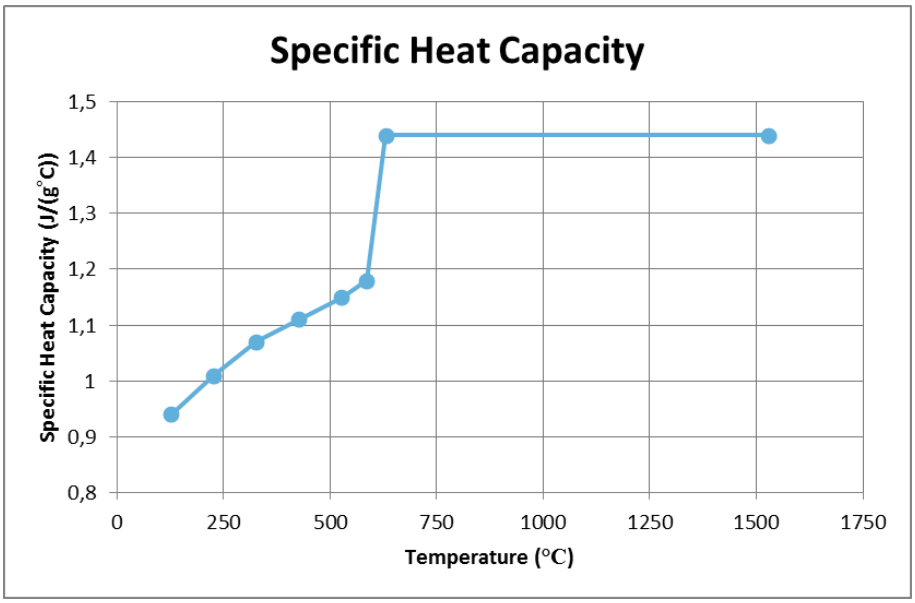

Figure 49: Temperature dependency of the specific heat capacity as applied in numerical models, after Richet et al. 1997, but adapted for the defined temperature limits to the solid and liquid state

18.5 Thermal Conductivity

The thermal conductivity is the amount of energy transmitted through a material of a unit surface over a unit length for a unit temperature gradient (Nodehi 2016). It is expressed in $\frac{Wm}{m^2K} = \frac{W}{m°C}$.

If its thermal dependence is taken into account, the value of the thermal conductivity varies with a maximum of 13 % (Nodehi 2016). The influence of this variation on finite element results of a glass beam under fire load is small.

To reduce model complexity, it has been chosen to model this property thermally constant, with a value of 1,2 $\frac{W}{mK}$ (Heller, Vervest, and Wilbrink n.d.).

18.6 Young's Modulus

In earlier research on glass at elevated temperatures and finite element analysis, it has been concluded that the influence of the Young's modulus on the deformation could only be validated for temperatures up to $600°C$(Nodehi 2016).

This is because of the viscoelastic behaviour of glass at these temperatures (Section 9). In this research, the effect of stress relaxation is translated in a reduction of Young's modulus (Section 17.4). The outcome is defined as follows: full stress will be developed in the solid state and virtually none in the liquid state.

In the solid state, the Young's modulus is constant and has been determined to be 70 GPa (Het Nederlandse Normalisatie-instituut 2014). In the liquid state, the Young's modulus is assumeed to be 1 % of the solid modulus, and is equal to 700 MPa. This estimation is acceptable, if the stress computed in this state is virtually zero. Interpolation between these values in the transition range is assumed to be linear (Figure 50).

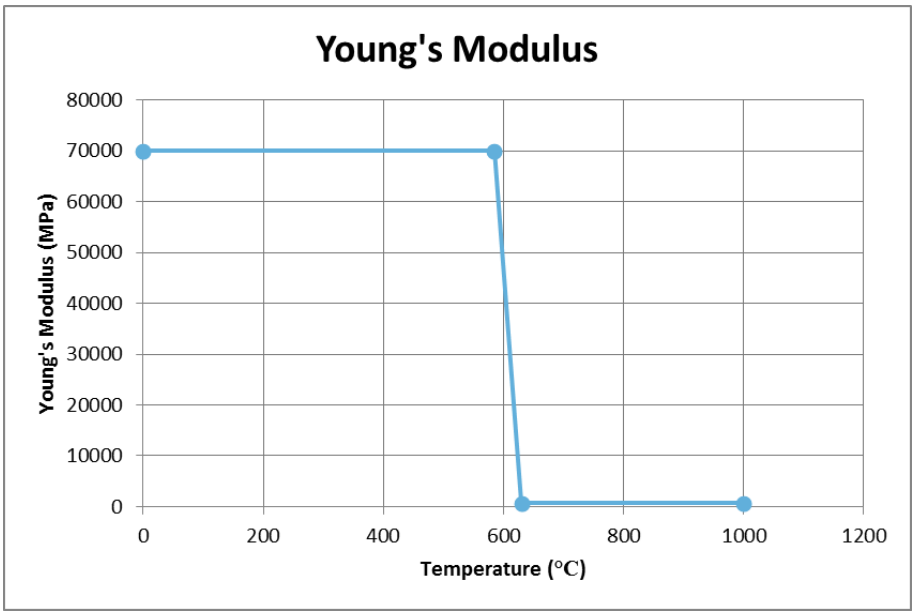

Figure 50: Temperature dependency of the Young's modulus as applied in numerical models

The relation in figure 50 is founded on literature, but contains simplifications and assumptions. However, it is stated that the relation is conservative. First, the value of the Young's modulus is overestimated in the liquid state, for a viscous liquid does not contain stress. Second, literature states that, as temperature rises, the Young's modulus of soda lime glass decreases to a value around 50 GPa before the annealing point (Heller, Vervest, and Wilbrink n.d.). This effect is purposely neglected. Third, the relation of temperature and viscosity, the linear interpolation presented in figure 26, used to define the transition range of temperature, is conservative. All three result in an overestimation of the

Young's modulus at a certain temperature and therefore in an overestimation of the stress, resulting in conservative results when calculating stress.

18.7 Coefficient of Linear Thermal Expansion

The coefficient for linear thermal expansion is a measure of the relative difference in length of a material for a unit temperature difference. It is a strain per unit temperature and therefore expressed in $^{\circ}C^{-1}$ (Rammig 2016). It is a key parameter in thermoelasticity theory (Section 8). Its value for soda lime glass is about $8,4 \cdot 10^{-6} ^{\circ}C^{-1}$ (Rammig 2016) (Leidse Instrumentmakersschool n.d.) (Heller, Vervest, and Wilbrink n.d.).

The coefficient of linear thermal expansion influences the thermal stress in the specimen (Section 8). In the finite element model, the stress should be reduced to zero when the glass becomes liquid. This has been modelled by reducing the Young's modulus, which is linearly related to the stress. In this regard, it seems to be unnecessary to adapt the coefficient of thermal expansion for the same transition. However, the coefficient of thermal expansion determines the unconstrained deformation of the glass. It will be explained with a mental experiment why this parameter should not be modelled as a constant value over temperature.

Suppose two adjacent, unconstrained elements, one solid and one liquid. The temperature of the liquid element is increased. If the coefficient of linear thermal expansion is constant, the strain of the liquid element increases accordingly. Because the elements are connected, the solid element will strain along, causing tensile stress in the solid element.

In reality, the increase of volume of the liquid volume will be accounted for by flow of molecules. The repositioning of particles will not cause stress in the adjacent solid volume.

If it is desired that the model does not compute stress in the supposed case, the strain of an element should be zero at any temperature beyond the transition range. This is represented by reducing the strain of an unconstrained volume to zero in the glass transition range, defined between $585^{\circ}C$ and $630^{\circ}C$. Above this temperature, in the liquid range, the thermal strain is zero, causing no stress in adjacent solid elements (Figure 51).

The linear coefficient of thermal expansion is the derivative over temperature of the thermal strain ($\epsilon_T = \alpha_T \Delta T$). This relation is demonstrated in figure 51.

The preheating temperature influences this relation. At the beginning of the analysis, the strain in the glass is assumed zero, so the strain at preheating temperature should be zero (Figure 51). If the preheating temperature is changed, the slope of the strain in the transition range is to be changed accordingly.

The differential relation between the coefficient of linear thermal expansion and thermal strain has been validated in the software by analyzing a basic model of a single element for this relation.

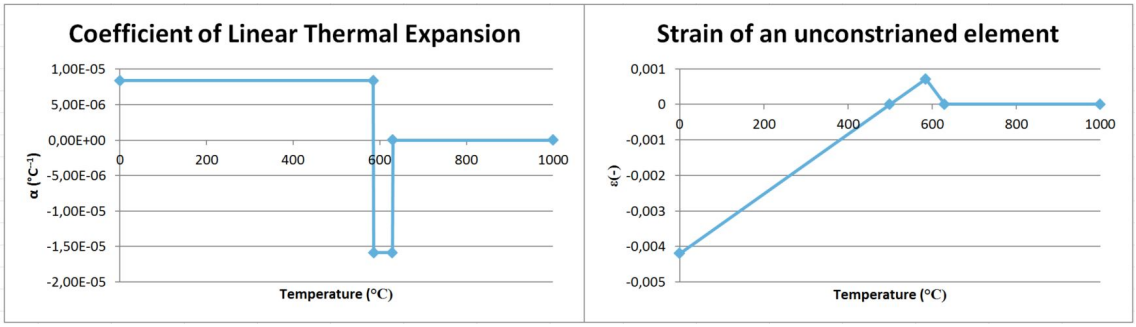

Figure 51: Left: the relation between coefficient of linear expansion related to temperature. Right: the effect of the coefficient on the strain of a volume. This is the integral of the graph on the left.

18.8 Other parameters

As described in section 16, the initial temperature is set to 500 $°C$, to represent the preheating temperature of the glass.
The Poisson's ratio of glass is 0,23 (Het Nederlandse Normalisatie-instituut 2014). The mass density is 2500 $\frac{kg}{m^3}$. The density has no influence on the analysis, because self-weight is neglected.

18.9 Assumptions and Simplifications

In this section and section 8 and 9, theories and properties have been presented to be applied in a thermal and mechanical numerical model. This cannot be done without simplifications and assumptions. Whenever this has been done, it has been explained why this decision would result in the best approximation or a conservative result. To provide an overview, a list is presented containing all significant the simplifications and assumptions.

- The relation of viscosity and temperature of glass has been interpolated linearly, with the viscosity on a logarithmic scale (Figure 26). This interpolation was conservative and based on data from Leidse Instrumentmakersschool n.d., NSG Group 2013 and Brow n.d.
- The upper tempertature limit to the solid range of glass is defined as the temperature at which 5 % of stress is relaxed in one second. This temperature is 585 $°C$. This limit is valid, provided that the thermal load speed is lower than 60$\frac{°C}{s}$.
- The lower temperature limit to the liquid range of glass is defined as the temperature at which 95 % of stress is relaxed in one second. This temperature is 630 $°C$. This limit is valid, provided that the thermal load speed is significantly lower than 60$\frac{°C}{s}$.
- Between the previously mentioned temperatures, the glass is in the transition range.
- It is assumed that the flame is similar to a bunsenflame. Therefore it is laminar and nonluminous. Its properties are then based on Wang et al. 2009 and supported by Het Nederlandse Normalisatie-instituut 2011.
- The variation over temperature of the radiative emissivity of glass is considered insignificant. Also, the radiative emissivity is assumed independent of the glass thickness. The emissivity of glass is assumed constant at a value of 0,8 (Het Nederlandse Normalisatie-instituut 2011).
- If the oven is opened, the surrounding temperature is immediately equal to room temperature,

$20\ ^{\circ}C$.

- The specific heat capacity of glass has been adapted to the transition range of temperature. The relation of the specific heat over temperature is linear in the transition range.
- The thermal conductivity of glass is assumed to be constant for all temperatures. This is validated to be an acceptable approximation in the research presented in Nodehi 2016.
- The Young's modulus is adapted to model stress relaxation. In the liquid range, the Young's modulus is assumed to be 1% of its value at room temperature. In the transition range of temperatures, the Young's modulus decreases linearly.
- The coefficient of linear thermal expansion is adapted in such a way, that its integral, the thermal strain, is zero for the liquid range. This strain reduces linearly in the transition range. The strain at the initial temperature is defined as zero.

19 Results of the Model Analysis

All results are presented and described in appendix A. A summary of the results is provided here. The researched parameters are divided into three categories. In the first part, the properties of the model are fine tuned, to reduce the numerical error to an acceptable level.
The second is the analysis, in which parameters are altered which can be influenced. By analyzing these, the ideal circumstances for the glass weld production can be found and applied.
The third part of the results is the sensitivity and contains the parameters which cannot be influenced. These are altered and the results of the model are compared to gain knowledge on the influence of the parameter on the process. Though elaborate research has provided reliable parameters, it is thorough to know what the influence on the results

In general, the weld time is around $60\ s$. The surface of the glass which is critical in most cases is the bottom surface of the flange. At weld time, the maximum temperature in the glass is about $1000\ °C$, the minimum $360\ °C$.

19.1 Model

The mesh size and time step are analyzed by refining them and comparing the results. If the results alter considerably, the finer mesh size or time step should be adopted. If the change is insignificant, it indicates that the finer option does not add value to the accuracy of the model and is therefore unnecessary.
A finer mesh and smaller time step increase computational time. Considering the amount of analyses performed, it was favoured to use the largest time step and mesh size that provide reliable results.

The mesh size applied in these analyses is fine in the front of the welding zone and coarse in the regions far from the welding zone. If there is critical stress, it is in or near the welding zone, making it the area of interest. The largest elements have $5\ mm$ edges, the smallest are $1,25\ mm$. This means that the thickness of the glass contains two to eight elements.
This is the finest mesh that was accepted in the educational version of the software. An option with elements of $0,625\ mm$ could not run. Smaller meshes in between did not return preferable results. Therefore this mesh was chosen and applied.

The time step has been analyzed similarly. The time step and amount of steps was not limited. The optimum was found at a time step of $2\ s$.

19.2 Analysis

The position of the flame has an essential influence on the welding process. If the glass is heated with a stationary point source, the temperature does not rise in the other end of the welding zone. Temperatures are not suited for welding.
A second flame position is along the welding zone at the side of the web and top of the flange, named *side* (Figure 52). This configuration resulted in critical stress at the front edge of the glass. Adding a heat source aimed to heat this area resulted in acceptable stress levels at the front. However, a critical area on the bottom surface of the glass remains.
The position which returns no critical stress on the surface of the glass, is the position *side, front and*

under. Here, the area on the bottom of the flange is heated as well. The stress remains below critical for more than thirty seconds after weld time. Note that, because the surface should be exposed to be able to heat it, the rest of the bottom surface is exposed to boundary conditions of heat loss to surroundings.

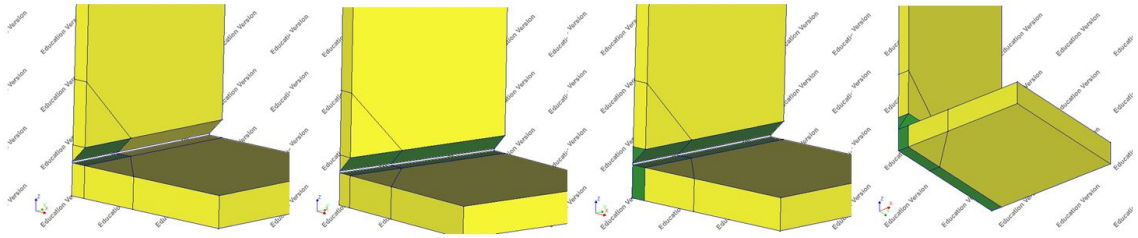

Figure 52: Geometries of different flame position configurations. The green area indicates the boundary surfaces of convective heat transfer from the flame. From left to right: *point*, *side*, *side and front* (default) and *side, front and under*.

The size of the flame is adapted as well for the position *side front and under*, by increasing and decreasing the heat boundary surface wit 50% (Figure A.17). The influence on the thermal analysis is significant, because the weld time decreases, and the minimum temperature in the glass at weld time increases. In the case of the smaller flame, the core of the welding zone reaches a maximum temperature below the threshold and has no weld time.
If the flame position is *side and front* and the size is varied, the results for the weld time are the same as for the other position. The stress at the bottom of the flange at weld time is not critical for the larger flame. Twelve seconds after weld time, the stress reaches critical level.

The preheating temperature has been adapted by changing the initial temperature of the glass elements. The results show a difference in the thermal results. As the preheating temperature rises, the weld time shortens and stress increases and vice versa.
If the initial temperature is set to room temperature, the weld time is postponed to more than five minutes. The stress at this time is critical on multiple surfaces of the web and flange.

The temperature of the surroundings is difficult to influence in the production process. However, considering further development of the welding process, this parameter is interesting to tune for process optimization. In this analysis, the surrounding temperature is adapted for convective and radiative heat loss.
The influence of the temperature of the surroundings on weld time is significant but small. At weld time, the minimal temperature in the glass is $361\ °C$ for surroundings at room temperature. If the surroundings are $500\ °C$, the minimum temperature is $500\ °C$.
The stress at weld time is not critical for surrounding temperatures of $400\ °C$ or higher. If the surrounding temperature is $500\ °C$, the stress remains not critical for more than thirty seconds after weld time.

The fourth parameter which can be influenced, is the glass thickness. It was researched what circumstances would be required if the glass was $4\ mm$ thick.
The thermal analysis shows that initially, the temperature in the core of the welding zone rises faster for the reduced thickness, though the temperature increase becomes slower after $20\ s$. However, the weld time is not significantly different.
The stress at the bottom surface of the flange is critical if only the thickness is adapted. Changing the

flame position to *side, front and under* resulted in surfaces without critical stress.
If the $4\ mm$ glass is not preheated, it takes long to heat the glass to the required temperature. The analysis was performed for ten minutes, within this time, the temperature of weld time was not reached. The stress was analyzed and shown to be critical.

19.3 Sensitivity

The sensitivity of the model is researched by adapting the remaining parameters individually and comparing the results to the results with default parameters. As a default situation, a situation is chosen in which the stress at weld time is critical. This way, it can be well compared what the influence of all parameters is on the size and position of the critical area.
The default parameters are presented in section 18 and listed in table A.1. Unless mentioned otherwise, the parameter is varied by increasing and decreasing the default value with 20%. In table 4, the influence of an increase in the parameters' values on model results is summarized.

Increased Property	t_{weld}	$T_{min}(t_{weld})$	$A_{crit}(t_{weld})$
Convection Coefficient, Flame to Glass	–	++	–
Flame Temperature	–	++	–
Convection Coefficient, Glass to Surroundings	0	0	0
Emissivity	0	-	+
Transition Range, width	0	0	-
Transition Range, time frame	0	0	-
Specific Heat Capacity	+	+*	-*
Thermal Conductivity	+	+	+
Coefficient of Linear Thermal Expansion	0	0	++
Young's Modulus	0	0	++

Table 4: Influenced of an increased parameter on the weld time, minimum temperature in the glass at weld time and the size of the critical area at weld time, resulting from the sensitivity analysis of the finite element model. * The influence is the same for the researched decrease in parameter value.

The convection coefficient governing heat gain from the flame to the glass has been varied to research the influence on the outcome of the analysis. Increasing the coefficient reduces weld time significantly and increases the minimum temperature in the glass at weld time. Additionally, the stress at t-weld is critical for all researched parameter values. The critical area increases as the coefficient decreases.

The temperature of the flame, influencing convective heat transfer, is varied between 727 $°C$ and 1927 $°C$ (1000 K and 2200 K). The temperature development and weld time are significantly influenced, as the weld time decreases and minimum temperature in the glass at this time increases if the flame temperature is increased. If the temperature of the flame is 1527 $°C$, the core of the welding zone can reach the required temperature. The analyzed values below reached a peak temperature below the threshold.
The values that returned a weld time have been analyzed mechanically. All showed critical stress, though for the highest flame temperature the critical area was very small. As the flame temperature increases, the critical area decreases.

The convection coefficient for heat loss to the surroundings has an insignificantly small influence on

the temperature development, weld time and minimum temperature in the glass. The difference in critical area is insignificantly small as well.

The emissivity of the glass, influencing radiative heat loss to surroundings, has an insignificantly small influence on the temperature development in the core of the welding zone and weld time. The influence on the minimum temperature in the glass at weld time is considerate, which decreases for an increased emissivity.
The difference in critical area is significant but small. The critical area increases if the emissivity increases.

The transition range is based on two definitions, the time frame and relaxed percentage, and influences three parameters, the Young's modulus, specific heat capacity and coefficient of linear thermal expansion (Section 18). Both time frame and percentage are varied to research sensitivity.
The percentage range is adapted to 1-99% and 10-90%. If the range is closer to 0 and 100%, the transition range is wider: the upper limit to the solid range decreases and the lower limit to the liquid range decreases.
The percentage range has an insignificant influence on the weld time or the minimum glass temperature at weld time. The influence on the critical area is significant, but small. As the range is wider, less elements are relaxed and in transition and the critical area is smaller.

The time frame is adapted to $0,1\ s$ and $5\ s$. If the time frame is changed, the transition range spans the same amount of degrees Celsius, but shifts along the temperature axis.
To find a time frame of relevant magnitude, it has been related to the load speed (Section 18). In Appendix A, it is shown that the time frame of $5\ s$ does not meet the requirement. Also, the time frame of $0,1\ s$ is conservative, considering the load speed.
The influence of the time frame on the weld time is insignificantly small. The temperature distribution at weld time is similar.
The influence on the critical area at the bottom surface of the flange is significant. If the time frame is larger, there are more elements at the front of the welding zone which are relaxed. However, for both decrease and increase in time frame, the critical area is smaller than for default.
An important observation is that all adapted transition ranges return a stress which is critical.

The specific heat of glass is dependent on the transition range. To find the sensitivity to this parameter only, it has been chosen to use the minimum and maximum value as a constant over temperature.
This parameter has a significant and considerable influence on the temperature development in the core of the welding zone and weld time. However, the minimum temperature increases significantly, for both extremes as a constant value for specific heat.
The mechanical analysis returns critical stress for the bottom surface of the flange for all researched values of specific heat. For both extremes, the size of the critical area is smaller than for the default, temperature dependent specific heat.

The thermal conductivity has a significant but small influence on the weld time and minimum temperature in the glass at weld time. As the conductivity increases, weld time and the minimum temperature in the glass increase.
The results of the mechanical analyses all show critical stress at the bottom area of the flange. As the conductivity increases, the critical area increases.

The coefficient of linear thermal expansion is analyzed for a constant value over temperature and for varying magnitudes of temperature dependent values. The parameter has no influence on the thermal analysis.

The mechanical results show a significant influence. As the coefficient increases, the critical area increases. For the lowest value, at 80% of the default value, the stress at weld time is not critical. If the coefficient is constant, the stress is divided over a larger area.

The Young's modulus has been adapted to a value constant over temperature. Additionally, the temperature dependent parameter has been varied. The thermal results show no difference.
The stress distribution for the constant Young's modulus is essentially different. Without the adaptations for the transition and liquid range, the stress is critical at the front of the welding zone in the flange and the web.
If the Young's modulus is temperature dependent, but increased, the critical area increases as well. The Young's modulus at 80% of the default value results in no critical stress at weld time.

20 Conclusions of the Model Analysis

The bottom surface of the flange is most likely to show considerable tensile stress as a result of thermal differentials. A few situations were found where this stress remained below the critical level. The first is in case the flame boundary surface is expanded to a part of the surface on the bottom of the flange, directly under the welding zone (Figure 52). The results for the analysis with flame position *side, front and under* showed that the stress on all surfaces is sufficiently low.
The second case in which thermal shock failure is not predicted is when the temperature of the surroundings is sufficiently large. If the temperature could be maintained at the initial temperature, the stress does not become critical before thirty seconds after weld time. This would provide sufficient time to create the weld.
If the coefficient of linear thermal expansion or the Young's modulus of the glass are 80% of the default value, the stress is not critical at weld time either. However, these parameters are glass properties and cannot be adapted for the production process if soda lime glass is to be used.
This observation supports the preference of preceding researchers to use borosilicate instead of soda lime, due to the lower coefficient of thermal expansion.

It is necessary to preheat the glass. The analyses performed with an initial temperature of room temperature returned critical stress on the web and flange.

There are two questions, which rose from the conclusions drawn above: Is it possible to weld thinner glass without a flame on the bottom surface or without preheating? The thickness of the glass was reduced to answer them.
The results show that in both cases, the stress is critical for a glass object of $4\ mm$ thickness. The thin objects are predicted to fail from thermal shock if the flame position is *side and front*. Adding a flame boundary to the bottom surface prevents critical stress and therefore thermal shock failure.
In case of flame position *side, front and under* without preheating, the specimen is predicted to fail from thermal shock failure. Preheating is also essential in case of $4\ mm$ thick glass. Because the surface to volume ratio is larger, the object cools relatively quick. Reaching the required temperature for the welding process requires more than ten minutes. This is considered too long for the production process, as the risk on human error increases if the process takes longer.

Because the main conclusions, requiring that a flame should heat the bottom surface and the glass has to be preheated, are not different for thick and thin glass, thicknesses in between were not researched.

The sensitivity of the model to parameters which cannot be influenced, is small. The largest influence on the stress distribution is observed for the time frame of the transition range, a constant coefficient of linear thermal expansion and a constant Young's modulus.
The transition range influences both the coefficient and the Young's modulus. The third parameter depending on it is the specific heat capacity. The thermal results are not significantly influenced by the transition range, so it is concluded that the change in specific heat due to an adapted transition range is insignificant.
The Young's modulus and coefficient of linear thermal expansion are both present in the equation, which links temperature difference to stress (Section 8). Therefore, changing these parameters has significant influence on the stress in the material. If either of these is constant for all temperatures, the critical area is present at multiple surfaces of flange and web. This shows the essential importance of mimicking liquid behaviour. Defining and applying the transition range, as performed in this model, evidently returns different results and conclusions.

Even though the influence of the transition range, Young's modulus and coefficient of linear thermal expansion are considerable, the main conclusion has remained the same for all results in this sensitivity study. The specimen is predicted to fail due to thermal shock. The size and position of the critical area changes for different parameter values, but the critical area was present for probable values. It is concluded that even though the sensitivity is considerable, the main conclusion, thermal shock failure or not, is reliable.

The sensitivity of the model to the specific heat returned ambiguous results. For the researched lower and upper limit, the critical area increased. The explanation has to be found in the simplification of the parameter for the sensitivity. The researched limits were constant for all temperatures, where the default parameter is temperature dependent. The reduction in complexity is the most likely explanation for why the minimum temperature in the glass at weld time and critical stress changed in the same direction for the lower and higher limit.

In table 4, it can be seen that there is a relation between an increase of the minimum temperature in the glass and the decrease of the critical area. In four sensitivity studies, it showed that adapting the parameter in such a way that results in an increase of minimum temperature, results in a smaller critical area. This relation is also observed in the analysis of the preheating temperature, the surrounding temperature and the flame size. This is logical, because the magnitude of the stress is related to the temperature difference in the material.
One sensitivity analysis did not conform to this relation: as the conduction of glass is increased, the minimum temperature and the critical area increased. The explanation is the following: if the glass conducts well, more energy is transported from the heat source to other regions of the object. The temperature gradient is larger near the heat source. This locally increased thermal gradient increases the local stress.

20.1 Discussion

In the model, it is assumed that at $t = 0$, the surroundings are instantaneously cooled to 20 $°C$ and the heat source is instantaneously added. In reality, the oven will be opened, causing the surroundings to cool more slowly. The heat loss in the model is overestimated. The flame will be positioned a few seconds later, so in the model the heat increase of this effect is overestimated. It has been estimated that one effect reduces the other. Additionally, because this concerns the first few seconds of the analysis, and the results are assessed at weld time, about one minute later, it is concluded that this effect is irrelevant for the main conclusions.

All results in which the flame position is *side and front* and the surrounding temperature is 20 $°C$ show critical stress, except for low values of the coefficient of linear thermal expansion or Young's modulus. This raises the question whether the model is designed in such a way, that peak stress is inevitable, resulting in critical stress.
A common rule of thumb in structural engineering, is that the stiff components attract the largest forces. Near the area where the stress is critical, the material is hot enough to be in the transition or liquid range. This causes a change in stiffness, which could explain the concentration of stress.
It has often been observed that the temperature difference between two adjacent elements is large enough to have one of them in the liquid and the other in the solid range. This creates a discrete change in stiffness of 1 to 100%. This can have a large effect on the stress distribution and maximum stress level.
It has not been possible to reduce this effect by refining the mesh. The available version of the used

software was educational and did not allow a finer mesh. The geometry was too complex to reduce the modeled object to a smaller volume, as the removed section of the object could not be easily summarized into nuanced boundary conditions for heat transfer and structural performance.
It is unknown whether this discrete change overestimates stress. This is why the stress has been analyzed using the critical area and not with the maximum stress. An example: It was not relevant whether the maximum stress was 60 or 80 MPa, It was important whether a portion of the surface was beyond the critical level. This way, the extremity of values was not relevant for the conclusions. Still, it has to be noted that this mechanism could have an influence on the phenomenon that in many cases, the stress was critical.

20.2 Glass Models of the Future

The model presented in this section uses solid elements, with properties that are adapted to mimic liquid behaviour. This is a simplification, and therefore not a representation of reality. In this thesis, this simplification is considered to provide sufficiently accurate results. Here, it will be explained what needs to be done if one would not accept such a simplification. What should one use to model the behaviour of glass in and beyond the transition range? The following answer is based on Veer, Bristogianni, and Justino de Lima 2018

A glass element is a network of atoms. These are bonded by covalent bonds, therefore, a single glass sheet is a macro-molecule.
At high temperatures, glass can be deformed plastically. This indicates the glass must be a set of large molecules, which are bonded by Van der Waals forces, because a single molecule cannot deform . It is possible that molecules break down and form while deforming glass.

There is an analytic theory, topological constraint theory, which explains why glasses are formed and allows to predict the transition temperature. This theory can be applied in molecular dynamics modelling, where atoms are modelled to make and break connections among them. This modelling technique can be used as a way to model what happens in glasses above the transition temperature. It can be used to model the split of a macro molecule in several large molecules and the interaction among them. However, to capture this, a model is required which is too large for the current state of the art. It is predicted this is possible within ten years.

20.3 Recommendations for Modeling

Until modelling on a molecular level is within reach, improvements can be made on the applied approach. It would be interesting to apply a finer mesh on the model and investigate if this reduces the calculated peak stress around elements in the transition range.

If the model is applied on a process with more products, the critical stress level should be reconsidered. Material factors and other reduction factors should be applied. Handling a lower level would result in less failed products among the produced batch.

20.4 Recommendations for Production

The aim of the model was to research whether the specimen would fail due to thermal shock failure during the production process of the weld, and to find the ideal circumstances for this process.

The main recommendation is to add a heat source to the bottom surface as well. Heating the area which otherwise becomes critical prevents high tensile stress, because the glass will become less viscous and relaxes.

A second recommendation is to keep the temperature of the surroundings as high as possible. Ideally, the environment is maintained at $500\ °C$, as this prevents critical stress. However, since the glass blower has to have access to the glass, this is not possible. It is recommended to minimize the opening through which hot air can escape.

A relation has been observed between the minimum temperature in the glass and the size of critical stress. Any measurement which increases this temperature is encouraged to be taken.

It is expected that it takes $60\ s$ to heat the glass from preheating temperature to sufficient temperature to create the welded joint. At this time, there will be local hot areas of $1000\ °C$.

21 Execution of the Glass Weld Experiments

After elaborate research on temperature development and thermal stress with finite element methods, the theoretic preparation for the weld experiments was finished. This section describes the experiments as performed for this thesis in June 2018. The experiments were performed at the Leidse Instrumentmakersschool, Leiden. The first and third experiment were executed by Frans Folst, the second by Tom Jansen.

21.1 Set-up

The aim during the experiment was to keep the glass at elevated temperature. Therefore, the glass weld was made in the oven in which the glass is preheated and cooled. The available oven is a box oven. The box is operable in vertical movement. The base of the oven is a insulating granular material. The box is an insulating material with heating coils on the inside.

The glass flange was laid on a messing plate on the base plate of the oven (Figure 53). The web was suspended with steel rods on the operable box (Figure 54). For this, two holes were drilled in the top of the web. This way, it is possible to lower the web on the flange as the weld is created.
For the first experiment, the edge of the web was not faceted.

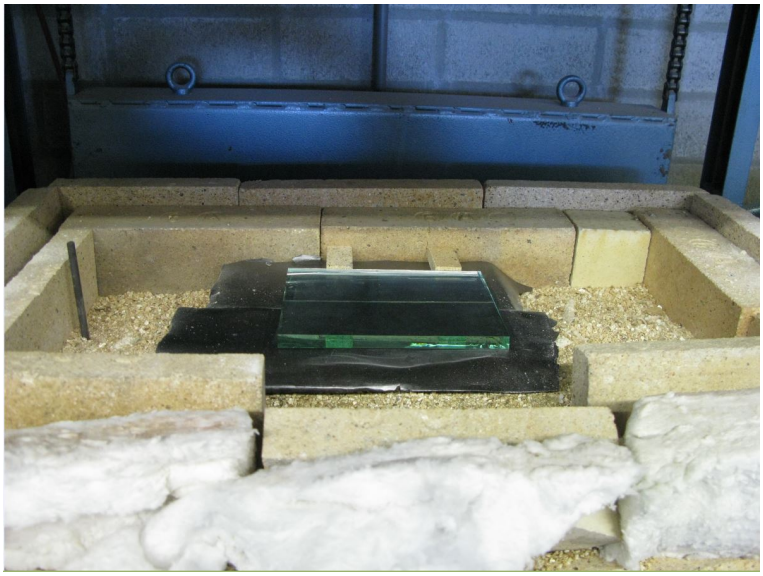

Figure 53: Positioning of the flange on the base of the oven prior to pre-heating. The ring of bricks closes the oven. The smaller ring on top is to be removed.

Because the box oven was the operating mechanism in this process, the box had to be at the right elevation during heating and cooling of the glass. This is done by a row of insulating bricks. Two layers of bricks were placed under the rim of the box. The thin layer on the top was to be removed at the start of the welding process, creating space to maneuver as the box is lowered to press the web on the flange. The bottom layer of bricks remains during the cooling stage. An additional benefit is that an opening in the oven could be made by removing one brick. This was used to let the line burner

Figure 54: Suspension of the web on steel rods attached to the oven's box, prior to pre-heating.

enter and it limited the size of the opening in the oven, as compared to an opening created by lifting the box.

The line burner was made of a copper tube in which holes were drilled (Figure 55). The copper was bent, capped and attached to a gas source. This allowed even heating of the welding zone.

Even though the advise resulting from the thermal analysis was to heat the bottom surface as well, this was not performed initially. If the bottom surface is to be heated the glass could not be placed on the oven's base. It had to be raised on two supports. If the glass was not supported fully, there was a risk that it sagged due to the heat, causing loss of shape.
Another solution was to put the flange on a small bridge of metal and heat the metal under the glass (Figure 56). Then, the heat would spread through the metal and the whole bottom surface would be heated instead of only the welding zone. This would influence the texture of this surface.
Because the practical issues of heating the bottom side would reduce the quality of the result and because the professionals had faith in the solution without bottom heating, based on their experience, it was decided to try the first experiment without heating the bottom. If the glass would fail, the other experiments would be performed as displayed in figure 56.

After the weld would be produced, the oven would be closed. The glass was to be kept at $500\ ^{\circ}C$ for four hours, after which the glass would be cooled to room temperature in 18 hours. Then it would be moved to another oven, where it would be reheated to $500\ ^{\circ}C$ and annealed slowly to room temperature. This was to release residual stress. It was annealed twice to make the first oven available for the next welding experiment in time.

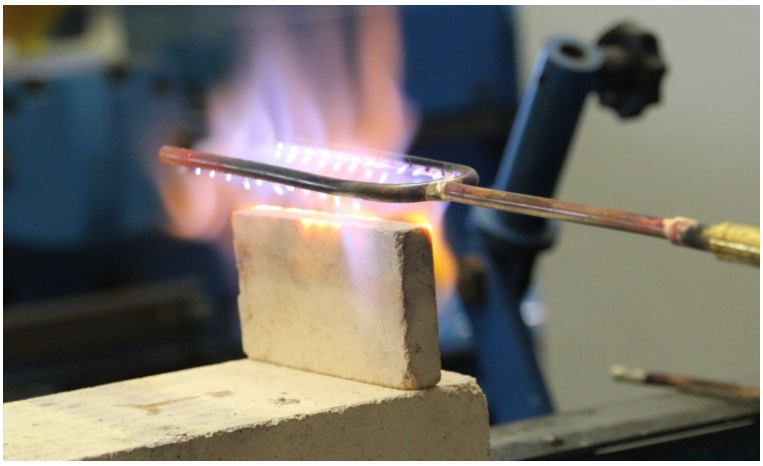

Figure 55: The gas line burner used in the third experiment. Note the red hot areas on the brick, in the focus point of the flames.

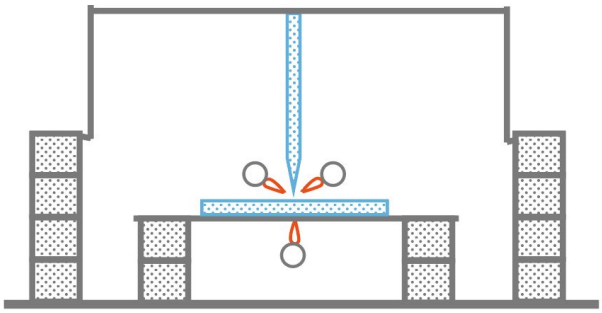

Figure 56: Cross-section of the production set up in case of an added flame at the bottom surface of the flange.

21.2 Observations and Improvements

The first experiment was executed as described above. The key moments are summarized in table 5 No failure was observed during production. There was a small complication with repositioning the brick to close the oven opening, delaying the process more than two minutes.

When the glass was removed from the first oven and placed in the second to anneal, it was confirmed that the glass had not broken from thermal shock failure. It was decided that the next experiment could be performed without a flame on the bottom surface of the flange as well.

The glass was fully transparent. The joint was a clear, all glass joint. It has been achieved to make a glass weld in 10 mm soda lime glass on the first try.

It was observed that the flange of the object was bent (Figure 57). Examining the video's resulted in the explanation. After the weld was formed, the heat source was removed. The oven had to be closed, but because the brick fell in the opening twice, this took longer than expected. When the brick was picked up to position it again, the box oven was lifted and lowered slightly. This moved the web.

	1	2	3
Start with removing bricks	0	0	0
Remove front brick	13	0	39
Burner in position	17	40	50
Lower oven, t_{weld}	84	116	231
Remove burner	122	113	253
Front brick repositioned	278	142	302

Table 5: Key moments in seconds after start in the execution of the weld experiments one, two and three.

Because the weld was cooling, the viscous glass joint moved along, bending the flange. It was noted to limit the movement of the box in the next experiments.

Figure 57: Welded specimen of first experiment, note the bent flange.

It was observed that the joint was aesthetically not yet ideal. The back of the weld had sharp corners, indicating that the temperature was not high enough for a smooth joint. Also, the desired filleted inner edge was not present. A sharp transition between web and flange was visible.

The most important observation from the first experiment was that the available time was longer than expected. In the finite element calculation, the available time up to thermal shock failure was $52\ s$ under these conditions (*default* in appendix A). The oven was open for more than four minutes. After the explanation for this difference was found, this is described in section 22, it was known that this prediction was too conservative for the real situation. The risk of thermal shock failure showed to be smaller than expected. This supported the choice to omit the flame on the bottom surface of the flange in the following experiments.

The second experiment was executed two days later. The main difference is that the line burner was removed before the web was lowered, so there was no local heating after the weld was formed.
The closing of the oven was without difficulty.

At the second experiment, the glass weld production has been captured best on camera (Figure 58). The image shows that the web was heated well and the flange was heated less. Judging from the glow of the material, it is estimated that the temperature difference between the elements was a few hundred degrees Celsius. This temperature difference at this elevation has shown not to cause thermal shock

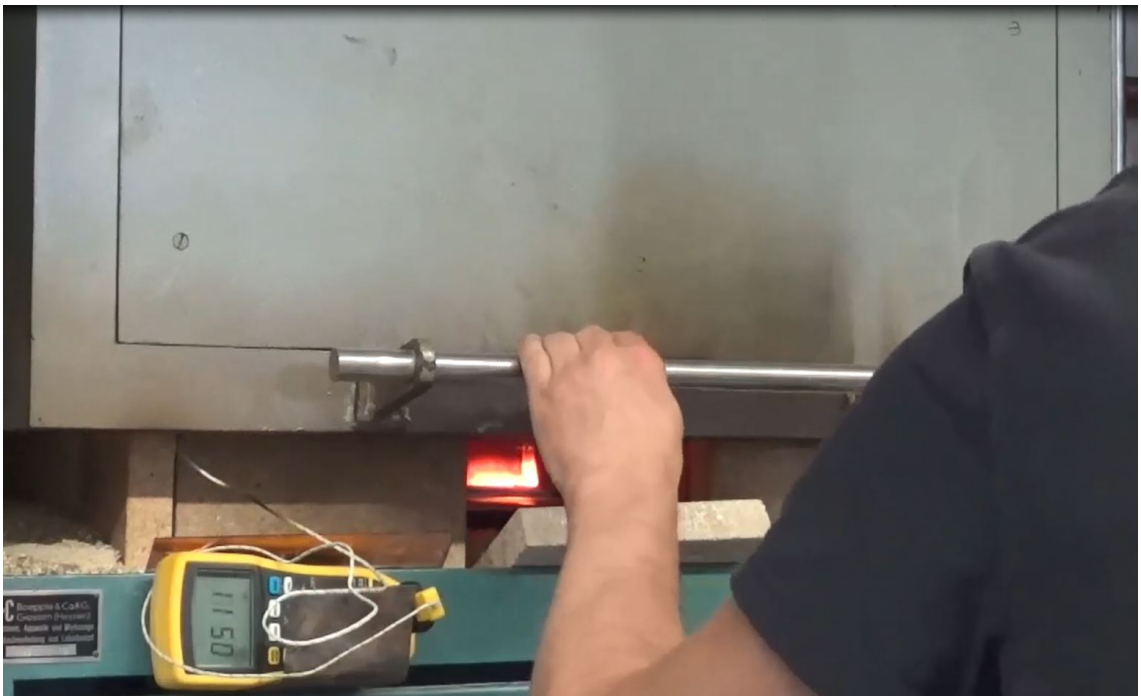

Figure 58: Lowering of the web on the flange at weld time during experiment 2.

failure. Most probably, the viscosity of the material was low enough to relax the thermal stress.

To gather data on the thermal conditions, three thermal couples were placed to measure the temperature. Two were positioned low in the oven, one was inserted at the top. These thermal couples measure with a wire, so they measure the instantaneous air temperature. They were monitored with a film camera and the data was noted afterwards when the footage was watched. The results are presented in figure 59.

When the glass weld was annealed, the object could be examined. The flange had a curvature, though smaller than in the first weld. The temperature difference of the elements was visible in the result: The web was molten upon the flange. There was a clear line between web and flange (Figure 64).

For the next and final planned experiment, it has been decided to heat the joint after the web is lowered. By heating the connection, it was aimed to melt both elements fully in joint and to soften the shape of the corner and edges to create a fillet in the inner corner of the weld.

At the third experiment, more experience was gained in the welding process. There was more confidence that the glass could withstand a longer production time.

A new burner was used (Figure 55). The holes were drilled in a different angle, resulting in a flame jet pointing horizontally and $45°$ downward . By testing the burner, it had been observed that an object $3\ cm$ below the burner would be in the focus point of these downward jets. The aim was to heat the web with the horizontal flames and the flange below with the downward flames. Both elements would become liquid and joint would become fully welded.

This time, the oven was opened for more than four minutes, and again it had proven not to be fatal.

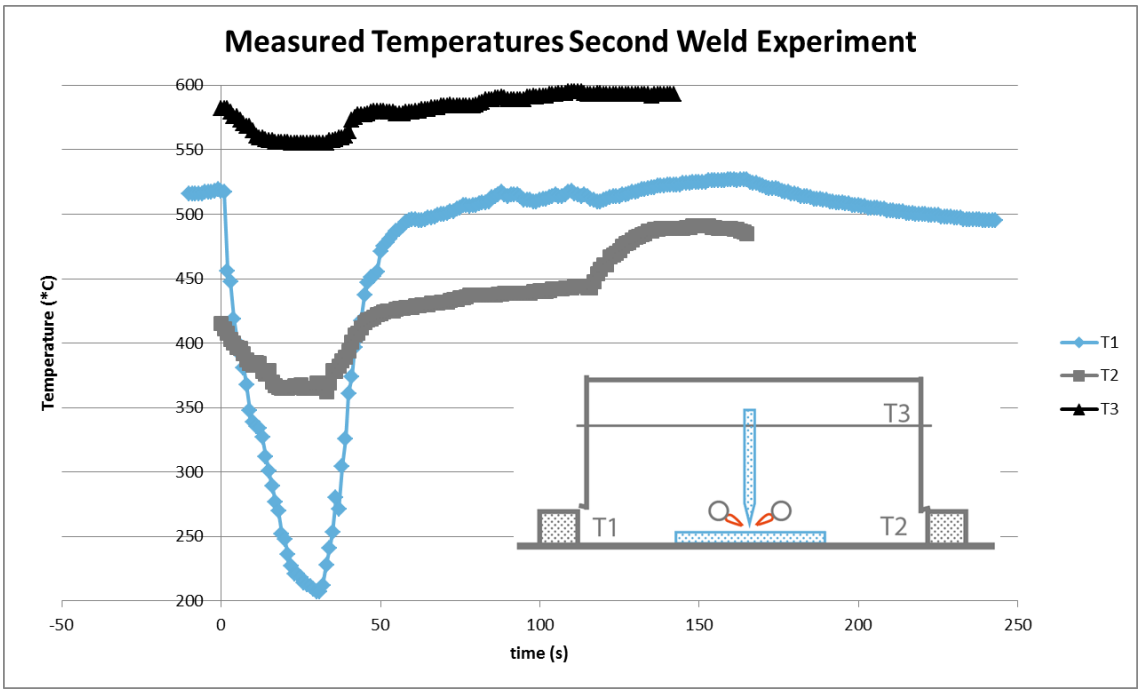

Figure 59: Measured temperatures during experiment two. Timescale matches table 5. T1 and T2 are at a low position in the oven. T3 is in a high position.

Again, temperature was measured with thermal couples, positioned in the same locations (Figure 60).

The third welded object showed the curved flange, of similar curvature as the second weld. For this weld, the edge of the web was positioned $5\ mm$ from the edge of the flange (Figure 65). Additionally, the joint is not in the center of the flange. It was difficult to position the glass accurately with the oven as an operating mechanism.

The inner corner of the weld was heated for 22 seconds after joining. This had the desired effect on the shape in the joint. A small seam between both elements was still visible.

The messing plate left residue on the bottom of the flange, creating a brown line.

Comparing the three specimen, they show interesting differences. The most significant ones have been described, but the pictures show the aesthetic differences in the joints best. (Figure 61 tot 66).

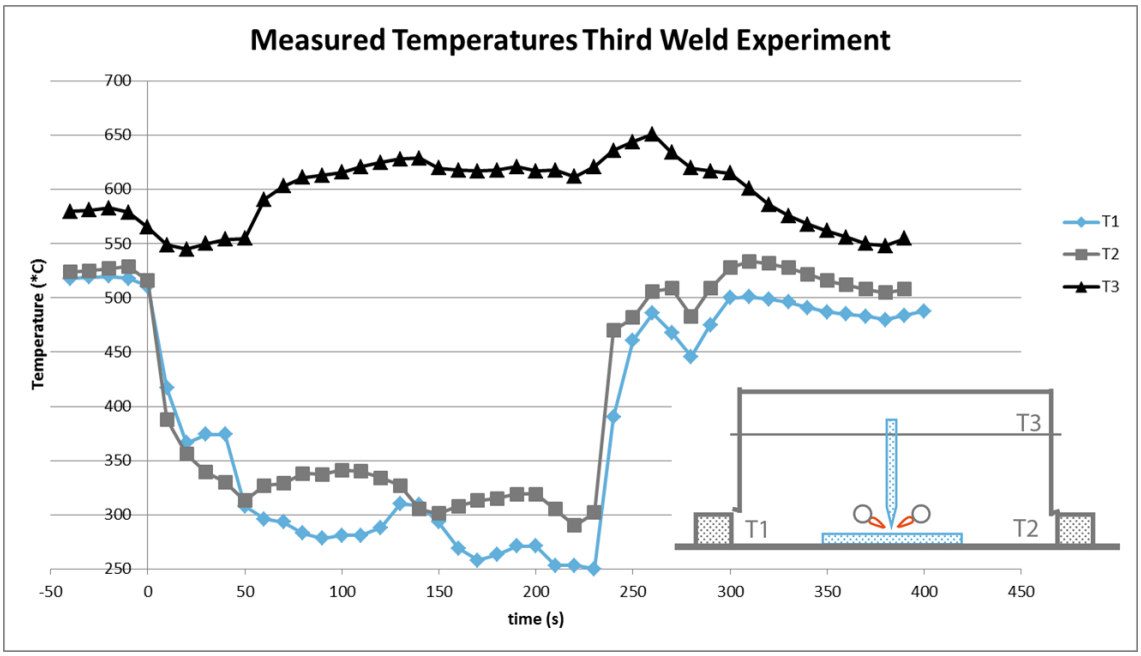

Figure 60: Measured temperatures during experiment three. Timescale matches table 5. T1 and T2 are at a low position in the oven. T3 is in a high position.

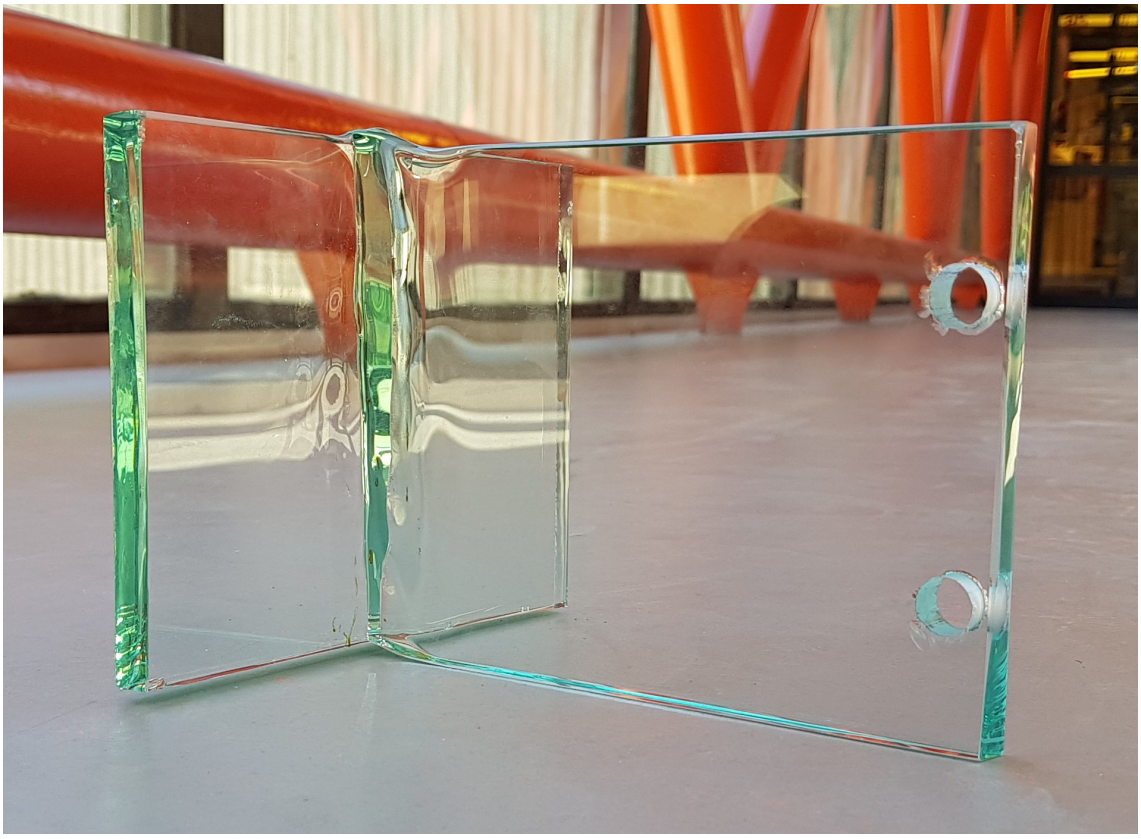

Figure 61: Product of the first weld experiment

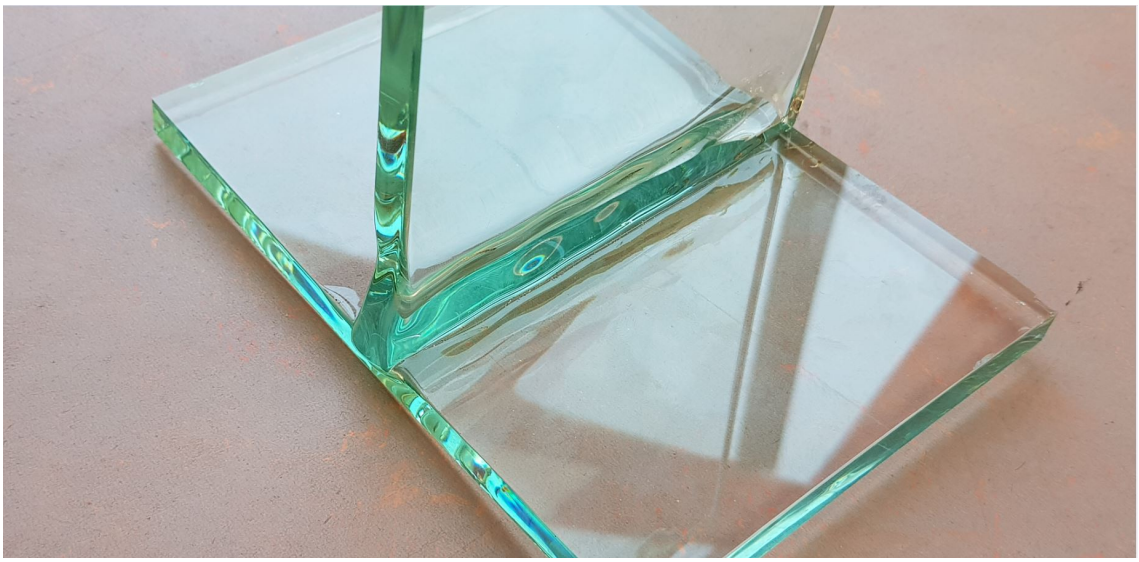

Figure 62: Product of the first weld experiment, close-up of the joint.

Figure 63: Product of the second weld experiment

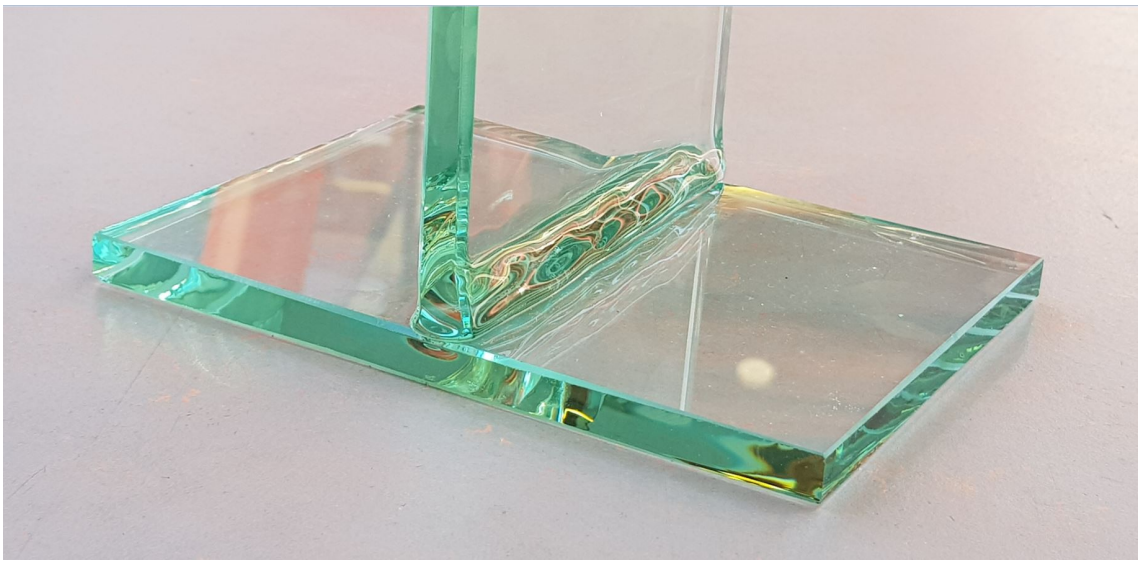

Figure 64: Product of the second weld experiment, close-up of the joint.

Figure 65: Product of the third weld experiment

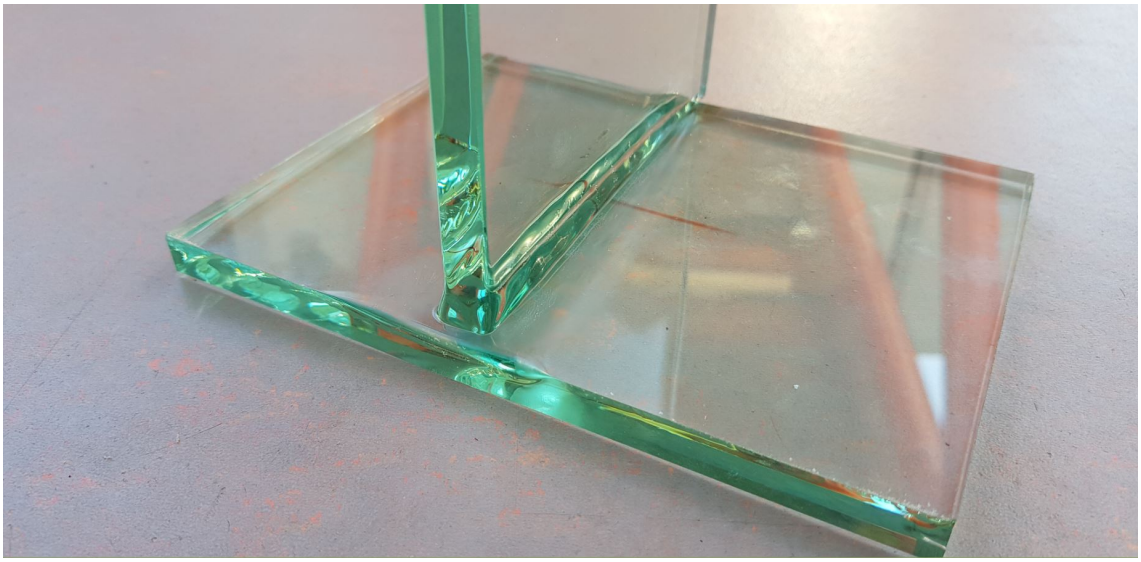

Figure 66: Product of the third weld experiment, close-up of the joint.

21.3 Fourth Welded Object

After the structural tests were executed, a fourth glass weld was made. The experiment was not filmed, but Frans Folst, the glass blower who performed the experiment, provided the following description:

The set-up was the same as for the other experiments. The web edge was not faceted prior to welding. The line burner was used to heat the plates for about 3,5 minutes. After pressing the glass web down on the flange by lowering the box oven, a point burner was used to heat the weld. This torch was not used in previous experiments. The joint was heated asymmetrically, the position of the burner alternated from left to right for about 3 to 4 minutes.
There were no thermocouples presents, but it is estimated that temperature levels were similar to those in the previous experiments. Occasionally, the burner accidentally hit the flange, resulting in irregularities on the glass surface.

The result is a fourth weld with a smooth, rounded fillet.
Visible air bubbles are observed in the weld.

Because the structural test was already executed, this object is not tested in the course of this thesis. The residual stress level is also not assessed in the course of this thesis. One conclusion can be drawn: it is possible to create a well filleted weld. Apart from this description, this fourth weld is outside the scope of this report.

21.4 Residual Stress

The residual stress in the objects was analyzed qualitatively with a polarization filter as described in section 10. The object showed grayish white regions (Figure 67 to 69).

The flange of experiment one shows a different pattern than the other two.

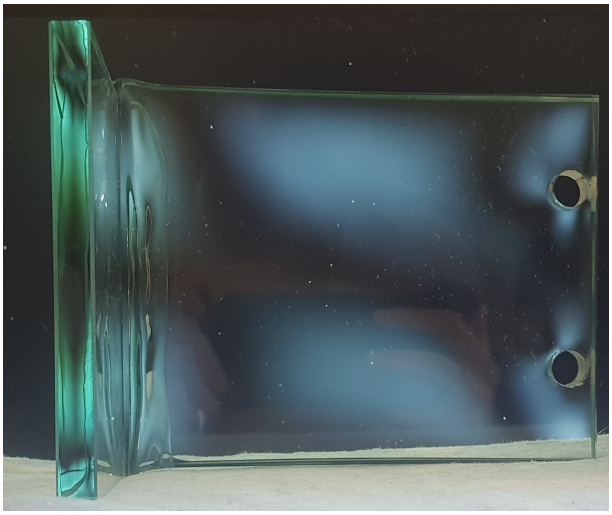

Figure 67: Polarized picture of the web of the specimen.

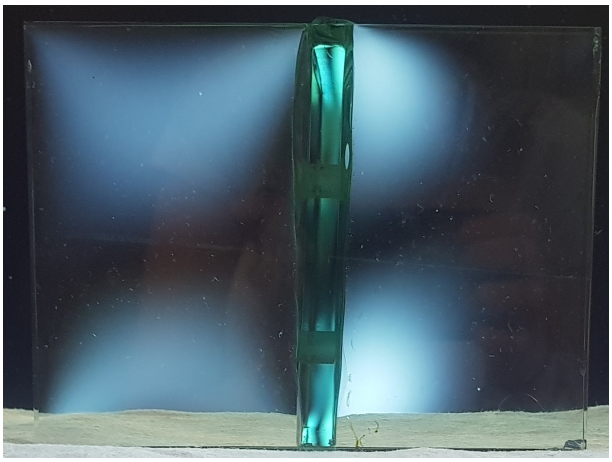

Figure 68: Polarized picture of the flange of the specimen of the first experiment.

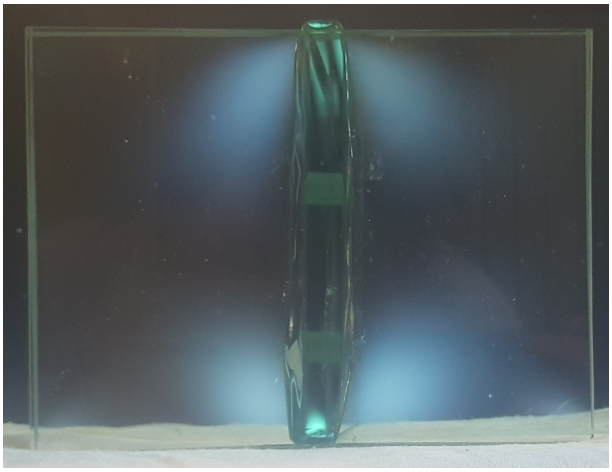

Figure 69: Polarized picture of the flange of the specimen of the third experiment. The picture for the second experiment's object is similar.

After the tests were performed, the remains of the webs have been analyzed with a SCALP. The results are presented in appendix C. The measuring error of the device is $5\ MPa$.

22 Validation of the Model

The success of the glass welding process created an inconvenience. Even though the glass was not heated on the bottom surface of the flange, thermal shock failure did not occur. This was against the predictions based on the thermal finite element model. Could this be explained?

22.1 Theories

The footage of the process shows that the thermal conditions have probably been different from the modeled situation. Both the heat loss and heat gain might have been different in reality.

Up to this chapter, the surrounding temperature has been considered as one parameter. In this step of the finite element analysis, it was considered that it is more realistic to split it in two parameters. The first is the surrounding radiative temperature of the surroundings, being the temperature of the thermal body with which heat is exchanged through radiation.
The second surrounding temperature is the surrounding convective temperature. This is the temperature of the air around the glass.

In the pictures, it is visible that the opening of the oven is small (Figure 58). The inside of the oven has a considerable thermal mass and maintains a temperature of $500\ °C$ throughout the process. The radiative temperature of the material outside the opening is lower, but the opening is so small that the view factor (Section 8) is insignificantly small for this effect to be relevant. Therefore, it suffices to model the inside of the oven at $500\ °C$ as radiative temperature for heat loss to the surroundings.

In the second and third weld production, thermocouples measured the air temperature in different positions in the oven. The minimum measured temperature is higher than $20\ °C$. Therefore, the surrounding temperature has been underestimated for heat loss to surroundings through convection. The difference is most probably caused by two phenomena. The opening on the oven is small, so the volume of cool air flowing in is too small to cool the inside of the oven. Secondly, the hot air from the flame remains in the oven. The heat source heats the glass and the surrounding air.

The heat gain from the flame might have been underestimated. It has been observed that the hot air of the flame flows along the web. Therefore, instead of cooling to surrounding temperature, this area is probably heated by the flame.

22.2 Model Adaptations

To verify these theories, the situation has been modeled. The radiative temperature of the surroundings has been set to $500\ °C$. The convective temperature has been set to $20\ °C$. This is a conservative underestimation, for the measured temperature was higher during the second and third experiment. However, the analysis of the model showed that convection has little influence on the process. The results are presented in Appendix B

The results show that the minimum temperature at weld time is $480\ °C$, this is more than $100\ °$ higher than with the default parameter values. The stress is not critical at 60 or $240\ s$ after starting the experiment.

These adaptations to the model prove to be sufficient to prevent thermal shock failure. The additional effect of higher convective temperature or the flame heating a larger surface is not required to prove why the glass did not break.

22.3 Discussion on the Model Validation

The model can be adapted for the situation as it presented itself during production. However, the original conclusions considering thermal shock failure have not been proven or disproven. It is unknown whether the values defined in section 18 are all correct. Especially, the transition range requires further validation, because its limits, though based on literature, are defined for this thesis and this situation. It is recommended not to apply the used definitions for the transition range temperature limits in other research or calculations, without further validation.

23 Conclusions of the Glass Weld Experiments

In the previous sections, the results of the welding experiments were presented. Several conclusions can be drawn, considering different aspects of the glass weld.

23.1 Welding Experiments

It is demonstrated that it is possible to weld 10 mm soda lime float glass.

Three transparent mono material joints are proof of the concept. The execution showed that the process was less sensitive to thermal shock failure than expected based on finite element analysis. The most probable explanation is that the factors influencing the heat loss of the glass have been estimated too conservatively.

Therefore, it is confirmed that glass welding is possible without thermal shock failure, if the glass is preheated and kept hot. It is carefully suggested that limiting radiative heat loss is sufficient.

It is important to heat both the flange and the web to get the unified glass joint which was the goal. The experiment in which this did not happen, resulted in a weld where the web was draped over a flange. Heating the joint after the elements are connected could be beneficial.

It showed to be difficult to position the web well on the flange. Especially in the third experiment, the web was off-set in two directions. This is most probably due to the indirect operation of the web. By managing the oven box, the glass was moved. Therefore, the glass had to be aligned before preheating.

Over the course of three experiments, the experience and confidence of the team increased. This is a promising prospect for further research. Building experience and intuition for this method does not require hundreds of trials. It could be that after a few repetitions, glass welding becomes a low risk and high quality process.

23.2 Residual Stress

There is residual stress in the welded specimen, but because the polarized light returned only white regions, the stress is concluded to be low. The used annealing schedule is adequate.

The pattern on the web shows stress paths between the holes in the glass and the joint. The most probable explanation is that the steel support system influenced the stress in the material during cooling. An interesting note, is that the glass to steel connection has not been critical under these circumstances.

The stress pattern in the flange of the first object is very different from the other two. Two aspects have been different for this experiment. First, due to complication while closing the oven, this specimen has been in an open oven without the line burner the longest. Second, the flange of this specimen is bent, indicating that the flange has been loaded in an unwanted manner during cooling.
Both factors could have contributed to the deviating and asymmetric residual stress pattern.

The quantitative SCALP measurements indicate small stress present in the webs of the welds, after the structural test was executed. The measuring error of the device is 5 MPa. The measured stress level

is within this error margin. It is concluded that the objects are practically free from residual stress.

23.3 Discussion

The performed experiments had the aim to produce welded glass T-shapes. Due to this mentality, it is unknown what the influence of many aspects has been on the result. The time the oven was opened or the glass was heated has been variable in all experiments, no conclusions can be drawn for these influences.

The heat loss due to radiation should be considered the most probable cause for difference between model and reality. It could be argued that this should have been known beforehand. If this was handled accurately in the model phase, more correct predictions could have been made, and maybe other aspects could have been researched which have now been neglected.
In reality, the difference between the model and the design of the set-up was too large. This is because the details of the set-up were finalized just before production and after the finite element results were obtained. A better control of the process could have aided the research.
Over-conservative assumptions have in all probability lead to pessimistic modelling.

In these experiments, soda lime float glass was used, though borosilicate has better resistance to thermal differences. Though borosilicate is more expensive, producing welds in this material would reduce risks.

The SCALP measurement was executed after the destructive structural test was performed. Fracture changes internal stress. The residual stress near the joint before fracture could have been larger.

It has been stated that the experience gained over the course of three experiments could indicate that optimizing the process should not require hundreds of repetitions. However, it should be noted that these relations are not likely to be linear and can therefore not be extrapolated with certainty.

23.4 Recommendation

It is recommended to align the conditions in the finite element model better with the actual situation.

It is recommended to do the experiments again, but not with the aim of production, but with the aim to find the limits of the process. Under what conditions does the glass crack due to thermal shock failure? If the limits of the material and process are known and can be used in optimizing the production process.

It is recommended to re-design the operation mechanism of the web. A different mechanism than the oven box could be considered. For example, an individual standard could be used, in which the web is positioned before preheating. If this standard is operable in all directions, the misalignment could be prevented.
The individual standard would be independent of the oven closure system. This would result in a separation of mechanical and thermal influences.

It is recommended to perform the SCALP measurements before destructive structural tests, to gain knowledge on the residual stress level near the joint.

The most important recommendation is to expand the possibilities. It would be interesting to research other glass configurations, or other sizes. Is it possible to make multiple welds in one object? Can 4 or 12 mm glass be welded similarly? Expanding the potential of the concept will contribute to its development.

Part V

Glass Fusion

This part describes the executed experiments to produce fused connections. The first section describes the method.
In the second section, the results of the experiments are presented. The final section contains the conclusions, discussion and recommendations of the fusion experiments.

24 Method of the Glass Fusion Experiments

The fusion experiments have been conducted in the Glass Cast laboratory of the faculty of Civil Engineering and Geosciences of the TU Delft. One experiment has been conducted at the Mechanical, Maritime and Materials Engineering Faculty.
The knowledge applied in the experiments, is based on the thesis of J. Mitchell 2015 and on the experience of Telesilla Bristogianni, a PhD candidate closely involved with this thesis. She has published research on cast glass bricks production and their structural applications.

Four experiments have been conducted. They were performedn in March, April, May and June of 2018. They are named experiment one to four.

24.1 Temperature

The aim during the fusion production is to globally heat the glass to a maximum temperature. Therefore, the temperature schedule of the oven is the most important production property.

Each step of the temperature schedule contains three aspects: the level, the ramp and the dwell. The level is the temperature to be reached in the step. The ramp is the speed with which the temperature should change before reaching the ramp, expressed in $\frac{^{\circ}C}{hr}$. The dwell is the amount of time the temperature level is to be maintained constant. The designed schedule is presented in table 6.

Step	t (hr) at start of step	Temperature Level (°C)	Ramp (°C/hr)	Dwell (hr)
0	0	25		
1	0	150	60	2
2	4,1	630	60	1,5
3	13,6	765	60	3
4	18,9	565	$*$	0
5	19,4	555	-60	2
6	21,6	505	-10	1,5
7	28,1	495	-10	0
8	29,1	25	-30	0
9	44,8	end		

$*$ Maximum cooling rate by quenching

Table 6: Designed firing schedule pf the fusion experiments.

A first step rises the temperature to 150 $^{\circ}C$. This is to allow water present in the mould material to vaporize.

The temperature level on which full fuse is to be achieved is 765 $^{\circ}C$ (J. Mitchell 2015). It was recommended to add a step before, with a level of 630 $^{\circ}C$. At this temperature, the glass is tack fused. Maintaining the glass at tack fuse temperature has been proven beneficial in preventing air bubble inclusions in the fuse (J. Mitchell 2015).

After the maximum temperature was reached, the specimen is to be cooled as quickly as possible to a level above the annealing point. This is to prevent crystallization of the glass. This process is named quenching and is applied from 765 to 565 $^{\circ}C$.

Residual stress in the material is prevented by bringing the object past the strain point with as little thermal difference in the object as possible (Section 10). This is the annealing phase. The object will be dwelled at 555, to reach a homogeneous temperature in the glass. The object is slowly cooled at a ramp of $10\ \frac{^{\circ}C}{hr}$, to allow the molecules to fixate while introducing a minimal temperature gradient. The glass is dwelled again at $505\ ^{\circ}C$, below the strain point, to relieve the stress which was created due to the minimal temperature gradient. To be conservative, cooling is to be done slowly down to a level beyond the strain point. After the oven reached $495\ ^{\circ}C$, the cooling rate could increase.

The maximal applied heating and cooling ramps were based on the present experience. With the aim to prevent thermal shock failure, the maximum heating rate was $60\ \frac{^{\circ}C}{hr}$ and the maximum cooling rate after annealing phase is $30\ \frac{^{\circ}C}{hr}$.

The difference between design and execution were small. For logistical reasons, it was convenient to increase the amount of time between start and quenching. This has been compensated by elongating the dwell at $150\ ^{\circ}C$ to a maximum of 3,5 hours in experiment three. Because the glass temperature is below the strain point, it is expected that this has no influence on the product.

24.2 Mould Production

As the glass is fused, it is kept in position by a mould. In the lab where the experiments were conducted, material and knowledge was available for gypsum moulds. The main ingredient is a powder named Crystal Cast M248, by Goldstar Powders, and is mixed with water.

Two moulds have been used in the experiments. The first is used in the first experiment. A glass T-shape was made by adhering two plates of 10 mm glass in a T-shape. The glass was coated with vaseline to prevent sticking, and timber walls were positioned around. The viscous water-powder mixture was poured in the formwork over the glass object, and left to harden for one day.
The next day, the glass was to be extracted from the hardened mould. However, this was not possible. The glass stuck to the mould or was wedged. Additionally, it was difficult to get grip on the glass or the mould without damaging them, reducing the amount of force to be applied. This has been solved by cutting the mould in two pieces and extracting the glass in another direction. The designed one piece mould resulted in two sections, split over the edge of the web. The mould was open at the front (Figure 70). During fusion, the opening was blocked with $10\ mm$ thick bricks positioned against the glass to prevent it from displacing.

The second mould was made in three pieces. Two sets of moulds were made and have been re-used for the second to fourth experiment. By accepting the two piece solution and redesigning the formwork, this mould allowed the edges of the web to be enclosed by the mould on both sides. The aim was to support the glass better on all sides.
The formwork consisted of timber elements. A timber positive T-shape was made. A second timber element was made as an outer formwork, with the purpose to make the mould slimmer and reduce material use. A third timber element was a plate which formed the edge of the mould at the web of the T-shape. This was kept in position with tape.
The mixture was poured in and hardened. The result was two mould segments, with a seam in between at the web of the T. The segments contained a $10\ mm$ indent in the web. For one of the segments, this edge was scraped of with a spatula, leaving a flat surface. Pushing the two together results in a $10\ mm$ thick space for the web, while all edges are supported by the mould (Figure 71).
The third element of the second mould is the base plate. This plate was rectangular, large enough to

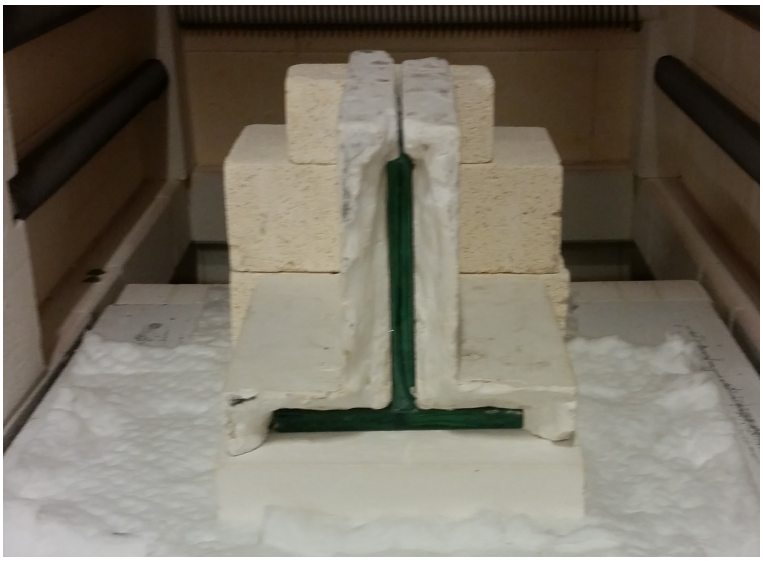

Figure 70: First fusion experiment prior to fusing, before all supporting bricks were in position. Note the first mould consisting of three elements with an open front.

fit two objects, and a few centimeter thick.

The T-shape mould segments of mould 2 have been re-used. Removing the fused object damaged the mould on the inside near the web. This was repaired by adding mould plaster. The quality of the moulds reduced over the re-usage.
Before the third experiment, a small fillet was scraped in the inside of the moulds at the corner of the fusion joint. It was aimed to create a filleted connection.

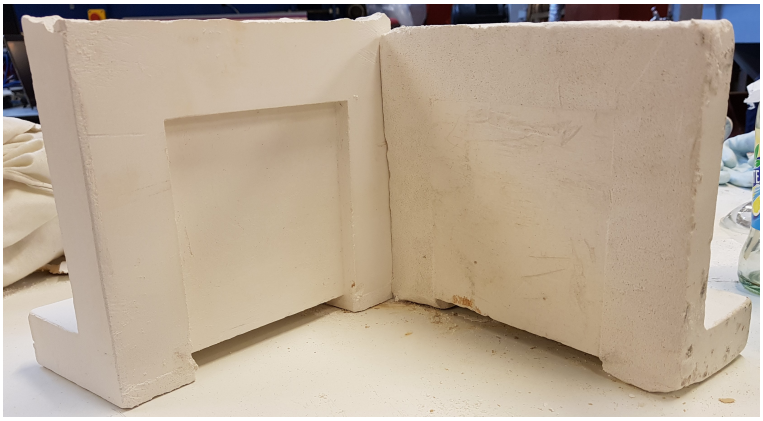

Figure 71: The two mould segments of the second mould. On one, there is a 10 mm indent for the glass web, the other is flat. There is space for the flange below.

The base plate broke due to ill treatment after the second experiment. A new one was made for the third experiment. At the fourth experiment, the plate was too big for the oven and a smaller, ceramic tile was used as a base plate.

24.3 Oven

Two ovens have been used in the experiments. The first is the oven at the civil engineering faculty and has been used for experiments one to three. In experiment two and three, two fused objects were produced in one firing.

For the first experiment, the moulds were placed on a fire resistant blanket (Figure 70). The back of the moulds was supported by three stacked bricks. Two glass plates, the web and the flange, were cleaned and inserted. The edge of the web which would be fused on the flange was a factory polished edge in all experiments. Ten millimeter thick ceramic tiles were used to close the gap in the moulds. More bricks were positioned around to prevent any displacement of the moulds.

The second and third experiment had the same oven set-up. As the oven was prepared, a fire resistant blanket was laid on the oven floor. The base plate was positioned on it. One mould segment, with the indent for the web, was positioned at the back. The glass flange and web were cleaned and positioned (Figure 72). The second mould segment, with a flat surface, was positioned. The other two mould segments and glass elements were placed similarly. A difference among these experiments, is that the glass for experiment three had ground and polished edges. Bricks were positioned around the base plate and mould segments to prevent movement (Figure 72)

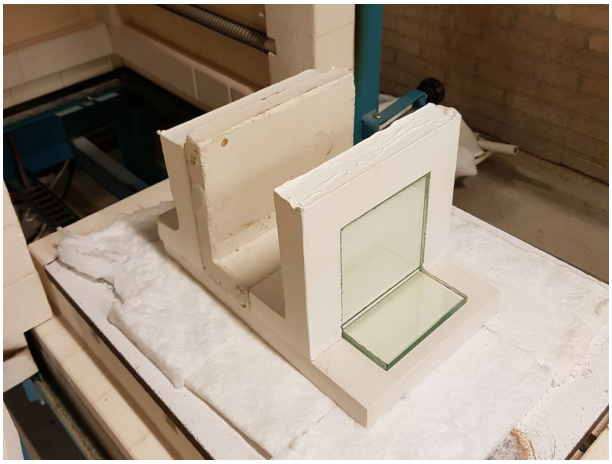

Figure 72: The positioning of the glass before the second and third experiment.

The oven is programmable. The quenching was not to be programmed, because the oven is not able to cool as quickly as desired while closed. The quenching is therefore performed by manually opening the oven door. This has been performed with caution, because the temperature is 765 $°C$. Heat resistant coats, masks and gloves were worn during the process.

The first oven was not available for the fourth experiments because of another prioritized project. Therefore, another oven at the university was used. This oven was smaller, allowing only one object to be fused. Based on experience from the previous experiments, it was decided not to use bricks as a supporting system (Figure 74).

The faculty's regulations did not allow opening of the oven during production. Quenching was not possible, and the cooling occured at the maximum rate the oven insulation allowed. It was not possible to monitor the temperatures automatically, so it is unknown what this rate has been. It was estimated

Figure 73: The moulds and bricks in position before experiment two and three.

Figure 74: The moulds in position before experiment four. The base plate is a ceramic tile and no bricks were used for support.

based on experience with this oven that the rate would be maximum $50\frac{^{\circ}C}{hr}$.
The absence of quenching forms a significant production difference between the product of experiment four and the others.

24.4 Summary of the Changes per Experiment

In this section, many aspects which have been changed or adapted throughout the series of experiments have been mentioned. To gain an overview, they are listed here.

Between the first and second experiment, new moulds were made. Two objects were fused instead of one. The orientation of the objects relative to the oven door is rotated $90°$.

For experiment three, a fillet was scraped out the inside of the mould segments. The segments, damaged during experiment two, were repaired with mould plaster. A new base plate was used. The edges of the glass were ground and polished before fusion.

In experiment four, only one fused object is produced. The re-used mould, damaged in experiment 3, was repaired in vain and remained damaged. The base plate was replaced by a ceramic tile and the bricks were not used to secure the position. Because quenching was not possible, cooling was done at the maximum rate the oven allowed.

25 Results of the Glass Fusion Experiments

25.1 Observations

The first observation of the specimens was while inside the mould segments. In all specimens, a displacement of the top edge of the web was observed (Figure 75). The maximum displacements measured 20 mm in experiment one, 21 and 24 mm in experiment two, 27 and 32 mm in experiment three and 27 mm in experiment fpur.
The deformation of experiment one led to the decision to make a new mould. The aim was to create a mould that was more tight, allowing less space for deformation.

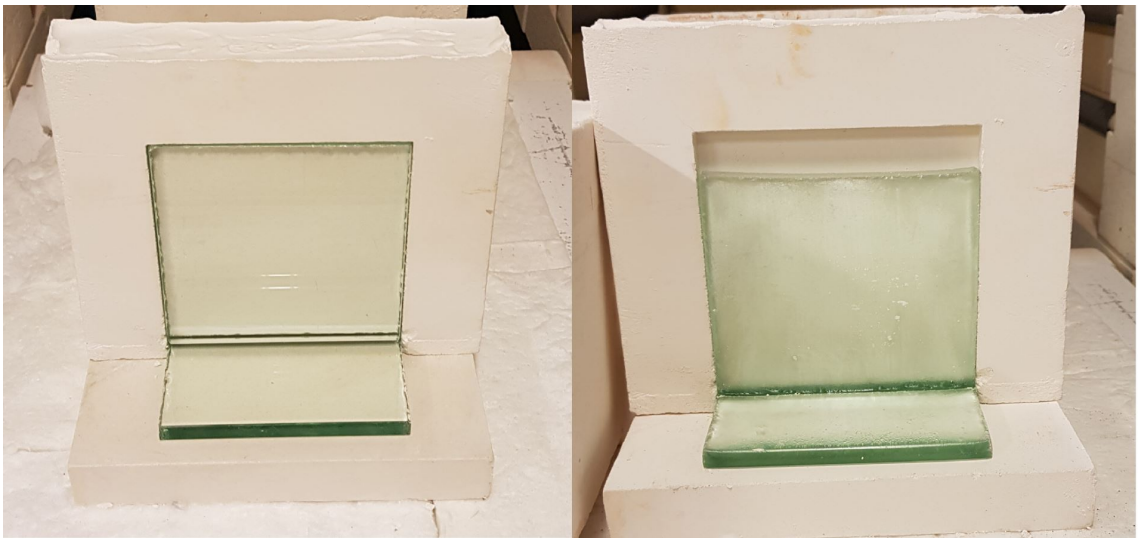

Figure 75: One object from the second experiment, before (left) and after (right) fusion. Note the deformation of the top of the web.

There was no glass residue on the outside of the mould or on the oven base.

The mould was removed and the specimen examined further. The surfaces had a rougher texture than prior to fusion. At some surfaces the spots on the mould surface match those on the glass surface, like on the bottom surface of the flange. At other surfaces, this was not observed, like on the top of the flange. The texture on the side of the web was finer than on the flange.
In all specimen, the top surface of the flange was smoother than the bottom. Also, it was the most transparent surface.
In the object of experiment one, this surface was least flat compared to other surfaces, with dents which could not be related to the mould.
For the objects of experiment two, the bottom surface of the flange showed the largest roughness, making it more transparent than the fine texture on the web. On both objects, a line was visible on the bottom surface, matching a flaw in the base plate.
The object of experiments three and four had surfaces of similar textures as the others. In all objects, the bottom surface of the flange matched the base plate texture.

The edges of the object were rounded. Most edges had a convex texture in both directions. This is not the case for the top edge of the web, which concaved significantly in both directions. The texture

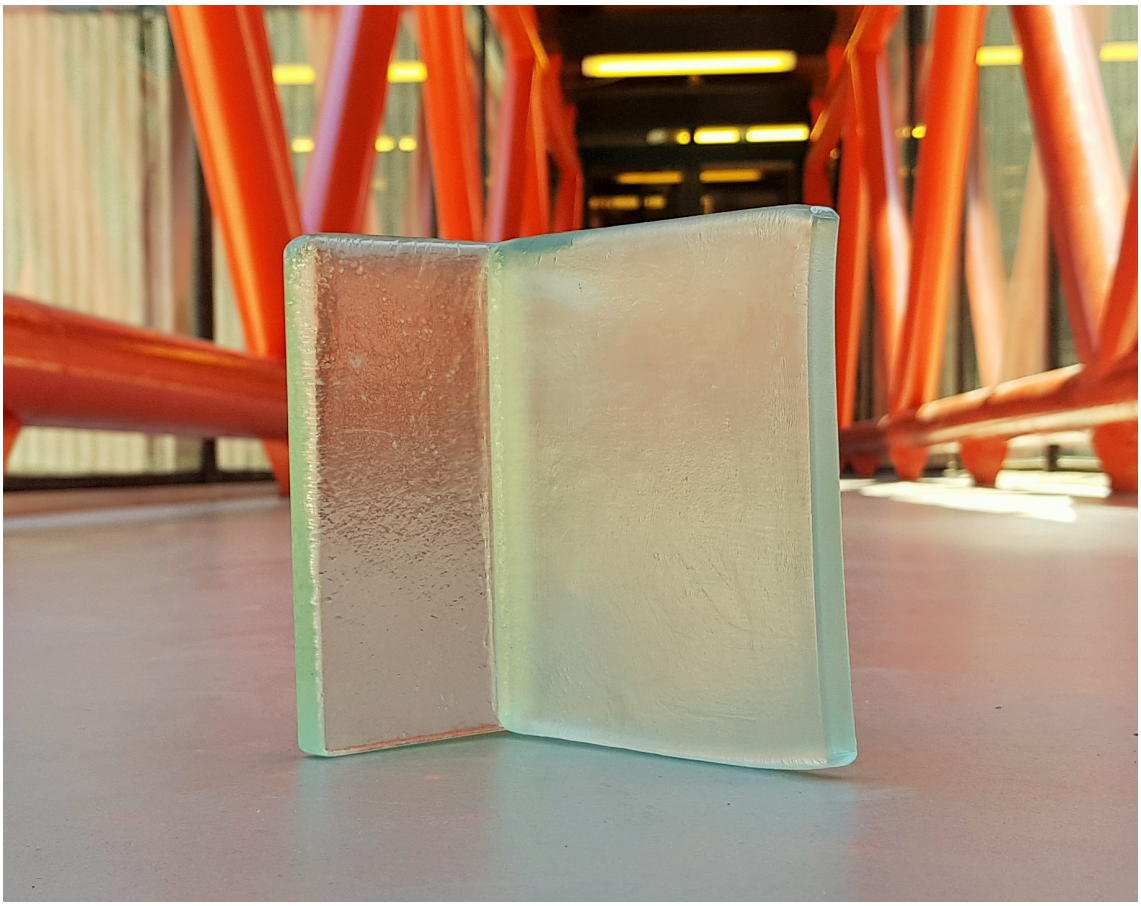

Figure 76: Texture on the surface of an object of experiment three. The left segment is the flange, which is more transparent than the web.

on the edges is rough and does not always match the mould or the marks which were present before fusion.
Some edges of the flange were rounded more than others. In experiment one, this was on the right side, in the others, this was at the front.
In experiment two, the front object had straighter edges than the back object. The back object had a deformed web edge, which could be linked to the shape of the mould. The top edge of the web was asymmetrically deformed. The front object had straight side edges for the web and a symmetrically deformed top edge.
The edges in the objects of experiment two showed sharper corners than experiment one's result. Also, the regions which showed marks of the cutting and grinding prior to fusion, where still marked after fusion. This led to the decision to grind and polish the glass in future experiments.
In the object of experiment four, an irregular volume of glass was present on the edge of the flange at the fuse (Figure 78). This could be related to the damage in the mould.

The glass panels are connected. The connection can take the self weight of the specimen in all angles.

There are no visible air bubbles or other types of contamination in the fused connections. The glass surfaces near the connection are deformed. There is a sharp groove between the flange and web, separating the parts visually. This seam is present in all specimens.

Figure 77: Edge quality of the objects of experiment two (left) and experiment three (right).

Figure 78: Irregular bulge on the object of experiment four.

In the first experiment, the sides of the joint were visually different. One side was straighter and showed a small fillet. The irregularities in the joint were most visible in this specimen. The web surface bulged over the seam
For experiment two, the shapes were straighter. The perpendicular angle and groove between elements led to the decision to apply a fillet in the moulds.
In the objects of experiment three, a softer fillet is observed, though the seam remains present (Figure 79).

25.2 Measurements of Dimensions

The thickness of the fused specimens was larger than of the original glass panels. The thickness was measured with a caliper which is accurate up to a tenth of a millimeter. The thickness was measured from at least one centimeter of the edge, on four positions on the web and eight on the flange. The results are summarized in table 7.

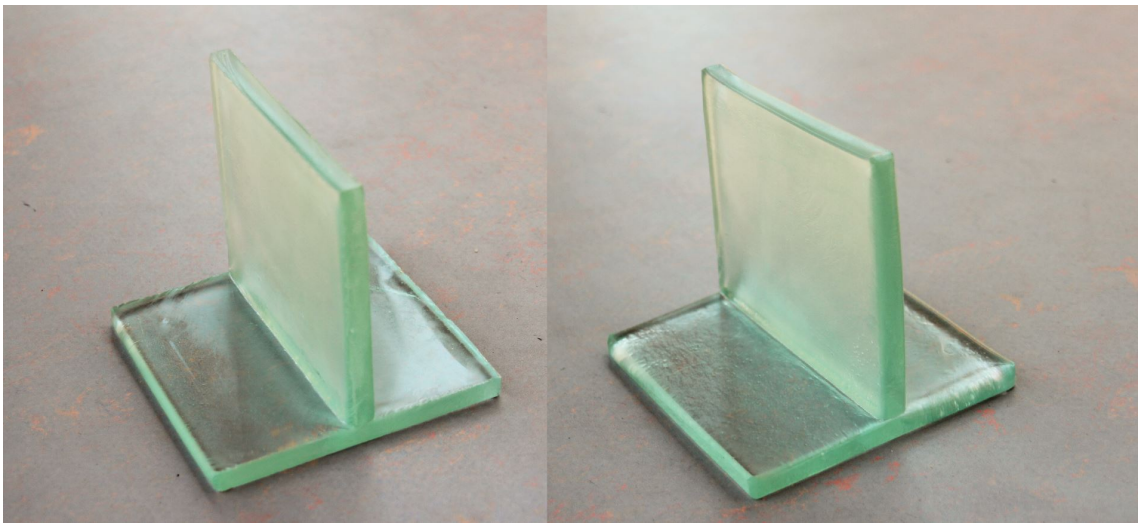

Figure 79: Difference in fillet between object of experiment two (left) and three (right).

Experiment (Object)	Min. web	Max. web	Min. flange	Max. flange
1	11,5	12,5	9,9	12,2
2(1)	11,6	11,8	9,9	10,5
2(2)	11,7	12,2	9,8	12,7
3(1)	11,5	12,0	10,1	11,0
3(2)	12,0	12,5	10,0	11,0
4	11,9	12,5	9,9	10,7

Table 7: Measured thicknesses in millimeter of the fused objects

25.3 Failure in Transport

Between experiment three and four, five fused objects existed. Four of them were temporarily stored at a different location, with the purpose of spreading knowledge on the production process. When all four were transported back, two of them broke.

One cracked in the web above and through the joint. The other cracked in the flange, through the joints edge. For the first time, observations beyond the surface could be made. The inside of the object was transparent glass. No air bubbles or imperfections in the glass could be distinguished with the naked eye.

The failed objects were from experiment two and three. They were objects 2(2) and 3(2) in table 7. After experiment four, the remaining intact objects were all from different experiments. These have been tested destructively, this is described in Part VI.

25.4 Residual Stress

After experiment one, the residual stress in the object was analyzed qualitatively with a polarization filter as described in section 10. The object showed grayish white regions (Figure 80). This led to the

conclusion that the annealing schedule was adequate to relieve residual stress in the experiment. No changes needed to be made to the schedule.

After experiment four, the four remaining objects were analyzed in the same manner to assess residual stress in the objects. The results showed grayish white areas, which confirmed the first observations.

Observing the flange through the filter, showed a pattern. If the flange is divided in four square segments, each of these contains a circular area where the glass is white.

The webs of the specimens shows almost no residual stress. Above the joint, a faint, blue gray area can be observed, indicating lower stress differences than the flange.

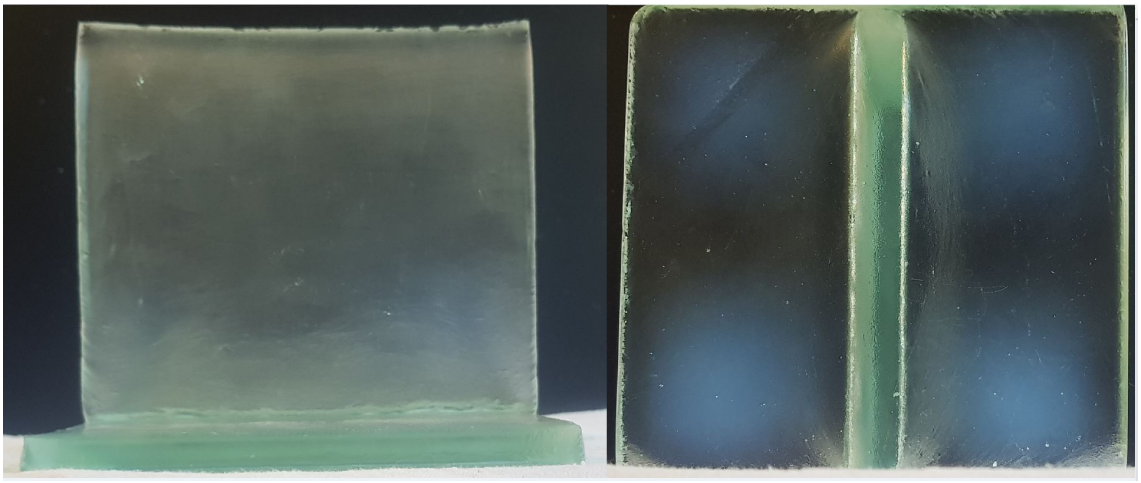

Figure 80: Typical residual stress indications in the fused objects' web (left) and flange (right) as observed with a polarization test.

26 Conclusions of the Glass Fusion Experiments

In the previous section, the results of the fusion experiments were described. Several conclusions can be drawn, considering different aspects.

26.1 Fusion Experiments

It has been demonstrated that the applied temperature schedule is suited to connect soda lime float glass panels.

The groove between web and flange in the joint indicates that there was surface tension during fusing. This could indicate that the connection is not fully fused, as it is possible that the molecules on the surface in the joint have not rearranged to create a homogeneous glass body.

The bottom surface of the object showed the most similarities with its mould. This is because gravity pushed the glass in the mould. The top surface of the flange was the smoothest. This is because this surface did not make contact with the mould and surface tension resulted in a smooth surface. The surface with the largest influence on the texture is the base plate.

The mould is not the only cause of the translucency. The top edge of the web is translucent as well in all objects, but this edge made no contact with the mould because of the deformation. A possible explanation is that this surface was cooled below a fixation temperature. As the inside of the object cooled, this edge shrank and wrinkled. This cannot be proven because it is unknown what the specimen looked like in the different stages of temperature inside the oven.

The objects did not crystallize. The translucency was due to the development of surface texture. The omission of quenching in experiment four did not result in a crystallized object. This is probably because the maximum temperature was below the glass working point. The material remained viscous, and the risk of molecular rearrangement and crystallization was not high at these temperatures. The risk of crystallization in glass fusing is lower than in glass casting.

The top edge of the web displaced in all experiments. It is most plausible that the moulds were not as tight as designed. Gravity made the glass move down and created a thicker, shorter web.

Even though the new moulds in experiment two resulted in a straighter product, the deformations were in the same order of magnitude. This suggests that in the new moulds, there was space for the glass to flow into. No success was achieved in making a one piece mould.
The deformations increased over the experiments. This has been related to the re-use of repaired moulds. This is supported by the bulge on the object of the fourth experiment. Here, additional new space was present in the mould, which was partially filled with glass. This has increased the deformation at the top. Re-using moulds which were damaged and repaired, shows to have a negative effect on the product's quality.
An additional influence on the deformation could be the polishing of the glass. This resulted in more space between glass and mould and more space for the glass to flow to.

The quality of the edges differentiated within and among the objects. Some edges were softened more. The most probable explanation, is that these edges had more space in the mould prior to fusing. The mould did not support these edges well.

The effect of polishing the edges was visible on the objects of experiment 2 and 3, as they showed less flaws at the edge (Figure 77).

The joint in the objects of experiment two was smaller than the joint in the first, indicating that it was achieved to create a tighter mould.

It was attempted to make a fillet in the joint by scraping the inner mould. It was achieved to create a small fillet in the glass, but the seam between the elements could not be prevented with this method (Figure 79).

The dimensions of the joint are variable. Even though the same moulds were used, the difference in thickness for the objects of experiments two to four is significant. More importantly, it has not been achieved to produce fused objects of $10\ mm$ thickness.

Between experiment one and two, the object was rotated $90°$ in the oven. No direct influence on the product has been observed.

The bricks used to support the moulds in the experiments were unnecessary. There were no negative effects of omitting them in the fourth experiment.

26.2 Unplanned Failure

The accidental failure of two specimens, showed that glass is, as is well-known, fragile. It functioned as a reminder to treat the specimens with care.

The most probable failure cause is an impact load, due to a bump during transport. It is probable that two glass elements hit each other, and that the glass failed as a result.

One specimen failed partially through the joint, but the other failed through the flange. This showed that the difference in strength between joint and elements was small enough to make failure in both sections possible.
The remains showed a first glimpse of the inside of the objects. It showed that the material was not crystallized. The translucency was due to the development of the surface texture. Visually, the joint seemed fully fused and homogeneous. However, since microscopic flaws could be present, it cannot be stated that the joint was perfectly homogeneous. If there were flaws, they were small enough to be invisible to the naked eye.

26.3 Residual Stress

The residual stress is white or grayish white in the polarized pictures (Figure 80).
The welded specimen were analyzed quantitatively with a SCALP, leading to the conclusion that the present residual stress is lower than the measuring error of $5\ MPa$ and that they are practically stress free (Section 23). SCALP measurements were not possible for the fused objects due to the rough surface texture.
The observed residual stress in the welded objects is larger, because the polarized pictures of the welds show brighter regions (Section 21). If the welds are practically stress free, the fused specimen are practically stress free as well.

Therefore, it is concluded that the magnitude of the residual stress is too small to form a significant risk of failure. The analyses give no indication that residual stress will play a significant role in the structural capacity of the objects. The applied annealing schedule is sufficient to relax residual stress.

26.4 Discussion

In all objects, a seam in the connection was observed, which has been attributed to a surface tension of both elements. If this tension is broken, the result could be a smooth, filleted joint. This full fuse of the surfaces could be aided by rising the temperature. The viscosity of the glass would reduce and the surface tension would break more easily with increased flow of glass. It is unknown at which temperature this effect would be obtained. However, there is a principle objection against this measure. Reducing the glass viscosity results in a process that is closer to glass casting. In that case, the product could have any shape and is no longer a system composed of glass panels. This is outside of the scope within which fusion is considered.
It is determined that raising the fusion temperature to a level beyond the working point changes the method to glass casting. The temperature levels between the used level and the working point are considered fusion and could be researched for their influence on the product.
It is unknown if the temperatures levels within the fusing process are high enough to prevent the seam between the elements.

There are several things which have been changed throughout the experiments. The only one that made a substantial difference is the change of the mould between experiment one and two. The other factors did not have an essential effect on the product.

It has not been researched what the effect is of different temperature schedules. This is a key parameter in the fusion process. All drawn conclusions are only applicable for one temperature schedule. As this schedule can vary in time and temperature, an infinite amount of possible schedules is not considered in this thesis.

It has been concluded that the risk of crystallization is smaller in fusing than in casting. The explanation is that the temperature was lower. This conclusion is therefore highly dependent on the maximum temperature and should not be extrapolated to other temperatures.

26.5 Recommendations

It is recommended to research the influence of different temperature levels and dwell durations.

It is also recommended to find a measure to control the dimensions of the product more accurately. It is suggested to produce a one piece mould.
It is proposed to apply the lost wax method (Figure 81) (Jacobs 2017). A positive mould is made of wax and the gypsum plaster is cast on it. The wax is removed by melting it. The glass is inserted, the remaining opening at the bottom of the flange is supported by a flat and smooth base plate. After fusion, the gypsum mould is dissolved in water.
The mould is not re-usable, but it has been concluded that re-using the gypsum mould is disadvantageous.

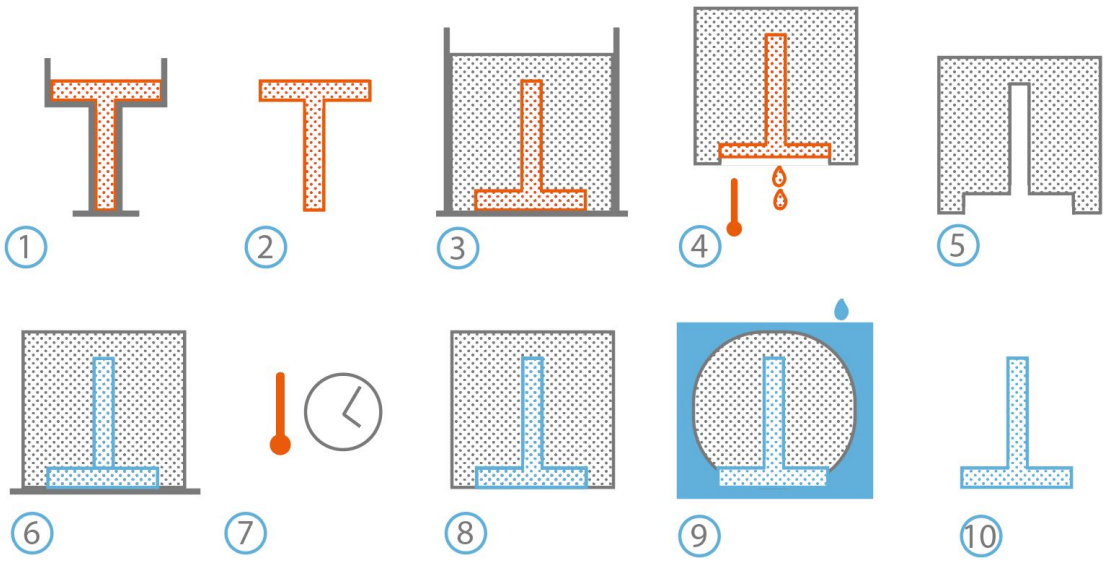

Figure 81: Fusion process using the lost-wax method: (1) casting molten wax in formwork, (2) positive wax mould, (3) casting gypsum mould, (4) removing wax by heating and melting, (5) negative gypsum mould, (6) positioning glass elements, (7) fusion, (8) product in gypsum mould, (9) dissolving mould in water and (10) final fused product.

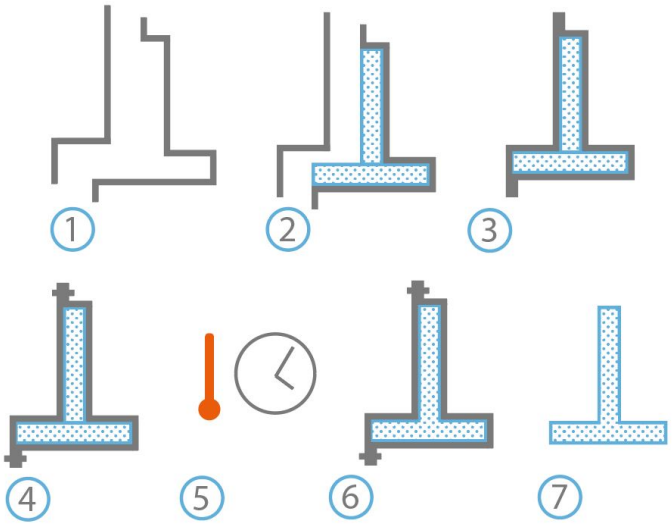

Figure 82: Fusion process using a steel mould: (1) two steel mould segments, (2) insertion of glass elements, (3) closing mould, (4) securing mould with bolts, (5) fusion, (6) product in mould and (7) final fused product.

Additionally, it is recommended to research the effect of the mould material more extensively. It is predicted that a difference in mould material can make a significant difference for the product.

In current practice, glass is hot bent. In this process, glass is heated and slumped in a steel mould (G. Mitchell n.d.). To prevent the glass from sticking to the mould, a mixture is applied on the surface before heating to 700 $°C$. This mixture contains clay and calcium carbonate. The result is a bent pane with a smooth surface.
It could be beneficial to apply these techniques on glass fusion. Steel has been the mould material for the Crystal Houses bricks, making it a logical choice for fusion moulds.
The difference between the bending and fusing practice is that with bending, temperatures are lower and the glass is viscous enough to partially bear itself. Not all its weight is supported by the mould. Therefore the stress of the mould on the glass is lower and the texture of the mould could have a smaller influence on the glass surface.
The used fusion temperature was higher and the low viscosity might influence the interaction with the mould surface, regardless of the mixture layer. This raises two questions: can glass be fused properly at lower temperatures, and does the mixture have a positive influence on the glass surface when fusing at higher temperature levels?

Using steel moulds can also be a way to control the dimensions of the product. In this case, it is recommended to make a mould of multiple pieces. After the glass is inserted, a bolted connection ensures that the available space in the mould is no larger than the desired thickness (Figure 82). After production, the glass can be extracted by unscrewing the bolts. This mould will probably allow less deformation than the moulds used in this thesis.

It is recommended to research the possibilities of post processing the product. The fused system can be polished to create a smooth surface and transparency. The residual stress in the product is small, therefore post-processing should be possible. In combination with mould improvements, this could be the solution to ensure the final product's dimensions.

Part VI

Analysis

This part is about the comparison of the connections. The welded and fused connections are compared with adhesive connections in a structural test.

The test method is presented. A finite element analysis of a perfect and homogeneous specimen is performed to predict the stress distribution.

The next section describes the test results. Possible causes of glass fracture are collected and some are determined to be the most likely cause of failure for the test. The structural model is adapted to the situation as it occurred in the tests to determine the most probable dominant cause of failure.

The next section contains the conclusions, discussion and recommendations of the structural test.

Then, focus shifts to qualitative aspects. The fused, welded and adhesive connection are analyzed for their aesthetics, accuracy and their requirement of time, energy, skill and money.

The final section of this part considers the options and obstacles for making larger heat bonded objects.

27 Method of the Structural Test

The comparison between the heat bonded joints and the suitable alternative has been made with a destructive structural test. The test has been performed in close collaboration with dr. ir. Fred Veer. His knowledge on glass and expertise in experiments is applied in many decisions in this process.

27.1 Goal of the Test

The goal of the test is to load the specimens to failure. The obtained results are the crack patterns and failure loads. By testing the welded, fused and adhesive specimens, the types of objects and types of connections can be compared.

27.2 Specimens

The specimens in the structural test are the products of the previous experiments (Table 8). These are three welded specimens and, after the accidental failure of two, four remaining fused specimen.

Five additional T-shapes have been made with an adhesive. Soda lime float glass panels, cut from the same panel as the one used in the fusion experiments, have been cut to 120 by 120 mm. The thickness is 10 mm. The edges were ground and polished. The edge of the web which was connected to the flange was the original factory polished edge.
The adhesive is Delo 4468. This transparent, UV-curing adhesive has been used in the Crystal Houses project in Amsterdam. After the glass was cleaned with propanol, the adhesive was applied on the flange. It was cured for about six seconds with a Delo UV-lamp. Then, the excess adhesive was wiped from the glass. Then, the adhesive was fully cured with the UV-lamp for about 40 seconds.

The welded specimens are different from the other two. The glass is not cut from the same plate, due to logistics. The used glass was on stack at the production location and the products were made in different locations. Though both were soda lime panels, the composition could have been different. A difference in composition can have an effect on the glass' properties (Veer, Bristogianni, and Justino de Lima 2018).
Another difference is the size. The flange and web of the glass were 120 by 160 mm before welding. This can have an effect of the structural behaviour. However, it is considered that this effect is probably insignificant under the used loading conditions, because the height of the connection is the same. For the same reason, the presence of holes in the web will probably not influence the results.

27.3 Shear Test

The best geometry to compare the connections to the parent material would probably be a connection between two parallel plates. This can be tested in a four-point bending test and compared to a larger glass plate without a connection. In this set-up, the stress in the joint is the same as in the material around it. This type of test can lead to conclusions about the comparison of strength between the connection and the parent material. This kind of test has been performed on welded and not-welded tubes in preceding research on welded joints (Giezen 2008).

Specimen	Connection Method	Experiment	Note
1	Adhesive		
2	Adhesive		
3	Adhesive		
4	Adhesive		
5	Adhesive		
6	Fusion	Fuse 1	
7	Fusion	Fuse 2	
-	Fusion	Fuse 2	Failed in transport, not tested
8	Fusion	Fuse 3	
-	Fusion	Fuse 3	Failed in transport, not tested
9	Fusion	Fuse 4	
10	Weld	Weld 1	Damaged in transport, tested
11	Weld	Weld 2	
12	Weld	Weld 3	

Table 8: Properties of the test specimens.

The geometry of the specimens, the T-shape, has been chosen because the product is a new typology for all-glass objects (Section 4). Therefore, the geometry was not chosen because it would be the best geometry for a structural test. A four-point bending test was not the best option with the size and shape of the products. Therefore, the specimens had to be loaded in a way that loads the joint differently from the material around it.

The connections are loaded in shear (Figure 83). A bending test has been considered, but discarded because this would be too sensitive for flaws in the seam of the joint. A tensile test has been discarded because this would give unnecessary complications with the set-up.

In the shear test, the object is positioned differently than it was during production. In the parts on welding and fusing, the bottom of the flange was the surface on the base of the oven. In the test, this surface is positioned vertical, and is therefore no longer a bottom. This surface is renamed the *back of the flange*. The *bottom* of the web and flange are now the edges which are at the bottom of the specimen in the orientation of the test.

The specimens are loaded in a test rig which can reach loads up to $100\ kN$. A steel element supports the specimen as it is loaded by the 'elephants foot', pressing down. The load is introduced in the glass web with a steel block and rubber strip. The rubber strip had to distribute the load on the web without peak stress. The steel block functioned as a spacer between the specimen and the large elephant's foot, to prevent the foot from pressing on the flange.

In the test design, it was determined that the flange was adhered to an aluminum support, which would be bolted to the steel support. Aluminum is chosen because it has approximately the same Young's modulus as glass, and no stress as a result of a stiffness change would be fatal to the specimen. The aluminum will support the vertical back of the flange and the bottom edge of the flange. The support at the bottom is $9\ mm$, generally one millimeter thinner than the glass, to prevent critical stress in this area.

The glass specimens are connected to the aluminum with a transparent adhesive. This is the same adhesive as used to make the adhesive specimens. The connections have been made with the same

process as described for the glass to glass joints.
All specimens contain an adhesive connection between glass and aluminum, but only the adhesive specimens contain an adhesive joint between glass web and glass flange. This connection will not be critical in the test because the area of the adhesive connection between the glass and aluminum is larger.

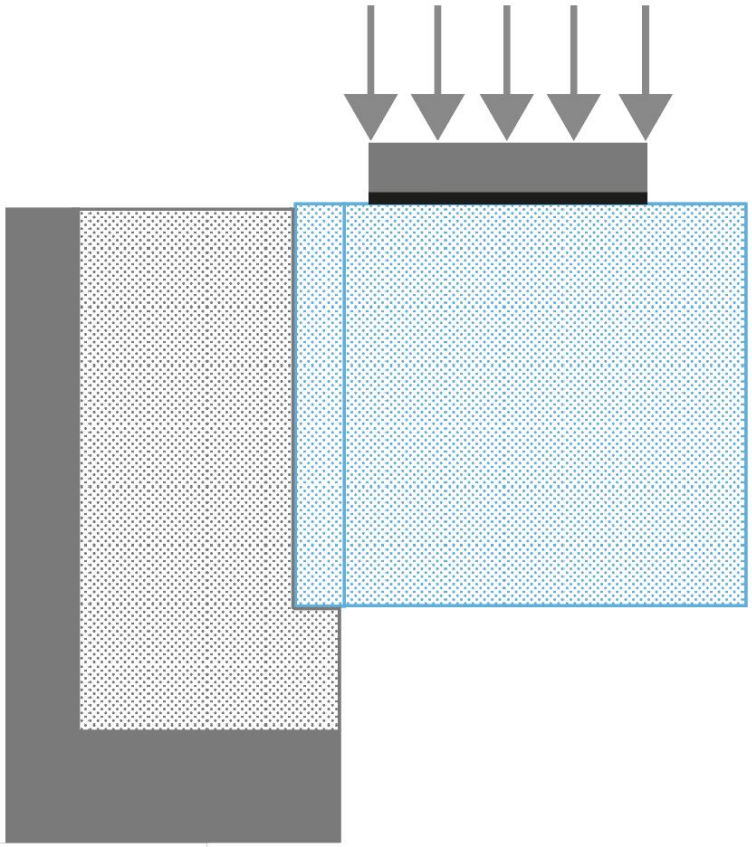

Figure 83: Design sketch of the shear test set-up, side view. The glass T-shape (dotted blue) is glued to an aluminum profile (dotted gray) which is attached to a steel test rig (gray). The load introduction block consists of steel and a rubber strip.

27.4 Structural Finite Element Analysis

The load situation has been analyzed prior to the experiment in finite element models. The same software is used as in the finite element model for the weld production (Section 17), thought this time, no thermal analysis is performed.

The glass T-shape was modelled with a perfect geometry. The connection was modeled as glass, so the virtual T-shape was perfectly homogeneous. By modelling the perfect situation, the differences between the model and test results can be explained by imperfections.

The results are presented in appendix D. The structural finite element model shows that the connection will be loaded in shear, and that this shear force will be well distributed.

The model also shows bending stress at the top and bottom of the connection, due to the eccentricity of the joint. The bending stress is maximum at the top and there is a possibility that this will be where the crack originates, though it should be noted that there are more possible causes for glass failure.

The finite element model demonstrates that it is complicated to perform a shear test on a T-shape geometry, without causing bending stress. However, after reconsidering other test set-ups, no better alternative was found, at it has been decided to perform this test.

27.5 Notes from Execution

The aluminum profiles had a thickness 6 mm behind the flange and 15 mm under the specimens. They were connected with bolts to the steel rig.

As the specimens were prepared, they were glued on the aluminum profiles. The welded profiles had a bent flange. The adhesive connection between flange and aluminum was not on the whole flange's surface. The adhesive surface was a few times wider than the glass joint. This can be seen in figure 84. The adhesive surface was the smallest for this specimen. It was concluded that the smaller adhesive joint is not likely to be critical or influence the stress distribution significantly.

During transport from the storage location to the test rig, a crack originated in specimen 10, a welded specimen (Figure 84). The most probable cause is accidental impact during transport. Residual stress could have contributed to the failure (Figure 68).
Because the adhesive and aluminum kept the flange in position, it has been decided to test the specimen.

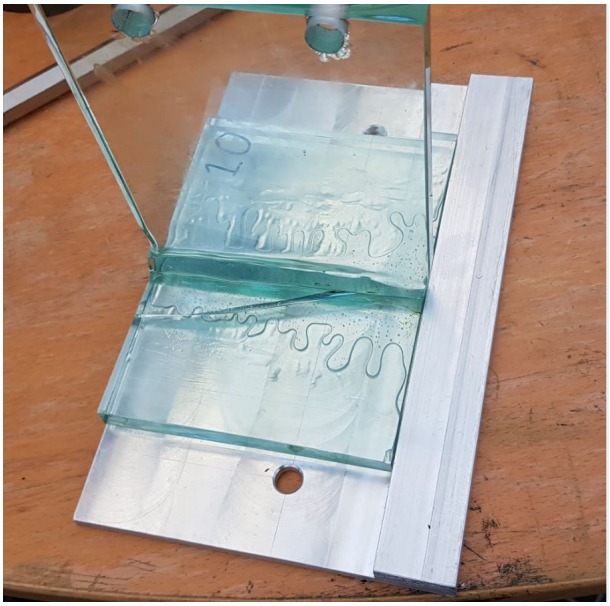

Figure 84: Specimen 10, showing the crack which originated during transport. Note the adhesive between the flange and the aluminum.

The load of the elephant's foot was transferred to the glass with a load introduction block. The block consisted of a steel block, 81 mm long and wider than the web, and a rubber strip. In the experiments,

the load introduction block was positioned on the web, with the edge $5\ mm$ from the joint. The web's edge of specimens 10 and 11 were not flat in this location. To prevent a load concentration, the block was positioned further away from the joint. The distance was $16\ mm$ for specimen 10 and $12\ mm$ for specimen 11.

The rubber strip was damaged throughout the experiments. The strip has been replaced after the testing of specimen 5, 6 and 9.

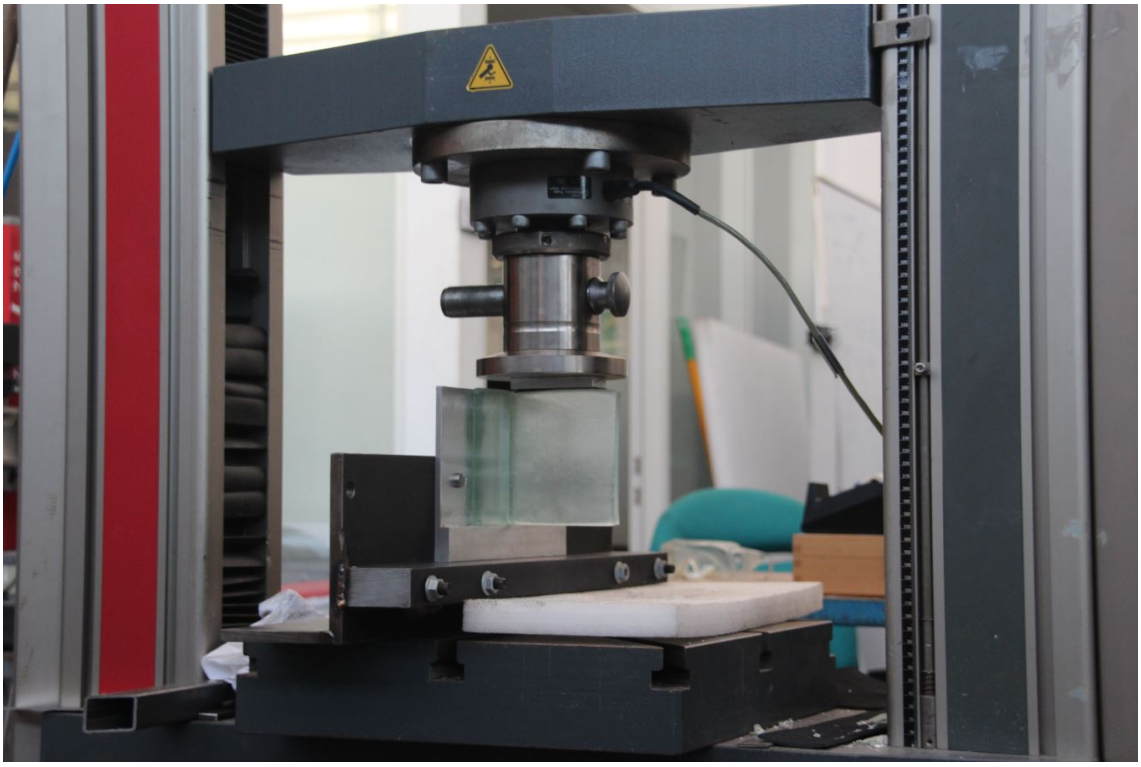

Figure 85: Picture of the execution of the test of specimen 7

28 Results of the Structural Test

The cracks in the specimen after the test are photographed and collected in appendix E. In figures 86, 87 and 88, the cracks in the glass elements are visualized. The dotted areas in specimen 6 and 7 indicate unknown cracks. Specimen 6 failed in many pieces and it was not possible to retrieve a crack image for this area from the footage or debris. At the time of writing, specimen 7 is connected, therefore it is unknown what the surface texture of the crack in or behind the joint is.

The adhesive specimens failed at the maximum load. For the fused and welded specimen, cracks appeared in the flange at loads before the failure load. These cracks appear as sudden reduction in load on the load-displacement curve of the results (Appendix F)). Therefore it is known that all fused and welded specimen showed initial cracks. The most plausible reason that cracks did not always coincide with failure, is because the specimen was glued to the aluminum profile and kept in position through a secondary load transfer mechanism through these materials. Due to observations during the test, in many cases it is known which cracks occurred when, but not all cracks have been noticed during the test.
For specimens 6 and 10, initial cracks are observed in the load-displacement diagram but were not noted during the experiments. Specimen 6 was the first to show an initial crack. This behaviour was not expected, and therefore there was no preparation for the phenomenon. It was only after the test of specimen 6, that it was decided to photograph initial cracks.
For specimen 10, the initial crack has not been photographed well, because it is not apparent on the pictures. The most plausible explanation is that the specimen was observed from the wrong side. The crack appeared on the other side of the welded joint, and the light distortion through the joint made it invisible on the photo taken.

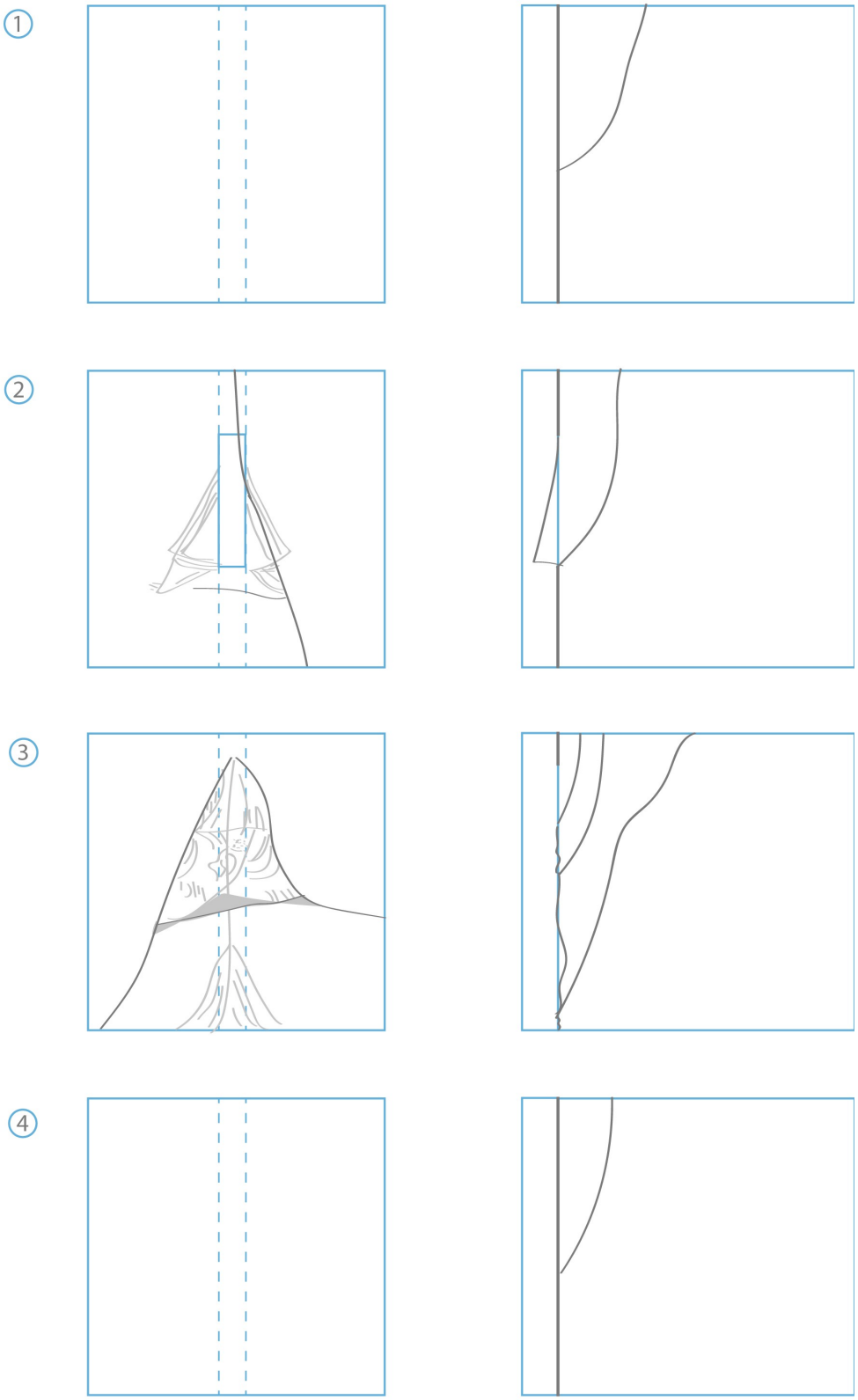

Figure 86: Cracks in specimens 1 to 4 (adhesive) after the shear test.

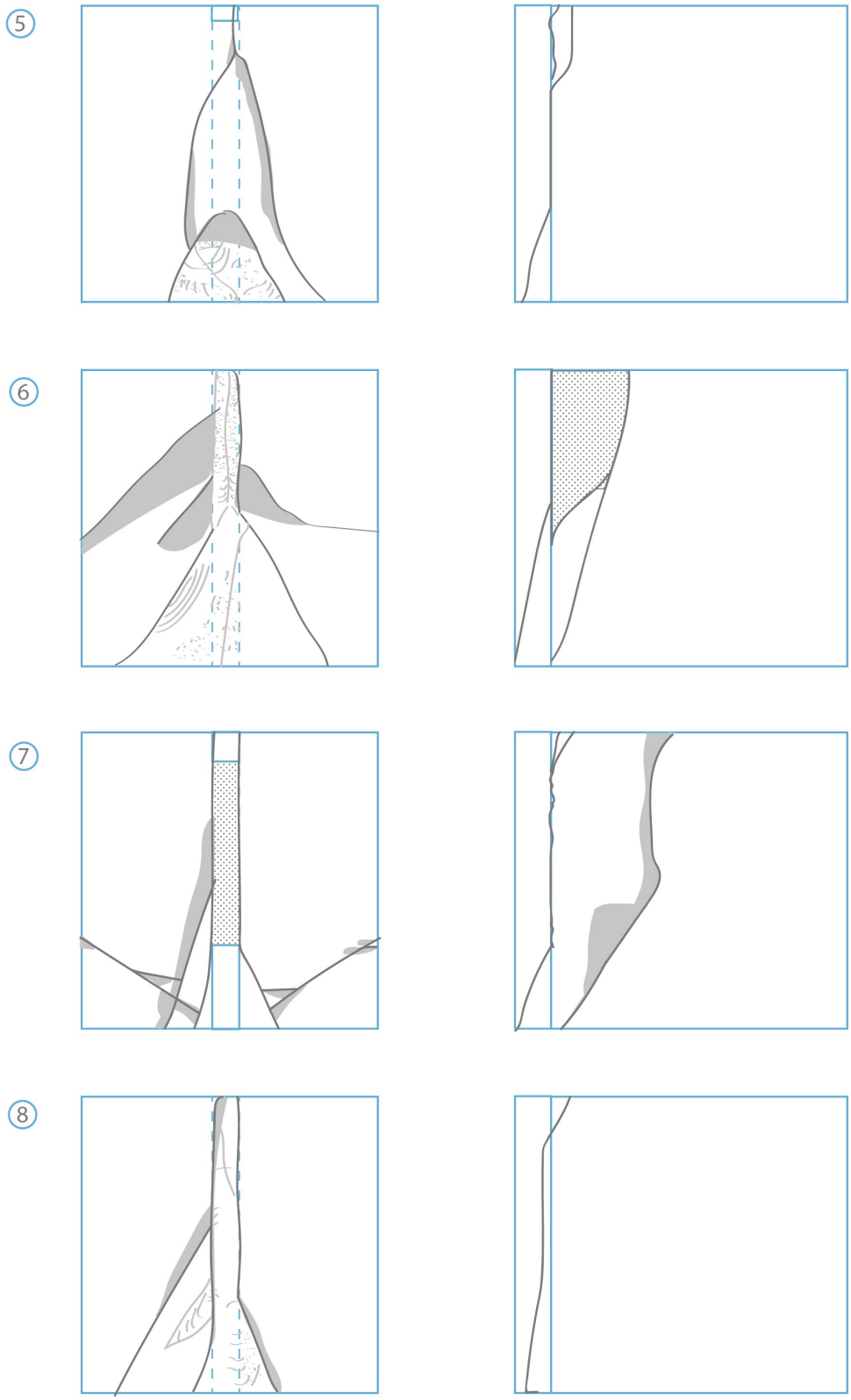

Figure 87: Cracks in specimens 5 (adhesive) and 6 to 8 (fused) after the shear test. The dotted areas indicate unknown cracks or crack surfaces.

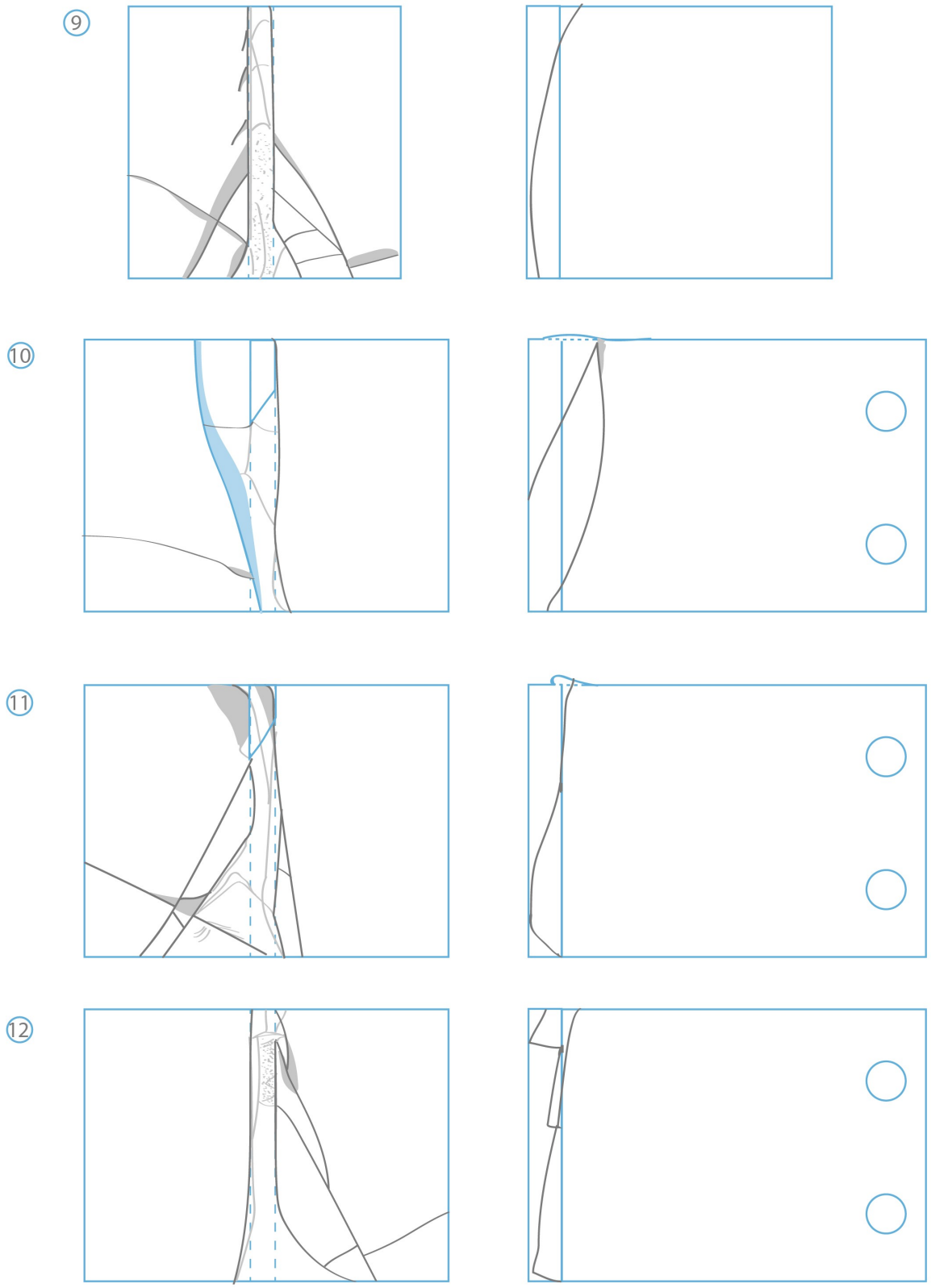

Figure 88: Cracks in specimens 9 (fused) and 10 to 12 (welded) after the shear test. The blue line in specimen 10 is the crack originated during transport.

28.1 Crack patterns

Many specimen show similar crack patterns. Four are described here, named Crack Pattern One to Four. The first noteworthy pattern is a crack through the flange of the specimen, through the edge of the joint (Figure 89). This crack bends at a few centimeter from the bottom edge and runs diagonal towards this bottom. This crack has been observed in all fused and welded specimens when the remains were examined. It has been observed that these cracks appeared as initial cracks in specimens 7, 8, 9, 11 and 12. They were present in the remains of specimen 6 and 10 as well, resulting in appearance in the remains of all fused and welded specimens.

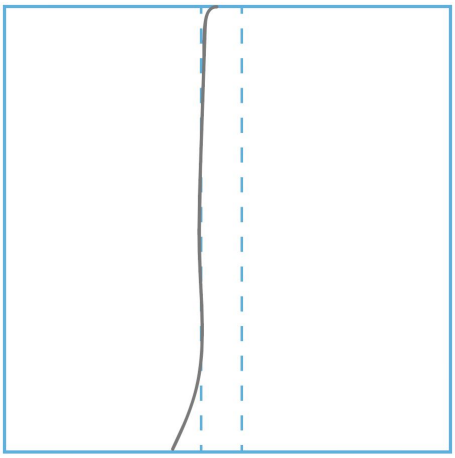

Figure 89: Crack Pattern One in the flange

Crack Pattern Two is a crack parallel to the diagonal section of the previously described crack and one end is connected to this crack, above where the first crack curves (Figure 90). This crack has been observed as an initial crack in specimen 7, 9 and 11. In these cases, it appeared after Crack Pattern One was observed. The crack pattern has been observed in the remains of all fused and welded specimen, except specimen 10.

Crack Pattern Three is a diagonal crack in the flange, on end connected to Crack Pattern One or Two, the other end is in the side of the flange (Figure 90). It is almost perpendicular to these patterns. It has been observed as an initial crack during the test in specimen 7 and 9, after observation of Crack Pattern One. It was observed in the remains of specimen 10 and 11 as well.

Crack Pattern Four is in the web and through the joint and has not been observed as an initial crack (Figure 91). Its appearance coincided with failure. The crack is between a point at or near the edge of the steel block introducing the load. The other end is beyond the joint, in the flange near the aluminum profile. It has been observed in all fused and welded specimen.
In some cases, specimen 6 and possibly 7, the crack is in the joint for a section of it. In others, specimen 9 and 10 the crack passes the joint without bending. The remaining specimens, 8, 11 and 12, show a bend, but the crack does not coincide with the joint plane.

Specimen 7, 8, 9 and 12 have remained connected after failure. In the case of specimen 12, the displacement at failure occurred partially instantaneously. Then, as the load was removed, the selfweight caused the web to slowly displace further until it was eventually separated from the flange. This took about 30 s. The webs of specimen 8 and 9 remained in position after failure. When the remains were

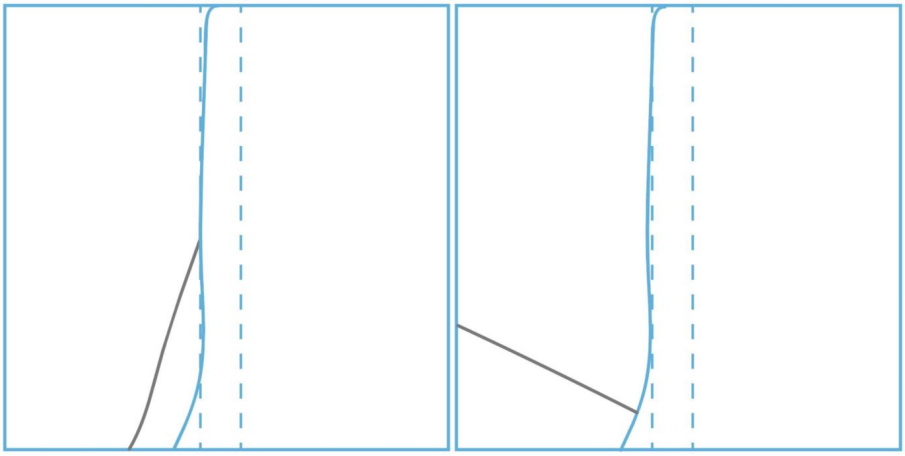

Figure 90: Crack Pattern Two (left) and Three (right) in the flange

examined, they were separated, though this required some light force to be applied manually. Specimen 7 had cracked in two positions on the web. One section has disconnected instantaneously, but the other is intact at the moment of writing.

The crack patterns have been observed in the fused and welded specimens. What kind of cracks are present in the adhesive specimens?
Specimens 1 and 4 have failed without a crack in the flange. These have delaminated. Specimen 2, 3 and 5 show diagonal cracks, resembling Crack Pattern One or Two, but are too different from the fused and welded specimen crack patterns to be assigned to these crack pattern types. Specimen 5 shows a crack through web and flange which resembles Crack Pattern 4. However, because the crack is clearly influenced by the joint, where a part of the joint has delaminated, it is too different from the others to be assigned to Crack Pattern Four.

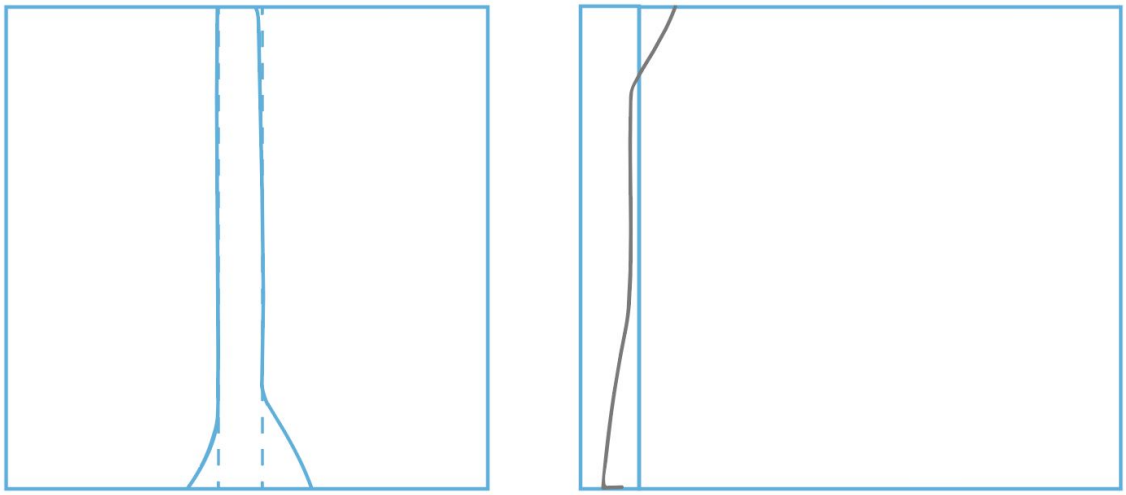

Figure 91: Crack Pattern Four in the flange and web. On the flange, the surface of the crack was between other cracks of Crack Patter One

28.2 Loads

The test rig measured the applied force and the displacement of the elephant's foot. The diagrams are presented in appendix F. The relevant loads on the specimens are gathered in table 9.

Specimen	Initial Crack Load (kN)	Failure Load (kN)
1	5,2	5,2
2	7,7	7,7
3	10,6	10,6
4	9,6	9,6
5	12,7	12,7
6	15,9	18,1
7	8,5	8,8
8	2,8	4,9
9	2,1	7,2
10	4,5	6,6
11	3,2	6,2
12	4,2	7,4

Table 9: Initial Crack Load and Failure Load for all specimens.

The initial cracks in the fused and welded specimens occurred at lower loads than the failure load. This load is named the initial crack load and is listed in table 9 as well. As the adhesive specimen showed no initial crack, the ultimate load has the same value as the load at which the first crack appeared.

Per connection method, the mean and standard deviation are presented in figure 92.

The area of the connection differs per specimen. This variable can be neutralized by dividing the load with it, resulting in a shear stress in the connection. This is not a stress capacity, because this is not always the area that failed. The presented shear stress should be considered as an engineering stress,

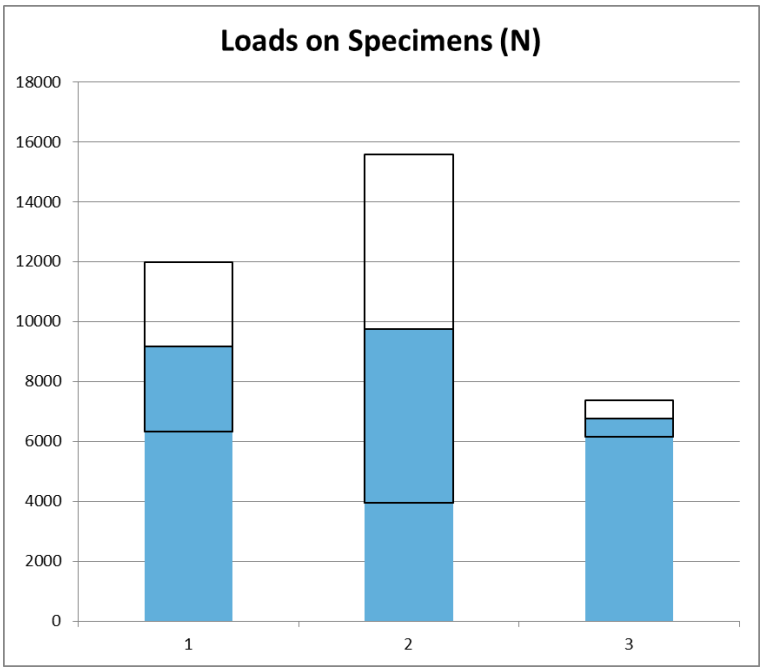

Figure 92: Ultimate loads on the specimens per connection method: adhesive (left), fusion (center) and weld (right). The mean value of the results is in blue. The black box indicates the standard deviation of the series.

a value to be used as a tool in design.

The area of the joint is measured by photographing the joint through the flange, with a ruler next to the joint to indicate the scale. By counting the pixels in the joint and scaling, the areas presented in table 10 are found. The mean and standard deviation of shear stress at failure per connection method are shown in figure 93.

The stress results show that the maximally obtained stress was in one of the adhesive specimens. The relative spread of the fused specimens is smaller for stress results than for load results. The relative spread of the stress results of the welds is larger than of the forces, but smaller than the stress spreads of the fusions.

Specimen	Area (mm^2)	Stress at Initial Crack (MPa)	Stress at Failure (MPa)
1	1200	4,4	4,4
2	1200	6,5	6,5
3	1200	8,8	8,8
4	1200	8,0	8,0
5	1200	10,6	10,6
6	1820	8,7	10,0
7	1370	2,0	6,4
8	1490	1,5	3,3
9	1670	1,3	4,3
10	1590	2,9	4,2
11	2050	1,6	3,0
12	1470	2,9	5,1

Table 10: Shear Stress at Initial Crack and Shear Stress at Failure for all specimen.

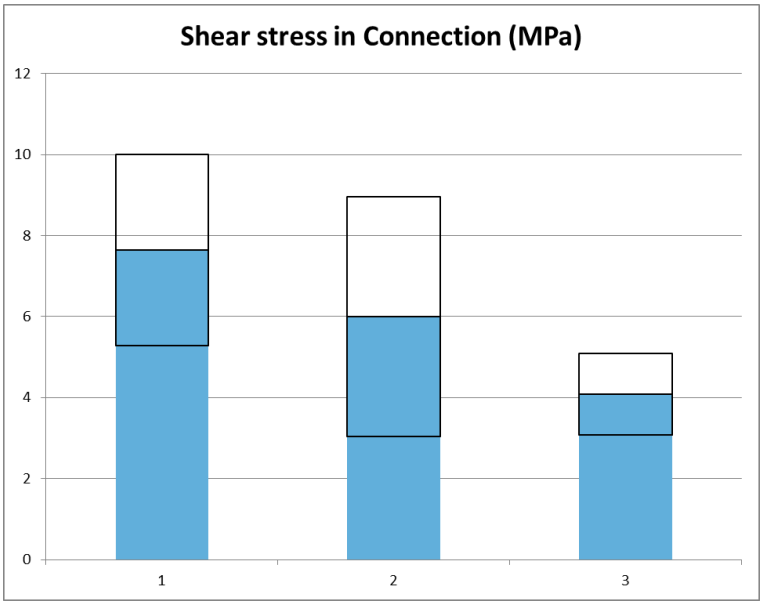

Figure 93: Shear stress in the connections at failure per connection method: adhesive (left), fusion (center) and weld (right). The mean value of the results is in blue. The black box indicates the standard deviation of the series.

29 Possible Failure Causes and Elimination

To explain the observed crack patterns, the possible causes are listed and eliminated to find the phenomenon which most likely have caused the crack pattern. The list of possible crack inducing phenomena is the following:

- Peak Stress
  - Damage
    Glass is sensitive to pre-existing damage on the surface and edge, because it causes a peak stress.
  - Geometry
    The perpendicular corner in the specimen is a location where stress peaks as well. A filleted joint reduces this stress. The seam between the web and flange of the fused and welded specimen increases stress locally.
  - Contact
    If two elements have a small contact area through which a force is transferred, local stress is high.
- Weakness in the Joint
  - Inhomogeneity
    This is related to the molecular scale of flaws in the joints. If the molecular structure of the joint is different from the structure in the web and flange, this could result in a lower stress capacity.
  - Pollution
    This is damage on a larger scale, like dust or air intrusion in the joint. These do not have to be visible to be present.
- Residual Stress
  Heat treated glass contains residual stress. If these are added to the mechanical stress, a fatal level might be reached unexpectedly.
- Overloading
  If the glass and all other circumstances are perfect, the stress distribution in reality is the same as predicted. Overloading causes cracks to occur where the calculated stress is maximum and above the capacity of glass. If the cause is overloading, it can be supported by finite element analyses.

29.1 Elimination

Residual stress is eliminated as a main cause for all cracks. The adhesive specimens are not heat treated and do not contain residual stress. The residual stress in the fused and welded specimen was analyzed qualitatively (Sections 26 and 23). It was concluded that the residual stress was low. It is possible that residual stress adds to mechanical stress or peak stress and therefore reduces the failure load. It is concluded that residual stress is never the only cause of failure.

Crack Pattern One, Two and Three are not caused by peak stress due to contact. It is plausible that a contact point between glass and aluminum increased stress, but the location where the cracks meet aluminum is too consistent for this to be likely. For the same reason, damage induced peak stress is

eliminated. Weakness in the joint cannot be the cause, because these crack patterns do not propagate through the joint.

Crack Pattern Four can, in some cases, not be caused by peak stress due to geometry. The peak stress is localized near the edge of the joint, through which this crack does not propagate in many cases. The pattern is too consistent to be caused by pre-existing damage.

Delamintation of the adhesive specimens is not related to peak stress, because this stress is in the glass. Overloading is not a likely cause, because the failure patterns are not consistent.

The diagonal cracks in the adhesive specimens are not caused by weakness in the joint, as they do not propagate through the joint. Overloading is unlikely to be the only cause, because the pattern is not consistent.

29.2 Remaining Causes

Crack Pattern One, Two and Three can be caused by overloading and peak stress due to geometry. Pattern Two and Three are secundary to Crack pattern One. It is plausible that the crack origin is in the surface of Crack pattern One, induced by surface irregularities. A combination of both causes is possible.

Crack Pattern Four is through the joint, so weakness in the joint should be considered. Overloading should be considered, because the pattern is present in many specimens and therefore probably related to the test design and set-up. Peak stress due to contact might have influence, because in many cases, the crack is at the edge of the block introducing the load.

The sections of the adhesive joints where delamination occurred were weaker than the surrounding glass. Delamination is most probably caused by pollution of the adhesive joint.

The glass cracks in the adhesive specimens are likely to be caused by peak stress due to pre-existing damage, in combination with overloading. Overloading has an influence, because the cracks show similarities with other observed failure patterns. Damage is of influence because the differences among the patterns is too large to be only caused by overloading.

Overloading has been named a possible cause for many observed failure patterns. However, the observed crack patterns were not predicted prior to the test. This led to the decision to model the test situation in finite element software with a support system which is more true to the situation. The aim is to research the influence of the dimensions of the aluminum profile and the support system on the stress distribution.

30 Analysis of the Glass-Aluminum Composite

The test result showed different behaviour than initially expected based on the finite element analysis. The behaviour was repetitive in the specimens. In the film footage, visible deformation of the flange at failure was observed: as the glass failed, it snapped beck in its original position. These observations indicated that the size and support method of the aluminum profile might be of influence on the observed crack patterns.

30.1 Mechanisms

The stiffness and support system of the glass aluminum composite could have caused a specific deformation. Two mechanisms cause important stress concentration.
As the object is loaded in shear, a mechanical arm causes a bending moment. The glass-aluminum object rotates around its fixation, the bolts. The top bends forward, the bottom remains in place because it is pressed on the steel. This results in a kink in the deformed shape (Figure 94). The section above the bolts is unconstrained and contains lower stress levels. The section below the bolts is constrained and highly stressed. The difference in stiffness causes peak tensile stress in the joint at a lower location than expected.

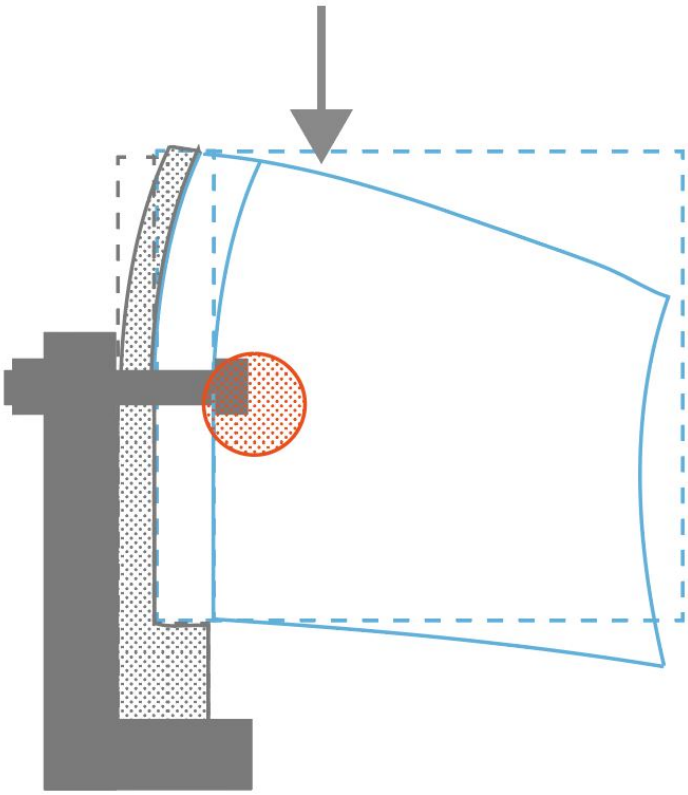

Figure 94: First mechanism of the glass aluminum composite. Side view of specimen. The red circle is where the stress peaks.

The second mechanism is best explained by a two dimensional model of the top section of the T-shape composite (Figure 95). As the specimen is loaded, the web deforms, its top section moving away from the flange. The system is anchored with the bolts. Considering the flange as a simply supported beam, and the joint to the web as a discrete change in rigidity of the beam's cross-section. This causes a peak stress in the edge of the joint, a tensile bending stress parallel to the beam.

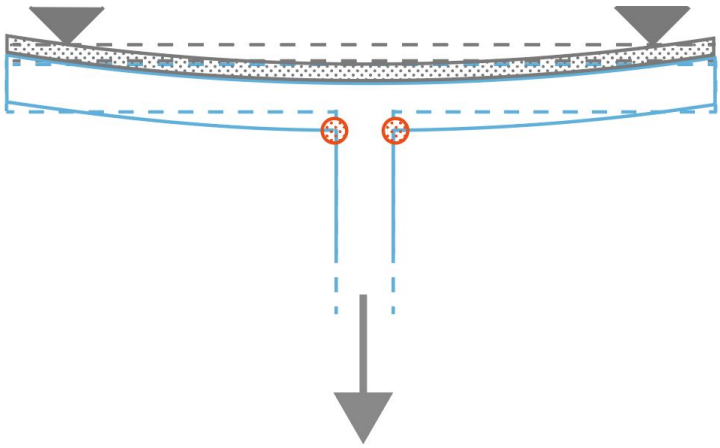

Figure 95: Second mechanism of the glass aluminum composite. Top view of specimen. The red circle is where the stress peaks.

30.2 Finite Element Analysis

A finite element model is made with the dimensions of the aluminum as applied in the test. Upon analysis of the footage of the test, the support of the aluminum was deducted to a mechanical scheme. The vertical and out of plane support of the aluminum profile is provided by the bolts. The steel behind the aluminum has functioned as a support for compressive forces.

The results of the finite element model show the described mechanisms and stress concentrations. The results are presented in appendix G.

A second model is made in which Crack Pattern One was simulated by splitting the geometry here and creating a $0,2\ mm$ gap through which load transfer is not possible. The results of this model are presented in appendix G as well.

Crack Pattern One is a result of overloading in combination with geometry induced peak stress. The stress distribution shows tensile stress peaks in a position and direction that match this pattern. This distribution is a result of the second mechanism described and illustrated in figure 95. The lowest load at which this pattern was observed does not result in critical stress levels, so the peak stress has contributed to the failure.

The second model shows that the stress in the crack surface of the flange can be critical. Additionally, it shows that the areas where Crack Patterns Two and Three propagated through are stressed as well, explaining the trajectory of the crack. On the other hand, it also shows that the flange section on the other side of the crack contains higher stress, which does not explain why Crack Patterns Two and Three would occur before Crack Pattern Four.

However, these patterns were not always observed before failure. Therefore it is concluded that the load distribution shows that these areas contain high stress due to overloading, and that peak stress due to damage in the pre-existing crack contributed to the crack origination.

Crack Pattern Four is most probably caused by the high stress in the joint. Due to the first mechanism described above (Figure 94), the stress parallel to the web surface is maximal at half the height of the specimen.
This is supported by the triangular base of the crack. The propagation of the crack causes a shock wave in the material that spreads in all directions. The lines of the triangular crack base meet at half the height of the specimen, indicating this could be the origin of the crack.
It is probable that peak stress due to damage or, in some cases, geometry contributed as well. It is also possible that weakening in the joint has contributed to the failure origin and crack path. This is most likely to have aided in the fused specimens 6 and 7, for these have failure plains parallel to the joint.

If it is accepted that the described mechanisms cause the crack patterns in fused and welded glass, it can be concluded that this model does not describe the adhesive specimens. These did not show initial cracks and did not show the described crack patterns. The model contained homogeneous glass, so it might be that the adhesive layer is not represented well by homogeneous glass. It is probable that strain in the adhesive redistributes stress over the joint differently than homogeneous glass in the model.
If the model predicts the behaviour of fused and welded glass better than that of adhered glass, it means that the fused and welded joints are closer to a homogeneous glass joint. It suggests that it has been succeeded to create an all glass connections, with a homogeneity of at least a quality that ensures failure to follow the patterns of an ideally homogeneous virtual model.

31 Conclusions of the Structural Test

In previous sections, the results of the structural test has been described. This lead to further analysis of the structural system, including the effect of the aluminum profile. In this section, conclusions are drawn.

31.1 Failure Patterns

The fused and welded specimen had initial cracks before failure. It is considered most probable that these cracks propagated well and that a secondary load transfer mechanism via adhesive and aluminum was in place. The stiffness of the composite did not reduce significantly. The adhesive specimens failed at first crack.

Crack Pattern One is most probably a result of a peak stress on the flange surface, because the web bends away from the flange (Figure 95). Finite element analyses showed that this mechanism is likely to be critical. However, because the load did not result in critical stress in all cases, peak stress due to the seam in the joint has most probably increased the stress.

Crack Patterns Two and Three are not as well proven with the finite element models. Therefore, irregularities in the crack surface of Crack Pattern One have probably increased the stress. Other causes, peak stress due to pre-existing damage and residual stress, could have had an influence as well.

Crack Pattern Four has probably originated in the edge of the connection, at a height halfway the specimen. This is the area stressed by the first mechanism of the glass aluminum composite (Figure 94). The energy released in the propagation of this crack has possibly caused the diagonal pattern near the bottom. The upward direction of crack propagation has followed the path of least resistance, which is possibly the stressed region between connection and the load-introducing block.

Crack Pattern Four bends near the joint in some cases. This is observed in the fused specimen, but not in the welded specimen. This could suggest that the fused joint is a weaker area than the glass surrounding it, which would most likely be caused by inhomogeneity, or (chemical) pollution during production. This observation suggests that the welded joints are more homogeneous than the fused connections. However, the series is too small to state this as a definite conclusion.

The adhesive joints show different fracture patterns. This difference is not directly relatable to the capacity, as the delaminated joints did not resist the highest or lowest loads.

It has been observed that the web and flange for specimens 7, 8, 9 and 12 where not fully detached after failure. There are three probable reasons for this. The first is that the adhesive between the glass and the bottom supporting aluminum keeps the cracked glass in position. The second possibility is that glass splinters in the crack interlock and cause friction which is able to keep the specimen together. This is a possibility for specimens 7, 8 and 9, because splinters were observed. The third is that the crack did not propagate through the glass completely due to a compressive stress field.

31.2 Failure Loads

The series tested was small, therefore no determining conclusions can be drawn from the experiment. The results only suggest an order of magnitude and a prediction of the consistency of results. The failure loads of all specimen have the same order of magnitude.

The specimen can be considered as a building component. In this case, the failure load is relevant. When the experiment is used to conclude something on the joint, the shear stress in the joint is relevant. This shear stress at failure is not a capacity, but an indication for a designing engineer.

Because the series is too small, no conclusions can be drawn based on the mean and standard deviation of the results. However, the results provide an indication of a maximum and minimum possible capacity. Experienced researchers in the field of structural glass apply a third of the minimum measured failure load as a statistical minimum representing the one in thousand failure load. The explanation about the value of this factor is provided in appendix H. This is a very rough and possibly not conservative estimation and can never be used in practice or construction. In this thesis it will only be applied to show what these results indicate, but not prove.

The initial crack load and stress are considered but are not used in the suggested statistical minimum and maximum load and stress. If the load is regarded, the composite is considered a building component. The component remained intact and able to bear load after the first crack. The ultimate failure load is more interesting in this case.
If the stress is considered, the concept of the joint is analyzed. The initial cracks have been attributed to the stiffness and supports of the components and are therefore not relevant for the concept of the joint.

The possible statistically minimum and maximum of the ultimate failure load of the specimens per connection method are displayed in figure 96.

The relative maximum of the fused joint is largest, 1116% of the possible statistical minimum. The weld has the smallest relative maximum with 358%. This is especially small considering that, by definition, this percentage has a minimum of 300%. The adhesive is in between, with 724%.

Considering the possibilities of the joint loaded in shear, a shear stress is obtained, removing the varieties in the joint's cross-sectional area among the specimen. The results are shown in figure 97.

The relative maximum stress of the adhesive is 724% of the possible statistical minimum, which is the same as for the loads, because the areas of all adhesive specimen are equal. For the fused joints this is 914%, the weld 499%. The expected spread of the fused joints is largest when considering loads and stress. For both quantities, the spread of the weld is smallest.

The highest minimum and maximum stress is measured in an adhesive specimen. This indicates, that with the current state of development, the most slender structure can be achieved with adhesive joints. However, this conclusion is not definitive due to the small series.

The fused joints show a large range for the capacity, though it reduces if the cross-sectional area is neutralized. This suggests that there are factors influencing the capacity which were different among the specimens. In section 25, differences among the specimens are described. Most differences are due to changes in the production process and had little influence on the appearance of the specimen. It cannot be concluded whether one of the observed differences has contributed to a difference in

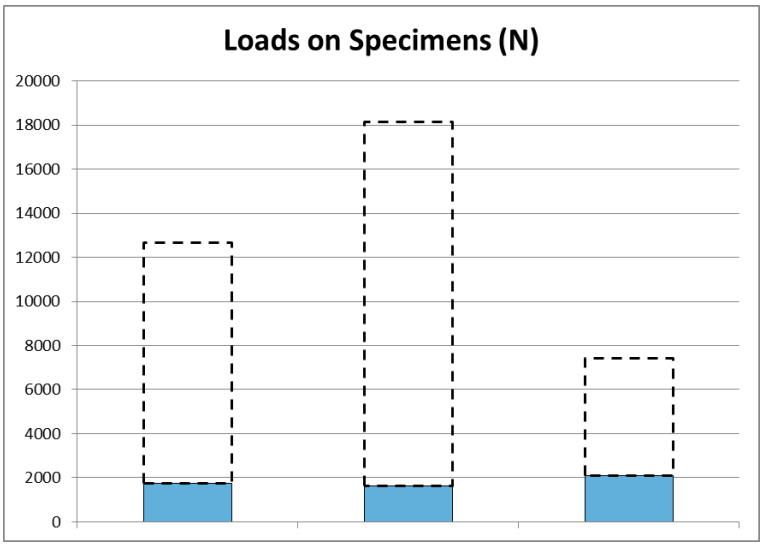

Figure 96: Ultimate load potential on the specimens per connection method: adhesive (left), fusion (center) and weld (right). The possible statistical minimum is indicated in blue. The upper segmented line is the possible maximum value. The segmented line circumferences the loads which are the expected load capacity of the system.

capacity of the fused specimen.
The cause of the differences among the test results of the fused specimen cannot be determined, though some factors are more likely to have had an influence than others. It has been stated that the fused joints are possibly not as homogeneous as the welded joints. The mould material becomes dust when contact causes abrasion. Dust could have settled between the glass elements before fusion, regardless of the cleaning of the glass seconds before positioning. In the welding process, this material was not used, so it is possible that less dust intruded the welded joints. This is a probable cause for the difference in spread of the results.
The large spread of the results for the fused objects, suggests that quality control of the production process can be the key step toimprove the structural performance.

The welded joints show good consistency in ultimate failure load. This is remarkable, considering the visible differences among the specimen and the accidental crack in one of the specimens before testing. The results suggest that it could be possible to obtain consistent capacity with welded connections. They also suggest that the load capacity is not highly sensitive to differences in the production process and differences in dimensions. It is possible that there is a dominant mechanism present which was consistent for these specimen, resulting in consistent failure loads.

31.3 Discussion

The welded specimen are larger than the others. However, this is not of key importance, because the length of the joint is the same for all specimens.
The flanges of the welded specimens are curved. The adhesive between glass and aluminum is therefore not on the whole surface, but only present in the area around the joint. It is unknown what effect this had on the crack patterns and failure loads.

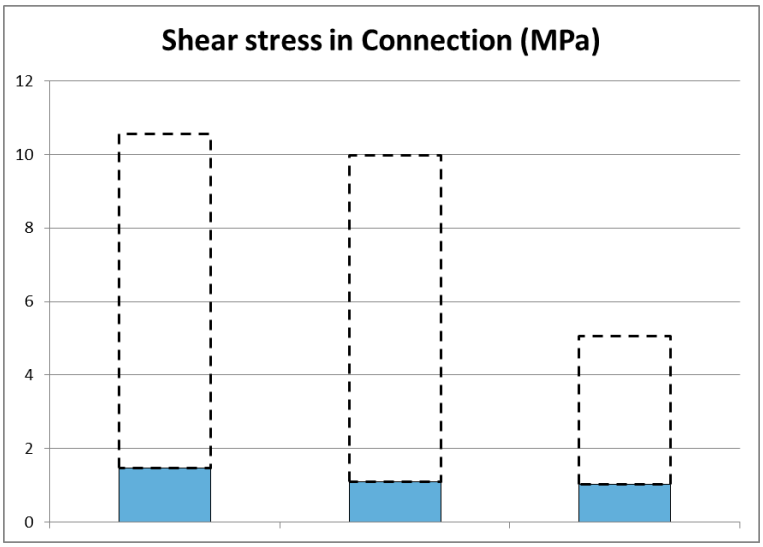

Figure 97: Shear stress potential on the specimens per connection method: adhesive (left), fusion (center) and weld (right). The possible statistical minimum is indicated in blue. The upper segmented line is the possible maximum value. The segmented line circumferences the stress levels which are the expected stress capacity of the connection.

Due to elimination, many causes of cracks have been indicated as unlikely and others are suggested to be the most probable cause. It is not proved whether these explanations are correct and they should, therefore, not be taken as an absolute cause of failure. All mentioned causes could have contributed to failure, for example a present residual stress or a contact point between glass and aluminum could have influenced the failure behaviour.

The most plausible cause of the observed crack patterns is the mechanical behaviour of the glass-aluminum composite. This is different from the behaviour as it was designed prior to the test. The thickness of the aluminum profile was too little to be considered stiff. The connection method to the steel element resulted in sections with a different rigidity and unforeseen stress concentrations.

The reason why this behaviour was not predicted, is that the thickness of the aluminum profile and its attachment to the steel system have not been considered well in the test design phase. The difference between the designed aluminum block and the eventually used slender plate has been too large. An order for aluminum profiles has been made without specifying the thickness.

This test has shown that a pure shear test is not easily performed on this type of geometry. The bending stress has most probably been fatal in the specimens.

This test loads the joint in a different manner than the other elements in the specimen. Therefore, the capacity of the joint and the glass cannot be compared. No conclusion can be drawn on whether the joint is stronger or weaker than the parent material.

The number of specimens is too small to draw conclusions on load or stress capacity. The results of this experiment can and should only be used for an indication of the order of magnitude. It is strongly advised against, to use the results in any application without further research. The small spread in results shown by the welds, could also be a materialization of a situation with low statistical

probability. It could have been luck.

31.4 Recommendations

The large spread among the fusion results is most probably caused by inhomogeneity and dust intrusion from the mould material. This contributes to the recommendations to research a different mould material for this process, as explained in section 26.

It is highly recommended to perform the test again with a larger series for statistical significance. Further research is recommended in different load situation as well. Little is known about the behaviour in tension, compression, bending, torsion, buckling or other cases.

A sufficiently large four-point bending test series is recommended to research whether the joint has the same capacity as the parent material.

It is recommended to ensure what the influence is on the mechanical behaviour, of the elements supporting the specimen. In this experiment, the influence of the aluminum on the glass was different than expected, resulting in a less pure test than predicted. Preventing this could have resulted in more knowledge on the mechanical behaviour of the joints. Therefore, it is advised to specify the dimensions of the support system while designing the test set-up.

32 Qualitative Comparison

With the structural test, the connection methods have been compared quantitatively. But there are more aspects to the connections methods and product properties which are relevant for any application in the building industry.

Glass structures are used to add prestige to a project. Aesthetics is a key element. Furthermore, it is ideal if the production, installation and maintenance of the product uses as little time, energy and money as possible.

The connection methods are in different states of development, one requires more future research than the other. In this section, the required additional research is not considered, because the investment in research should, ideally, never block innovation.

32.1 Aesthetics

Aesthetics are subjective, and there is no stage for taste in this thesis. However, glass is an interesting material because it is transparent. It is used due to a world wide fascination for dematerialized structures. Transparency is a criterion.

Figure 98: Adhesive (left), welded (center) and fused (right) objects.

The fused product is therefore not ideal, because of the translucency. The translucency is partially a result of the texture of the mould. Different mould textures will result in different glass textures. The mould will not be as smooth as the glass surface of a float glass production process, because this is smoothened by surface tension on a molecular scale. With every mould material, grinding and polishing is necessary to obtain a transparent product.

Polishing the object will provide sufficient transparency. Cast glass objects need to be polished after cooling as well, for the same reason. The Crystal Houses project in Amsterdam proves that polishing provides a transparency which is sufficient for a project. The difference is that the fused products are more slender, and therefore fragile, than cast products, and should be polished with caution.
It has been concluded that other factors aid to this effect, because not all texture can be related to the moulds and because edges which did not touch the mould are translucent as well. It is unknown what the effect of these factors is when a different mould type or material is used. However, these effects can still be undone with post-production polishing.

Te adhesive joint is transparent. The texture of the glass is unchanged and the adhesive is transparent. The edges of the glass reflect and refract lights differently than a homogeneous glass joint. From some viewing angles, the perpendicular connection is less visible (Figure 99).

The welded glass joint is transparent because the glass is smoothened by surface tension during cooling. The texture of the surface is smooth, but in the products of this thesis, the surface itself was not flat. This effect can be a wanted aesthetic quality or not and is therefore subjectively advantageous or not. It has been observed that in the production, improvement is made in the shape of the joint. In the second experiment, only the web was heated well, and the result showed this difference in heating. This has been improved in the third welding experiment, where both elements were molten and the joint showed a smoother transition from web to flange.
The welded joint is less visible from several viewing angles. It has been observed that from most angles, the visibility of the welded and adhesive joints is similar 99.

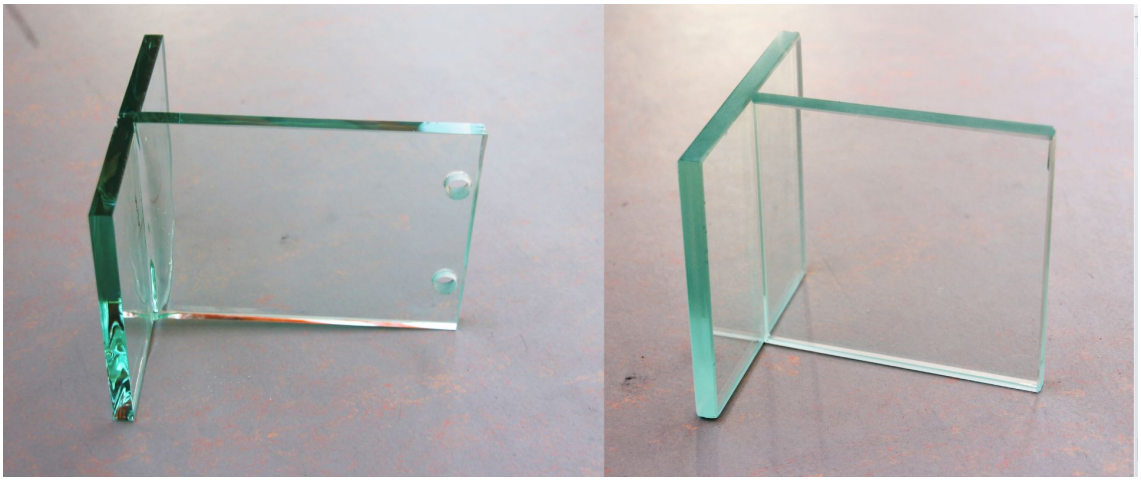

Figure 99: The welded (left) and adhesive (right) joint from an angle at which the connection is less visible.

It has not been achieved to create a smooth circular fillet in any of the joints. This fillet is aesthetically interesting, because it adds a new feature to perpendicular glass connections. It is also considerd that this fillet can have beneficial influence on the structural capacity, because fillets reduces peak stress.
The adhesive systems showed a seam because it is a composite. In the fused objects, it has been tried to create a fillet, but this has not succeeded. It is unknown if this is a possibility in fusion, at a temperature low enough not to be considered casting. In the welded systems, the seam was present. Considering the improvements made in the welding experiments, it is predicted that the welded process could be improved with the aim of creating the desired fillet in the connection.

32.2 Accuracy

The accuracy of the product is the possibility to produce an object with the desired shape and measurements. This property is important, because in the building industry, it has to be possible to design elements to an accuracy of millimeters. The adhesive specimens provide good accuracy. The adhesive is thin and the glass can be cut to size.

The fused specimen showed poor accuracy in this thesis. The thickness varied from $9,9$ to $12,5$ mm within one specimen. Additionally, the length of the web was variable due to deformation. It as been recommended to change the mould to improve this. Further research is necessary to create tolerances which are acceptable in the building industry.

The welded products had a thickness that remained 10 mm at a certain distance of the weld. Because no material was added when connecting the elements, the web is shortened in the process of pushing the viscous region's together. The length of the web has therefore been variable among the welded products.
Additionally, in all specimens, the flange was bent.
It is predicted that improving and controlling the glass weld production process will result in products with better accuracy. For example, prescribing the distance over which the web has to be lowered fixates the length of the web in the product.
Further research into prevention of a curved flange is necessary to result in a product with sufficient accuracy.

Post processing the products, cutting and polishing after the connection is made, is a possibility. The products are annealed and can be cut. It is advised to improve the annealing schedule if this solution is applied.

32.3 Time

Adhesive connections are made in a matter of minutes. Heat bonded joints are created in a matter of days. Therefore, the adhesive joints require the least amount of time. This makes them more convenient, easier to do again and therefore beneficial.

The heat bonded joints require more time because they have to be annealed. Where the process of casting a glass brick can take more than three days, the production of fusing and welding has taken two (Jacobs 2017).

The time the fuse requires is all passive. Once the oven is closed, no attention needs to be given to it until the product is taken out. Especially because in the production process applied in this thesis, quenching by opening the oven showed to be superfluous.

The time the weld requires is passive at preheating and annealing, and active for a few minutes while welding. The duration of the active process for the weld is the same order of magnitude as for the adhesive.

Though a large section of the time requirement is passive for human attention, it is not for equipment. While the products are heated and cooled, the ovens are occupied. An example of a logistic inconvenience resulting from this, presented itself in the welding process. To make the box oven available for

the next experiment, the object was relocated to a second oven. The glass system had to be cooled for relocation and reheated for annealing in the second oven.

32.4 Energy

The time use in the oven introduces the next subject, the use of energy during the experiments. It is unknown what the energy usage of the adhesive joint is, because the production process of the adhesive is out of the scope of this thesis.
Considering the adhesive, it should be noted that the energy required to recycle the system is significant, because recycling components is more complex than recycling mono materials (Section 7).

The fused systems require a significant amount of energy, which is used to fuel the oven. The welded systems require the same oven usage, though oven temperatures are lower, and the energy for the welding torch. Its energy source is fossil fuel and there is currently no suitable alternative, using a renewable source.
It is concluded that the weld requires most energy and least sustainable energy compared to fusion.

32.5 Skill

The amount of skill required differs per method. The least skill is required for the fused method. Most skill is in manufacturing the moulds. If these can be re-used, all required skill is in positioning the glass and moulds in the oven. In this thesis, the skill required to create the fused connections showed to be not too challenging.

More skill is required for the adhesive. The manufacturers for the Crystal Houses project have been trained specially for this purpose. In this thesis, the adhesive bonds were made with less protocol and accuracy than in the Crystal Houses project. In the structural test, two out of five adhesive specimens delaminated, emphasizing the importance of skill in the production process.

The welded products require not only skill, but also experience. The manufacturers were professional glass blowers. Their experience was required to know the moment when the glass' viscosity was low enough to press the elements together.

32.6 Money

The time, energy and skill listed above can also be expressed in money. High requirement of these results in a more expensive product.

The costs made related to this thesis cannot be used well to compare this. As a project of the TU Delft, the facilities and manhours of the university were relatively cheap, as opposed to the external facilities and manhours at the LiS for the welds.

It is reasoned that the weld is more expensive because of the required skill and experience. Manufacturers can charge a higher fee for rare skills.

Another option is to train someone for the glass welding purpose, but this investment will be of sig-

nificant size as well. The investment in training adhesive joint manufacturers is estimated to be lower.

It is estimated that, after research and development is invested in, the fused and adhesive joints are in the same order of magnitude of price. The energy requirement of fusion and the skill requirement of adhesion could result in similar orders of magnitude.

The weld will be most expensive, even after research and development. This is mostly due to required experience with glass at elevated temperature. If the process can be improved into a protocol, it is possible to prescribe the time at which the weld is to be formed. In this case, the experience with the glass would be less necessary.

Money has always been an obstruction with heat bonded glass joints. This thesis has taken one factor, which drove up the price, out of the comparison: material. Glass welds were previously researched in borosilicate glass, because it is less sensitive to thermal shock. In this thesis, it has been demonstrated that welding cheap soda lime glass with a structurally relevant thickness is possible.

33 Heat Bonds on a Larger Scale

In this thesis, the heat bond has been researched on a scale of a few hundred millimeters. The product's had a size of 120 to 160 by 130 to 170 mm. Building components can be designed larger. Based on the results of this research, a vision is presented on the options and obstacles of producing and implementing larger, heat bonded systems.

For both method, the product's size is limited by the oven size. To produce larger heat bonds, larger ovens are required. These ovens exist, but are used in other industries. For upscaling glass heat bonds, it is recommended to look at the steel industry. In the steel industry, annealing ovens of considerate size are used. The temperature required for annealing steel is 725 $°C$ to 1150 $°C$, depending on the carbon content (Dossett and Boyer 2006).
When using soda lime glass, the required oven temperature for welding is 500 $°C$, and for fusing it is 765 $°C$. Note that, as a result of the recommended research into temperature schedules, these temperatures may vary in future processes, but they are not predicted to exceed 1150 $°C$.

Figure 100: Large industrial annealing oven (Electrotherm Electrical & Metal Products Ltd. 2018)

In the steel industry, industrial annealing ovens of several meters in size are used (Figure 100). For example, an industrial machinery producer describes a box oven they offer, with an inner working zone of $2,5$ by $4,4$ by $1,5$ m, which can reach temperatures up to 1200 $°C$ (Electrotherm Electrical & Metal Products Ltd. 2018). Much larger ovens are not likely to be required, because transport, most likely by road, imposes another limit on the size.

For the fusion process, larger moulds should be produced. It is recommended to research the influence of mould types and materials on the product (Section 26). These results can be implemented when increasing sizes of glass fusion.

The second element to be enlarged for the welding process is the welding torch. By using a longer tube to make the line burner and increase the gas outflow, this can be done relatively easily. If the burner becomes too large to hold or handle, it is advised to use robotic arms for this. These are also applied in industry for mass producing forging (Figure 101) (Electrotherm Electrical & Metal Products Ltd. 2018).

Figure 101: Robotic arm operating in oven (Electrotherm Electrical & Metal Products Ltd. 2018)

If a large oven is used in the welding process, manually welding can become impossible due to the heat. In the small scale process, manual welding was performed to introduce the heat and press the elements together. If this is not possible in the larger scale process, due to exposure of the welder to heat, it is recommended to use robotic arms.
In the small scale process, the experience of professional glass blowers was used to determine the moment at which the weld should be formed. This could still be done in the large oven with remote controlled robotic arms, if cameras or transparent oven walls are used to make observations outside the oven possible.
The large oven requires investment. If investments are made, it is recommended to invest in an automated process as well. A thermal final element model, like the one made for this thesis, can be used to predict the time required for heating and making the connection. It is predicted that after elaborate research, the glass welding process can be automated like the steel welding process.

In both production processes of this thesis, gravity is used to press the web on the flange. It is recommended to rotate the elements before connecting them, to a composition that benefits from gravity during production.
If the size of systems is increased, it is possible that rotation is not desired or too complicated. If this is established, it is recommended to research production processes with a different orientation, for example a vertical heat bond.
Based on their experience, the glass blowers who made the welds for this thesis advise to benefit from gravity if possible. In another configuration, the heated glass could not stick as easily. Viscous glass moves inward, towards a spherical shape. Making a vertically positioned joint could be complicated if the elements move away from each other.

Considering the structural strength of large heat bonded joints, little can be concluded based on this thesis. It has been recommended to perform more structural tests. Until these are performed and a proper statistical analysis is executed, no definitive conclusions can be drawn on the structural capacity of heat bonded joints. Drawing conclusions on the heat bond's capacity in case of larger sizes would therefore be premature.
The spread of results for the fused and adhesive specimens indicate that it is important to improve quality control and prevent dust intrusion. These aspects are to be considered when the sizes of heat bonds are enlarged.

As for all glass structures, the design of a glass component and its application should take into account the safety of the structure and the replacement strategy in case of failure. If the size of heat bonded systems is increased, it should be taken into account that the heat bonded system fails if an element of the system fails. In case of damage, the consequences are larger for larger elements. Replacement of larger elements could impose challenges.

In summary, the required large oven exist, because they are used in the steel industry. Larger heat bonds can be welded with robotic arms an fused with large moulds. If required, it is recommended to research the possibilities of different orientation of elements during production. It is premature to predict the strength of large heat bonds. When enlarging and implementing heat bonded systems, transport, structural safety and replacement should be considered properly.

Part VII

Conclusions

34 Conclusions

34.1 Research Questions

The aim of this section is to provide an answer on the research questions. The main question is the following:

What is the best method, among glass welding and kiln formed glass fusing, to produce heat bonded systems for applications in glass structures?

To define the term 'best', the following set of sub-questions is used:

- How can the structural safety of a heat bond be ensured?
- Which method results in a system with the least residual stress?
- How can thermal shock failure be prevented during the welding process?
- How can the tolerances of the fused product be limited, to make the product applicable in structures?
- Which method, among heat bonded joints and suitable alternatives, has the best structural performance?
- How do the methods, heat bonded joints and suitable alternatives, compare on qualitative aspects?

34.2 Structural Safety

- The structural safety of the heat bonded system can be provided by tempering, laminating and reinforcing the glass system, though this requires additional research.
- Outside of the system, safety can be provided by protecting, overdimensioning and creating a secondary load transfer mechanism.

34.3 Residual Stress

- The welded objects have a very low residual stress level and are practically stress free.
- The residual stress in the fused objects is lower than in the welded objects.
- For all specimen, it is concluded that the applied annealing schedule has been appropriate to prevent residual stress sufficiently.

34.4 Weld Production

- It is possible to weld soda lime float glass of a structurally relevant thickness.
- The risk of thermal shock failure can be reduced by heating the to be welded areas from all sides or by maintaining the surroundings at elevated temperature. The latter has been applied in the experiments of this thesis.

34.5 Fusion Production

- It is possible to fuse soda lime float glass of a structurally relevant thickness.
- The mould has a paramount influence on the quality of the product. It has an influence on the texture of the surface and the aesthetics of the product. It also influences the deformations during production and the dimensions of the product.

34.6 Structural Test

- The cause of failure is most probably a combination of elevated stress due to the stiffness and support of the test set-up and peak stress due to irregularities on the glass surface. Other causes could have contributed to failure.
- Considering the test specimens as a structural object, the expected statistical minimum load capacity is largest for the welded specimen. The expected statistical maximum load capacity is largest for the fused specimen.
- Considering the test specimens as a connection method, the expected statistical minimum and maximum stress at failure are largest for the adhesive specimen.
- The small spread of the welded results suggests that it could be possible to obtain consistent capacity with welded connections.

34.7 Qualitative Aspects

- The aesthetic difference between the specimen is large. The welded and adhered products are more transparent than the fused product.
- The welded and fused objects were not produced with an acceptable accuracy of dimensions for structural applications.
- The welded glass product requires most time, energy, skill and money. The adhesive product requires the least time and energy.

34.8 Best

Both methods require further research and development. In the current state of development, glass fusion results in less residual stress, requires less skill and is cheaper to produce. Glass welding shows to result in a transparent glass to glass connection and its structural performance is promising.

35 Discussion

In the welding and fusion experiments, the aim has been to produce specimens. This has obstructed scientific gathering of knowledge about influencing factors. Preference has been given to creating a product, and the limits of production are therefore unknown.
This has two important consequences. The influence of different temperature schedules on a fused object is not researched. The current process worked, and the risk of creating a poor connection was not taken. Another example is the thermal shock failure during welding. The expected failure did not occur, which was related to conditions being estimated differently. It has not been researched whether the expected would occur if the conditions of model and reality match, because producing glass welds was preferred.

In the structural test, the influence of the stiffness and supporting system of the aluminum has been too large.

In the structural test, the joint and the other sections of the specimen were loaded differently. It can therefore not be concluded whether the connection was stronger or weaker than the parent material, or whether the joint was homogeneous.

No conclusion can be drawn on the aesthetics of the joints, because any conclusion would be subjective. For similar reasons, it is up to each individual to add the benefits and disadvantages presented in this thesis and decide which method is best.

From the qualitative analysis, the adhesive objects show great potential. This should not be taken as a reason to stop pursuing the fused or welded connection. If practical matters would dominate, innovation is discouraged. The qualitative comparison should be used to analyze feasibility and to compare. The qualitative analysis can be used as an encouragement to research and develop the adhesive joint.

This thesis is an exploratory study into heat bonded systems. The surface of the topic has been brushed, to peek into the possibilities and challenges of this concept. All conclusions are based on results of small series: three welding experiments, four fusion experiments and a structural test with series of five, four and three specimens per type. With more repetitions, it could be that the population of the results has a different average. It is possible that results obtained and used in this thesis, are statistical outliers. Therefore, all conclusions drawn in this thesis, can be proven to be untrue by future research.

36 Recommendations

Further research to heat bonded systems is highly encouraged. To create transparent glass to glass connection, further research in the adhesive joint is also recommended. Additional research is required to obtain knowledge about:

- whether the results are similar for larger sample sizes. This can be achieved by doing the performed experiments again.
- the safety measures for the heat bonded system. The suggested tempering, laminating and reinforcing of heat bonded systems have yet to be researched.
- the possibilities in combination with other techniques. Could a cast component be fused on a float glass panel? Can a hot bent element be welded on another bent element? Are there adhesives which remain functional at elevated temperature levels? etc.
- the limits of the weld production process. How long can the oven be open before thermal shock failure? Is welding possible with larger thicknesses? Are other configurations or products possible? etc.
- validating and improving the thermal finite element model. By finding the limits of the welding production process, the model can be calibrated and thoroughly validated. Then, the production process can be improved by researching theory.
- improving the weld production process. Can a seamless fillet weld be made? Can the curvature of the flange be limited? Can the accuracy be improved? etc.
- the limits of the fusion production process. What is the influence of the maximum temperature on the product? What is the influence of the dwell duration on the product? etc.
- improving the fusion production process. It is suggested to research mould materials with smooth textures and post-fusion polishing. How can the product be more accurate? How can transparent fused objects be produced? Can a seamless, filleted fusion be made? etc.
- the possibilities of the adhesive joint. What are the limits to the production process? What is the statistical distribution of failure loads? Is the adhesive joint stronger than glass? What is the structural behaviour when the adhesive T-shape is combined with safety measures like laminating or reinforcing? etc.
- the structural behaviour of all transparent joints under different loading conditions. What is the behaviour in tension, bending, dynamic loading etc.?
- the statistical distribution of the failure of joints. This could possibly result in capacity values and design criteria.

Bibliography

Aben, H. et al. (2010). "On Non-destructive Residual Stress Measurement in Glass Panels". In: *Estonian Journal of Engineering*.

ABT Ingenieurs in Bouwtechniek (n.d.). *Kasteel Ruurlo*. URL: www.abt.eu/projecten/kasteel-ruurlo.aspx.

Anderson, A. (2012). "Separation of Laminated Sheets". (Somerville, Australia).

Aurik, M. (2017). "Structural Aspects of an Arched Glass Masonry Bridge". Delft.

Belis, J. et al. (2006). "Seamless Connection of Soda-Lime Float Glass by Welding: Preliminary Test Results". In: *International Symposium on the Application of Architectural Glass*. Munich, Germany.

Blandini, L. (2016). "Transparent, Complex, Sustainable Challenges for Contemporary Facade Engineering". In: *Challenging Glass Conference*. Ghent, Belgium.

Borom, M. (1980). "De Mechanische en Chemische Aspecten van Glasverbindingen". In: *Mikroniek*.

Bos, F.P. (2009). "Safety Concepts in Structural Glass Engineering". PhD thesis. Delft. ISBN: 978-90-8570-428-7.

Bos, F.P., C. Giezen, and F. Veer (2008). "Opportunities for the Welding and Hot-Shaping of Borosilicate Glass Tubes in Building Structural Applications". In: *Challenging Glass Conference*. Delft.

Brow, R.K. (n.d.). *Summary of Chapter 6, Viscosity, of Introduction to Glass Science and Technology by J.E. Shelby*. URL: http://web.mst.edu/~brow/PDF_viscosity.pdf.

Bullseye Glass Co. (2009). *TechNotes 1 to 7. A Technical Supplement from Bullseye Glass Co.* August 2009. Bullseye Glass Co.

Dispersyn, J. and J. Belis (2016). "Numerical Research on Stiff Adhesive Point-Fixings between Glass and Metal under Uniaxial Load". In: *Glass Structural Engineering*. Cham, Switzerland: Springer International Publishing.

Dossett, J. and H. Boyer (2006). *Practical Heat Treating: Second Edition*. Novelty, United States of America: ASM International.

Dow Corning (2014a). *Dow Corning 121 Structural Glazing Sealant, Product Information*.

— (2014b). *Dow Corning 993 Structural Glazing Sealant, Product Information*.

Electrotherm Electrical & Metal Products Ltd. (2018). *High temperature Box Furnaces*. URL: www.electrothermindustry.com/High-Temperature-Box-Furnaces.

Gardon, R. (1956). "The Emisivity of Transparent Materials". In: *Journal of the American Ceramic Society*.

Giezen, C. (2008). "Development of a Structural Element of Glass with Glass Welding Processes". Delft.

Hagl, A. (2012). "Tensile Loading of Silicone Point Supports - Revisited". In: *Challenging Glass Conference*. Delft.

— (2016). "Development and Test Logistics for Structural Silicone Bonding Design and Sizing". In: *Glass Structural Engineering*. Cham, Switzerland: Springer International Publishing.

Hasselman, D.P.H. (1969). "Unified Theory of Thermal Shock Failure Initiation and Crack Propagation in Brittle Ceramics". In: *Journal of the American Ceramic Society*.

Heller, P., J.C.G. Vervest, and H.F. Wilbrink (n.d.). *Vademecum voor de Glastechniek*. Leiden: Leidse Instrumentmakersschool and Kluwer Technische Boeken BV.

Het Nederlandse Normalisatie-instituut (2011). *NEN -EN 1991-1-1-2+C1: Belastingen op constructues - Algemene Belastingen - Belasting bij Brand*.

— (2014). *NEN 2608 - Vlakglas voor Gebouwen - Eisen en Bepalingsmethode*.

Jacobs, E. (2017). "Structural Consolidation of Historis Monuments by Interlocking Cast Glass Components". Delft.
Klein, J. and N. Oxman (2015). "Additive Manufacturing of Optically Transparent Glass". Cambridge, United States of America.
Krom, D. de (2014). *Glazen Serre Kasteel te Ruurlo, Berekening Glasconstructies*. Delft.
Leidse Instrumentmakersschool (n.d.). *Glasinstrumentmaken*. Leiden.
Louter, P.C. (2011). "Fragile yet Ductile". PhD thesis. Delft. ISBN: 978-90-8570-743-1.
Mitchell, G. (n.d.). *How is curved glass made?* URL: www.sciencefocus.com/science/how-is-curved-glass-made.
Mitchell, J. (2015). "Precision Air Entrapment through Applied Digital and Kiln Technologies: A New Technique in Glass Art". PhD thesis. Sunderland, United Kingdom.
Nijsse, R. (2003). *Glass in Structures*. Basel, Switzerland: Birkhäuser - Publishers for Architecture. ISBN: 3-7643-6439-4.
— (2008). "Corrugated Glass as Improvement to the Structural Resistance of Glass". In: *Challenging Glass Conference*. Delft.
Nodehi, Z. (2016). "Behaviour of Structural Glass at High Temperatures". Delft.
NSG Group (2013). *Technical Bulletin, Properties of Soda-Lime Silica Float Glass*. Toledo, United States of America.
O'Callaghan, J. (2008). "Glass Structures from Stairs to Cubes". In: *Challenging Glass Conference*. Delft.
O'Callaghan, J. and C. Bostick (2012). "The Apple Glass Cube: Version 2.0". In: *Challenging Glass Conference*. Delft.
Oikonomopoulou, F., T. Bristogianni, et al. (2016). "Challenges in the Construction of the Crystal Houses Façade". In: *Challenging Glass Conference*. Ghent, Belgium.
— (2017). "The Construction of the Crystal Houses Facade: Challenges and Innovations". In: *Glass Structures and Engineering*.
Oikonomopoulou, F., F. Veer, et al. (2014). "A Completely Transparent, Adhesively Bonded Soda-Lime Glass Block Masonry System". In: *Journal of Facade Design and Engineering*.
Rammig, L. (2012). "Direct Glass Fabrication - New Applications of Glass with Additive Processes". In: *Challenging Glass Conference*. Delft.
— (2016). "Residual stress in Glass Components". In: *Challenging Glass Conference*. Ghent, Belgium.
Richet, P et al. (1997). "Configurational Heat Capacity and Entropy of Borosilicate Melts". In: *Journal of Non-crystalline Solids*.
Rick Mather Architects (n.d.). *All Glass Extension*. URL: www.rickmather.com/project/search/all_glass_extension.
Schipper, R. (2011). *Large Transparent Glass Surfaces*. Delft.
Schittig et al. (1999). *Glass Construction Manual*. Basel: Birkhäuser - Publishers for Architecture. ISBN: 978-3-7643-8122-6.
Shorr, B.F. (2015). *Thermal Integrity in Mechanics and Engineering*. Heidelberg, Germany: Springer Verlag. ISBN: 978-3-662-46968-2.
Solla, I. (2011). *The Louvre pyramids revisited*. URL: facadesconfidential.blogspot.nl/2011/10/louvre-pyramids-revisited.html.
Stelzer, I. (2010). "High Performance Laminated Glass". In: *Challenging Glass Conference*. Delft.
Takeuchi, T., K. Sugizaki, and K. Yasuda (2012). "Design of Suspended Glass Ceiling Structure in High Seismic Hazard Zones". In: *Challenging Glass Conference*. Delft.
Teeuwen, A.S. (2016). "An Edge-integrated Connectin for Segmented Glass Beams". In: *Challenging Glass Conference*. Ghent, Belgium.

The Engineering ToolBox (n.d.). *Specific Heat of Solids*. URL: www.engineeringtoolbox.com/specific-heat-solids-d_154.html.

Veer, F. (2016). "Fatigue and Creep Behaviour of Stainless Steel/Glass SentryGlas Joints". In: *Challenging Glass Conference*. Ghent, Belgium.

Veer, F., T Bristogianni, and C. Justino de Lima (2018). "A Re-evaluation of the Physiochemistry of Glass on the Basis of Recent Developments and its Relevance to the Glass Industry". In: *Challenging Glass Conference*. Delft.

Wang, Y. et al. (2009). "Convective Heat Transfer of the Bunsen Flame in tge UL94 Vertical Burning Test for Polymers". In: *Journal of Fire Sciences*.

Appendices

A Results and Interpretation of the Thermal Finite Element Analysis of the Glass Weld Production Process

In Part IV, the production process of glass welds is analyzed in a finite element model. The aim of this model is to research thermal and stress development during the process.
This appendix contains the gathered results in data, graphs and plots. For every varied parameter or combination of varied parameters, thermal and mechanical results are displayed and interpreted. The conclusions are gathered in section 19.

Unless mentioned otherwise, the default parameter values are used. These are explained in section 18 and summarized in table A.1

Propterty	Unit	Value	Comment
Mesh size	mm	1,25 to 5	
Time step	s	2	
Preheating Temperature	$°C$	500	
Flame position			At the front and along the welding zone
Convection Coefficient, Flame to Glass	$\frac{W}{m^2°C}$	50	
Flame Temperature	$°C$	1727	
Convection Coefficient, Glass to Surroundings	$\frac{W}{m^2°C}$	4	
Emissivity	-	0,64	
Surrounding Temperature	$°C$	20	
Transition Range	$°C$	585 to 630	
Specific Heat Capacity	$\cdot 10^6 \frac{J}{m^3°C}$	2,1 to 3,6	Depends on transition range
Thermal Conductivity	$\frac{W}{m°C}$	1,2	
Coefficient of Linear Thermal Expansion	$\cdot 10^{-6} °C^{-1}$	8,6 to 0	Depends on transition range
Young's Modulus	GPa	70 to 0,7	Depends on transition range
Poisson's Ratio	-	0,23	
Glass Density	$\frac{kg}{m^3}$	2500	Software demands parameter, no influence on analyses
Glass Thickness	mm	10	

Table A.1: Default parameter values for FEA of glass weld production process

A.1 Additional Result Definitions and Interpretation

There are a few definitions in the presentation of the results, which require further explanation. A few have been dealt with in section 17.3. The following are additional, to help understand the results as presented in this appendix.

Most of the stress plots are manually scaled, as opposed to an automatically scaled plot based on the extreme stress values. This has several reasons. One is that in most results, one numerical extreme

causes a peak stress which is not relevant, but scales all results. Therefore, almost all significant areas contain only one or two colours, making it difficult to interpret the plot. Secondly, the automatically scaled results do not show well if the stress capacity is passed. Thirdly, using the same colour scale on all images makes it easier to compare the stress plots.
The scale of the principal stress plots also requires elaboration. The limit to the tensile capacity of glass is $45\ MPa$. It is desired to distinguish the areas where the stress is larger than the capacity by a red colour. Another desire was to distinguish all elements with the principal stress in compression. The scale that meets these requirements is a scale from -9 to $54\ MPa$, divided in seven color segments. The dark blue areas (smaller than $0\ MPa$) indicate compression, the red areas (larger than $45\ MPa$) indicate that the tensile stress capacity is surpassed. These red areas are therefore also referred to as critical areas.
It is important to note that the scaled stress plots show no extreme values. Even though the accompanying legend suggests it, it is not valid that the maximum stress is $54\ MPa$ and the minimum is $-9\ MPa$. The manually scaled plots can be recognized by their -9 to 54 scale with round numbers. Also, the figure description contains the word 'scaled'.

In most cases, the bottom surface of the specimen contains the critical area. Therefore, the results of this surface are useful for comparison. In figure A.1, it is shown how this surface is orientated in all plots. The front of the object is at the bottom of the image, in all plots of the bottom surface.

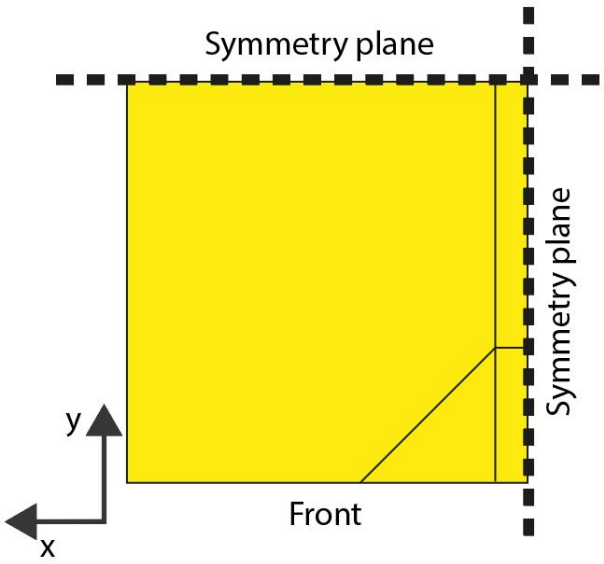

Figure A.1: Orientation of the bottom surface. The front of the welding zone is at the bottom of the pixture in all plots of this bottom surface.

If the mechanical analysis is performed for the weld time only, computational time is lower than if it is computed for all time steps. By computing the stress at weld time, the only relevant lost information is the earliest time at which critical stress occurs. This information is an interesting number for the comparison of the results. However, it has been chosen to compare the results based on the size and area of the critical stress region at weld time. The reduction in computational time makes this option more practical.
For a random sample of cases which show no critical stress at weld time, it has been checked whether there was any critical stress before weld time. Since this was not observed, it has been accepted to draw conclusions based on the stress distribution at weld time.

A.2 Default

The results for the default analysis are those with which all others are compared. It has been chosen to use a combination pf parameters that results in a specimen with critical areas, see the explanation provided in section 19.

The weld time of the default parameter combination is 60 s. At this time, the bottom surface is predicted to crack due to critical stress. To be more precise, the earliest time at which the surface shows critical stress is 52 s.

Figure A.4 and A.2 show that the automatically scaled stress plots show the extremes but are not as easily interpreted as the scaled plots. The automatically scaled plots are almost all turquoise and green. It is unclear where the stress is larger than the capacity. This supports the decision to mainly use scaled stress plots. Figure A.5 shows the relation between temperature and stress relaxation, as

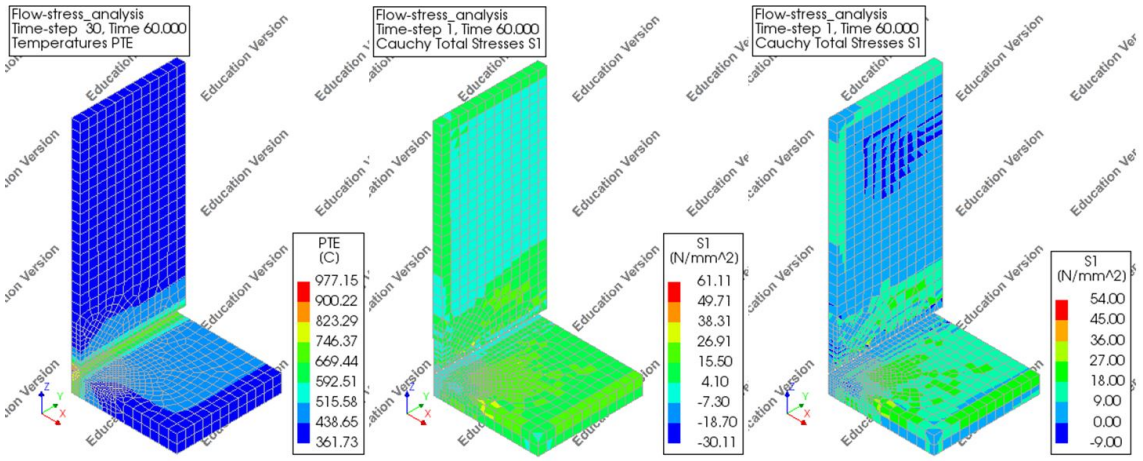

Figure A.2: Temperature distribution (right), automatically scaled principal stress (center) and scaled principal stress (right) for the default parameter combination at weld time.

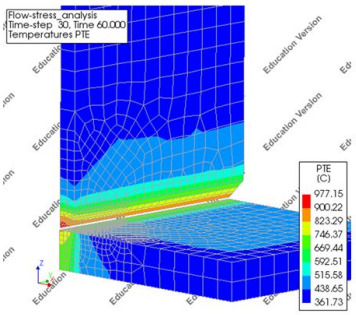

Figure A.3: Temperature distribution at weld time, close-up.

described in section 9 and applied in section 18. The material with a high temperature is less viscous. Flow then results in the reduction of stress. At the front of the weld, the hot areas, about 600 $°C$ or warmer, show little stress. At this temperature, the glass is in the transition phase and the stress is

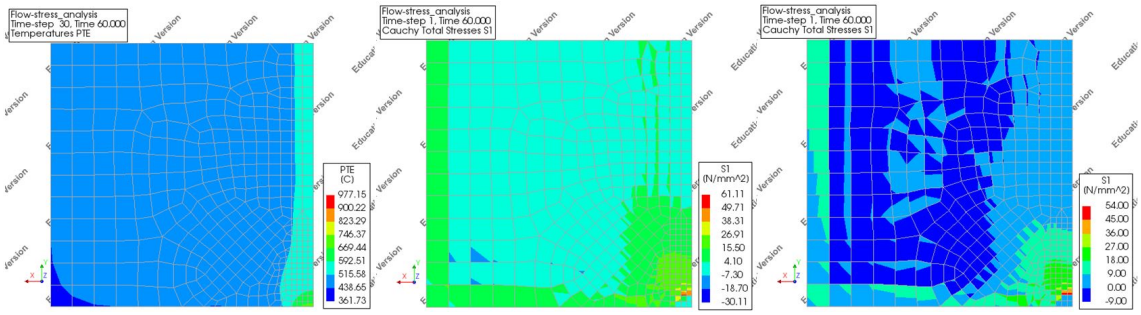

Figure A.4: Plots for the bottom surface, with the temperature distribution (right), automatically scaled principal stress (center) and scaled principal stress (right), for the default parameter combination at weld time.

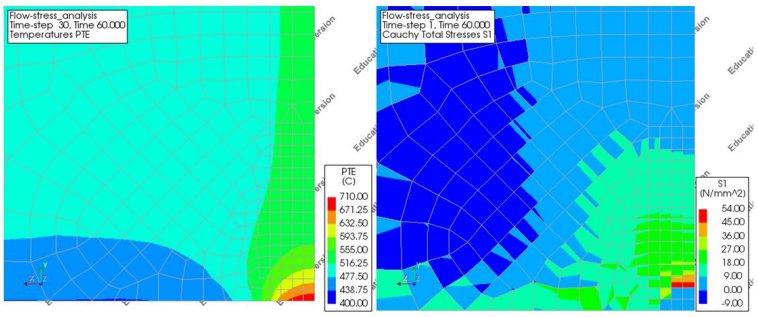

Figure A.5: Close-up plots for the bottom surface, with the temperature distribution (right) and scaled principal stress (right), for the default parameter combination at weld time.

reduced.

A.3 Mesh Size

The mesh size is adapted to fit basic requirements. The method was according to a finite element analysis philosophy: refine the mesh size, if the results change significantly, the previous mesh size was too coarse, if not, the previous mesh size can be adopted. The maximum mesh size is $5\ mm$, when the thickness is composed of two elements. In the welding zone, the maximum size is set to $2,5\ mm$, resulting in four elements to span the thickness.
The minimum mesh size was limited by the software. The educational version of Diana has a maximum amount of elements in the model.

The mesh sizes used were *all 2,5*, where alle elements were $2,5\ mm$, the default mesh, *1,25, 2,5 and 5*, containing $5mm$ elements with $2,5\ mm$ elements in the welding zone and $1,25\ mm$ elements in the front of the welding zone, and the third mesh size is *2,5 and 1,25*, where the elements in the welding zone were $1,25\ mm$ and the others were $2,5\ mm$. The finest mesh, where the elements in the welding zone are $0,625\ mm$, contained too many elements for the software in educational version.

Mesh size	all 2,5	1,25, 2,5 and 5 (default)	2,5 and 1,25
$t_{weld}\ (s)$	62	60	60

Table A.2: Weld time for varying mesh sizes

The difference in thermal results is not significant (Table A.2).

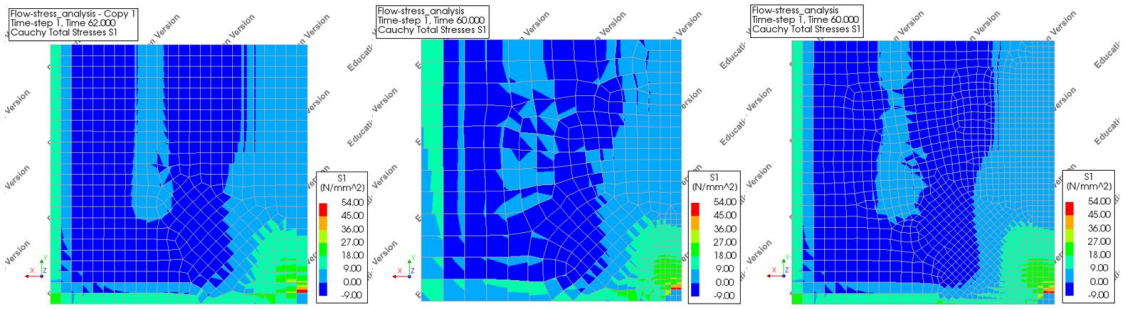

Figure A.6: Principal stress plot, scaled, at weld time of the bottom surface for varying mesh sizes with all 2,5 (left), 1,25, 2,5 and 5 (default) (center) and 2,5 and 1,25 (right)

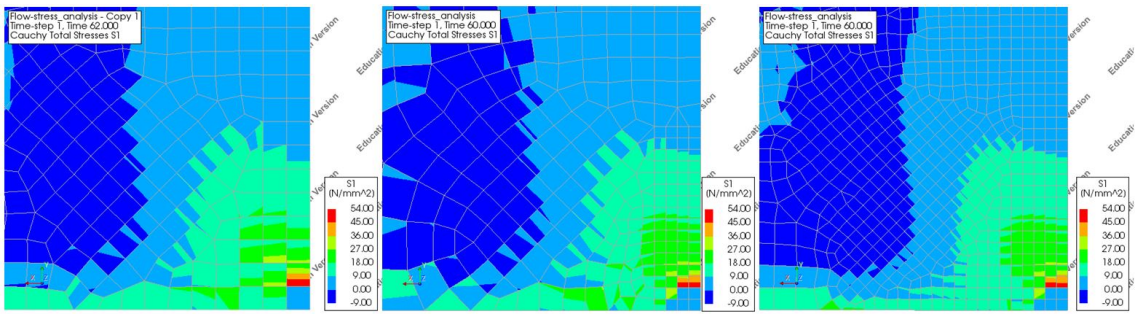

Figure A.7: Principal stress plot, scaled, at weld time, close-up of the bottom surface for varying mesh sizes with all 2,5 (left), 1,25, 2,5 and 5 (default) (center) and 2,5 and 1,25 (right)

The difference between *all 2,5* and the default mesh show that the critical area is at the front of the welding zone. It is preferred to use a fine mesh there, because this will benefit the accuracy of the results.
The difference between the default mesh and the *2,5 and 1,25* mesh show that this affects the borders of stress in green and blue, at $9MPa$ or lower. The fine meshed results show more continuity. This accuracy is not necessary to draw the main conclusion, because whether the stress is critical is not related to this stress level.

The default mesh is preferred, because it balances the computational time and model accuracy in the area of interest, the front of the welding zone.

A.4 Time Step

The time step of the analysis determines the time difference for every step of the calculation. The smaller the time step, the smaller the numerical errors. A small time step results in more computations and a longer analysis time. These effects should be balanced when choosing the time step.

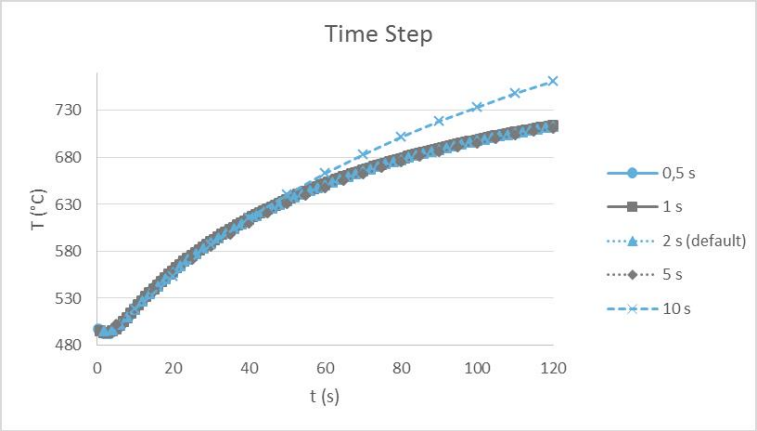

Figure A.8: Temperature at the core of the welding zone over time for different time step sizes.

Time step (s)	0,5	1	2 (default)	5	10
t_{weld} (s)	59	60	60	65	60

Table A.3: Weld time for varying time steps

The times step influences the increase pf temperature. Figure A.8 shows that the results diverge significantly for a time step of $10\ s$. It is concluded that this time step is too large.
The weld times show one exceptional result, which is for the time step of $5\ s$.

The first observation is that the stress is not critical for a time step of $0,5\ s$. However, the time required to perform this analysis is too long to be practical in this research. A larger time step, the default time step of $2\ s$, is preferred. The stress plots show that this time step is conservative, compared to smaller time steps.

For the other time steps, the critical area has similar size. For the time steps of $5\ s$ and $10\ s$, the red area is larger on one element than on the other. This discrete change shows that the results among

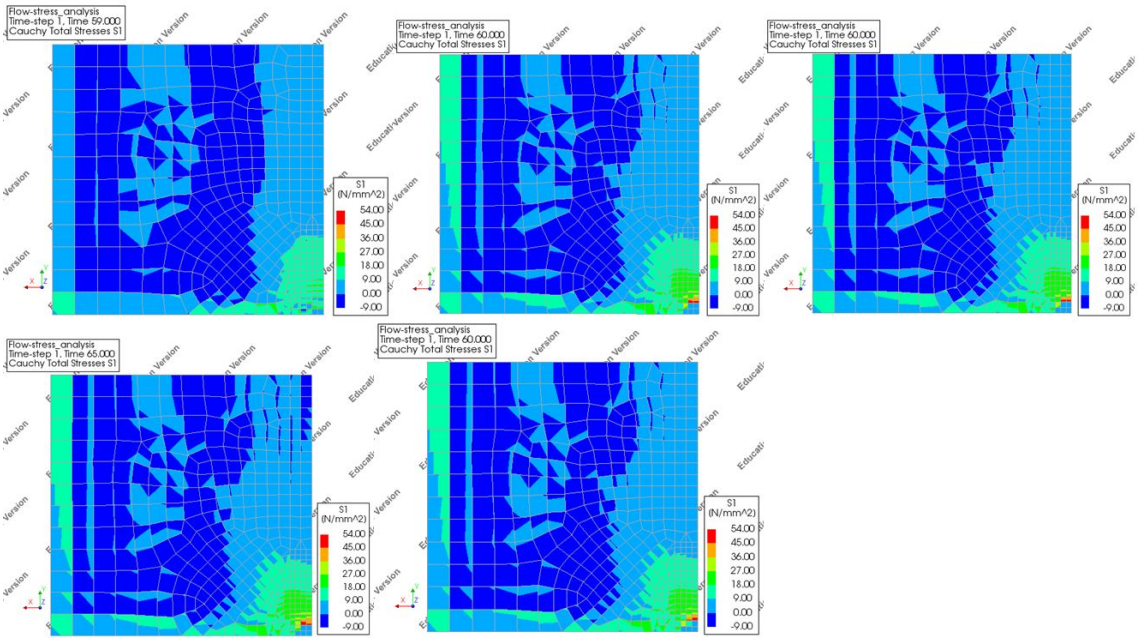

Figure A.9: Principal stress plot, scaled, at weld time of the bottom surface for varying time steps. Left to right, top to bottom: $0,5\ s$, $1\ s$, $2\ s$, $5\ s$, $10\ s$

elements are further apart than for the smaller time steps. A smaller time steps returns results, which are more coherent among elements.

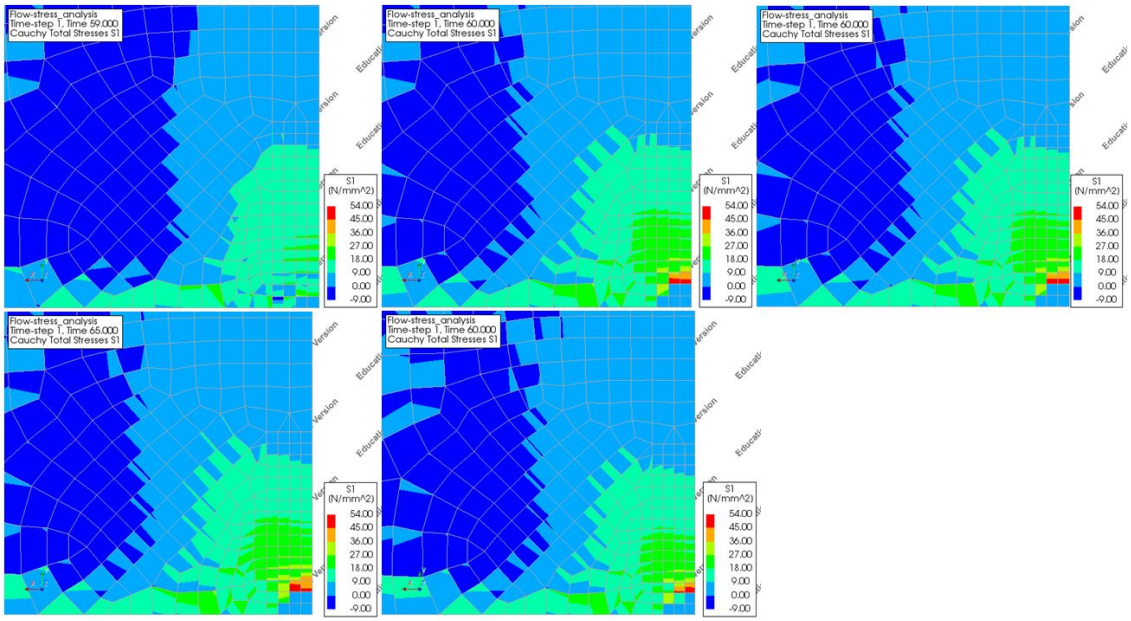

Figure A.10: Principal stress plot, scaled, at weld time, close-up of the bottom surface for varying time steps. Left to right, top to bottom: $0,5\ s$, $1\ s$, $2\ s$, $5\ s$, $10\ s$

A.5 Preheating Temperature

The glass will be preheated in an oven before welding. In the model, this is accounted for by an initial condition. At the start of the analysis, the temperature of the glass is the preheating temperature, which is homogeneous over the material.
Several preheating temperature levels are analyzed. All preheating temperatures are below the annealing point. Also, the model is analyzed for the case without preheating, an initial condition of $20°C$.

Preheating temperature ($°C$)	540	500 (default)	450	20
t_{weld} (s)	40	60	84	340

Table A.4: Weld time for varying levels of preheating temperature

From figure A.11, it can be seen that the change in initial temperature mainly shifts the starting point of the analysis and that the thermal behaviour is similar afterwards. The weld times shift along: it decreases at a warmer start level and vice versa.
If the glass is not preheated, the glass can be welded after almost six minutes after the oven is opened.

Figure A.14 shows large areas of critical stress for the sample with an initial temperature of $20\ °C$. One can distinguish a tensile arch in the glass. The glass in the welding zone expands but is constrained, causing compression. This needs to be internally compensated by a tensile stress, manifested in the shape of an arch. This picture is the exact opposite of a reinforced concrete beam loaded with a distributed force: in that case, a tensional force in the reinforcement causes a compression arch in the beam.

It is concluded that the specimen will fail due to thermal shock failure.

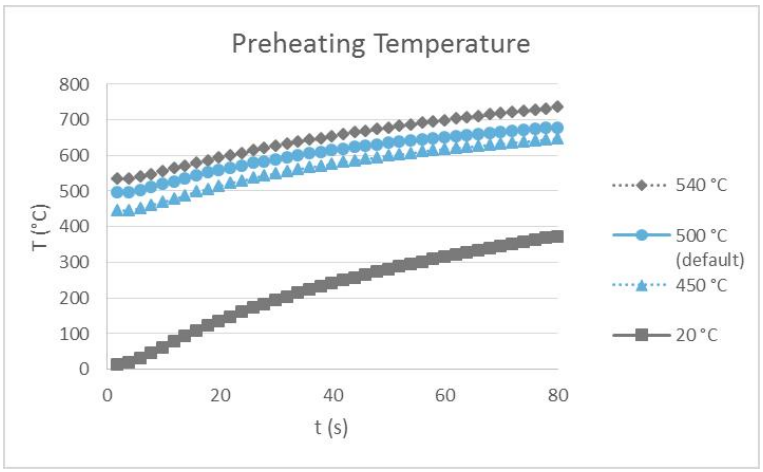

Figure A.11: Temperature at the core of the welding zone over time for different levels of preheatng temperature.

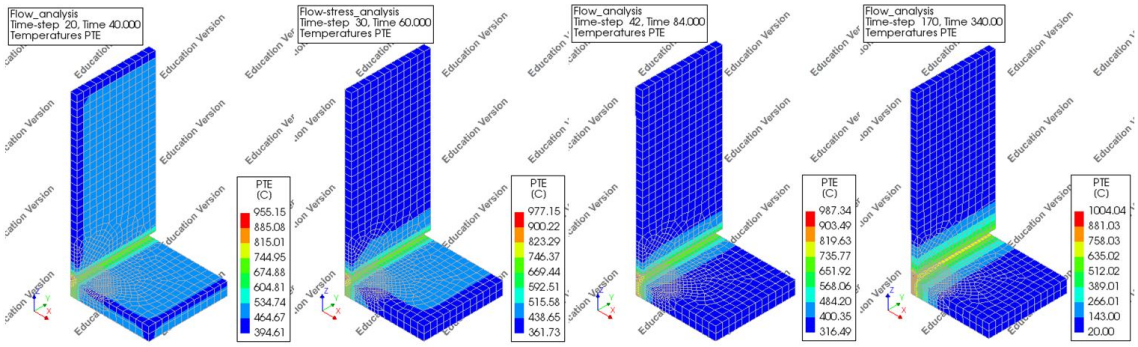

Figure A.12: Temperature distribution at weld time for varying levels of preheating temperature. Left to right: $540\ °C$, $500\ °C$ (default), $450\ °C$ and $20\ °C$.

Figure A.15 shows that with a preheating temperature of $540\ °C$, the stress is not critical at weld time. Further research shows that the stress becomes critical twelve seconds later (Figure A.15). If the weld can be produced within that time frame, it might be possible to weld without thermal shock failure. It has been chosen not to pursuit this case in practice for two reasons. The first is that twelve seconds is estimated to be too short to manipulate the glass and close the oven door. The second reason is that $540\ °C$ is close to the annealing temperature. Using a high preheating temperature increases the risk that the glass deforms due to transition.

For a preheating temperature of $450\ °C$, the critical area is similar to that of the default preheating temperature, but the area with stress above $9\ MPa$ is larger. There is more tension in this specimen at weld time. It is concluded that the preheating level of $500\ °C$ is preferred for the production process.

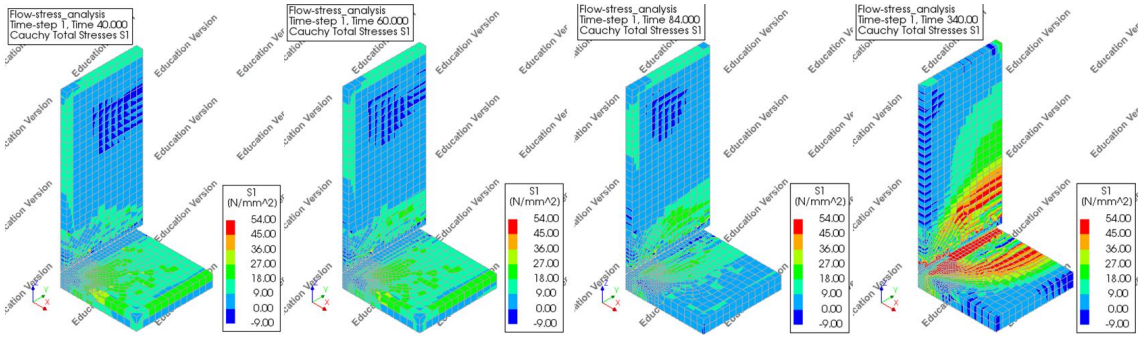

Figure A.13: Principal stress plot, scaled, at weld time for varying levels of preheating temperature. Left to right: 540 $°C$, 500 $°C$ (default), 450 $°C$ and 20 $°C$.

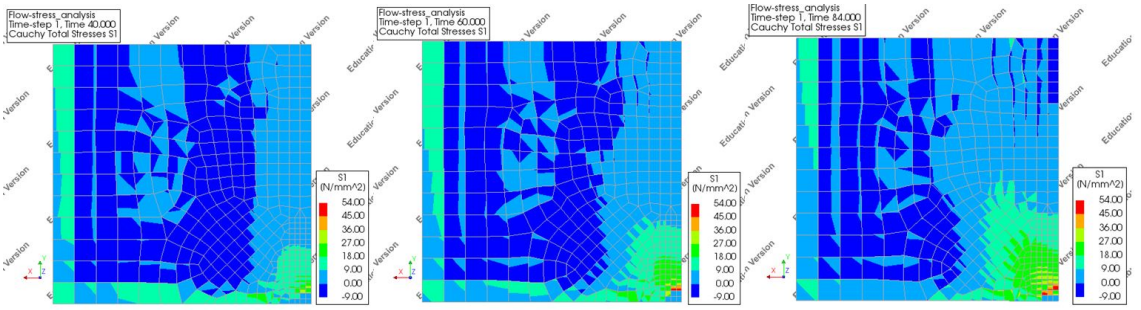

Figure A.14: Principal stress plot, scaled, at weld time of the bottom surface for varying levels of preheating temperature. Left to right: 540 $°C$, 500 $°C$ (default) and 450 $°C$.

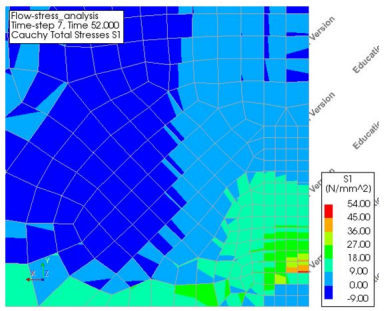

Figure A.15: Principal stress plot, scaled, after 52 s, close-up of the bottom surface for a preheating temperature of 540 $°C$

A.6 Flame Position and Size

The position and size of the flame is one of the parameters which are easily altered in the welding practice. In the model, this parameter is represented by the boundary surface on the glass that is affected by convective heat transfer from the flame to the glass. The default position is chosen in such a way that the stress is critical, as explained above. The default size is based on the geometry of the faceted edge. The air at this edge cannot escape upwards, creating a space where convective heat is transferred maximally. However, to investigate sensitivity, different sizes are analysed.

The flame positions to be investigated are named *point*, *side*, *side and front* and *side, front and under* and are shown in figure A.16.
It is important to note that the bottom surface is fully insulated for the positions *point*, *side* and *side and front*. In the *side front and under* position, the bottom has to be exposed to position the flame under this surface. Therefore, the remaining area on this surface is no longer insulated, but exposed to the surroundings. This area is therefore changed to a boundary surface, with the properties of convective and radiative heat loss to the surroundings.

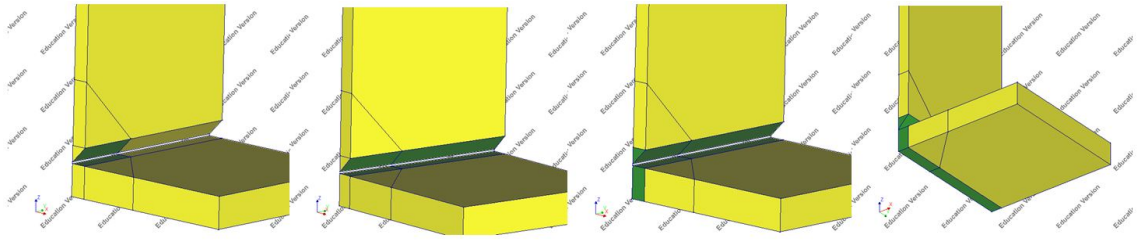

Figure A.16: Geometetries of different flame position configurations. The green area indicates the boundary surfaces of convective heat transfer from the flame. From left to right: *point*, *side*, *side and front* (default) and *side, front and under*.

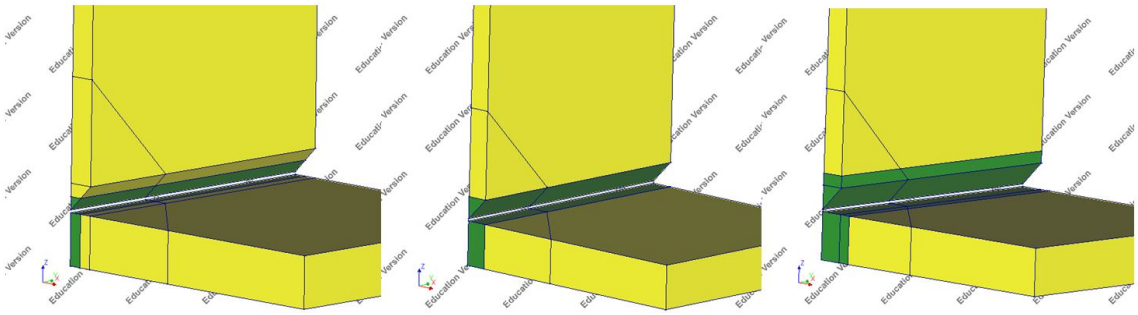

Figure A.17: Geometetries of different flame sizes. The green area indicates the boundary surfaces of convective heat transfer from the flame. From left to right: smaller (min $2,5\ mm$), default and larger (plus $2,5\ mm$). Faceted edges are of the same size for all images.

Flame position and size	point	side	side and front (default)	side, front and under	smaller	larger
$t_{weld}\ (s)$	-	60	60	60	-	42

Table A.5: Weld time for varying time steps

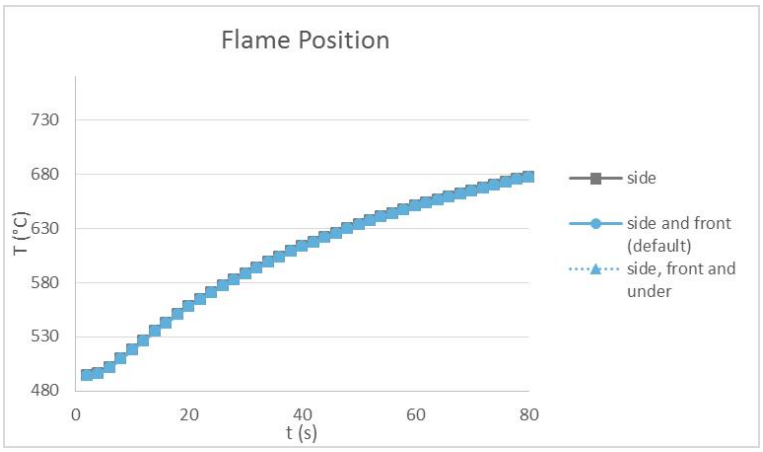

Figure A.18: Temperature at the core of the welding zone over time for different flame positions.

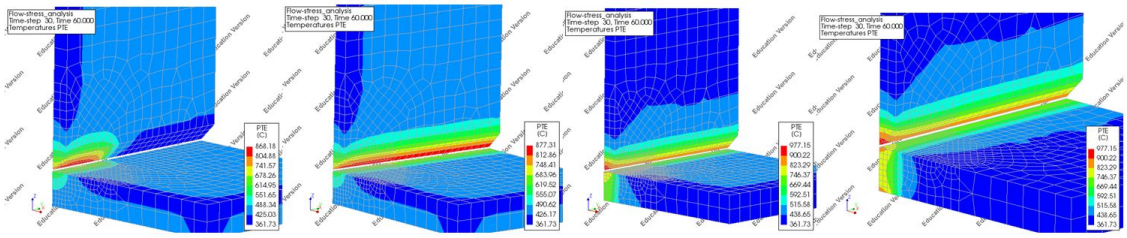

Figure A.19: Temperature distributions at weld time for different flame position configurations. From left to right: *point*, *side*, *side and front* (default) and *side, front and under*. Because position *point* has no weld time, the temperature at 60 s is shown.

There is no weld time for the *point* position, because the core of the welding zone near the symmetry plane is not well affected by locally heating the welding zone near the edge.
The weld time of all positions where the side is heated is the same. This is because the point where the temperature is measured to determine the weld time is not affected by the boundary surface at the front or the bottom of the object.

Figure A.20 shows that heating the front of the welding zone is necessary to prevent critical stress at the front edge of the glass. Figure A.21 shows that if the bottom surface of the object is heated, no critical stress occurs. After thirty seconds, still no critical stress is present under this condition (Figure A.22). It is estimated that this will provide enough time to produce the weld.
The band along the welding zone is blue, indicating relaxed stresses. The surface is hot enough for the glass to be in the transition or liquid range.
It is recommended that the bottom surface of the object, of the flange, is locally heated during the weld production.

If the size of the boundary surface considering the heat gain of the flame is altered, the temperature development changes. The sizes vary from 50 to 150% of the default surface.
In the case of the smaller surface, the temperature development in the core of the welding zone remains too low and has a maximum of 565 $°C$ at 114 s.

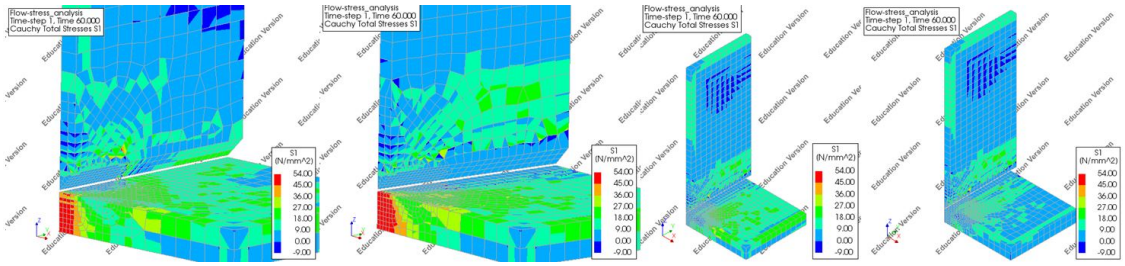

Figure A.20: Principal stress plots, scaled, at weld time for different flame position configurations.From left to right: *point*, *side*, *side and front* (default) and *side, front and under*. Because position *point* has no weld time, the temperature at $60\ s$ is shown.

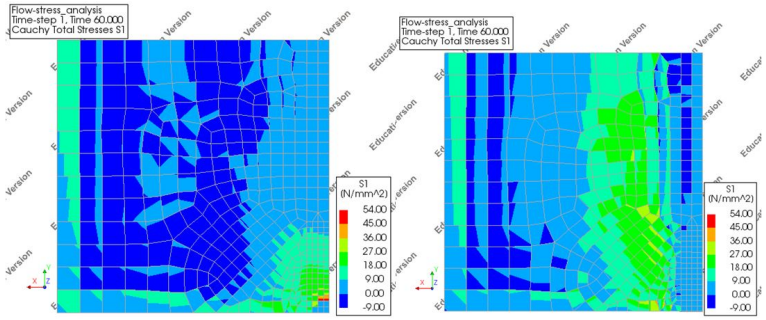

Figure A.21: Principal stress plots, scaled, at weld time of the bottom surface for different flame position configurations. *Side and front* (default) (left) and *side, front and under* (right).

The stress plots in figure A.24 is for the position *side, front and under* and shows that the size of the flame boundary surface affects the width of the area where the stress is relaxed. It affects the width of the band where the material is in transition or liquid range.
The stress plots in figure A.25 show that if the flame boundary surface is larger and the position is *side and front*, there is no critical stress at weld time. The default result shows critical stress for the earliest time of $52\ s$, which is later than the weld time for the larger flame boundary surface. With this flame configuration, the earliest time to show critical stress is $52\ s$ as well. This indicates that the flame size does not affect stress relaxation at the bottom.

The available time between weld time and critical stress, is considered too short to manipulate the glass and produce the weld.

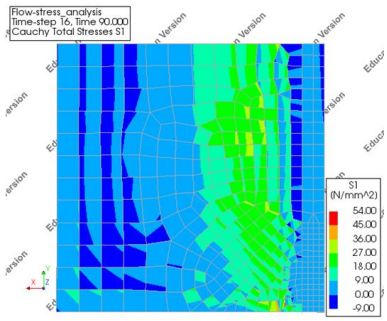

Figure A.22: Principal stress plot, scaled, thirty seconds after weld time of the bottom surface for flame position *side, front and under*.

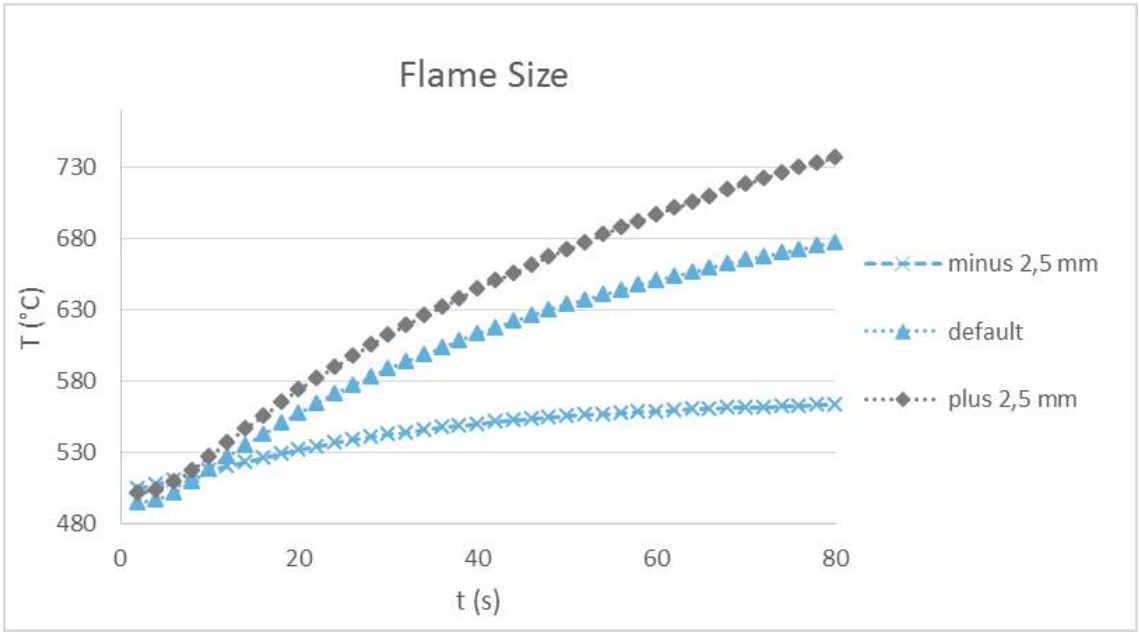

Figure A.23: Temperature at the core of the welding zone over time for different flame sizes.

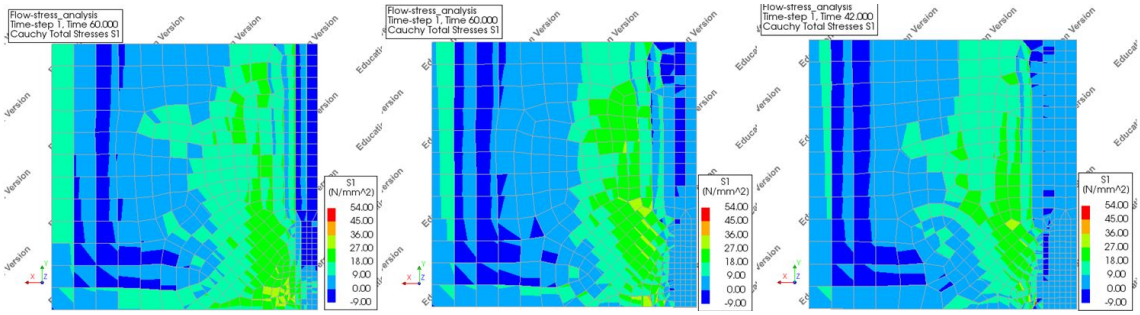

Figure A.24: Principal stress plots, scaled, at weld time of the bottom surface for different flame sizes, position *side, front and under*. From left to right: smaller, default, larger. Because the smaller size has no weld time, the temperature at 60 s is shown.

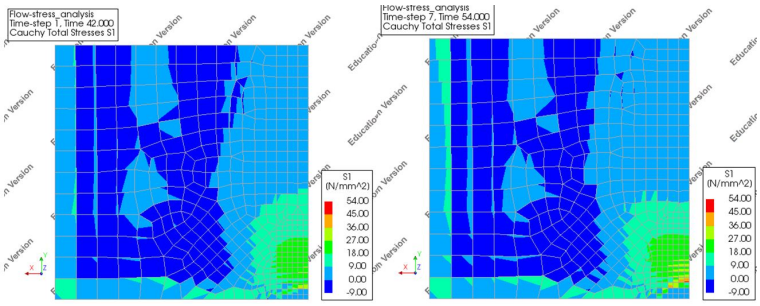

Figure A.25: Principal stress plots, scaled, for the results of the combination of the flame position *side and front* and larger size at weld time and twelve seconds later.

A.7 Convection Coefficient, Flame to Glass

The default value is based on a bunsen flame and the eurocode. To test the sensitivity of the model to this parameter, its value is varied by 20%. The thermal analysis shows significant variations (Table A.6, Figure A.26). The quicker energy is transferred to the glass, the quicker it heats to the required temperature.

Convection coefficient, flame to glass ($\frac{W}{m^2°C}$)	40	50 (default)	60
t_{weld} (s)	88	60	48

Table A.6: Weld time for varying convection coefficients for heat transfer from the flame to glass.

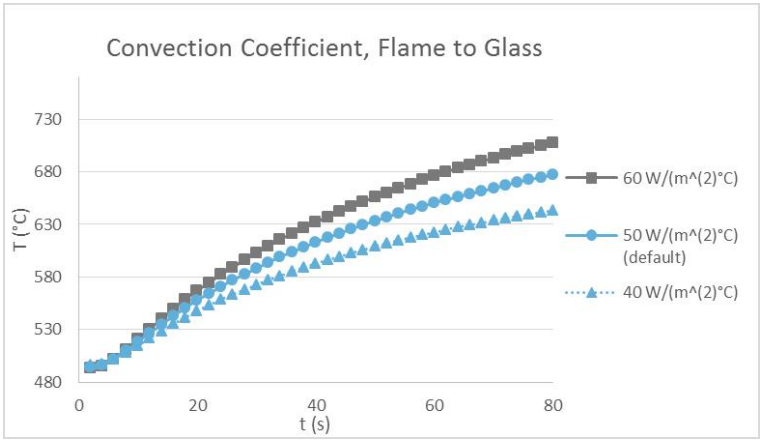

Figure A.26: Temperature at the core of the welding zone over time for different convection coefficients for heat transfer from the flame to the glass.

The stress distributions show a significant difference. With a lower conduction coefficient, the critical area is larger (Figure A.31). For the analysed conduction coefficients, the results show critical stress and predict thermal shock failure.

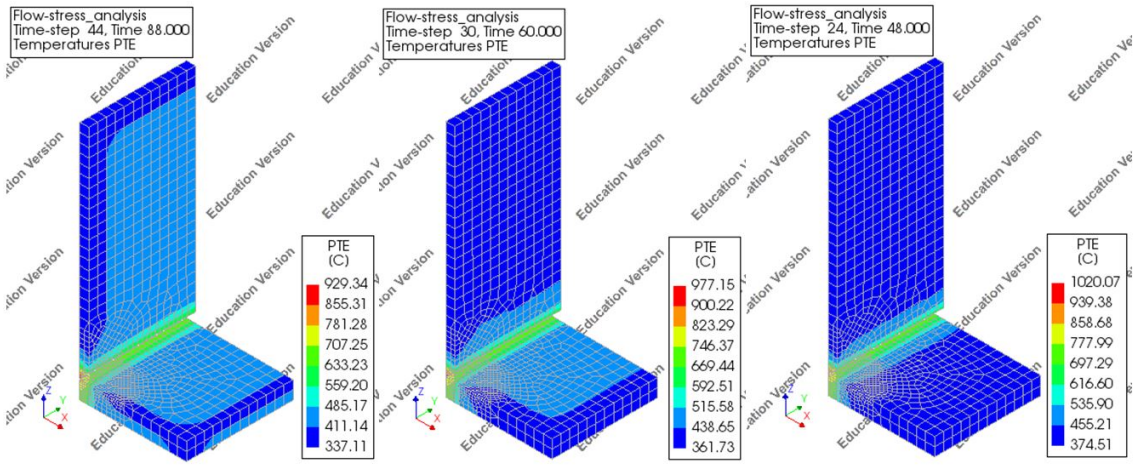

Figure A.27: Temperature distributions at weld time for different convection coefficients for heat transfer from the flame to the glass. From left to right: 40 $\frac{W}{m^2°C}$, 50 $\frac{W}{m^2°C}$ and 60 $\frac{W}{m^2°C}$

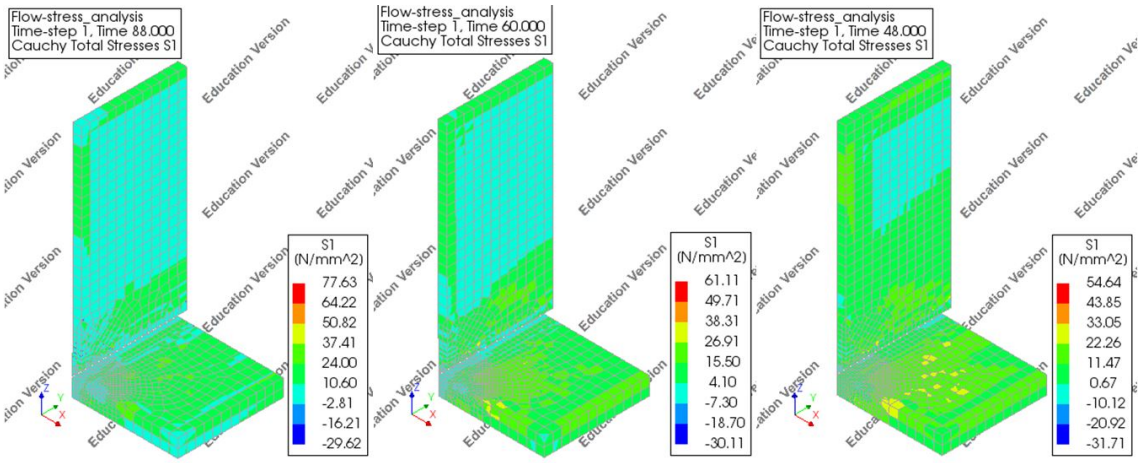

Figure A.28: Principal stress plots at weld time for different convection coefficients for heat transfer from the flame to the glass. From left to right: 40 $\frac{W}{m^2°C}$, 50 $\frac{W}{m^2°C}$ and 60 $\frac{W}{m^2°C}$

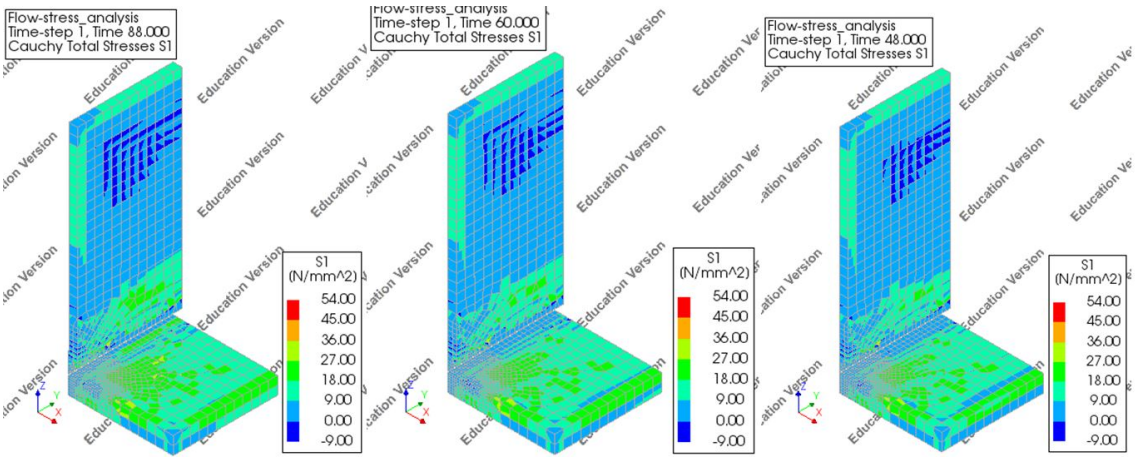

Figure A.29: Principal stress plots, scaled, at weld time for different convection coefficients for heat transfer from the flame to the glass. From left to right:40 $\frac{W}{m^2°C}$, 50 $\frac{W}{m^2°C}$ and 60 $\frac{W}{m^2°C}$

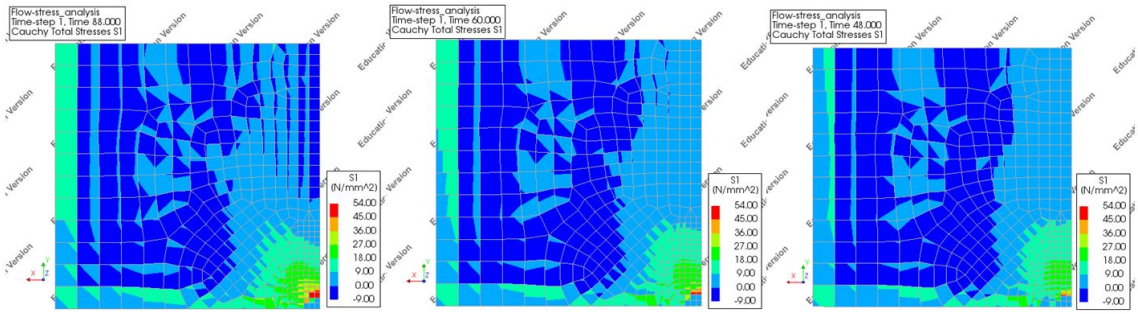

Figure A.30: Principal stress plots, scaled, at weld time of the bottom surface for different convection coefficients for heat transfer from the flame to the glass. From left to right: 40 $\frac{W}{m^2°C}$, 50 $\frac{W}{m^2°C}$ and 60 $\frac{W}{m^2°C}$

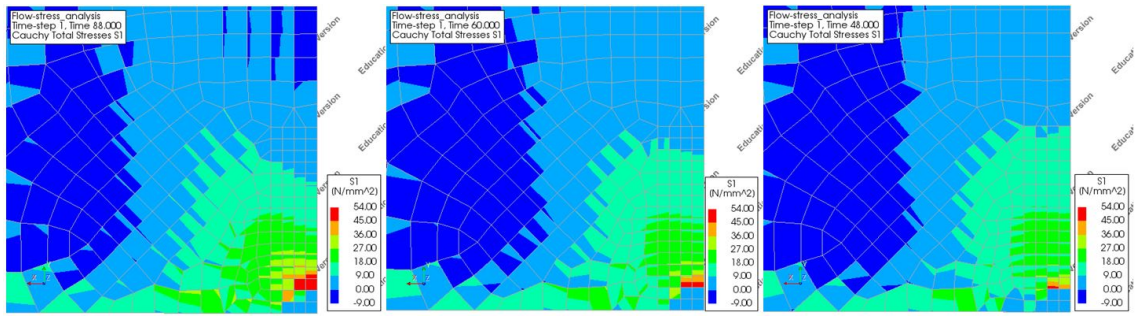

Figure A.31: Principal stress plots, scaled, at weld time, close-up of the bottom surface for different convection coefficients for heat transfer from the flame to the glass. From left to right: 40 $\frac{W}{m^2°C}$, 50 $\frac{W}{m^2°C}$ and 60 $\frac{W}{m^2°C}$

A.8 Flame Temperature

The properties of a bunsen flame are applied as default values. The bunsen flame is 2000 K, 1727°C. The sensitivity is tested by analyzing the model for several values.

Flame temperature(°C)	727	1227	1527	1727 (default)	1927
t_{weld} (s)	-	-	86	60	48

Table A.7: Weld time for varying flame temperatures.

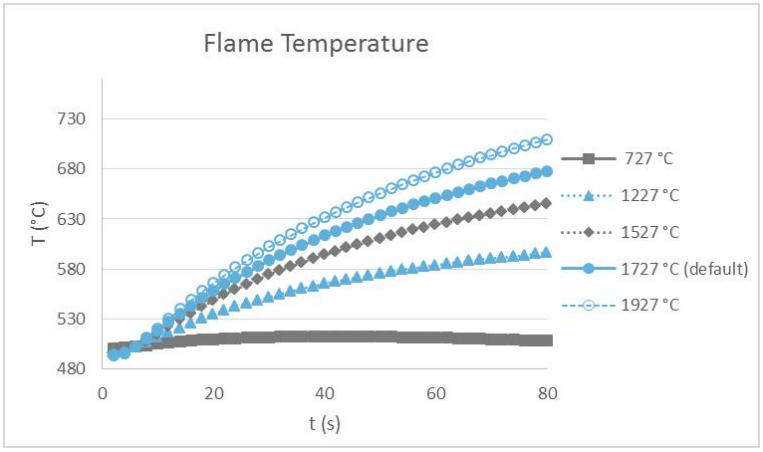

Figure A.32: Temperature at the core of the welding zone over time for different flame temperatures.

If the flame is 1527 °C or warmer, the glass can reach the required temperature. A higher flame temperature results in a shorter weld time.

The values for flame temperatures that return a weld time, are analyzed for mechanical behaviour. The close-up of the principal stress plot (Figure A.37), shows that the stress is critical in all cases.

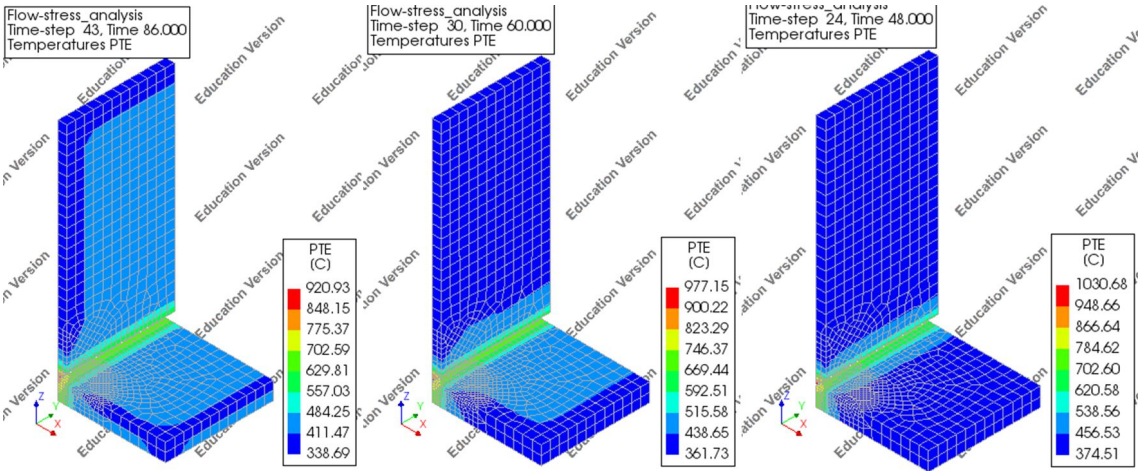

Figure A.33: Temperature distributions at weld time for different flame temperatures. From left to right:1527 $°C$, 1727 $°C$ (default) and 1927 $°C$

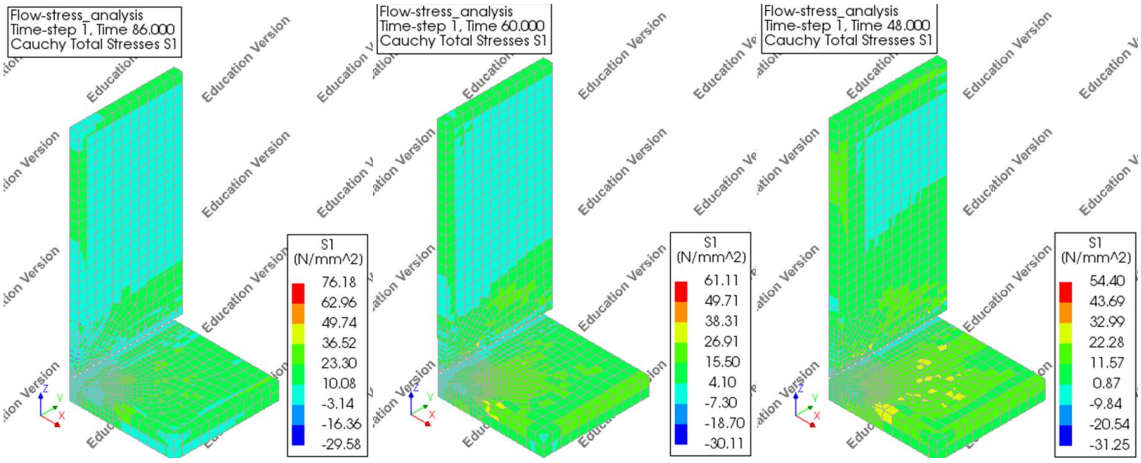

Figure A.34: Principal stress plots at weld time for different flame temperatures. From left to right:1527 $°C$, 1727 $°C$ (default) and 1927 $°C$

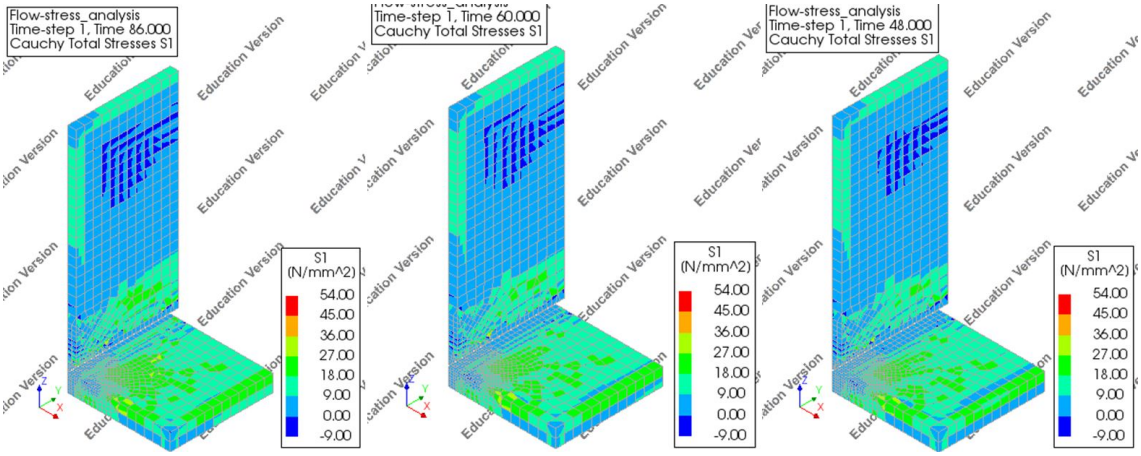

Figure A.35: Principal stress plots, scaled, at weld time for different flame temperatures. From left to right:1527 $°C$, 1727 $°C$ (default) and 1927 $°C$

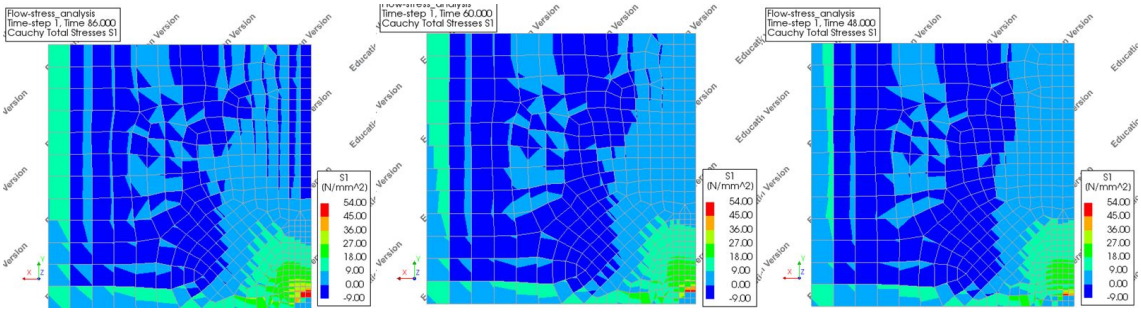

Figure A.36: Principal stress plots, scaled, at weld time of the bottom surface for different flame temperatures. From left to right:1527 $°C$, 1727 $°C$ (default) and 1927 $°C$

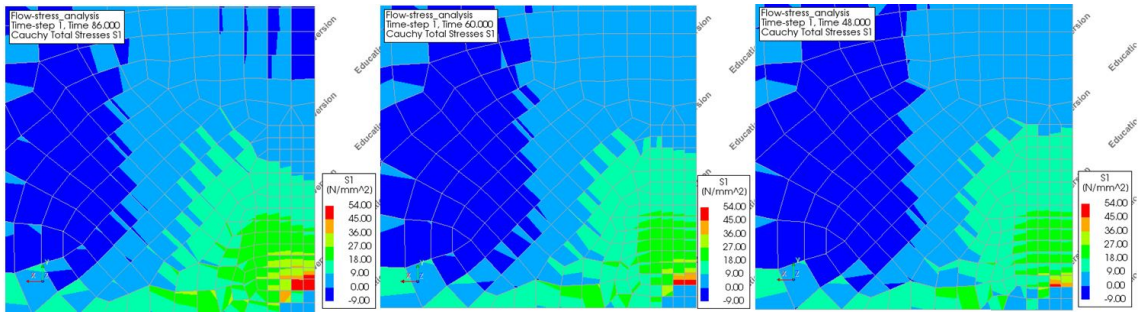

Figure A.37: Principal stress plots, scaled, at weld time, close-up of the bottom surface for different flame temperatures. From left to right:1527 $°C$, 1727 $°C$ (default) and 1927 $°C$

A.9 Convection Coefficient, Glass to Surrounding

There is a second convection coefficient, determining the scale of the heat loss to the surroundings. Note that the heat loss to the surroundings works through two mechanisms, the other being radiation. The convection coefficient is varied with 20% to analyze the model's sensitivity.

Convection coefficient, glass to surroundings ($\frac{W}{m^2°C}$)	3,2	4 (default)	3,8
t_{weld} (s)	60	60	62

Table A.8: Weld time for varying convection coefficients for heat transfer from the glass to surroundings.

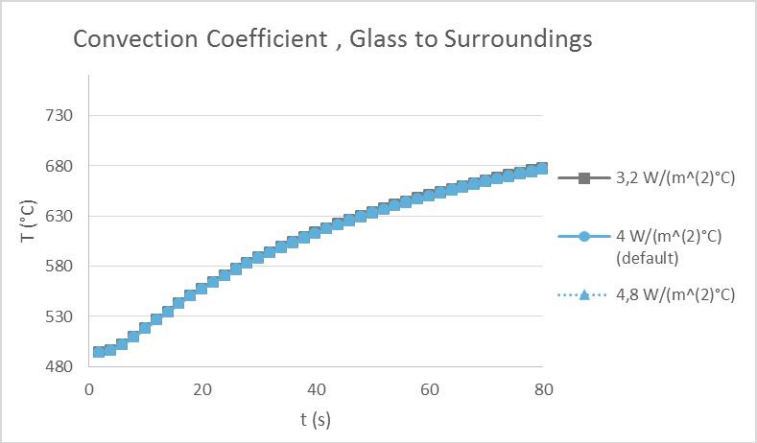

Figure A.38: Temperature at the core of the welding zone over time for different convection coefficients for heat transfer from the glass to surroundings.

The influence of the coefficient to the weld time is insignificant. The small difference in the thermal analysis is most visible in figure A.38.

There is a difference among the stress plots (Figure A.43). However, this difference is considered insignificant as well. This is not odd, because the coefficient of conduction influences the thermal analysis. If the difference in the thermal analysis is insignificant, it should be as well in the mechanical analysis.

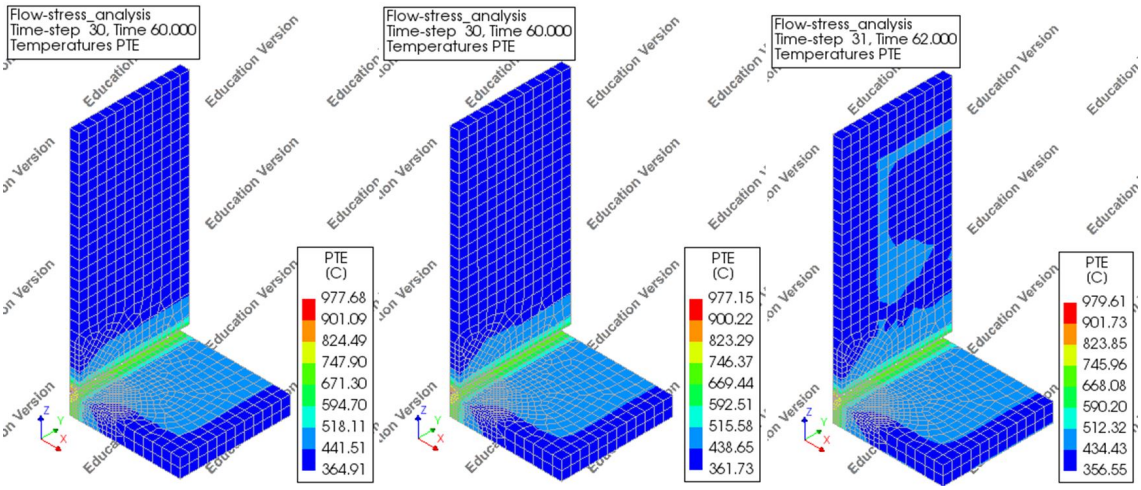

Figure A.39: Temperature distributions at weld time for different convection coefficients for heat transfer from the glass to surroundings. From left to right: $3,2\ \frac{W}{m^{2\circ}C}$, $4\ \frac{W}{m^{2\circ}C}$ (default) and $4,8\ \frac{W}{m^{2\circ}C}$

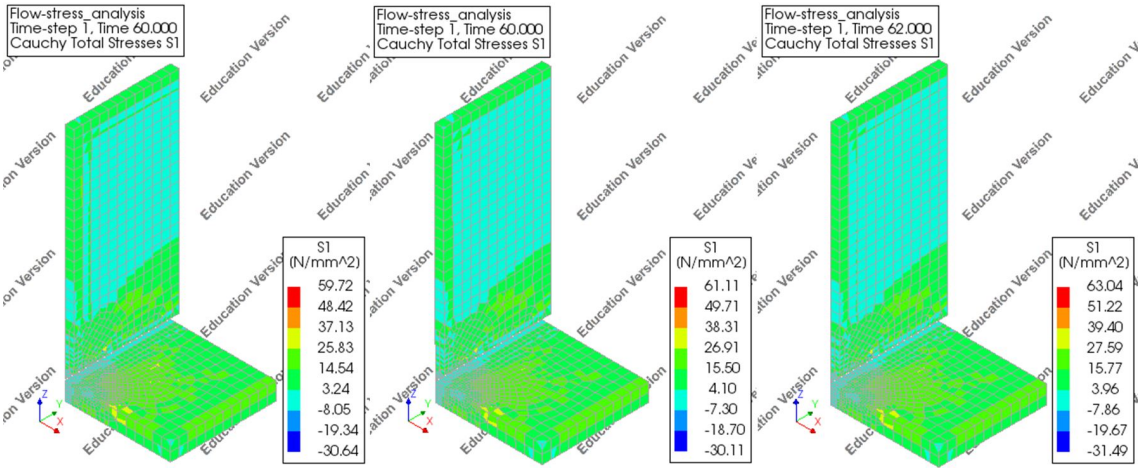

Figure A.40: Principal stress plots at weld time for different convection coefficients for heat transfer from the glass to surroundings. From left to right: $3,2\ \frac{W}{m^{2\circ}C}$, $4\ \frac{W}{m^{2\circ}C}$ (default) and $4,8\ \frac{W}{m^{2\circ}C}$

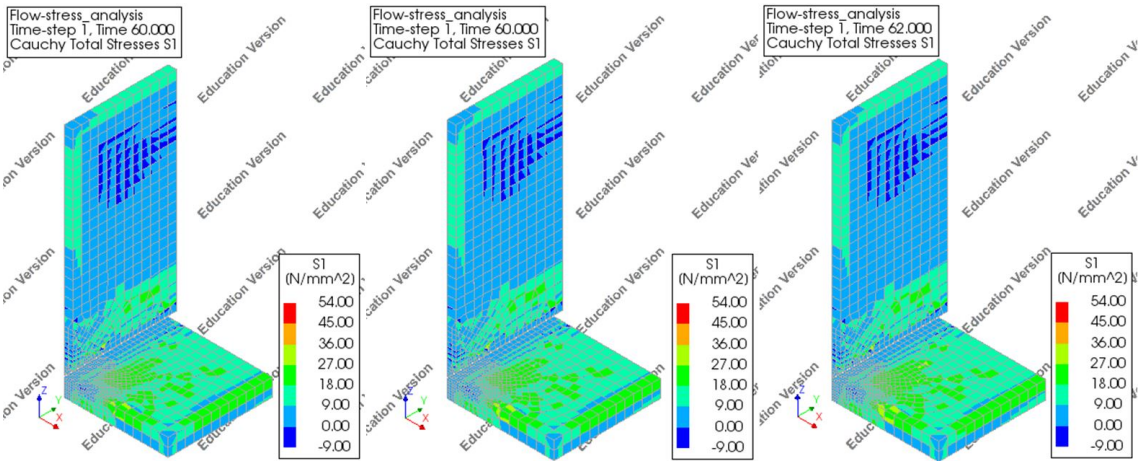

Figure A.41: Principal stress plots, scaled, at weld time for different convection coefficients for heat transfer from the glass to surroundings. From left to right: $3,2\ \frac{W}{m^{2\circ}C}$, $4\ \frac{W}{m^{2\circ}C}$ (default) and $4,8\ \frac{W}{m^{2\circ}C}$

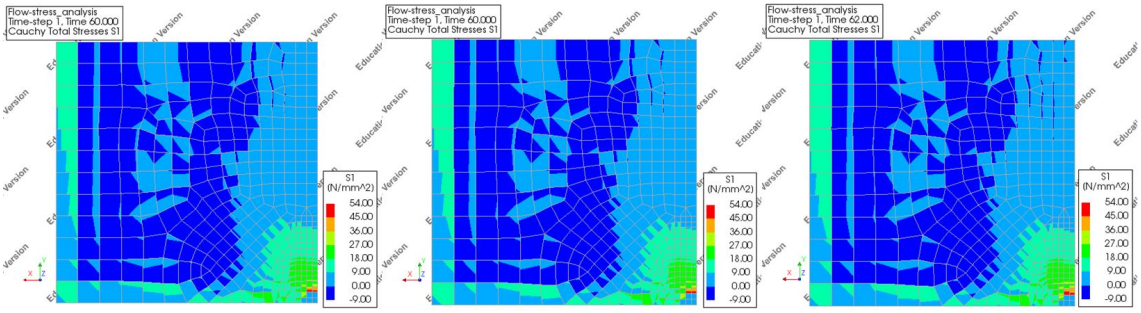

Figure A.42: Principal stress plots, scaled, at weld time of the bottom surface for different convection coefficients for heat transfer from the glass to surroundings. From left to right: $3,2\ \frac{W}{m^{2\circ}C}$, $4\ \frac{W}{m^{2\circ}C}$ (default) and $4,8\ \frac{W}{m^{2\circ}C}$

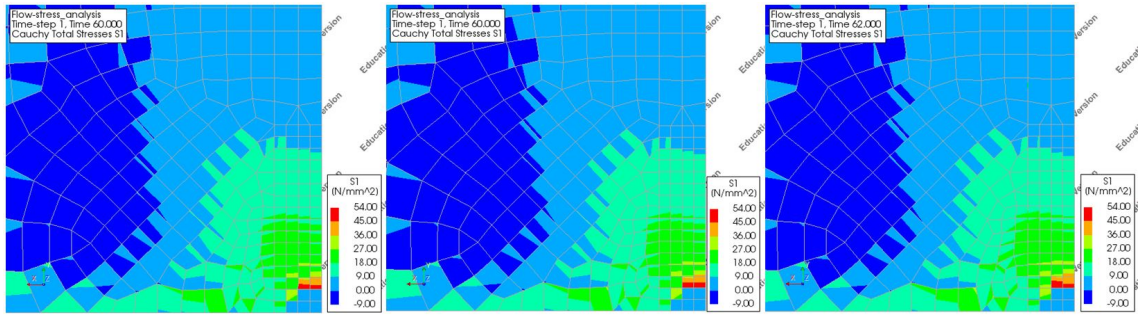

Figure A.43: Principal stress plots, scaled, at weld time, close-up of the bottom surface for different convection coefficients for heat transfer from the glass to surroundings. From left to right: $3,2\ \frac{W}{m^{2\circ}C}$, $4\ \frac{W}{m^{2\circ}C}$ (default) and $4,8\ \frac{W}{m^{2\circ}C}$

A.10 Emissivity

The second phenomenon considering heat loss to surroundings, is radiation. This is scaled with the emissivity factor. The sensitivity of the model is analyzed by varying the emissivity factor with 20%.

Emissivity (-)	0,512	0,64 (default)	0,768
t_{weld} (s)	58	60	64

Table A.9: Weld time for varying emissivity factors.

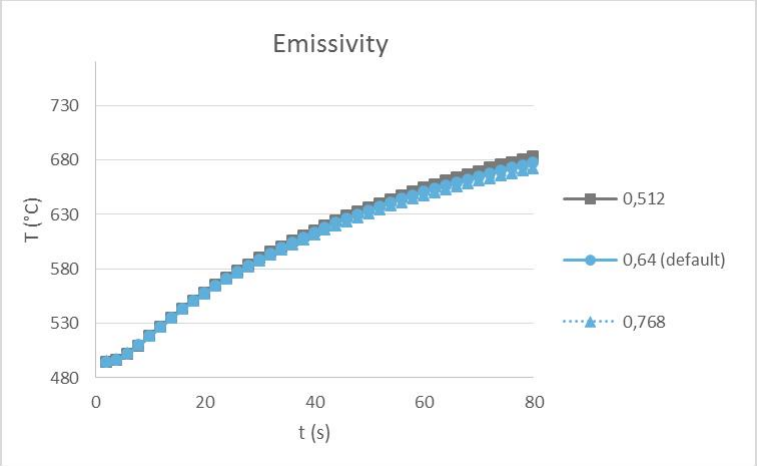

Figure A.44: Temperature at the core of the welding zone over time for different emissivity factors.

The variation of the emissivity makes a difference to the thermal results that is significant. A lower emissivity results in a shorter weld time.

The stress plots show a different distribution as well. The lower the emissivity, the smaller the critical area.

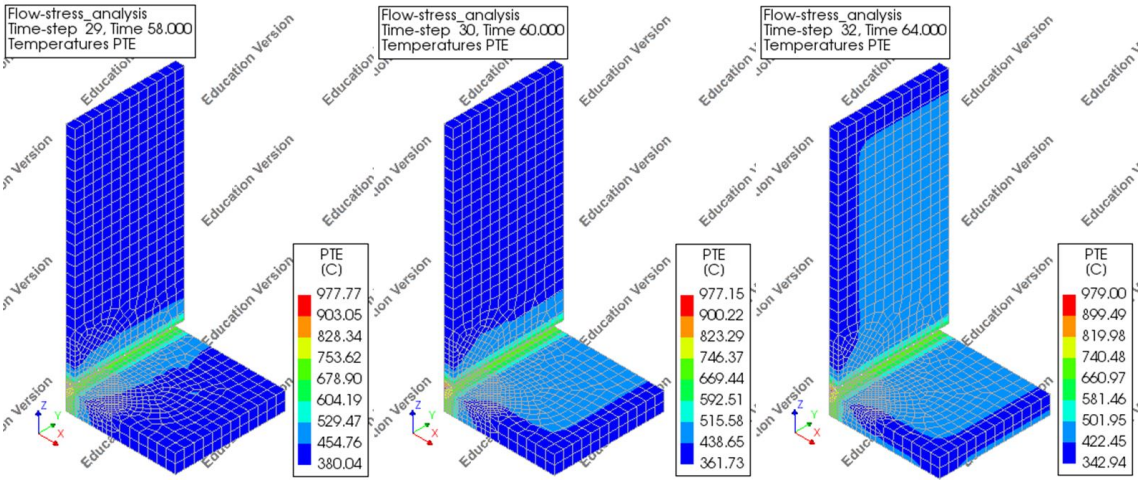

Figure A.45: Temperature distributions at weld time for different emissivity factors. From left to right: 0,512, 0,64 (default) and 0,768

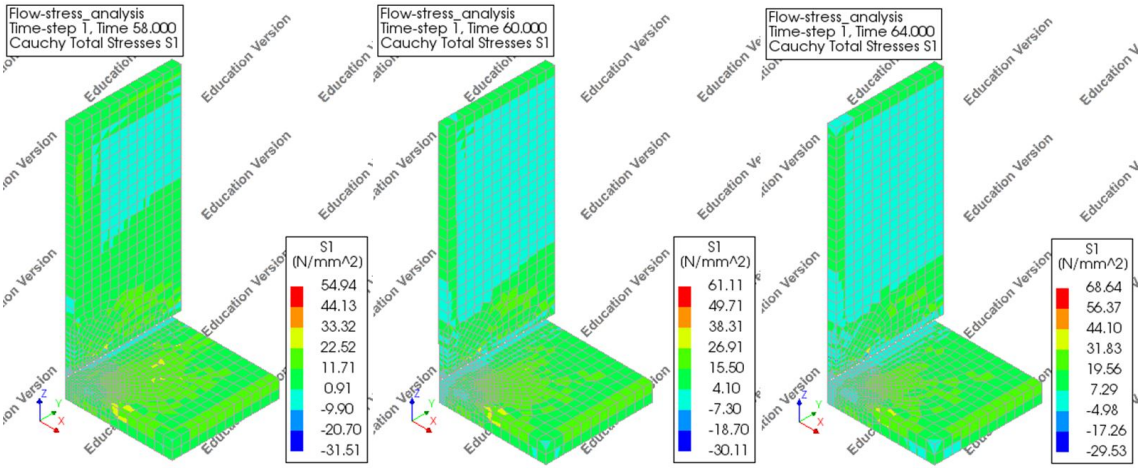

Figure A.46: Principal stress plots at weld time for different emissivity factors. From left to right: 0,512, 0,64 (default) and 0,768

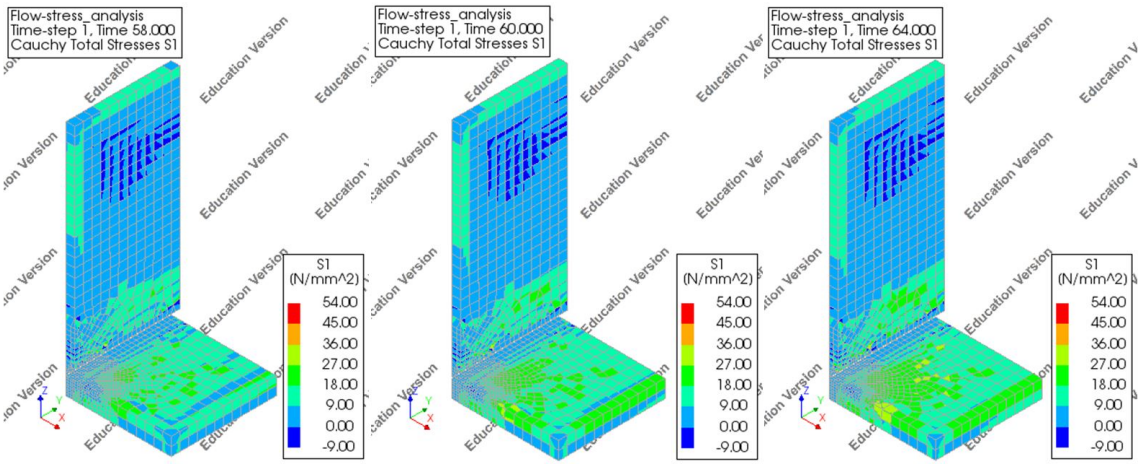

Figure A.47: Principal stress plots, scaled, at weld time for different emissivity factors. From left to right: 0,512, 0,64 (default) and 0,768

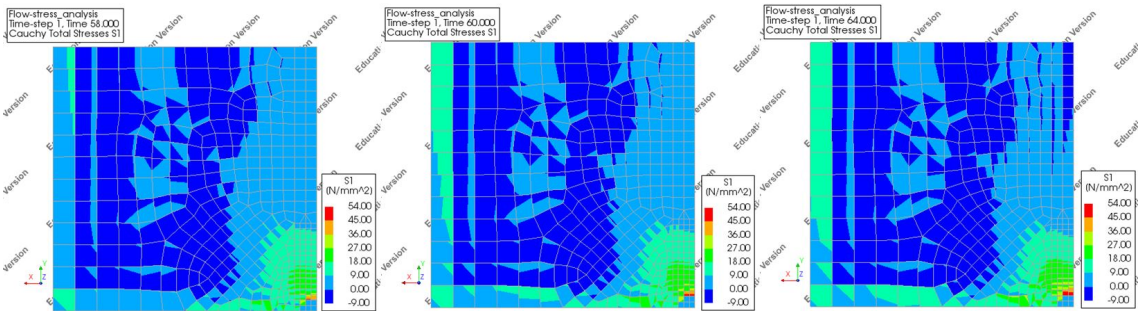

Figure A.48: Principal stress plots, scaled, at weld time of the bottom surface for different emissivity factors. From left to right: 0,512, 0,64 (default) and 0,768

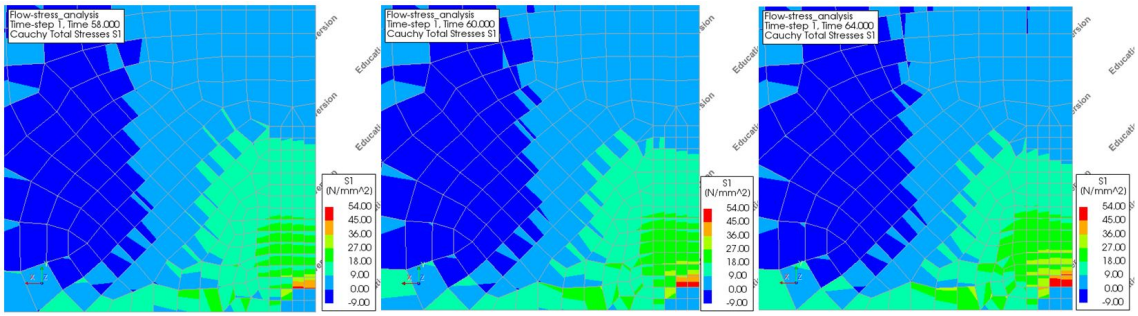

Figure A.49: Principal stress plots, scaled, at weld time, close-up of the bottom surface for different emissivity factors. From left to right: 0,512, 0,64 (default) and 0,768

A.11 Surrounding Temperature

Heat loss to surroundings occurs through two phenomena, which are both related to the temperature of the surroundings. This temperature is by default room temperature. It is analyzed whether a change in surrounding temperature would reduce the critical stress area.
In practice, the question is whether maintaining a certain temperature around the glass will result in a bottom surface without critical stress. Note that in all analayses, the preheating temperature is fixed at 500 $°C$.

Surrounding temperature ($°C$)	20 (default)	100	200	300	400	500
t_{weld} (s)	60	60	58	58	54	52
t_{fail} (s)				70	82	>82
Production time (s)	-	-	-	12	28	>30

Table A.10: Weld times for varying surrounding temperatures. Failure times and production times ($t_{fail} - t_{weld}$) are listed for those showing no critical stress at t_{weld}.

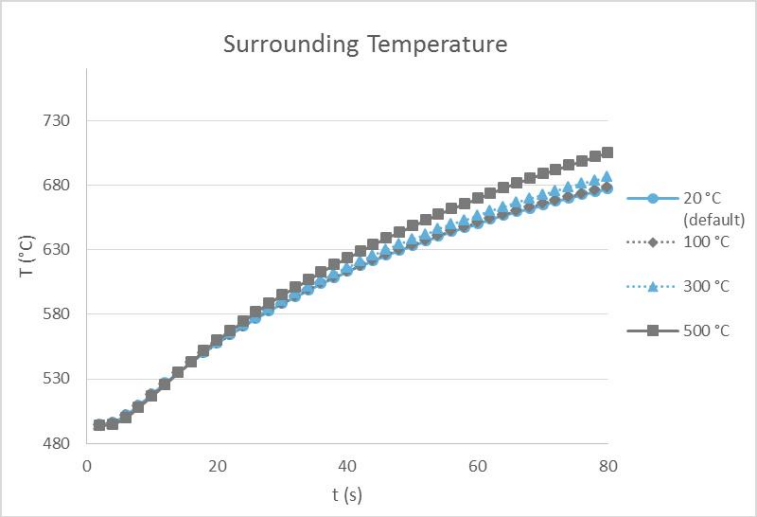

Figure A.50: Temperature at the core of the welding zone over time for different surrounding temperatures.

The thermal results are influenced by this parameter. In figure A.51, it can be seen that the minimum temperature in the glass raises along with the surrounding temperature. The temperatures in the core of the welding zone are also influenced, resulting in slight, but significant change in weld time.

The stress plots vary significantly for the analyzed situations. The most important conclusion is that the stress plot is not critical at weld time for a surrounding temperature at 300 $°C$ or higher. Further research has provided the first time step at which critical stress occurs (Table A.10). It shows that with a surrounding temperature of 300 $°C$, the production time is too short. The available time for 400 $°C$ surroundings is considerably larger and might be large enough to manipulate the glass. The results for 500 $°C$ provide sufficient production time

The conclusion is that if the temperature of the surroundings is maintained at a higher level, the risk of thermal shock failure is smaller. The glass could be welded withoutchanging the flame position.

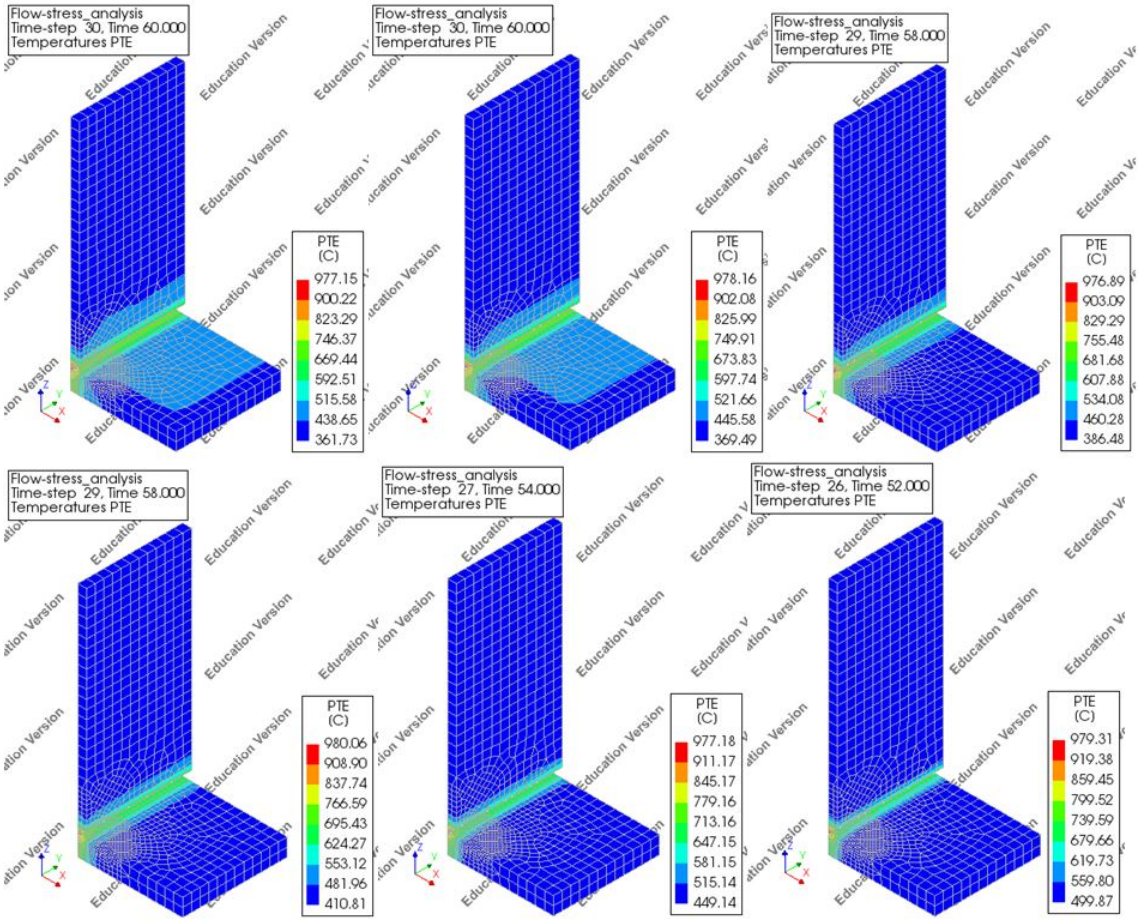

Figure A.51: Temperature distributions at weld time for different surrounding temperatures. From left to right, top to bottom: 20 $°C$, 100 $°C$, 200 $°C$, 300 $°C$, 400 $°C$, 500 $°C$

Practically, this is challenging, for humans cannot be in these conditions. Until the process is automatized or remote controlled in a climatized space, this is not practical.

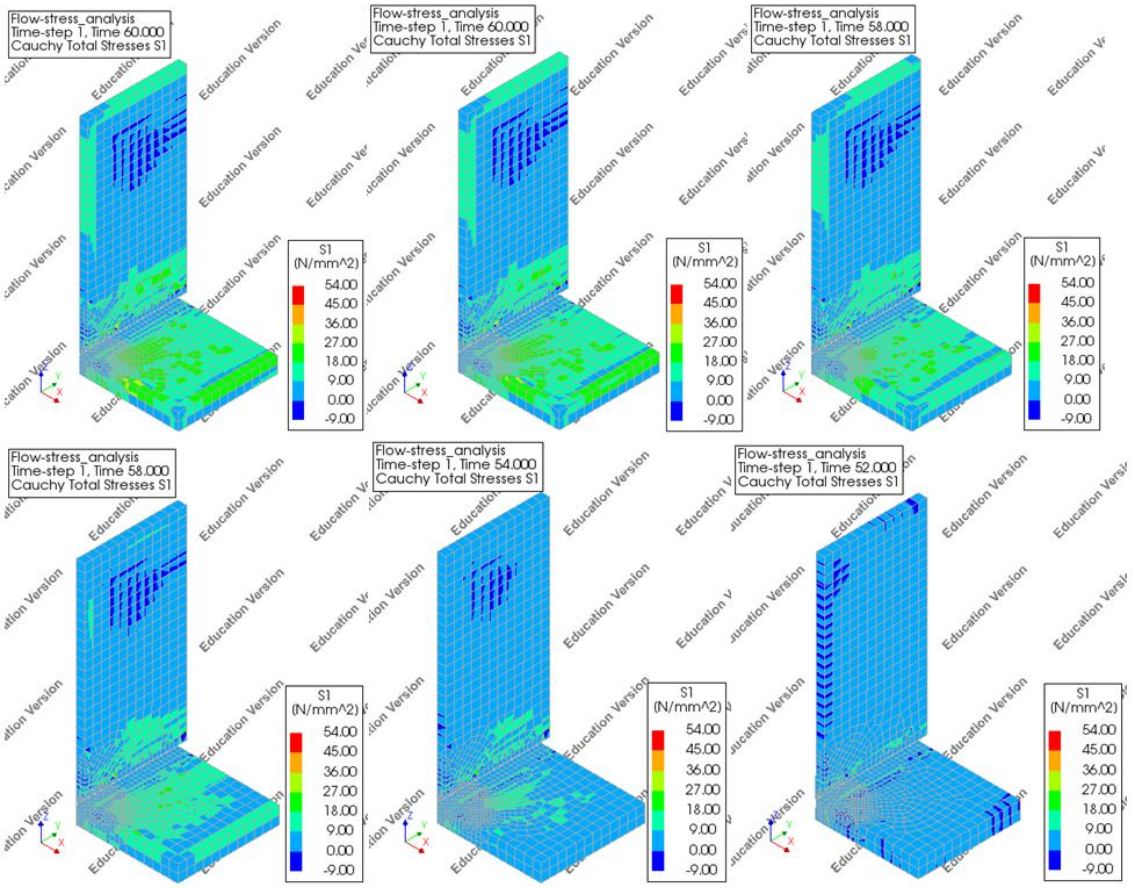

Figure A.52: Principal stress plots, scaled, at weld time for different surrounding temperatures. From left to right, top to bottom: 20 $°C$, 100 $°C$, 200 $°C$, 300 $°C$, 400 $°C$, 500 $°C$

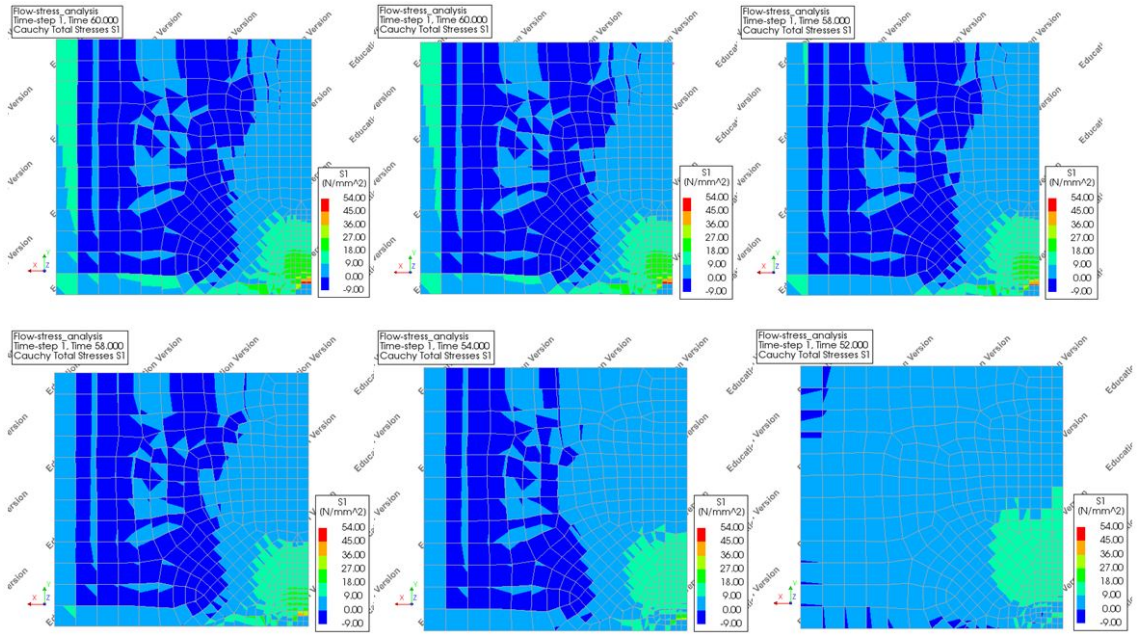

Figure A.53: Principal stress plots, scaled, at weld time of the bottom surface for different surrounding temperatures. From left to right, top to bottom: 20 $°C$, 100 $°C$, 200 $°C$, 300 $°C$, 400 $°C$, 500 $°C$

A.12 Transition Range

The transition range determines at which temperature the viscoelastic behaviour of glass causes stress relaxation. In section 18, the transition range is defined as the temperatures at which 5 to 95% of the stress in the glass is released in a time frame of 1 second. Here, the values of this percentage and time frame are varied, to investigate the sensitivity of the results to this definition.

Using the relation between temperature and viscosity of figure 26 and the formulas in section 9, the temperatures are found for different definitions of the transition range. These are displayed in figure A.54 and listed in table A.11. It is observed that the percentage influences the width of the transition range and that altering the time frame displaces the transition range along the temperature axis.

The transition range is an indirect parameter. It is not an input parameter of the model, but it has influence on several parameters. These are the specific heat capacity, coefficient of linear thermal expansion and the Young's modulus, as described in section 18. These are adapted for each transition range accordingly to perform the analyses.

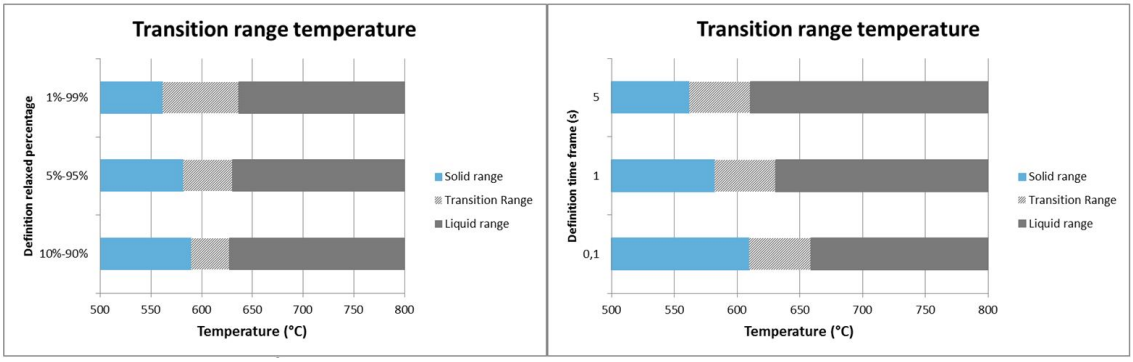

Figure A.54: Temperature ranges for the solid, transition and liquid range. Left: constant time frame, varying relaxed percentage. Right: varying time frame, constant relaxed percentage.

Transition range	5-95%, 1 s (default)	1-99%, 1 s	10-90%, 1 s	5-95%, 0,1 s	5-95%, 5 s
Temperatures ($°C$)	585 - 630	562 - 637	590 - 628	610 - 659	562 - 611
t_{weld} (s)	60	62	60	60	62

Table A.11: Temperature range and weld times for varying definitions of the transition range

The thermal analysis results show that the transition range definition makes a difference in the temperature development, though it is very small. This is due to the adaptation of the specific heat capacity. The differences are too insignificant to dram conclusions on the influence of the definition. It is concluded that an adaptation in this temperature range for the specific heat capacity can alter the weld time with two seconds.

Stress relaxation can only be accepted if the stress development due to loading is slower than the stress relaxation. For example, a very short time frame for impact loads, and a longer time frame for slowly pressing the glass. In this thesis, it has been defined that the increase in temperature has to be lower than 60 $°C$ in the time frame (Section 18).

In table A.12, it is checked whether this requirement is met. This is done by measuring the maximum

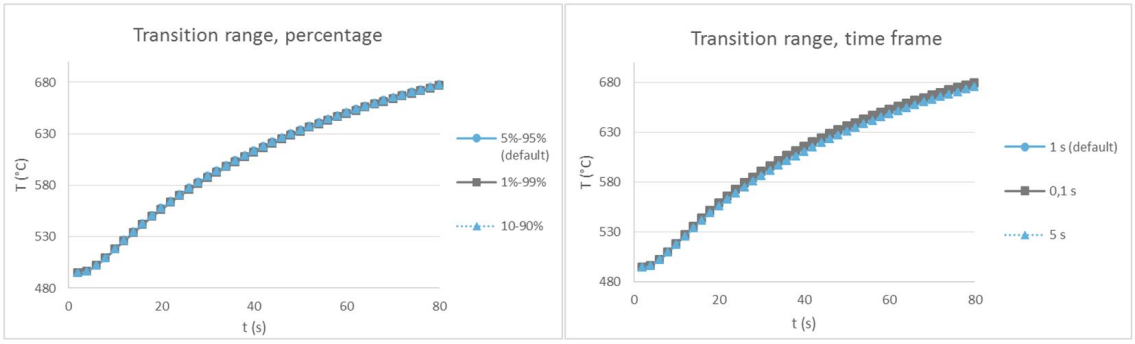

Figure A.55: Temperature at the core of the welding zone over time for different transition range definitions. Left: constant time frame, varying relaxed percentage. Right: varying time frame, constant relaxed percentage.

increase of temperature. Due to its proximity to multiple flame boundary surface, this is at the front of the welding zone in the tip of the faceted edge, in the first time step. Using this point and time step results in a conservative check, because the temperature rate at the position and time of interest, the bottom surface at weld time, is a fraction of it.
Table A.12 shows that the criterion is not met for a time frame of $5\ s$. It also shows that for the time frame of $0,1\ s$, the criterion is too conservative. The criterion is barely met for the time frame of $1\ s$. However, because the measuring point and time is conservative, it is decided that this time frame is conservative enough to be accepted for these load conditions.

Transition range time frame	5-95%, $0,1\ s$	5-95%, $1\ s$ (default)	5-95%, $5\ s$
Maximum Temperature Increase, Allowed ($\frac{^\circ C}{s}$)	600	60	12
Maximum Temperature Increase, FEA result ($\frac{^\circ C}{s}$)	58	57	55

Table A.12: The maximum allowed increase in temperature and maximum increase in temperature from the results of the FEA for different definitions of transition range time frame.

In figure A.59, it is visible that the stress plot for 5-95% and 10-90% are similar. The difference is almost indistinguishable. The difference between the 1-99% and the 5-95% range is more clear, because it shows less blue elements at the front of the welding zone, indicating less stress relaxation. One element has a moderate stress level (green), probably because it is in transition. In both plots, this element is approximately $630\ ^\circ C$. In the 1-99% range, this temperature is in the transition range, resulting in a moderate stress level. In the 5-95% range, this temperature is in the liquid range, returning low stress.

The influence of the time frame is visible when the stress plots of the bottom at t_{weld} are compared. The difference in the size of the critical area for differnt time frame definitions is insignificantly small. The significant difference is the location of the stress peak.
The time frame of $0,1\ s$ returns a more rigid material. There are two elements with a low stress at the front, indicating the relaxed, liquid state.
For a time frame of $5\ s$, the material is more relaxed, as seven elements are relaxed at the front as opposed to five for the default parameter. The critical elements are positioned further away from the edge. Two adjacent element are in the transition range, which is indicated by their substantial, but not

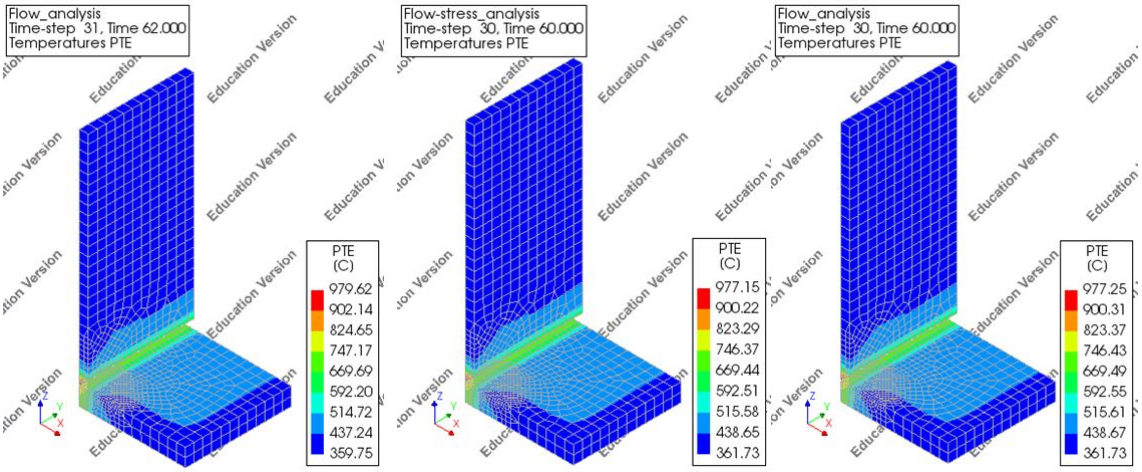

Figure A.56: Temperature distributions at weld time for different surrounding temperatures. From left to right: 1-99%, 5-95% (default) and 10-90%. All transition ranges are defined with a 1 s time frame.

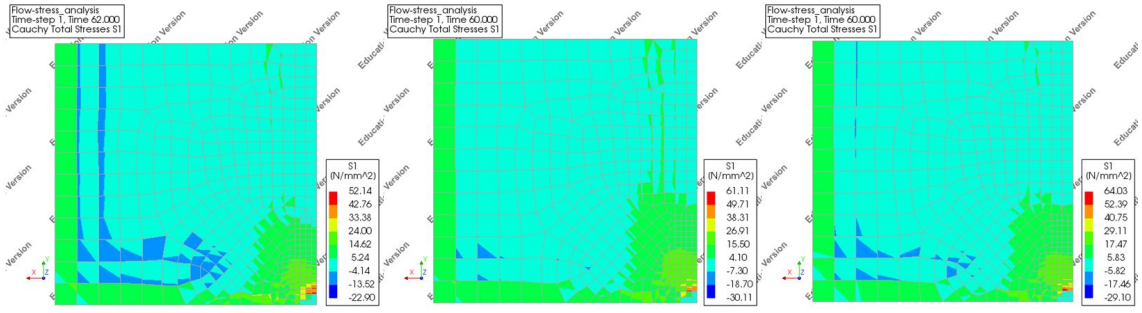

Figure A.57: Principal stress plots at weld time of the bottom surface for different definition of the relaxed percentage. From left to right: 1-99%, 5-95% (default) and 10-90%. All transition ranges are defined with a 1 s time frame.

critical stress level.

This supports the expected influence of the time frame of the transition range: if the the time frame is larger, the material is relaxed at lower temperatures, resulting in more relaxed elements at t_{weld}.
The most important conclusion is that for all three time frames, the specimen is predicted to fail due to thermal shock. The stress limit is exceeded in all analyses, at a surface area of similar size. The definition of the time frame influences the exact stress distribution, but not the final conclusion to be taken from the results.

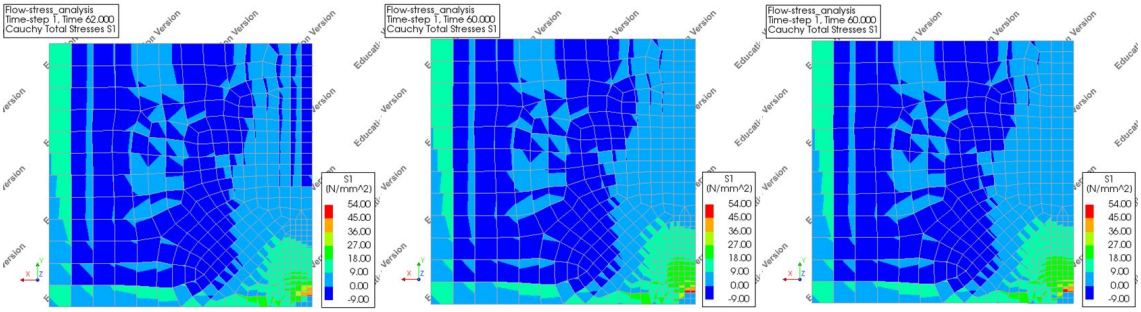

Figure A.58: Principal stress plots, scaled, at weld time of the bottom surface for different definition of the relaxed percentage. From left to right: 1-99%, 5-95% (default) and 10-90%. All transition ranges are defined with a 1 s time frame.

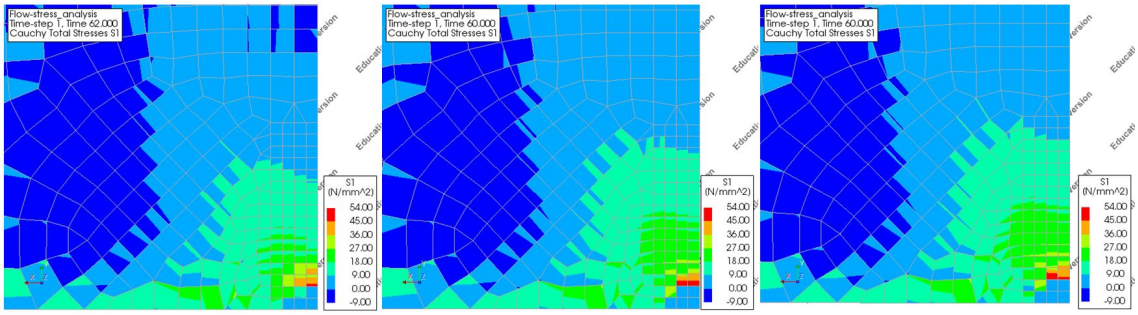

Figure A.59: Principal stress plots, scaled, at weld time, close-up of the bottom surface for different definition of the relaxed percentage. From left to right: 1-99%, 5-95% (default) and 10-90%. All transition ranges are defined with a 1 s time frame.

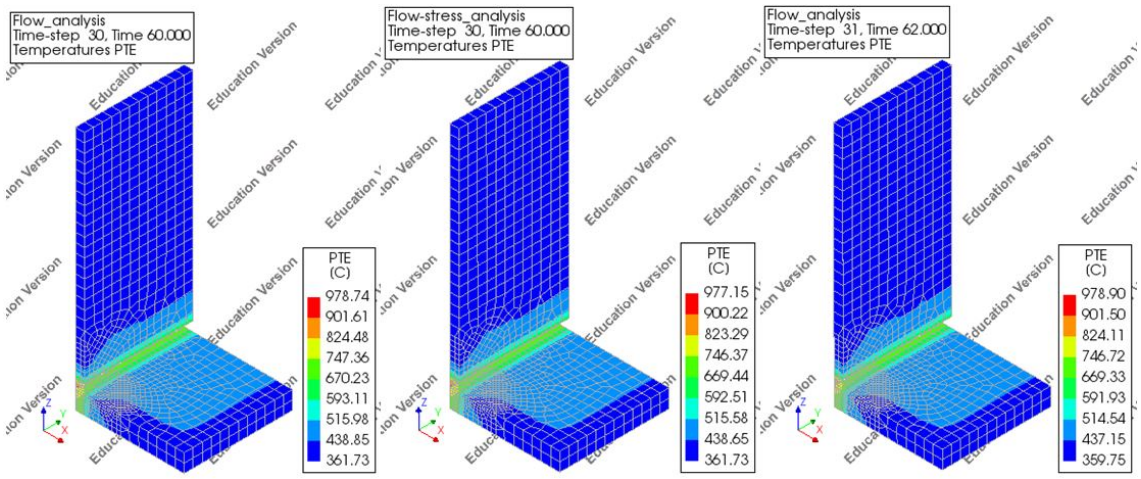

Figure A.60: Temperature distributions at weld time for different surrounding temperatures. From left to right: $0,1$ s, 1 s (default) and 5 s. All transition ranges are defined with a relaxed percentage of 5-95%.

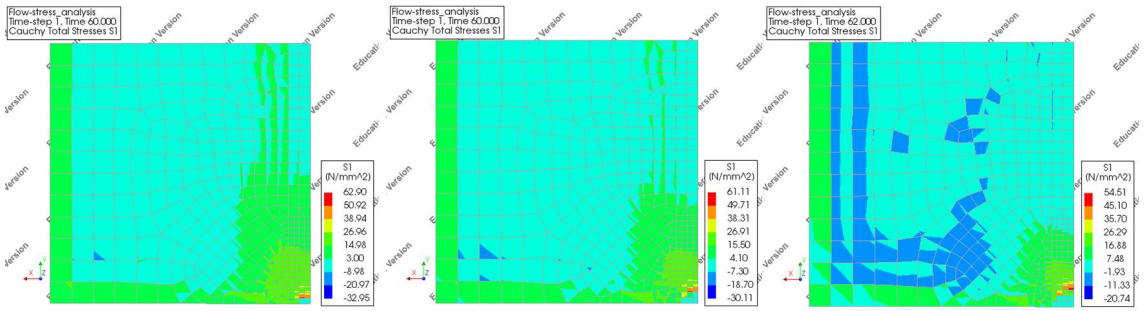

Figure A.61: Principal stress plots at weld time of the bottom surface for different definition of the time frame. From left to right: $0,1\ s$, $1\ s$ (default) and $5\ s$. All transition ranges are defined with a relaxed percentage of 5-95%.

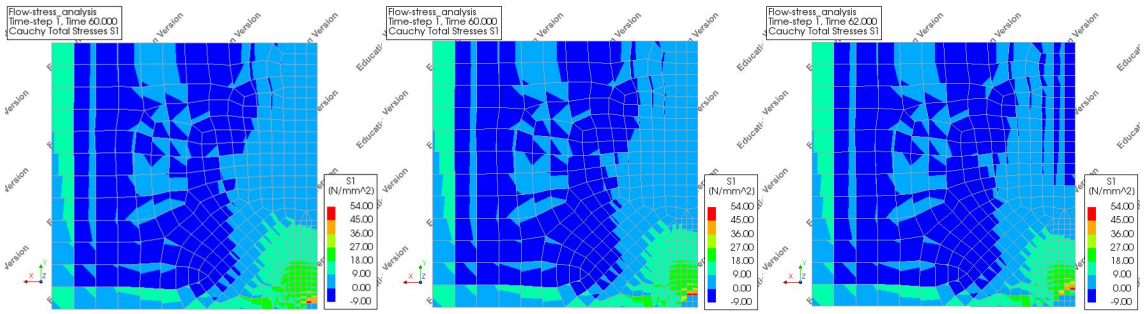

Figure A.62: Principal stress plots, scaled, at weld time of the bottom surface for different definition of the time frame. From left to right: $0,1\ s$, $1\ s$ (default) and $5\ s$. All transition ranges are defined with a relaxed percentage of 5-95%.

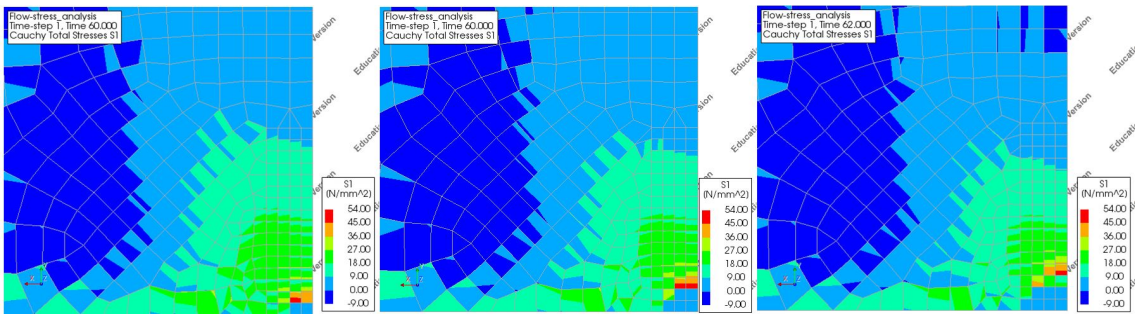

Figure A.63: Principal stress plots, scaled, at weld time close-up of the bottom surface for different definition of the time frame. From left to right: $0,1\ s$, $1\ s$ (default) and $5\ s$. All transition ranges are defined with a relaxed percentage of 5-95%.

A.13 Specific Heat Capacity

Altering the specific heat capacity changes the amount of energy required to change the temperature. The parameter's default value is temperature dependent (Figure 49). The sensitivity of the model is tested by analyzing it for its minimum and maximum value constant over temperature.

The specific heat can be measured in energy per unit of temperature per unit of volume, which the software requires, or energy per unit of temperature per unit of mass, which the literature provided. These units are related by the volumetric mass of glass. However, it can be argued that this is not a constant value over temperature, as the material expands.
It has been researched if this would be of significant influence. Using the coefficient of linear thermal expansion and assuming the mass of the glass remains constant, the density has been adapted to a temperature dependent desity. This made no significant difference to the value of the specific heat capicity in energy per unit of temperature per unit of volume ($\frac{J}{m^3°C}$) and is therefore neglected.

Specific heat capacity ($\cdot 10^6$ $\frac{J}{m^3°C}$)	constant 2,1	2,1 to 3,6 (default)	constant 3,6
t_{weld} (s)	40	60	66

Table A.13: Weld time for varying values of specific heat capacity.

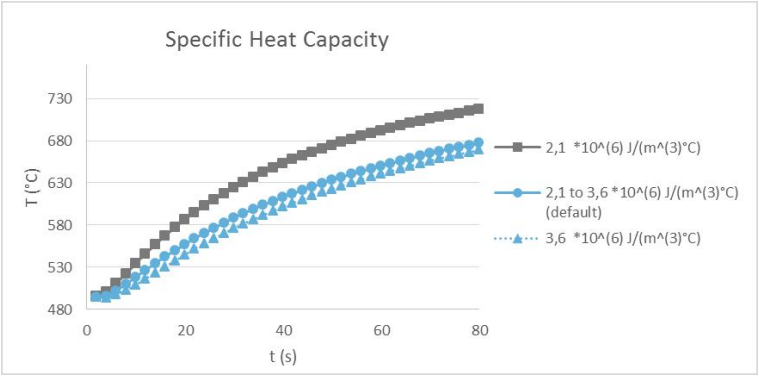

Figure A.64: Temperature at the core of the welding zone over time for different values of specific heat capacity.

The specific heat influences thermal results such as weld time significantly. The difference between minimum constant specific heat capacity and default is larger than of that between maximum and default. This is not odd, because the minimum value is by default applicable in lower temperature ranges. For the ranges of this analysis, 300 to 900 $°C$, specific heat is closer to the maximum value.

The stress plots at weld time for different specific heat values show a difference which is considered insignificantly small.

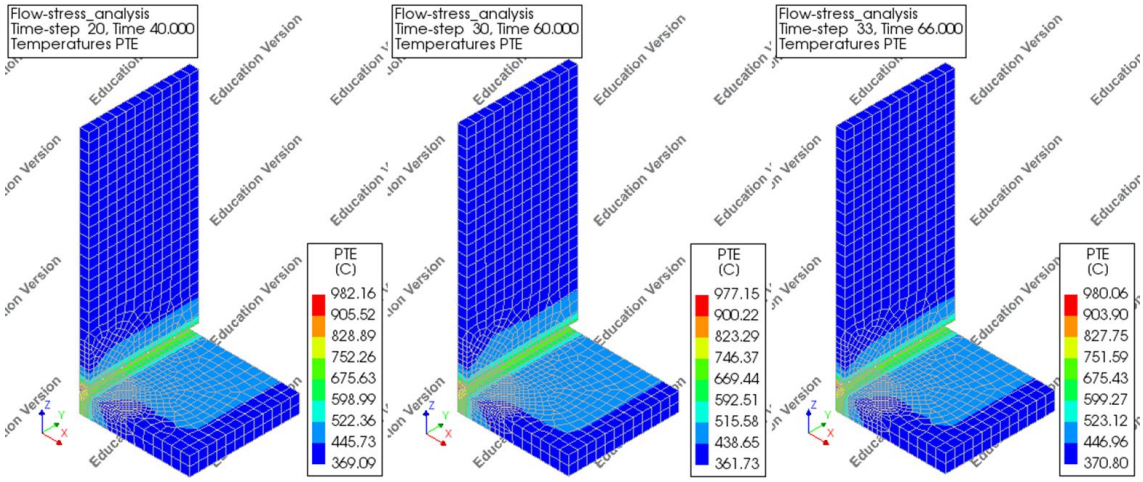

Figure A.65: Temperature distributions at weld time for different values of specific heat capacity. From left to right: constant $2,1 \cdot 10^6 \frac{J}{m^3°C}$, $2,1$ to $3,6 \cdot 10^6 \frac{J}{m^3°C}$ (default) and constant $3,6 \cdot 10^6 \frac{J}{m^3°C}$

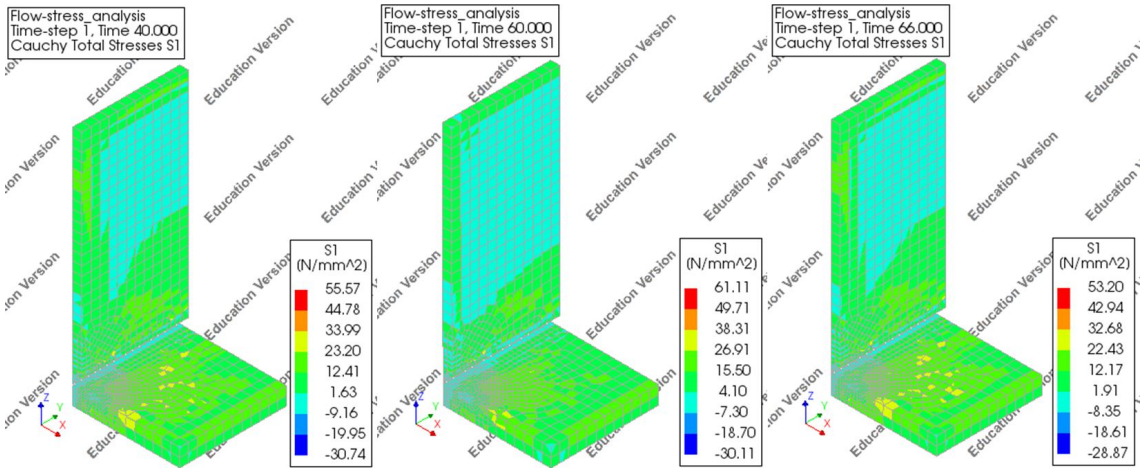

Figure A.66: Principal stress plots at weld time for different values of specific heat capacity. From left to right: constant $2,1 \cdot 10^6 \frac{J}{m^3°C}$, $2,1$ to $3,6 \cdot 10^6 \frac{J}{m^3°C}$ (default) and constant $3,6 \cdot 10^6 \frac{J}{m^3°C}$

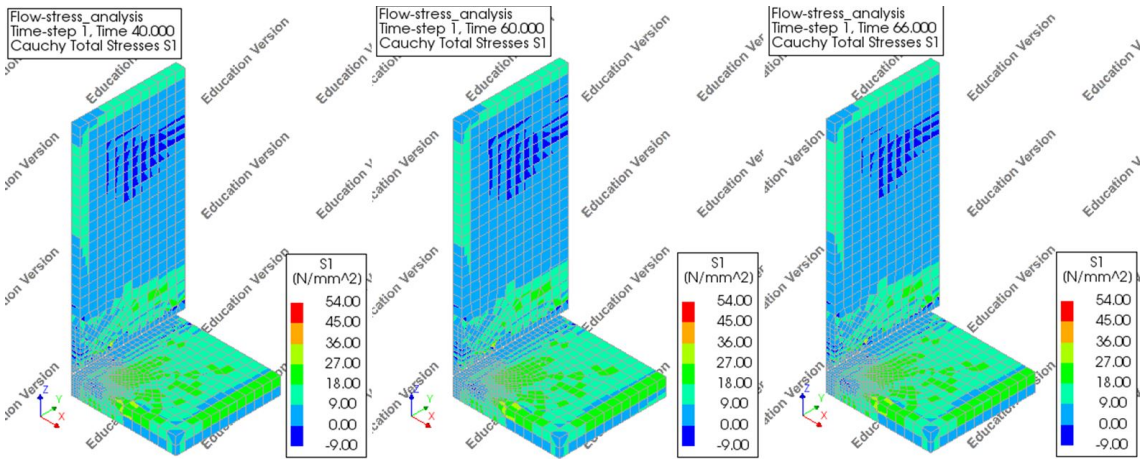

Figure A.67: Principal stress plots, scaled, at weld time for different values of specific heat capacity. From left to right: constant $2,1 \cdot 10^6 \frac{J}{m^{3\circ}C}$, $2,1$ to $3,6 \cdot 10^6 \frac{J}{m^{3\circ}C}$ (default) and constant $3,6 \cdot 10^6 \frac{J}{m^{3\circ}C}$

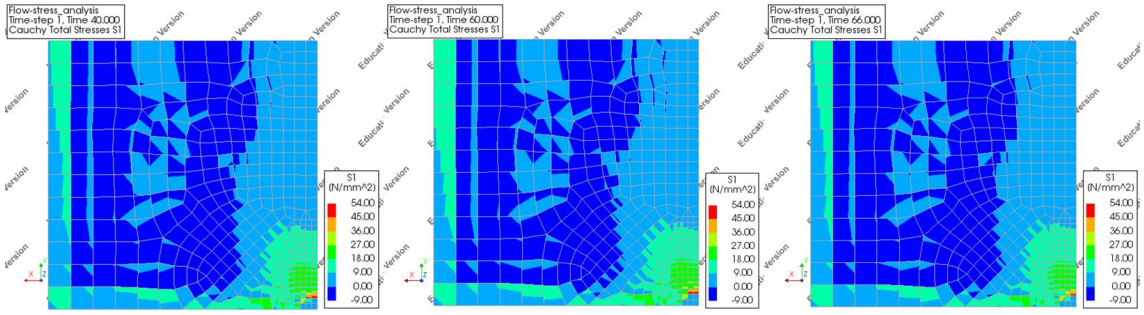

Figure A.68: Principal stress plots, scaled, at weld time of the bottom surface for different values of specific heat capacity. From left to right: constant $2,1 \cdot 10^6 \frac{J}{m^{3\circ}C}$, $2,1$ to $3,6 \cdot 10^6 \frac{J}{m^{3\circ}C}$ (default) and constant $3,6 \cdot 10^6 \frac{J}{m^{3\circ}C}$

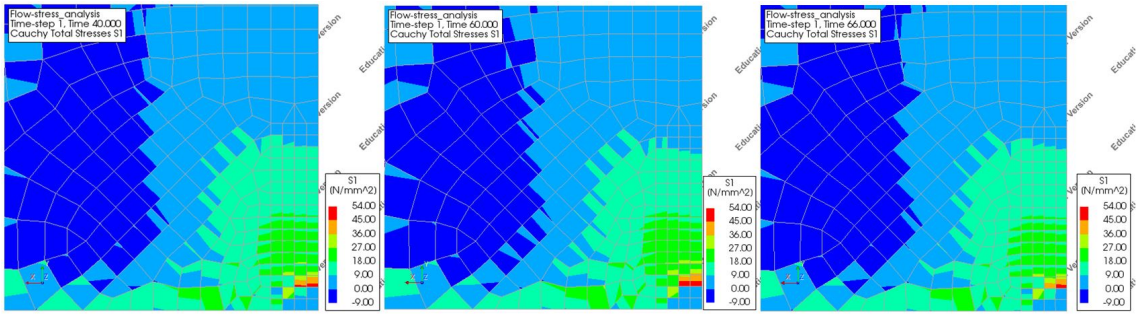

Figure A.69: Principal stress plots, scaled, at weld time, close-up of the bottom surface for different values of specific heat capacity. From left to right: constant $2,1 \cdot 10^6 \frac{J}{m^{3\circ}C}$, $2,1$ to $3,6 \cdot 10^6 \frac{J}{m^{3\circ}C}$ (default) and constant $3,6 \cdot 10^6 \frac{J}{m^{3\circ}C}$

A.14 Thermal Conductivity

The thermal conductivity of glass influences the spread of heat through the material. The sensitivity of the model to this parameter has been analyzed by varying it with 20%.

Thermal conductivity ($\frac{W}{m°C}$)	0,96	1,2	1,44
t_{weld} (s)	58	60	64

Table A.14: Weld time for varying values of thermal conductivity.

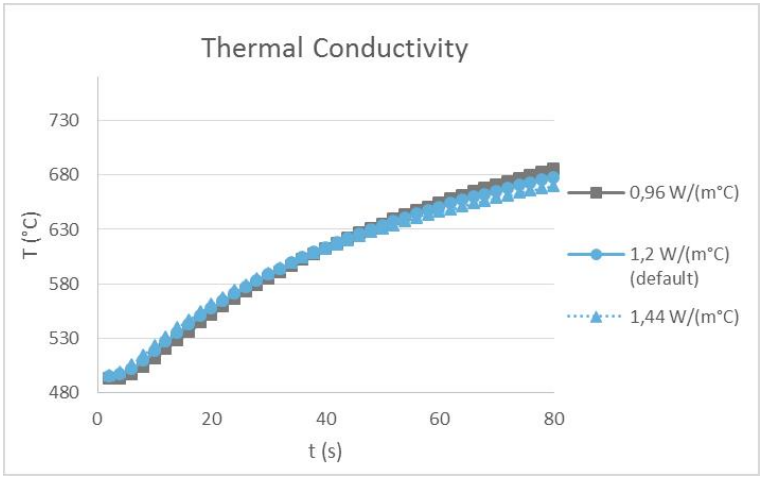

Figure A.70: Temperature at the core of the welding zone over time for different values of thermal conductivity.

The thermal conductivity of glass has a small influence on the weld time, but a significant influence of the temperature distribution at weld time. Minimum termperatures in the glass varies from 355 to 364 $°C$.

The stress plots show differences, though all predict the specimen to fail at weld time.

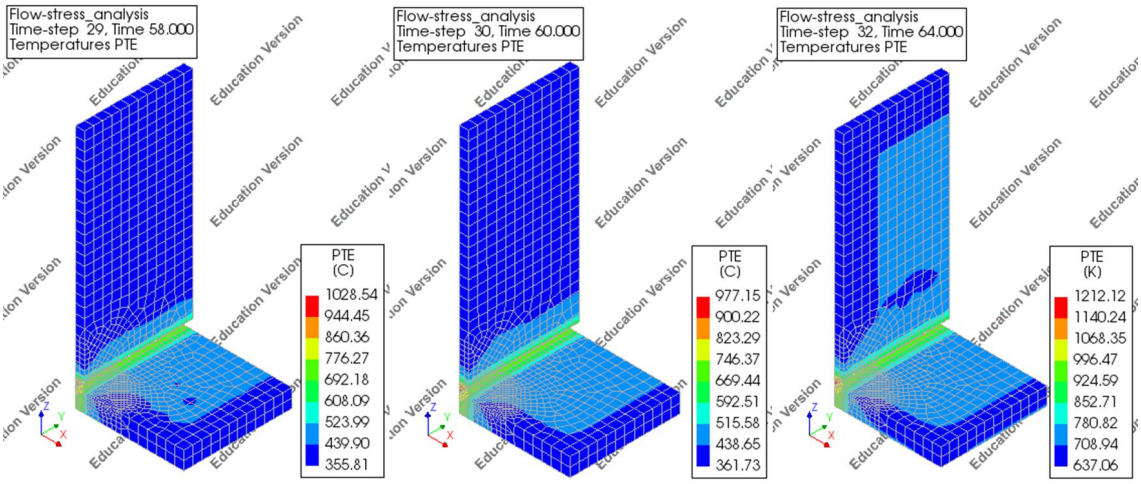

Figure A.71: Temperature distributions at weld time for different values of thermal conductivity. From left to right: $0,96\ \frac{W}{m°C}$, $1,2\ \frac{W}{m°C}$ (default) and $1,44\ \frac{W}{m°C}$

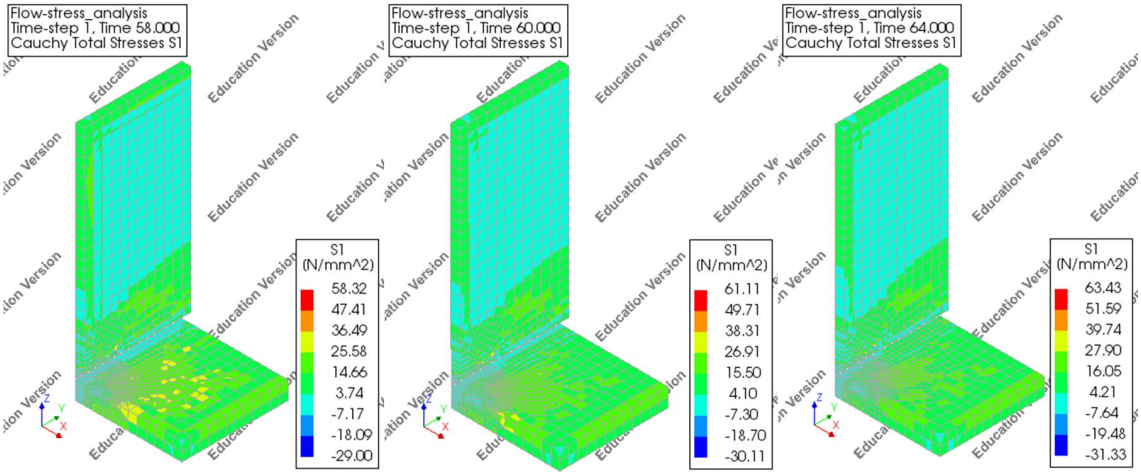

Figure A.72: Principal stress plots at weld time for different values of thermal conductivity. From left to right: $0,96\ \frac{W}{m°C}$, $1,2\ \frac{W}{m°C}$ (default) and $1,44\ \frac{W}{m°C}$

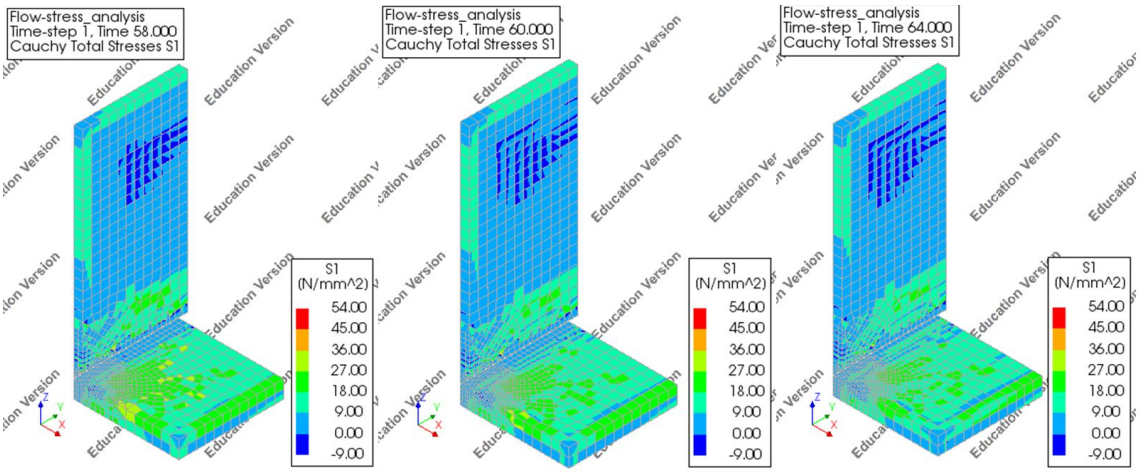

Figure A.73: Principal stress plots, scaled, at weld time for different values of thermal conductivity. From left to right: $0,96\ \frac{W}{m°C}$, $1,2\ \frac{W}{m°C}$ (default) and $1,44\ \frac{W}{m°C}$

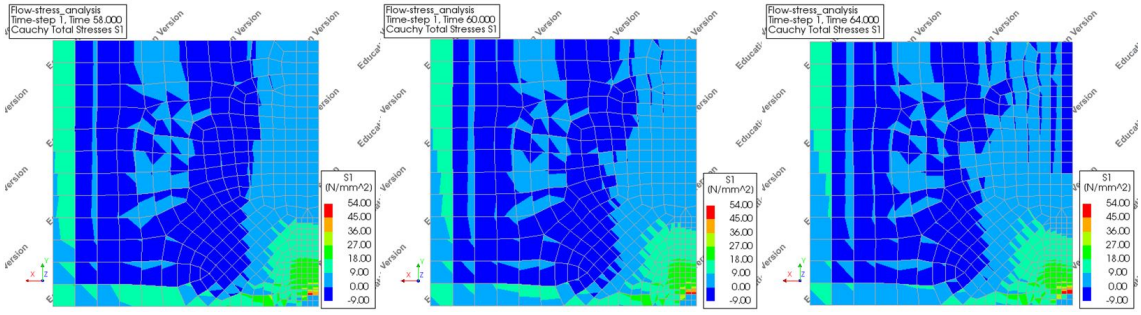

Figure A.74: Principal stress plots, scaled, at weld time of the bottom surface for different values of thermal conductivity. From left to right: $0,96\ \frac{W}{m°C}$, $1,2\ \frac{W}{m°C}$ (default) and $1,44\ \frac{W}{m°C}$

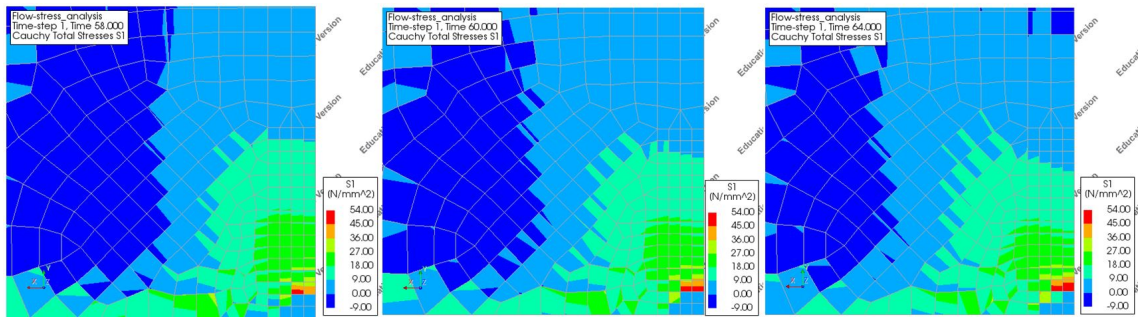

Figure A.75: Principal stress plots, scaled, at weld time close-up of the bottom surface for different values of thermal conductivity. From left to right: $0,96\ \frac{W}{m°C}$, $1,2\ \frac{W}{m°C}$ (default) and $1,44\ \frac{W}{m°C}$

A.15 Coefficient of Linear Thermal Expansion

The magnitude of thermal stress for a certain temperature difference is dominated by the Young's modulus and coefficient of linear thermal expansion. The sensitivity of the model to the latter is analyzed by varying it and interpreting the results. The coefficient depends on the transition range, this dependency has been analyzed in another section. Here, the influence of a constant coefficient is analyzed as opposed to the variable default, which returns no expansion in the liquid range. Also, the magnitude of the variable coefficient is varied with 20%.
As explained in section 18, the coefficient is adapted for the liquid range to model the mechanical influence, not because a liquid does not expand.

Coefficient of linear thermal expansion ($\cdot 10^{-6} °C^{-1}$)	constant, 8,4	variable, 6,72	variable, 8,4 (default)	variable, 10,08
t_{weld} (s)	60	60	60	60

Table A.15: Weld time for varying coefficients of linear thermal expansion.

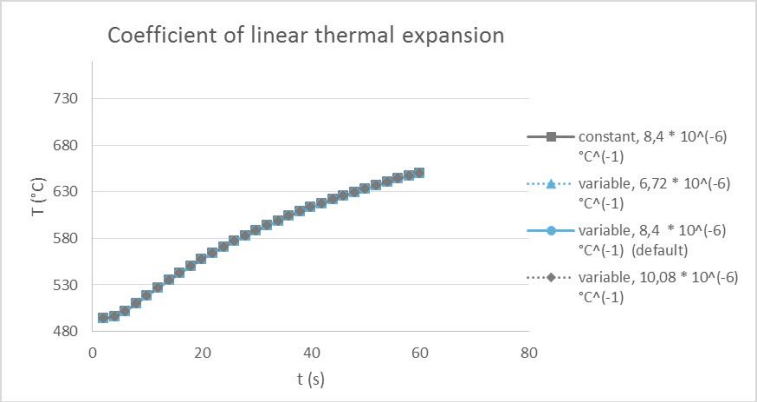

Figure A.76: Temperature at the core of the welding zone over time for different coefficients of linear thermal expansion.

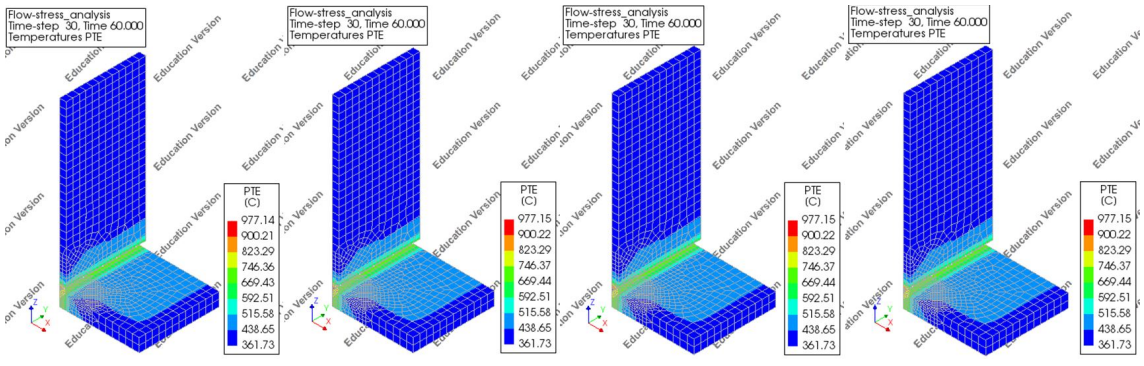

Figure A.77: Temperature distributions at weld time for different coefficients of linear thermal expansion. From left to right: constant $8,4 \cdot 10^{-6} °C^{-1}$, variable $6,72 \cdot 10^{-6} °C^{-1}$, variable $8,4 \cdot 10^{-6} °C^{-1}$ (default) and variable $10,08 \cdot 10^{-6} °C^{-1}$

The coefficient of linear thermal expansion has no influence on the thermal analyses (Figure A.77).

This is not odd, for the parameter is supposed to have no influence on heat transfer.

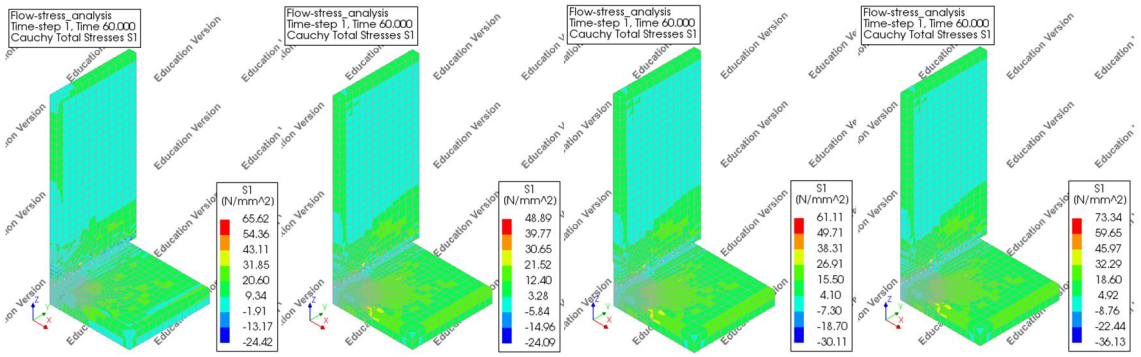

Figure A.78: Principal stress plots at weld time for different coefficients of linear thermal expansion. From left to right: constant $8,4 \cdot 10^{-6} °C^{-1}$, variable $6,72 \cdot 10^{-6} °C^{-1}$, variable $8,4 \cdot 10^{-6} °C^{-1}$ (default) and variable $10,08 \cdot 10^{-6} °C^{-1}$

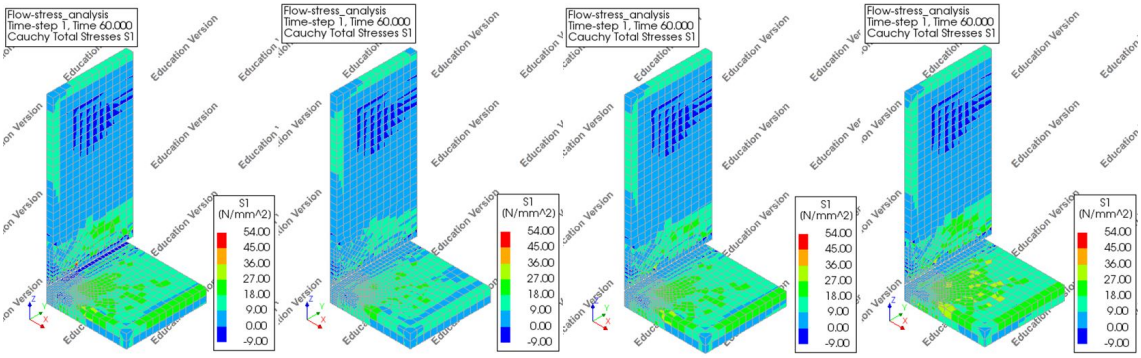

Figure A.79: Principal stress plots, scaled, at weld time for different coefficients of linear thermal expansion. From left to right: constant $8,4 \cdot 10^{-6} °C^{-1}$, variable $6,72 \cdot 10^{-6} °C^{-1}$, variable $8,4 \cdot 10^{-6} °C^{-1}$ (default) and variable $10,08 \cdot 10^{-6} °C^{-1}$

The stress plots show significant difference. In case of a constant coefficient, the area in tensile stress is larger than in the default case. Also, it is observerd that more elements on the bottom sruface contain stress levels of 36 MPa or larger (orange and red)(Figure A.81). It seems the larger stress is spread over more elements, instead of higher, more local stress. The larger stress peaks in the variable cases might be caused by a discontinuity (relaxed and not expanded to rigid and expanded) among the elements.

The variable coefficients show increasing stress for an increasing coefficient. This is directly related to the influence of the coefficient on thermoelasticity.

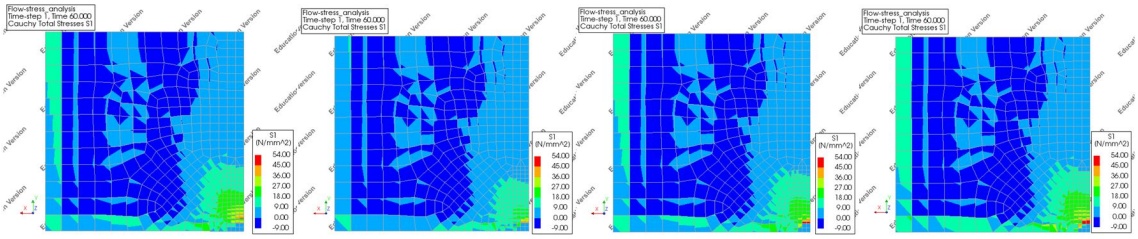

Figure A.80: Principal stress plots, scaled, at weld time of the bottom surface for different coefficients of linear thermal expansion. From left to right: constant $8,4 \cdot 10^{-6} \circ C^{-1}$, variable $6,72 \cdot 10^{-6} \circ C^{-1}$, variable $8,4 \cdot 10^{-6} \circ C^{-1}$ (default) and variable $10,08 \cdot 10^{-6} \circ C^{-1}$

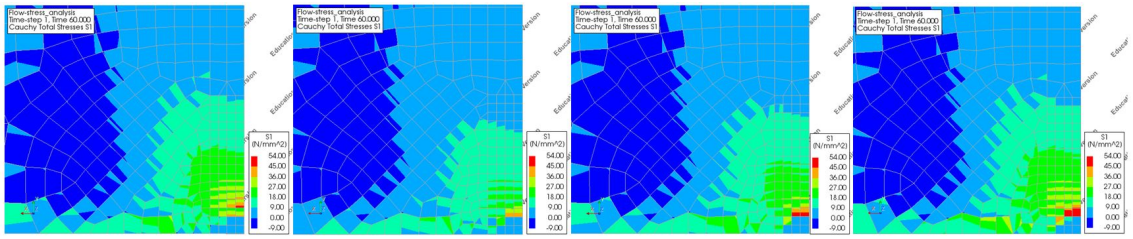

Figure A.81: Principal stress plots, scaled, at weld time, close-up of the bottom surface for different coefficients of linear thermal expansion. From left to right: constant $8,4 \cdot 10^{-6} \circ C^{-1}$, variable $6,72 \cdot 10^{-6} \circ C^{-1}$, variable $8,4 \cdot 10^{-6} \circ C^{-1}$ (default) and variable $10,08 \cdot 10^{-6} \circ C^{-1}$

A.16 Young's Modulus

As the Young's modulus was related to the transition range, it is modelled to be temperature dependent. To investigate the sensitivity, it is researched what the results are for a constant Young's modulus. Furthermore, the variable modulus is adapted with 20%.

Young's modulus (GPa)	constant, 70	v. 0,56 to 56	v. 0,7 to 70 (default)	v. 0,84 to 84
t_{weld} (s)	60	60	60	60

Table A.16: Weld time for varying Young's moduli. *v.* stands for *variable*

The thermal calculations are not influenced by the adaptation in Young's modulus. This is logical, for the modulus has no influence on heat transfer and distribution.

The stress plot for the constant Young's modulus does not show the same pattern as the other stress plots. Especially figure A.85 shows that critical stress occurs in positions where the elements are relaxed for the variable Young's modulus.

The variable Young's moduli of different sizes show that the stress increases for an increase in Young's modulus. The influence is the same as the influence of the coefficient of linear thermal expansion. This is logical, since both are linearly related to the thermoelastic stress and were both varied with 20 %.

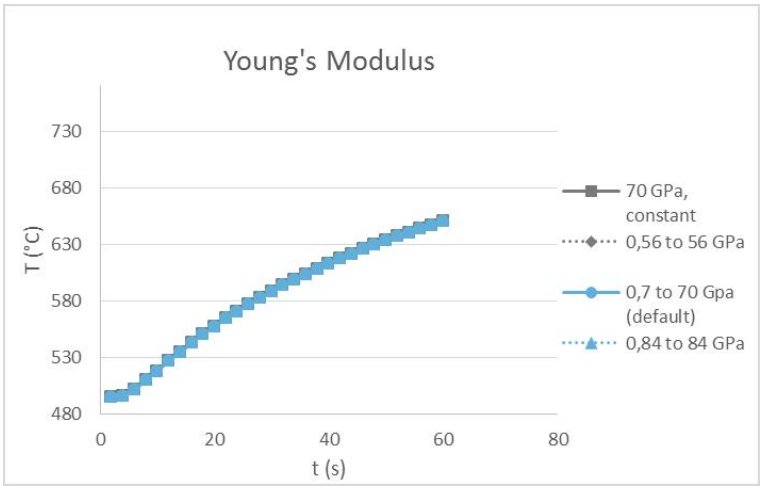

Figure A.82: Temperature at the core of the welding zone over time for different Young's moduli.

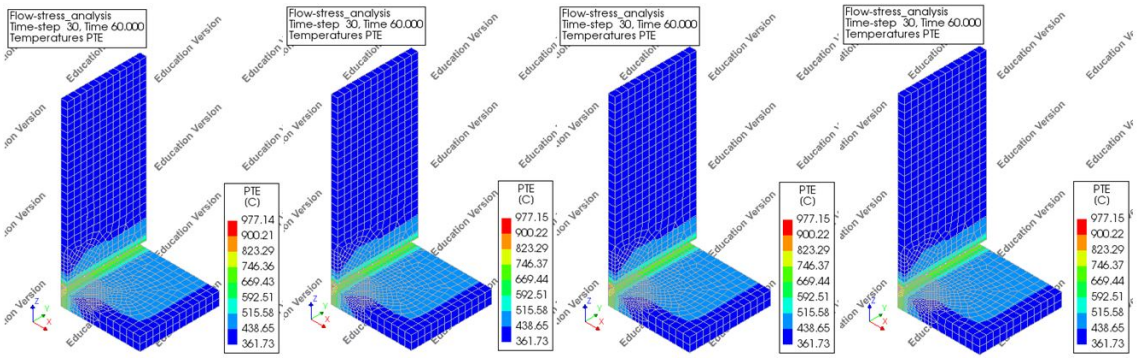

Figure A.83: Temperature distributions at weld time for different Young's moduli. From left to right: constant, 70 GPa, variable, 0,56 to 56 GPa, variable, 0,7 to 70 GPa (default) and variable, 0,84 to 84 GPa

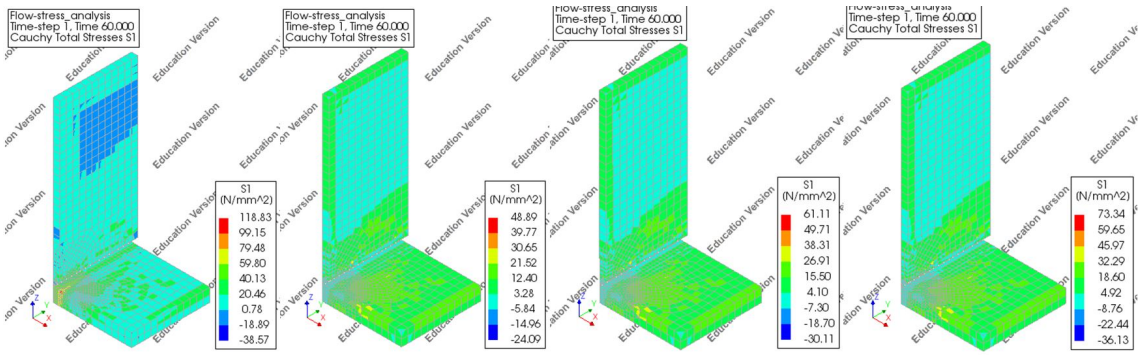

Figure A.84: Principal stress plots at weld time for different Young's moduli. From left to right: constant, 70 GPa, variable, 0,56 to 56 GPa, variable, 0,7 to 70 GPa (default) and variable, 0,84 to 84 GPa

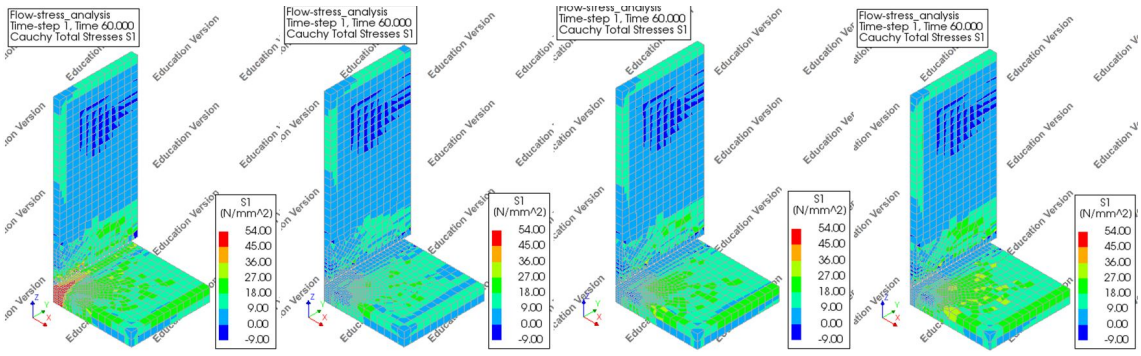

Figure A.85: Principal stress plots, scaled, at weld time for different Young's moduli. From left to right: constant, 70 GPa, variable, 0,56 to 56 GPa, variable, 0,7 to 70 GPa (default) and variable, 0,84 to 84 GPa

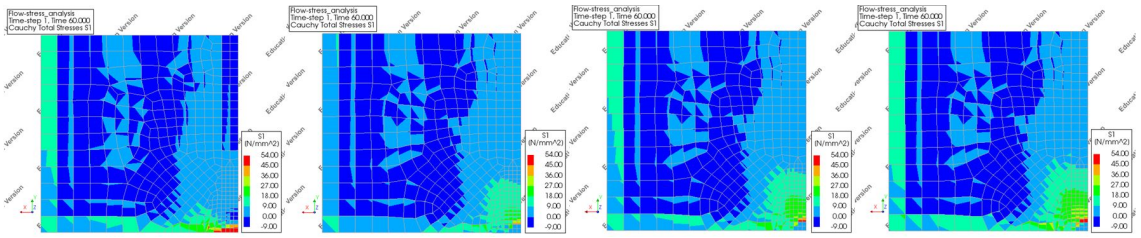

Figure A.86: Principal stress plots, scaled, at weld time of the bottom surface for different Young's moduli. From left to right: constant, 70 GPa, variable, 0,56 to 56 GPa, variable, 0,7 to 70 GPa (default) and variable, 0,84 to 84 GPa

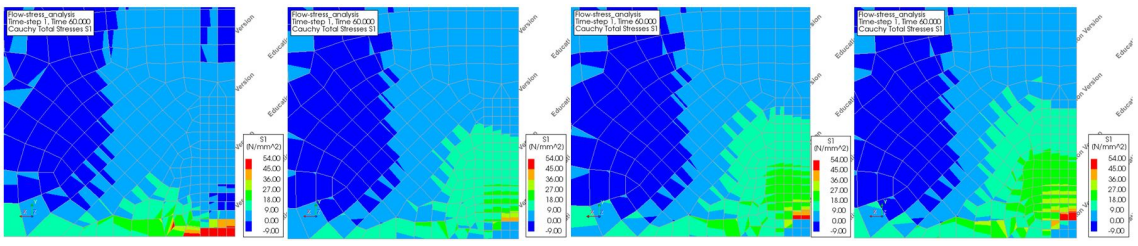

Figure A.87: Principal stress plots, scaled, at weld time, close-up of the bottom surface for different Young's moduli. From left to right: constant, 70 GPa, variable, 0,56 to 56 GPa, variable, 0,7 to 70 GPa (default) and variable, 0,84 to 84 GPa

A.17 Glass Thickness

The results of all analyses above cause wonder whether the stress would also be critical if the glass is thinner. The model has been adapted to represent glass of the same size but of a thickness of $4\ mm$. It has been analyzed if the default parameters would result in stress of a not critical level.

Thickness (mm)	10 (default)	4
t_{weld} (s)	60	62

Table A.17: Weld time for varying glass thickness

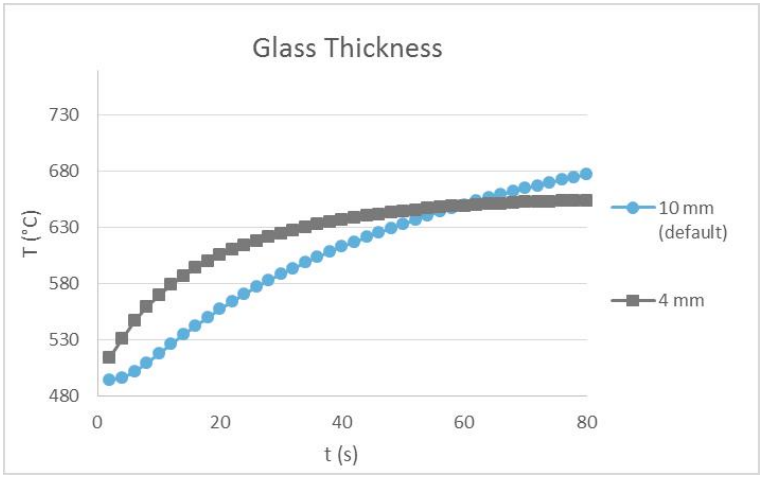

Figure A.88: Temperature at the core of the welding zone over time for different glass thicknesses

The influence on the thermal analysis is significant, though this is not well visible in the weld time result. The influence can be spotted in figure A.88, showing a larger temperature increase in the beginning that flattens after thirty seconds.

The stress plots show that the stress is critical on the bottom surface. The $4\ mm$ specimen is also predicted to fail in default settings. Therefore, it has been decided not to research the thicknesses between 4 and $10\ mm$.

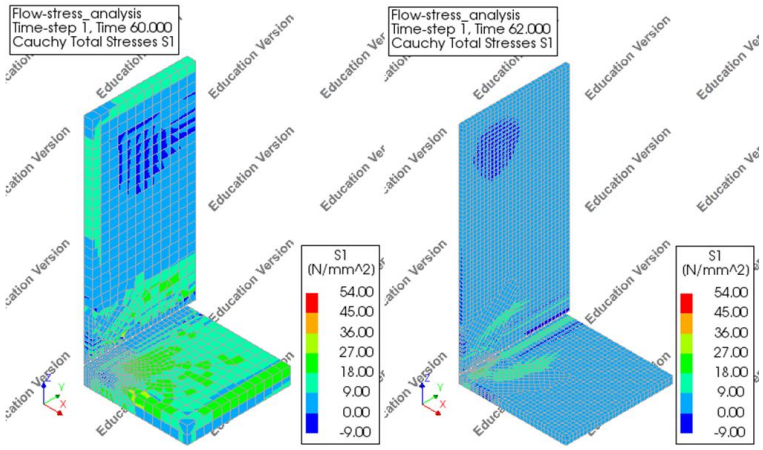

Figure A.89: Principal stress plots at weld time for different glass thicknesses. Left: 10 mm and right, 4 mm

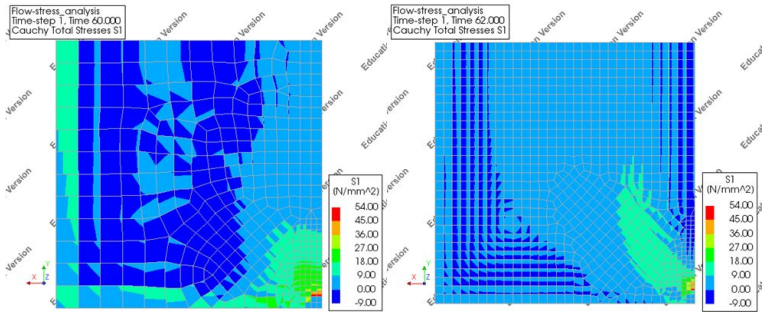

Figure A.90: Principal stress plots, scaled, at weld time of the bottom surface for different glass thicknesses. Left: 10 mm and right, 4 mm

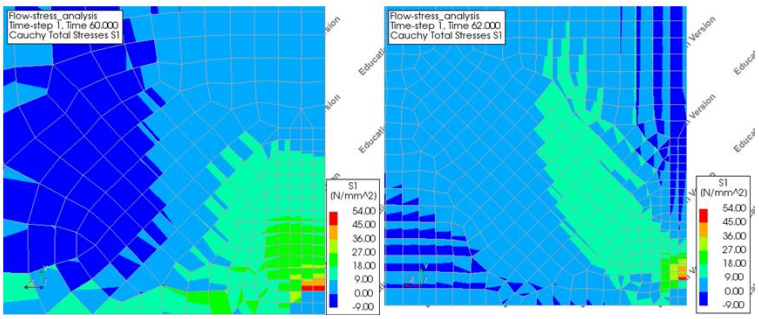

Figure A.91: Principal stress plots, scaled, at weld time, close-up of the bottom surface for different glass thicknesses. Left: 10 mm and right, 4 mm

A.18 Glass Thickness and Flame Position

The $4\ mm$ thick glass has been predicted to fail in default settings. Therefore, it has been analyzed what other parameters should adapt to prevent critical stress. The analyses on the $10\ mm$ specimens returned that the flame position is a key element. Therefore, the analysis of the $4\ mm$ model has been performed for a larger and *side, front and under* flame position.

The increase of the boundary surface affecting the flame might be a realistic option. As the model was scaled to the new thickness, the boundary surfaces were scaled along. One can argue that this is not correct, for the same type of burner is used and the same kind of boundary is required. On the other hand, the size of the surface was based on the air pocket between the faceted web edge and the flange, which reduces for a smaller thickness.
The analysis is performed with boundary surfaces for the flame of the same size as for the default model, position *side and front*. The results (Figure A.92) show no critical stress at weld time, shortened from 60 to $14\ s$, or thirty seconds later. However, between these moments the stress reaches critical levels and decreases again. This set-up is also predicted to fail while the glass is being manipulated to form the weld.

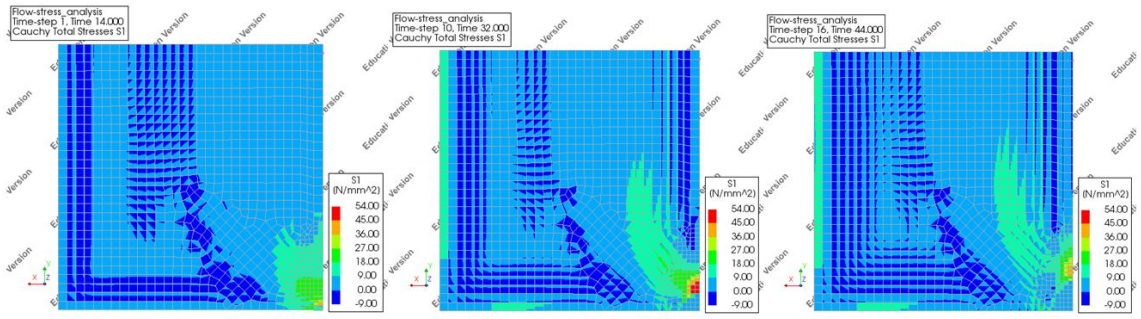

Figure A.92: Principal stress plots, scaled, of the bottom surface for a $4\ mm$ thickness and larger flame. Left to right: at $14\ s$ (weld time), at $32\ s$ and at $44\ s$.

In the case of a $10\ mm$ glass thickness, the method to prevent critical stress showed to be adding a flame to the bottom of the specimen. It is researched whether this measurement will be sufficient for the $4\ mm$ specimen as well.
Figure A.93 shows that the stress in the specimen is not critical at weld time. The stress is larger than in the $10\ mm$ case with a flame in position *side, front and under*. This is probably due to the smaller size of the flame boundary surface for the model with a $4\ mm$ glass thickness.
Figure A.94 shows that the stress is not critical for thirty seconds after weld time, providing enough time to create the weld. The stress has not reached a critical level inbetween.

It is concluded that the addition of a flame on the bottom surface is sufficient to prevent thermal shock failure for the glass thickness of $4\ mm$.

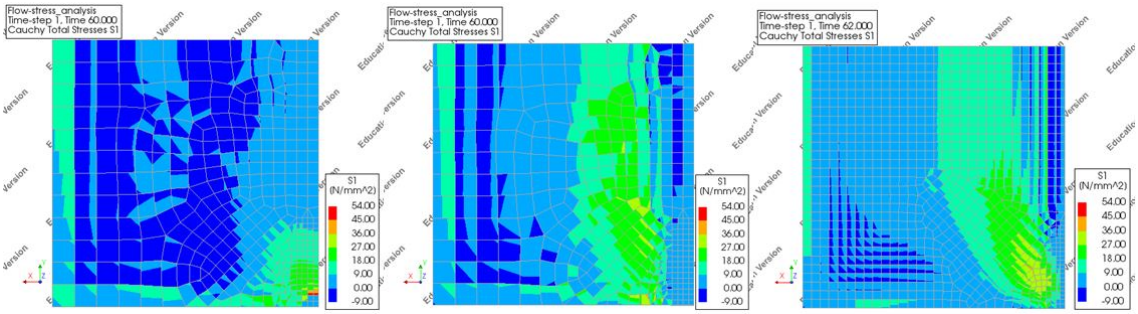

Figure A.93: Principal stress plots, scaled, at weld time of the bottom surface. Left to right: deafult, thickness 10 mm and flameposition *side front and under*, thickness 4 mm and flameposition *side front and under*

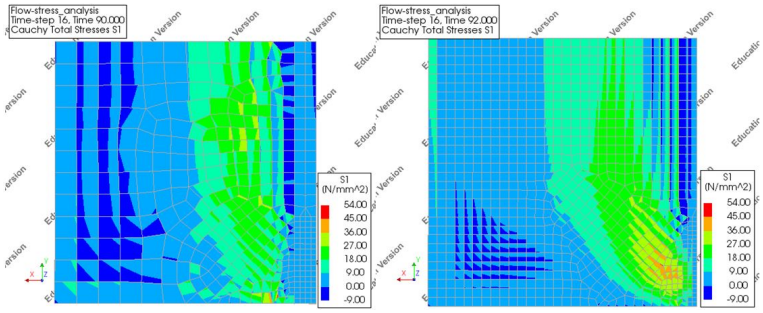

Figure A.94: Principal stress plots, scaled, thirty seconds after weld time of the bottom surface. Thickness 10 mm and flame position *side front and under* (left), thickness 4 mm and flame position *side front and under* (right)

A.19 Flame Position, Preheating Temperature and Glass Thickness

After the model with a 4 mm thickness has been analyzed for different flame positions, the question arose whether it is still necessary to preheat the glass, if the flameposition is *side, front and under* and if the thickness is 4 mm.

Figure A.95 shows the results for the default model and two models with a flame positioned at *side, front and under* and a preheating temperature of 20 $°C$,no oven. The first has thickness of 10 mm, the second is 4 mm. Both of the not preheated specimens show critical stress in the flange and web. It is concluded that preheating the glass is a necessity, even if the flame is positioned at the bottom surface and even if the thickness is reduced.

Thickness (mm), Preheating Temperature ($°C$)	10, 500 (default)	10, 20	4, 500	4, 20
t_{weld} (s)	60	62	340	>600

Table A.18: Weld time for varying glass thicknesses and preheating temperatures.

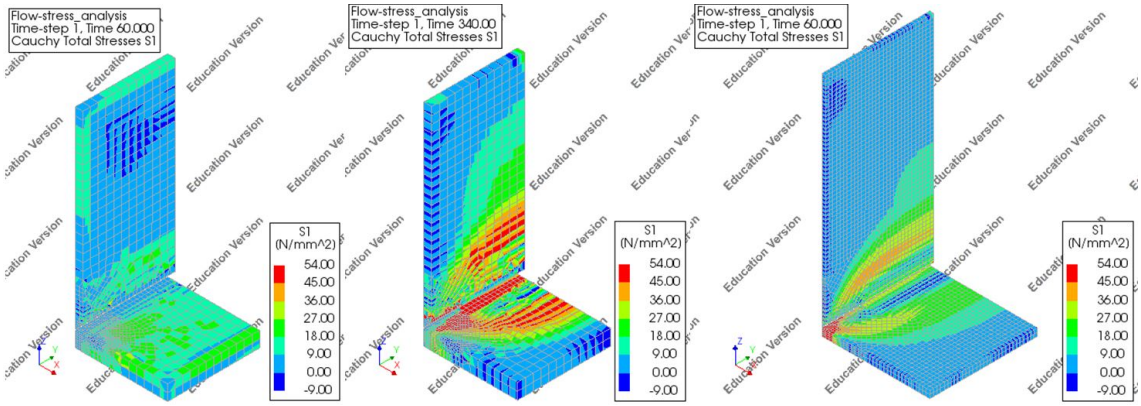

Figure A.95: Principal stress plots, scaled, at weld time and after 60 s for the right image. Left to right: default, thickness 10 mm and preheating temperature 20 $°C$, thickness 4 mm and preheating temperature 20 $°C$.

B Validation of the Thermal Finite Element Model

To explain why the glass weld production succeeded, the thermal conditions were analyzed as they occurred (Section 22). The finite element model has been adapted to calculate whether it would predict thermal shock failure. If this is not the case, it can be concluded that the difference between the prediction and reality is due to too conservative thermal conditions. This appendix contains the results of the thermal finite element model for the adapted thermal conditions.

The model has been run applying the validation case, which is default settings with an adapted radiative temperature. This temperature is chaned to 500 $°C$. The analysis has been performed to check the stress at one and four minutes after the opening of the oven.

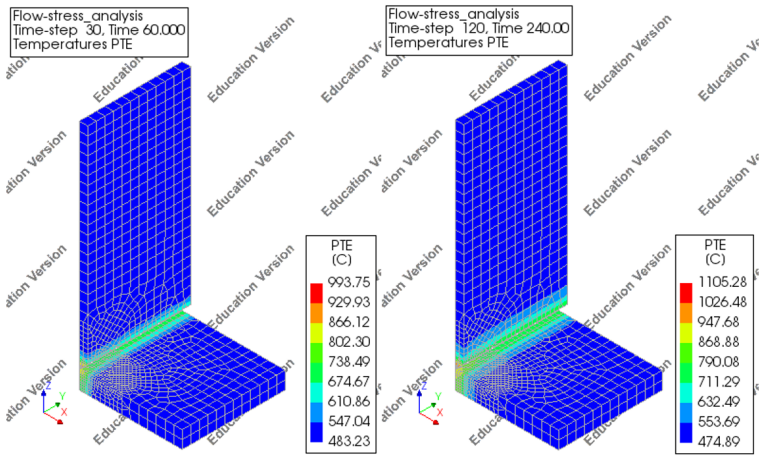

Figure B.1: Temperature distributions at 60 s (left) and 240 s (right) for the validation case.

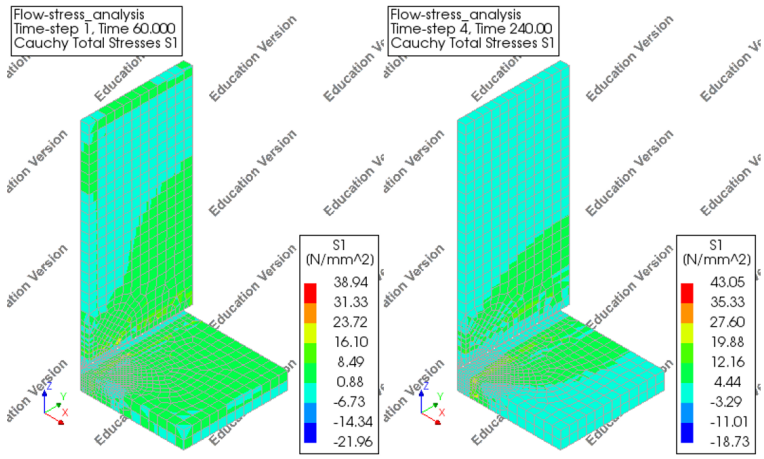

Figure B.2: Principal stress plots at 60 s (left) and 240 s (right) for the validation case

Weld time is at 52 s.
The plots in this section show no critical stress. In figure B.2, it can be seen that even the numerically errored extremes remain below 45 MPa. The minimum temperature in the glass after one minute is more than 100 $°C$ higher than the default case.

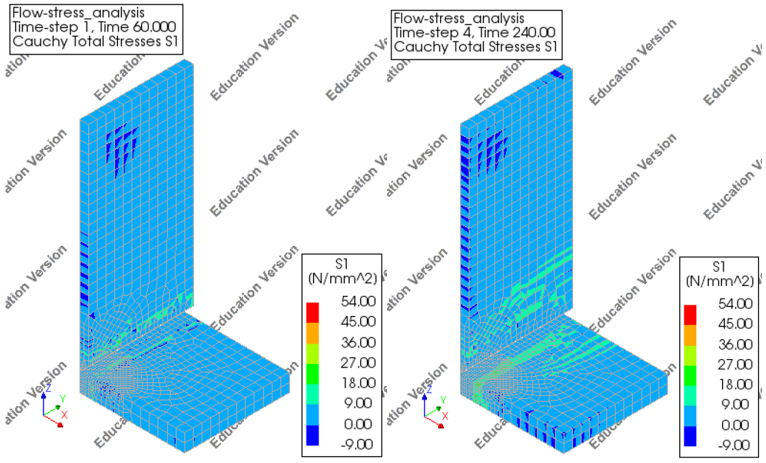

Figure B.3: Principal stress plots, scaled, at 60 s (left) and 240 s (right) for the validation case.

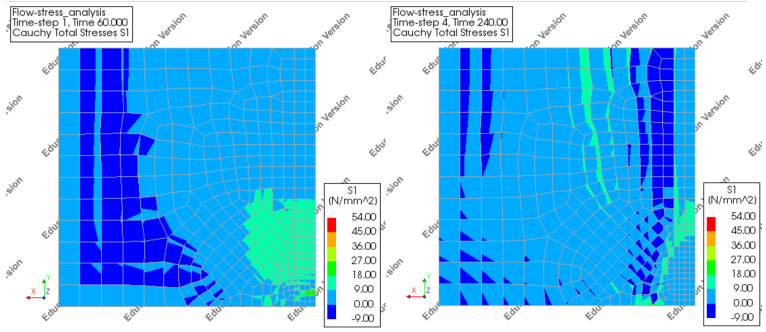

Figure B.4: Principal stress plots, scaled, at 60 s (left) and 240 s (right) of the bottom surface for the validation case.

It has been concluded that raising the radiative temperature of the surroundings provides the low stress as observed in the experiments. Therefore, it has been decided not to adapt parameters to the other beneficent observations.

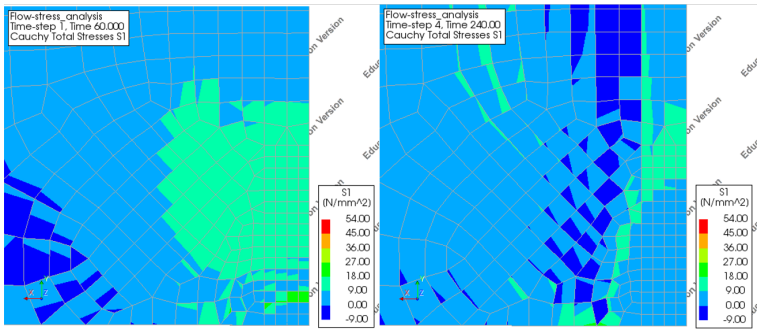

Figure B.5: Principal stress plots, scaled, at 60 s (left) and 240 s (right), close-up of the bottom surface for the validation case.

C Results of the SCALP Measurements of the Webs of the Welds

Note that the measurements are executed after the destructive structural tests were performed. The specimen numbers correspond to those of the structural test: specimen 10 was produced in the first welding experiment, 11 in the second and 12 in the third.

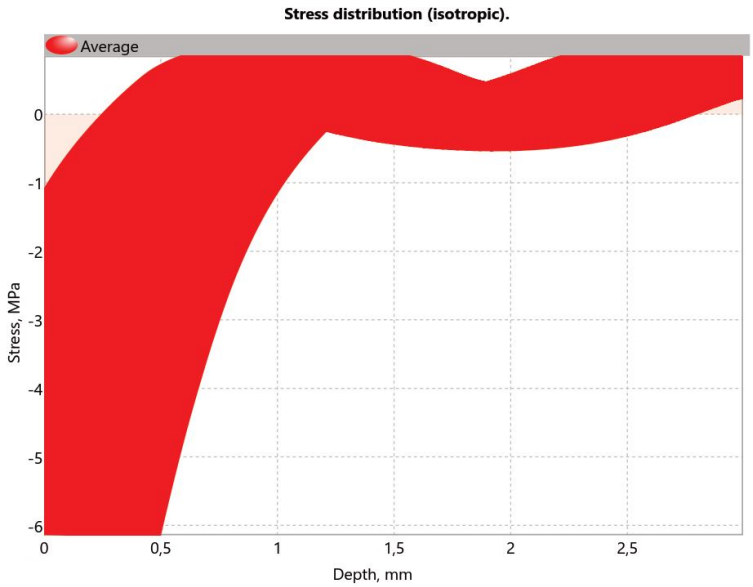

Figure C.1: SCALP Result Output for the remains of the web of specimen 10, between the holes

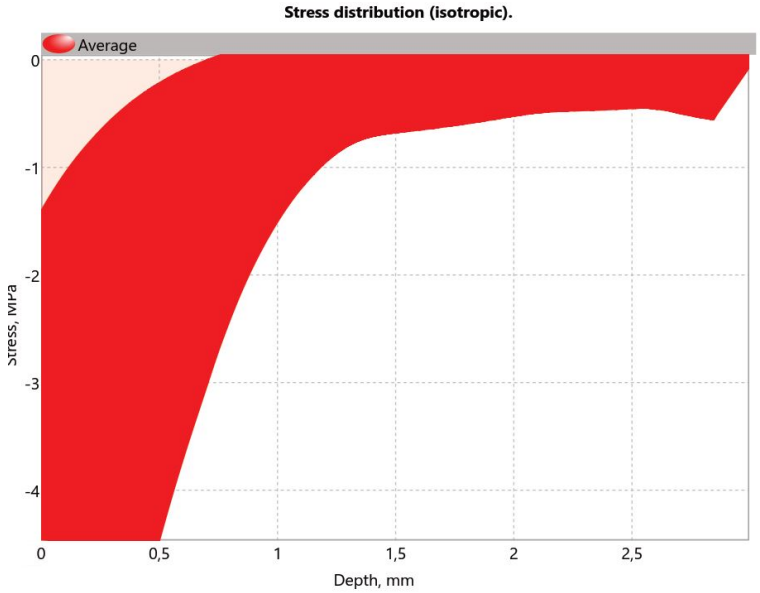

Figure C.2: SCALP Result Output for the remains of the web of specimen 10, near the weld

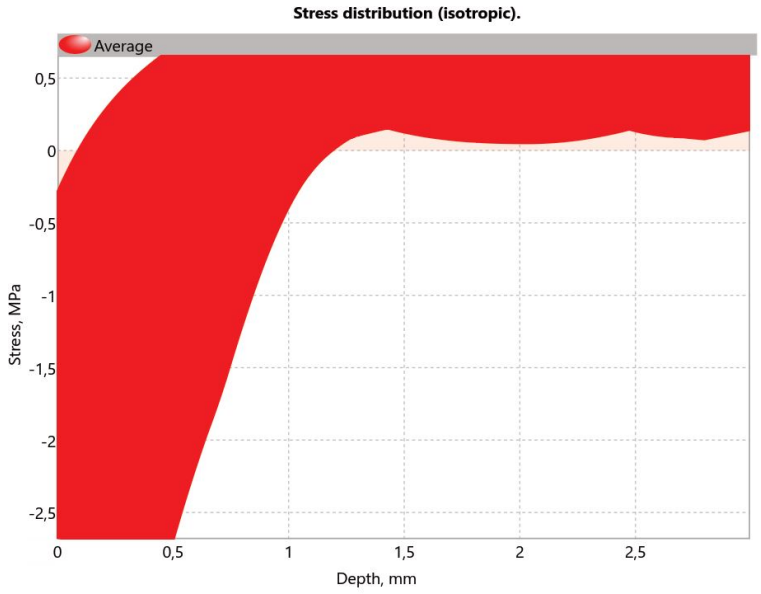

Figure C.3: SCALP Result Output for the remains of the web of specimen 11, near the holes

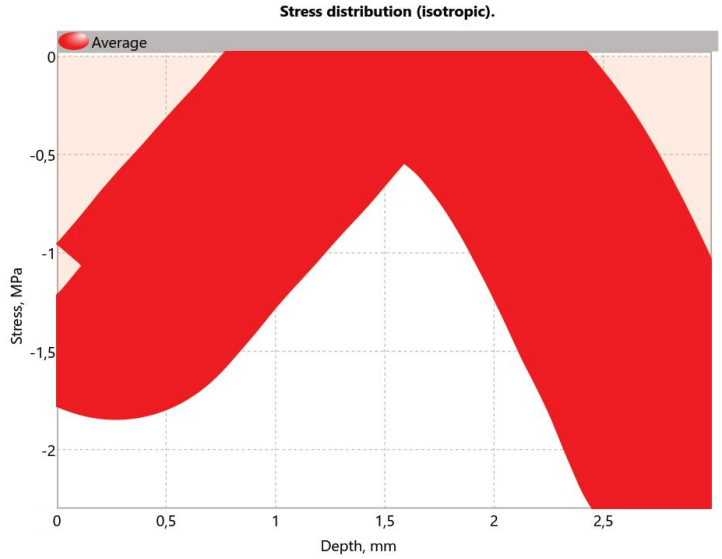

Figure C.4: SCALP Result Output for the remains of the web of specimen 11, near the weld

Figure C.5: SCALP Result Output for the remains of the web of specimen 11, parallel to the weld

Figure C.6: SCALP Result Output for the remains of the web of specimen 12, between the holes

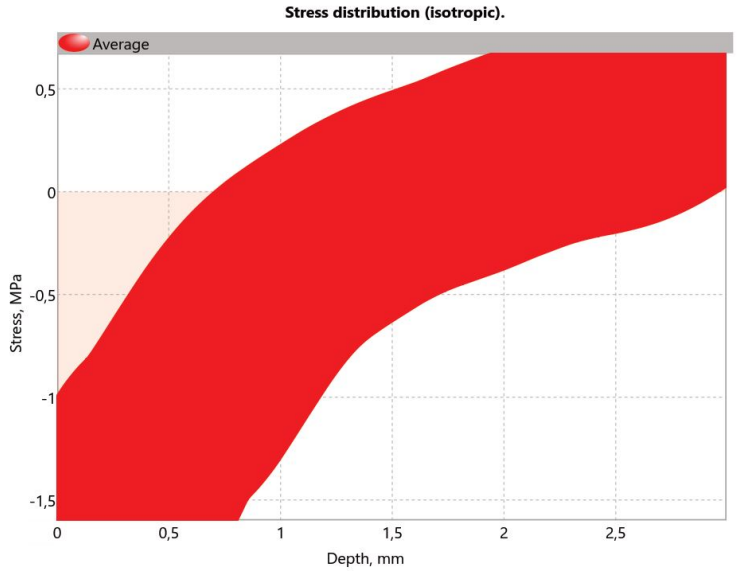

Figure C.7: SCALP Result Output for the remains of the web of specimen 12, near the weld

D Results of the Structural Finite Element Analysis of the Shear Test

Before the execution of the structural shear test, the design (Figure 83) is modelled in finite element software.

The specimen are modelled for the perfect situation. The geometry is perfect and the surface quality is perfect. The connection between the aluminum and glass is an adhesive in the test. Since this adhesive is very stiff, the adhesive is not modelled. The glass elements are connected to the aluminum elements without an interface.

The geometry of the model and the supports are displayed in figures D.1 and D.2. The applied material properties are presented in table D.1.

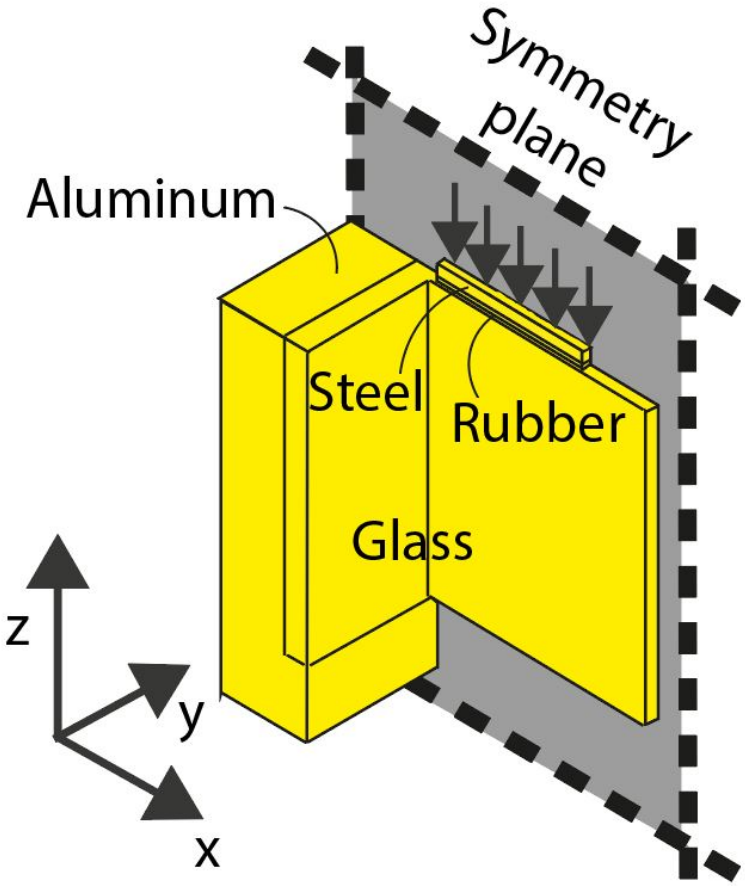

Figure D.1: Geometry of the model of the shear test

There are interfaces between the steel and rubber and the rubber and glass. This interface has an insignificantly low shear stiffness, ensuring that only normal stress is transferred from the elephant's foot to the glass.

The load applied on the specimen in the model is $80\ kN$.
The results od the linear elastic analysis are presented in figures D.3 toD.5. The largest stress is normal bending stress parallel to the web edges (X-direction, figure D.3). This is caused by a bending

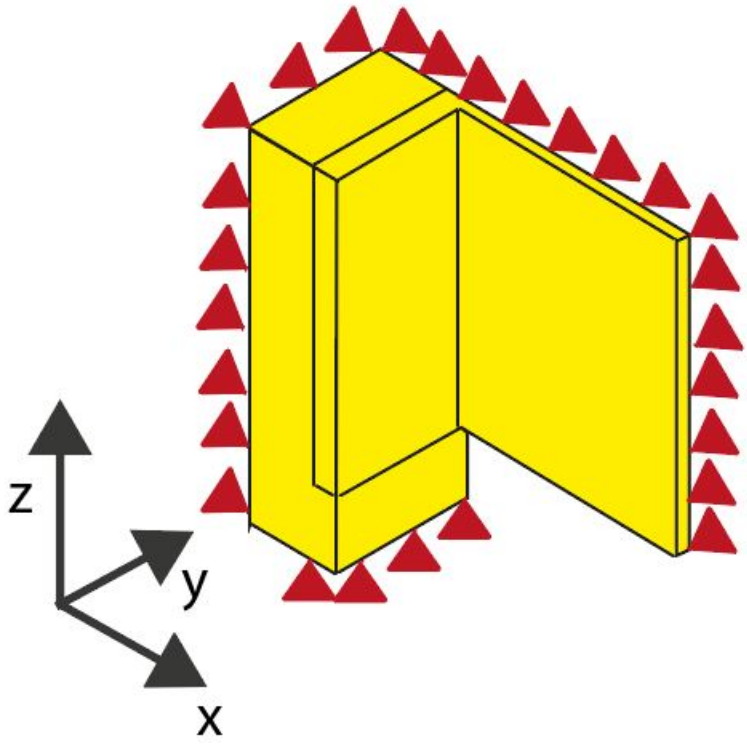

Figure D.2: Geometry of the model of the shear test

Parameter	Glass	Aluminum	Steel	Rubber
Young's Modulus (GPa)	70	69	210	1
Poisson's ratio (-)	0,23	0,33	0,20	0,49

Table D.1: Material properties applied in the structural finite element models of the test

moment. The magnitude of the stress is related to the magnitude of the load. As a test, $80\ kN$ is chosen. Considering the magnitude of the stress, which is about ten to twenty times larger than the glass stress capacity, the failure load is expected to be lower.

The shear stress is significant and well distributed in this test set-up. The advantage of this set-up is that the whole connection is loaded in shear. This does not load the connection in bending, which is sensitive to surface flaws.

It shows to be difficult to load this geometry in shear. Even though the bending stress will occur, it has been decided that this set-up is the best way to test the T-shape geometry.

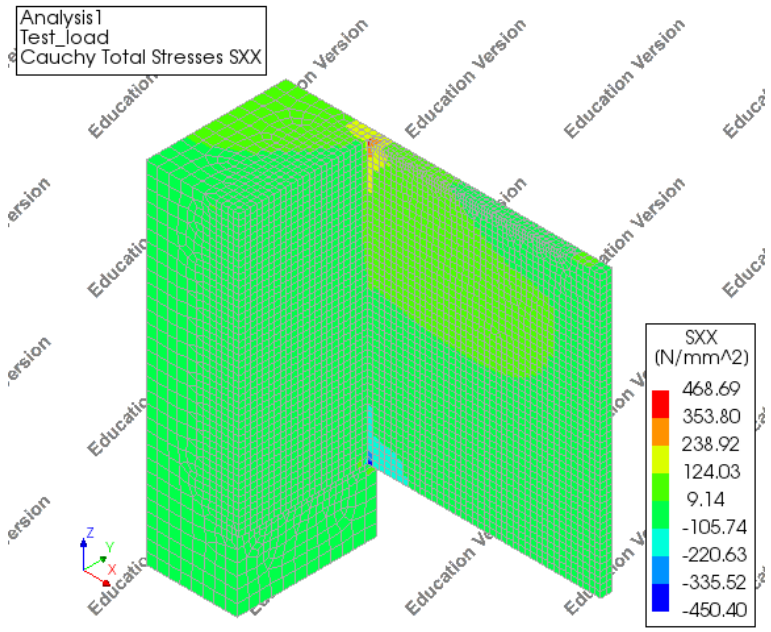

Figure D.3: Unscaled stress distribution, normal stress in X-direction

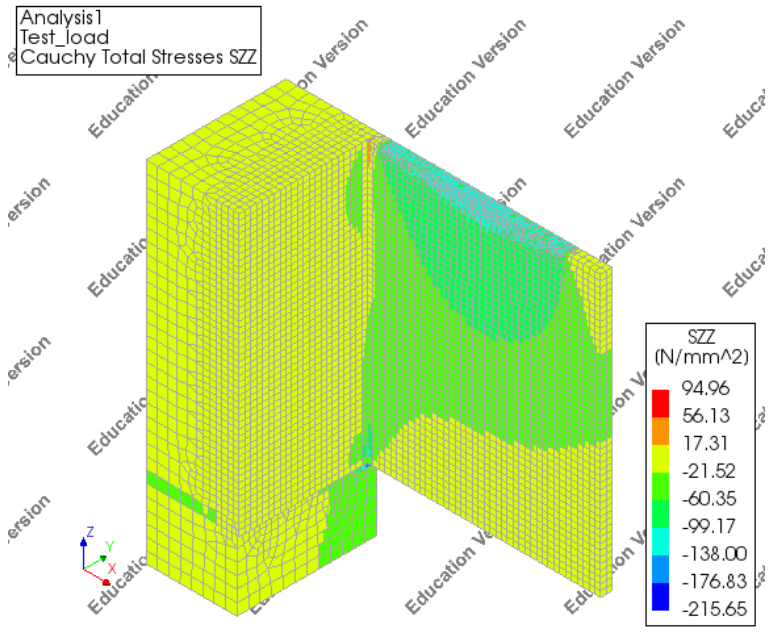

Figure D.4: Unscaled stress distribution, normal stress in Z-direction

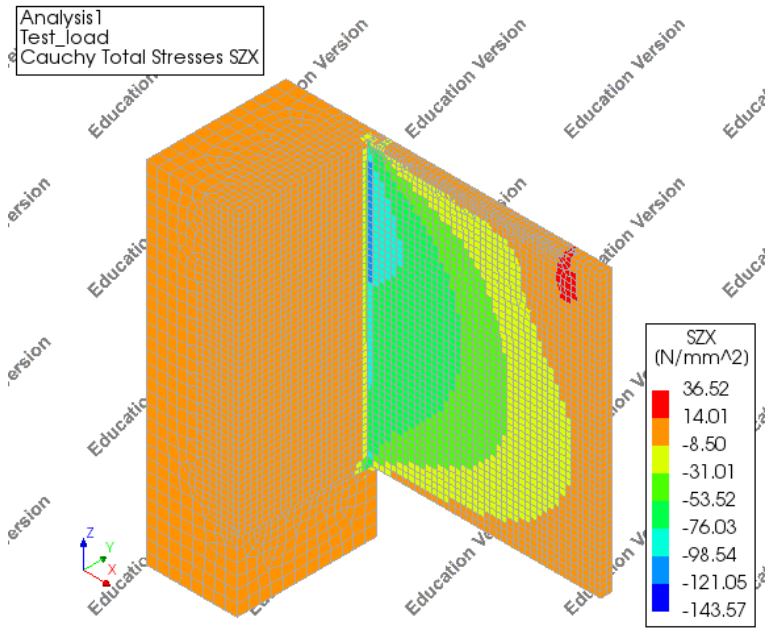

Figure D.5: Unscaled stress distribution, shear stress in Z-direction on surface with normal in X-direction

E Photographs of the Specimens after the Structural Test

This appendix contains photographs of the specimens after the structural shear test was performed. The specimen numbers correspond to those used for the structural test.

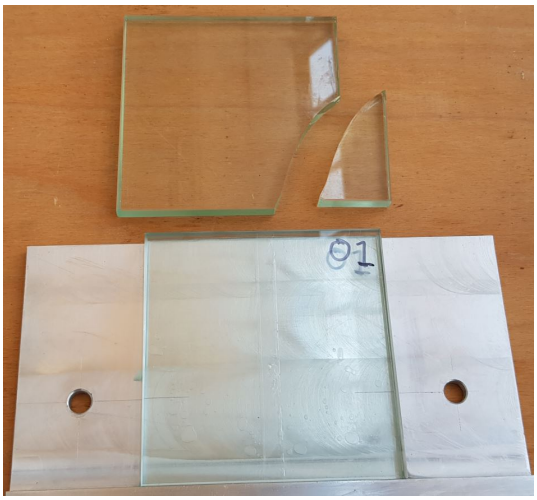

Figure E.1: Cracks in Specimen 1

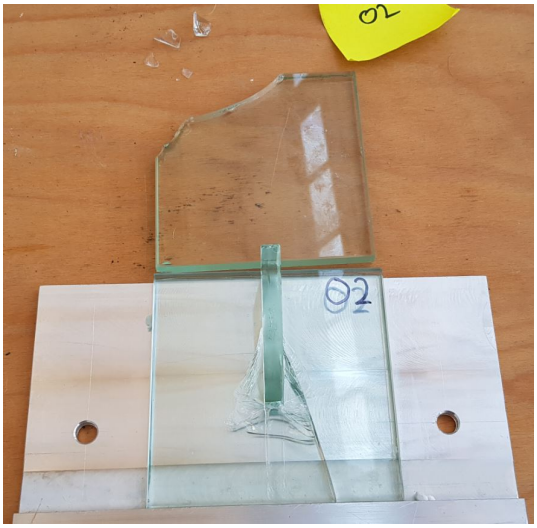

Figure E.2: Cracks in Specimen 2

Figure E.3: Cracks in Specimen 3

Figure E.4: Cracks in Specimen 4

Figure E.5: Cracks in Specimen 5

Figure E.6: Cracks in Specimen 6

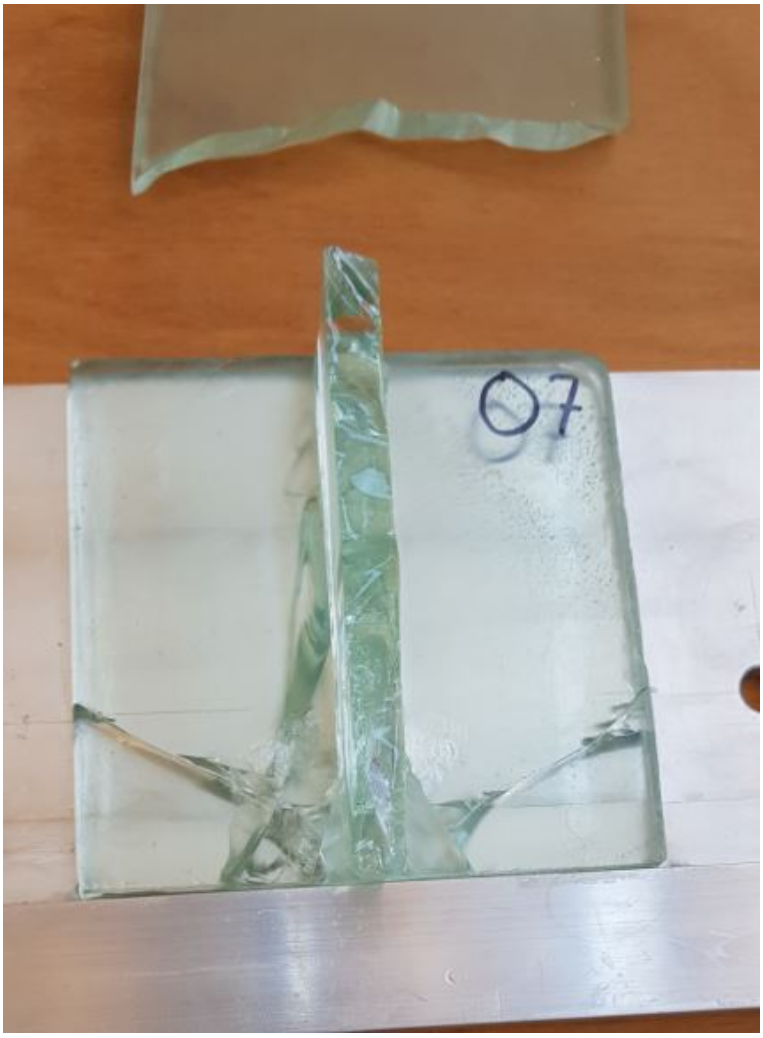

Figure E.7: Cracks in Specimen 7

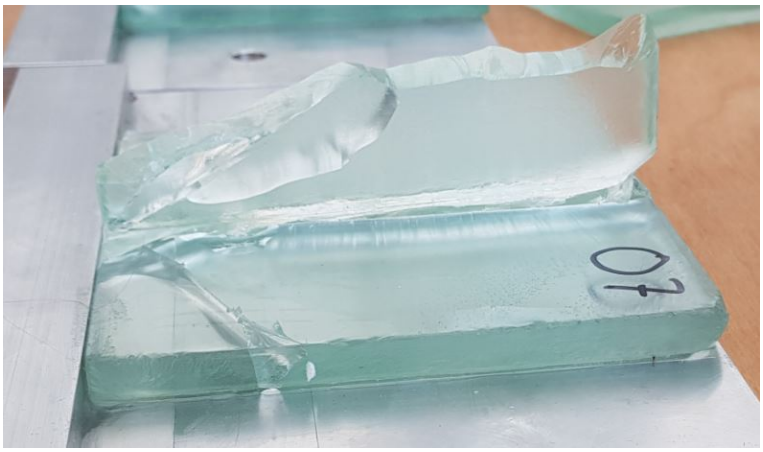

Figure E.8: Cracks in Specimen 7, side view

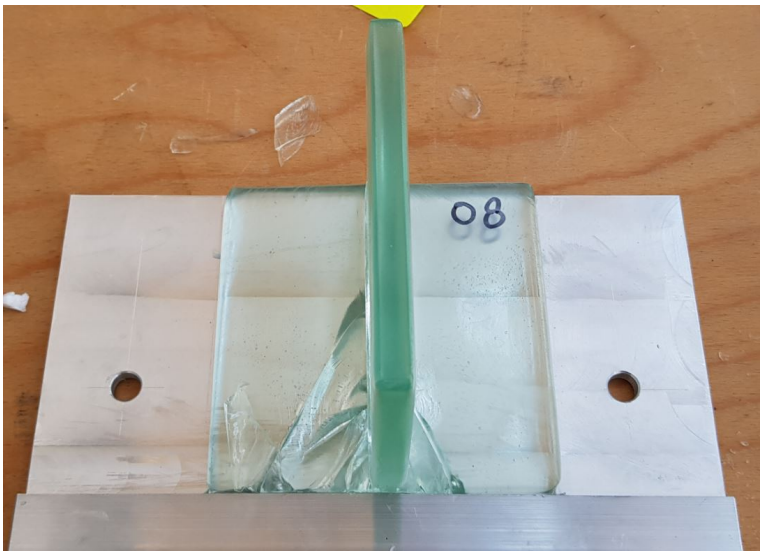

Figure E.9: Cracks in Specimen 8

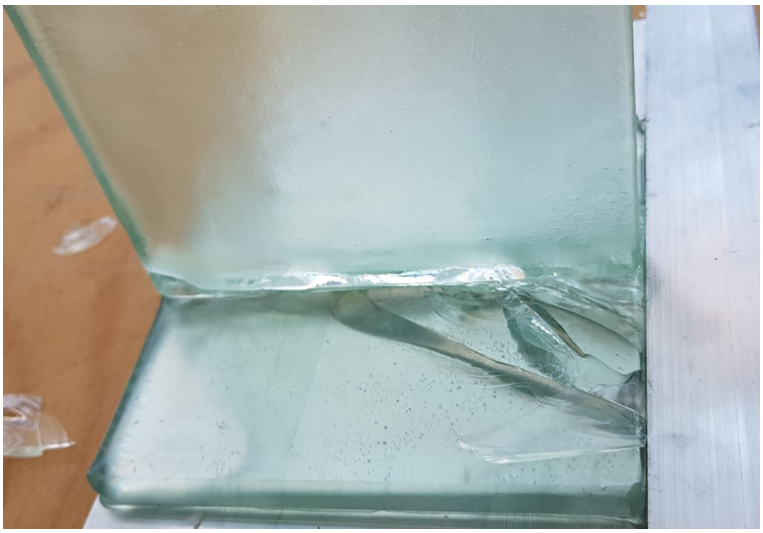

Figure E.10: Cracks in Specimen 8, side view

Figure E.11: Cracks in Specimen 9

Figure E.12: Cracks in Specimen 9, side view

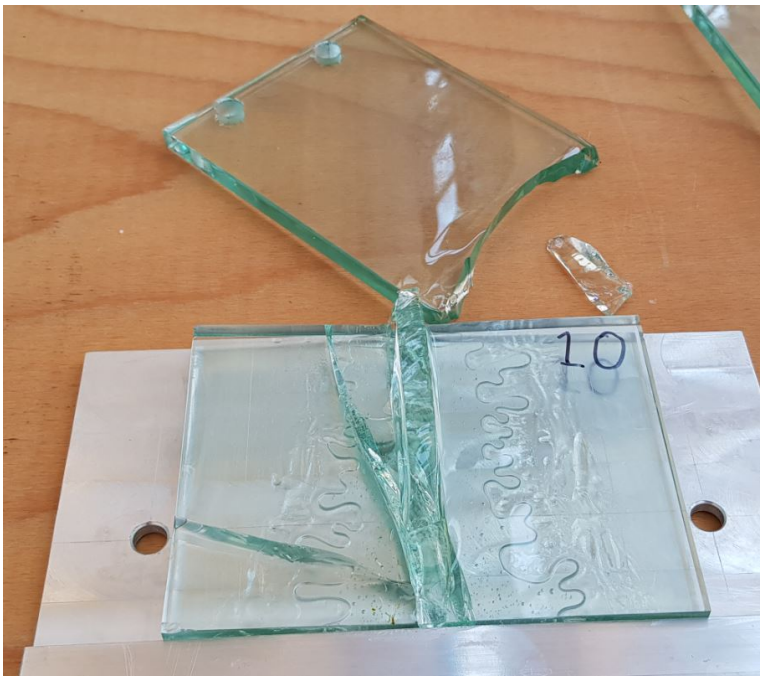

Figure E.13: Cracks in Specimen 10

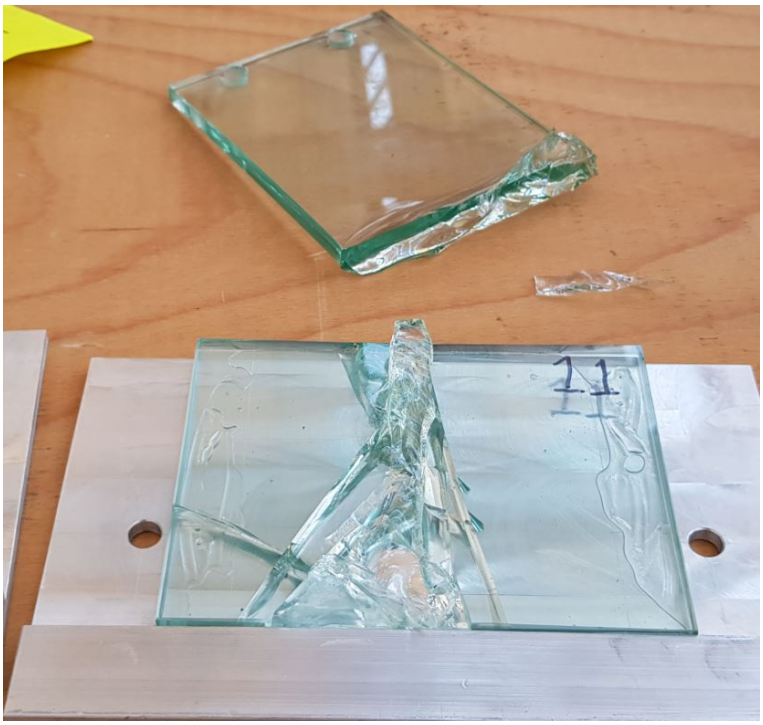

Figure E.14: Cracks in Specimen 11

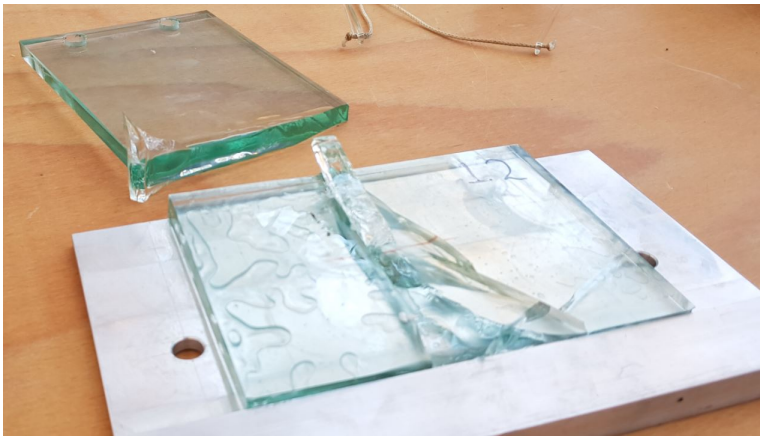

Figure E.15: Cracks in Specimen 12

F Force Displacement Diagrams of the Shear Test

This appendix contains the output of the measurement equipment of the structural shear test. They are, combined with the crack observations, the results of the test (Section 28). The numbers of the specimen correspond to table 8.

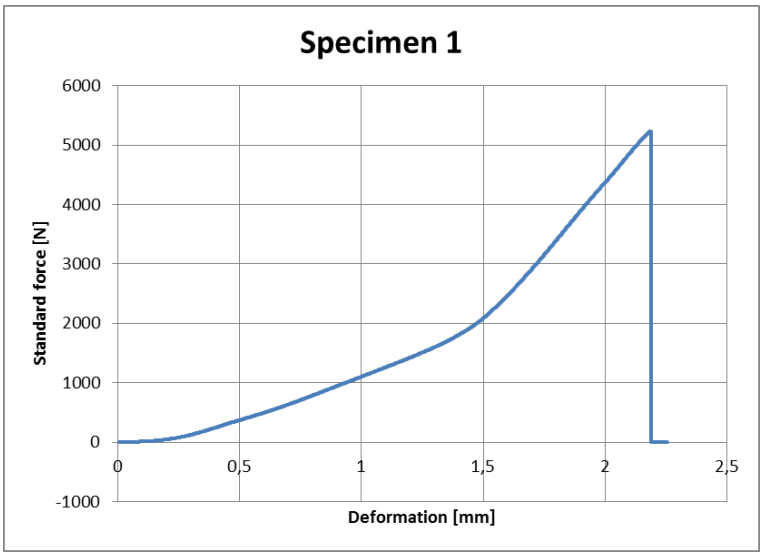

Figure F.1: Force-displacement diagram of the shear test of specimen 1

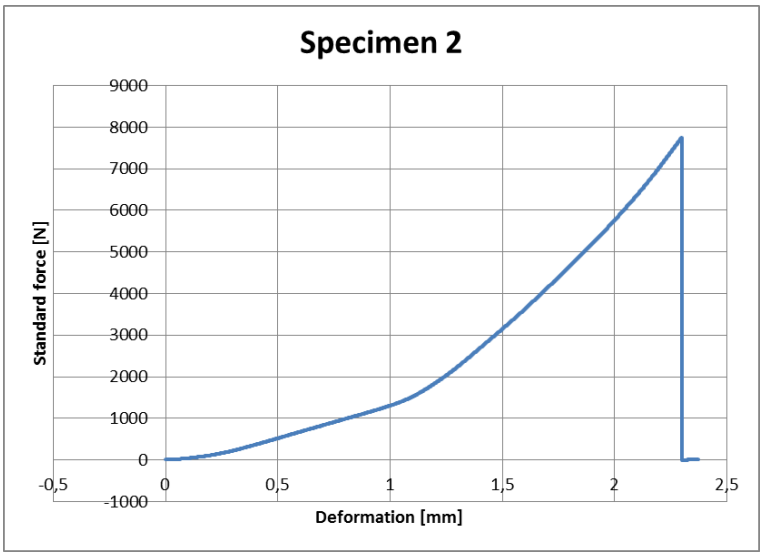

Figure F.2: Force-displacement diagram of the shear test of specimen 2

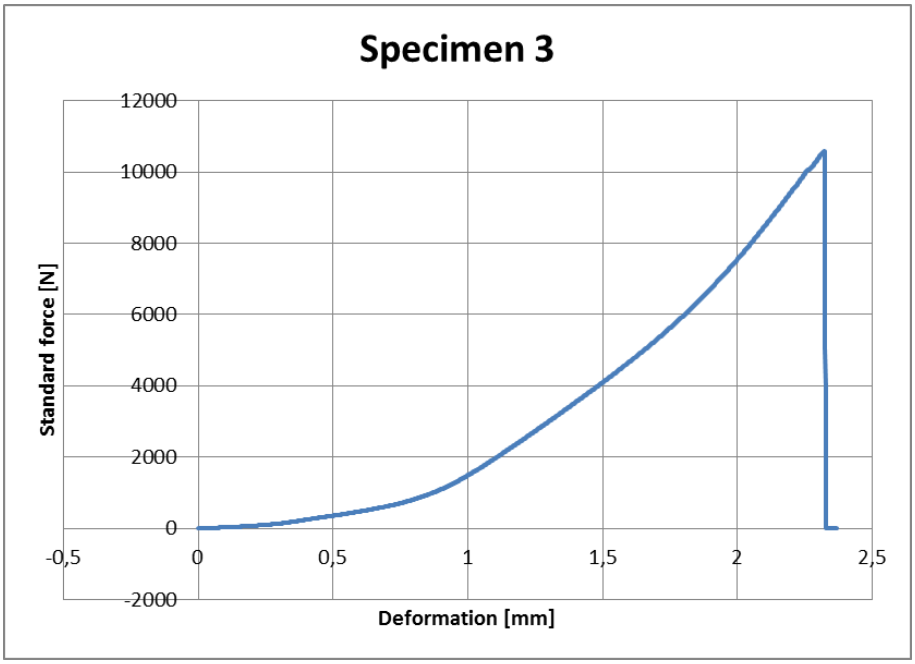

Figure F.3: Force-displacement diagram of the shear test of specimen 3

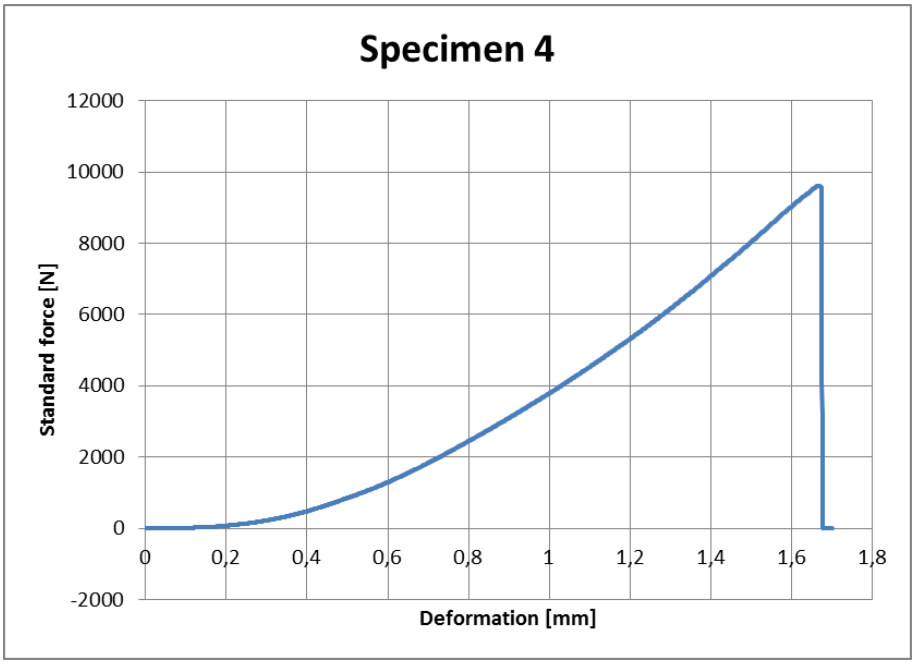

Figure F.4: Force-displacement diagram of the shear test of specimen 4

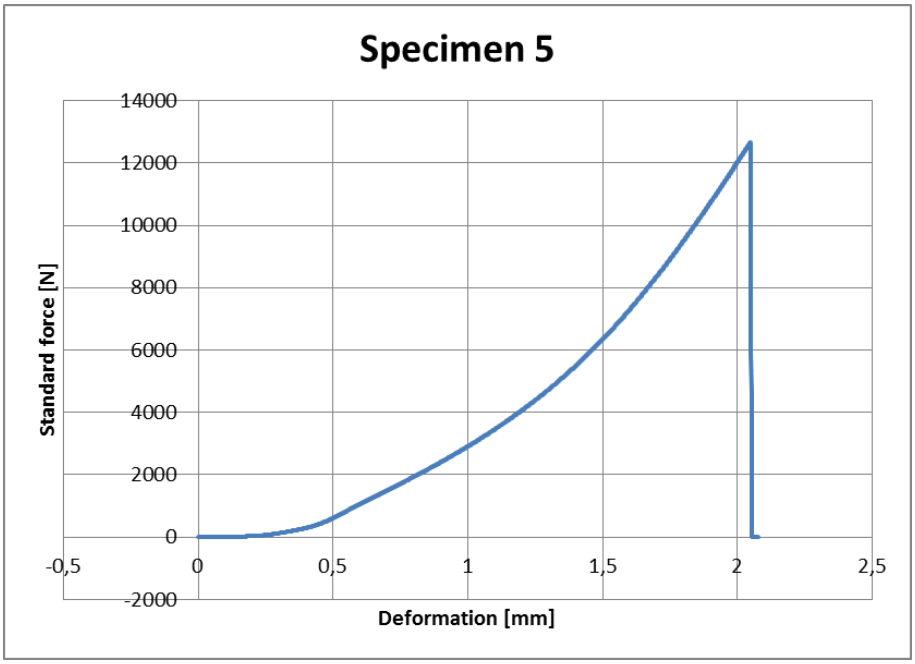

Figure F.5: Force-displacement diagram of the shear test of specimen 5

Figure F.6: Force-displacement diagram of the shear test of specimen 6

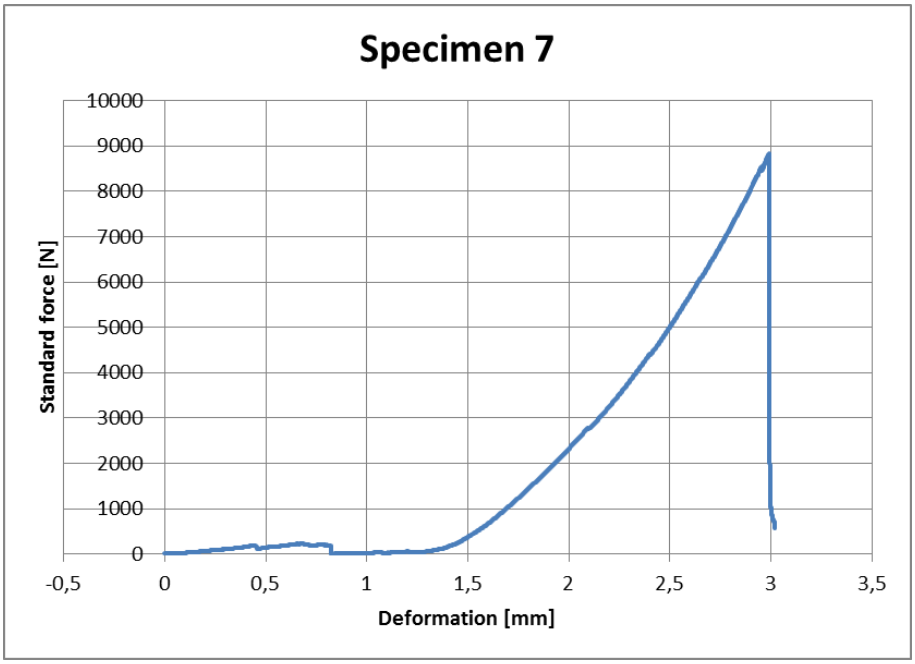

Figure F.7: Force-displacement diagram of the shear test of specimen 7

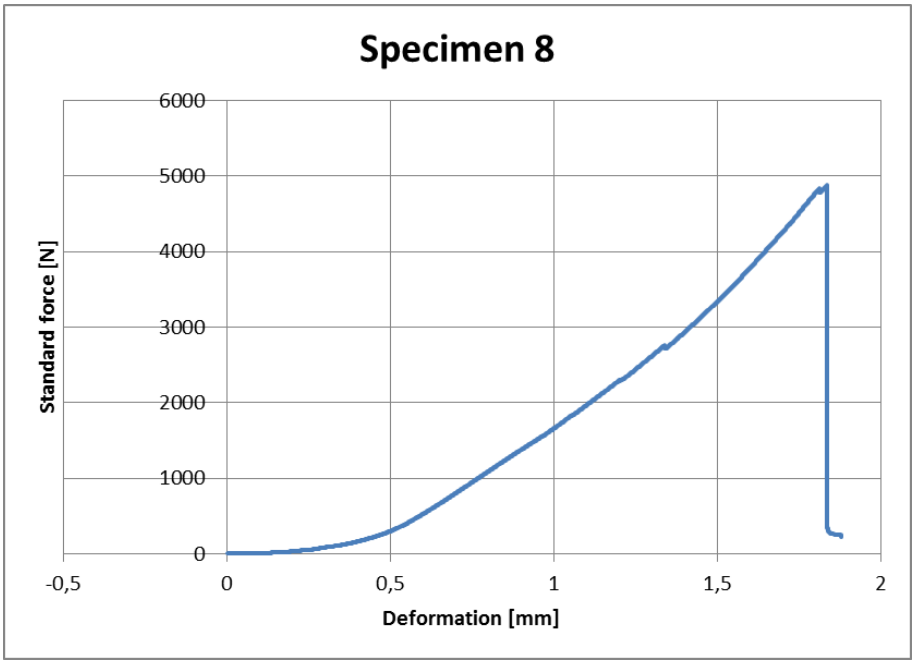

Figure F.8: Force-displacement diagram of the shear test of specimen 8

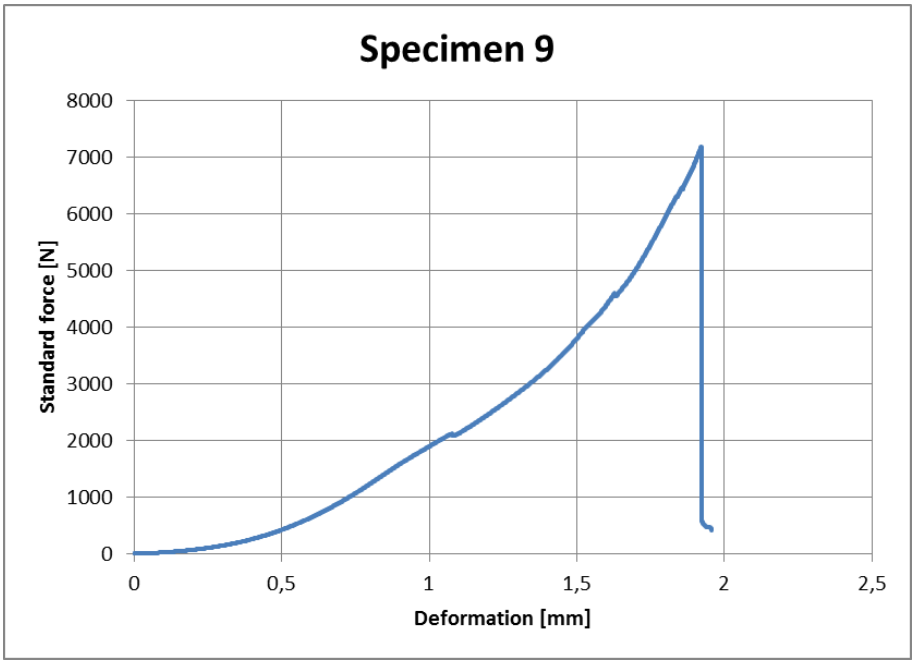

Figure F.9: Force-displacement diagram of the shear test of specimen 9

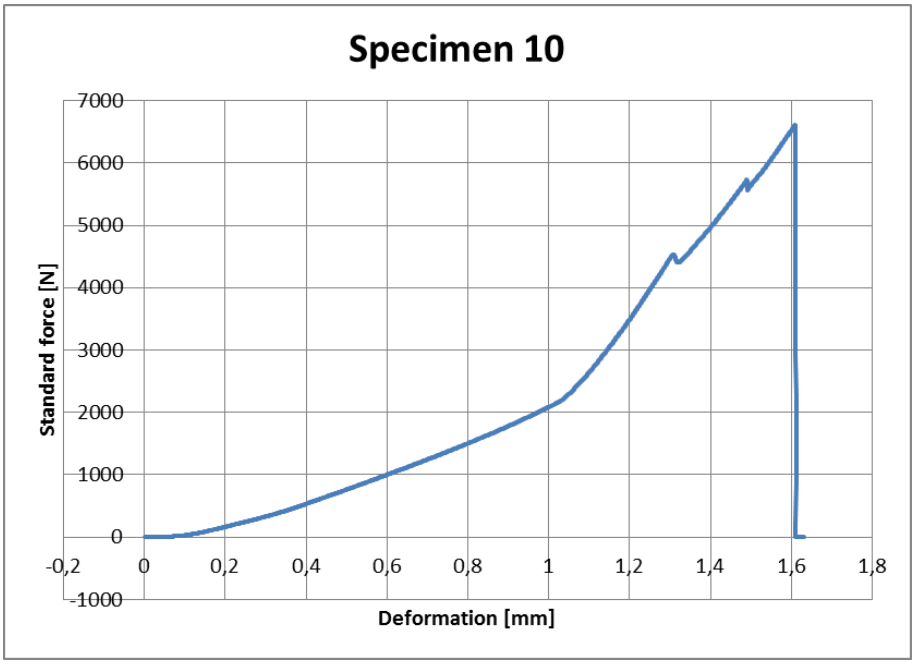

Figure F.10: Force-displacement diagram of the shear test of specimen 10

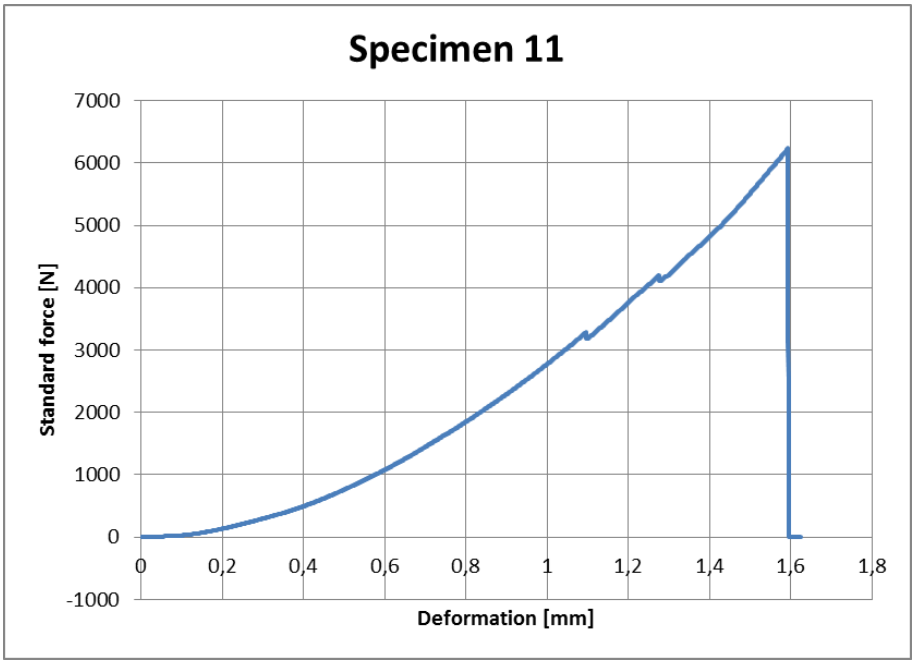

Figure F.11: Force-displacement diagram of the shear test of specimen 11

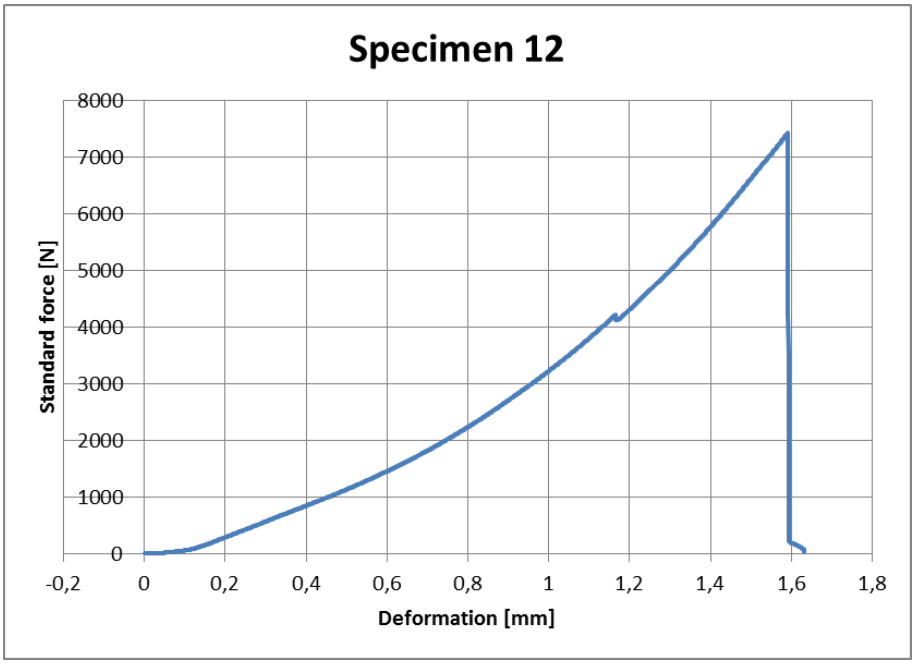

Figure F.12: Force-displacement diagram of the shear test of specimen 12

G Finite Element Analysis Results of the Glass Aluminum Composite

In section 30, the mechanisms of the test set-up, functioning as a glass-aluminum composite, are described. In this appendix, the finite element model and results are presented which support the observed mechanisms.

G.1 Perfect Specimen

The structural glass finite element model has been adapted. The dimensions of the aluminum and the supports have been matched with reality as it presented itself in the structural experiments.
First, a model was made with a perfect geometry. The material parameters are the same as for the structural finite element model made before the test. The glass joint was modelled perfectly homogeneous. The adhesive between glass and aluminum is not modelled. The load on the specimens is 2 kN

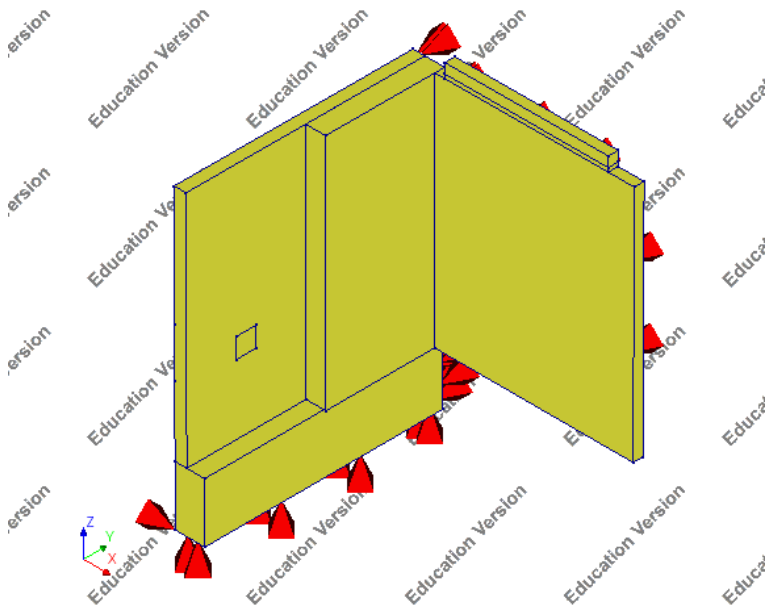

Figure G.1: Geometry of the model of the glass-aluminum composite

The most important result of this model is the stress parallel to the flange's surface. This is shown in figure G.3. This images confirms that the second composite mechanism, the one in figure 95, has occurred, because it shows the glass in the flange near the joint is highly stressed.

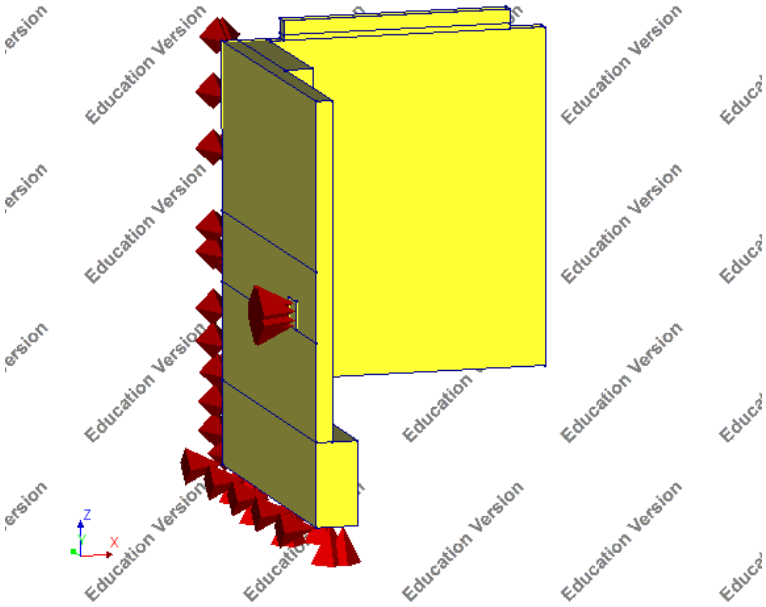

Figure G.2: Geometry of the model of the glass-aluminum composite, back view showing bolt support.

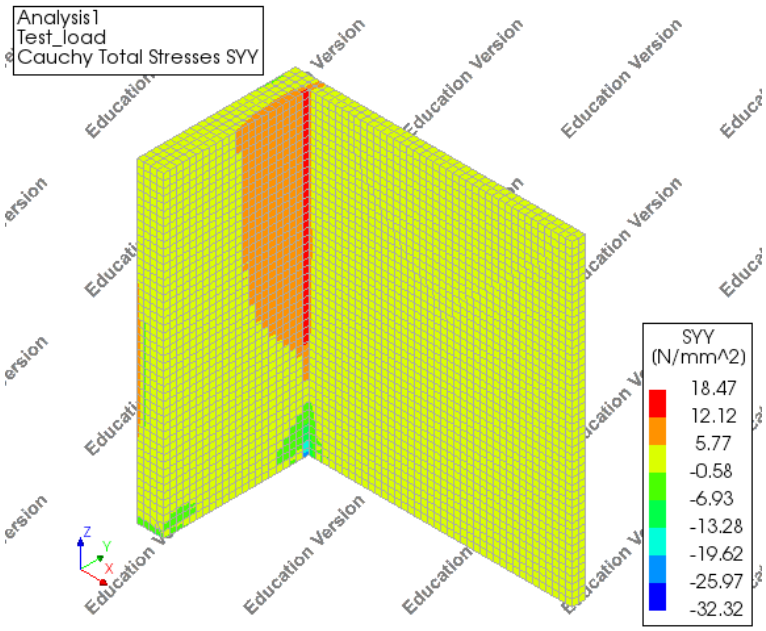

Figure G.3: Unscaled stress plot of the glass of the specimen, showing the normal stress parallel to the flange's surface.

G.2 Cracked Model

After the origination of Crack Pattern One, the fused and welded specimens were loaded further. To model the stress distributions of that situation, the glass-aluminum composite model is adapted. The shape of Crack Pattern One is drawn in the model and the glass flange is split and spaced $0,2\ mm$. No interaction in the crack is modelled (Figure G.4). It is assumed that the crack has propagated through the flange completely. The load on the specimens in $10\ kN$.

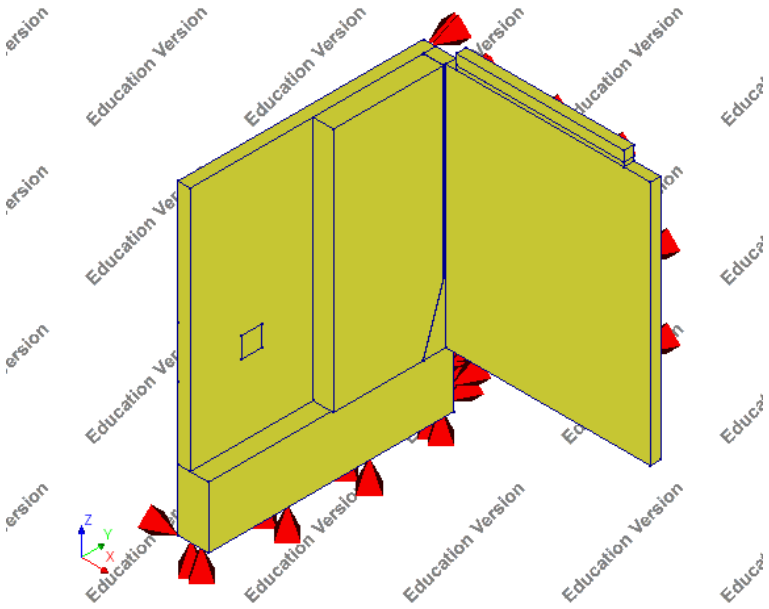

Figure G.4: Geometry of the model of the glass-aluminum composite, with Crack Pattern One in the flange

The important stress plots are shown in figures G.5 and G.6. The first shows the principle stress near the crack. It shows stress is elevated in the crack's surface. The second plot supports first glass-aluminum composite the mechanism shown in figure 94. It shows the stress peaks in the stiff part of the T-shape. The deformations are exaggerated by the software. It shows a discrete bend near the height of the bolted connection between aluminum and glass.

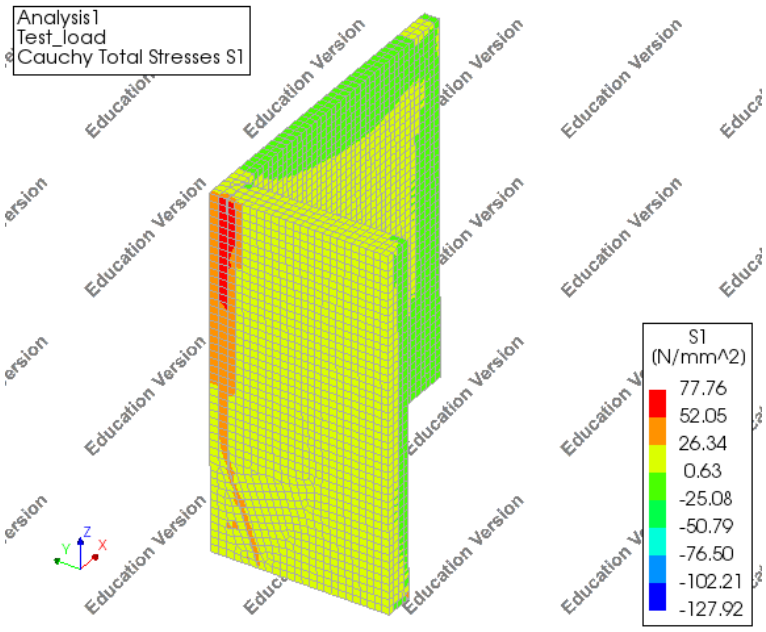

Figure G.5: Unscaled stress plot of the glass of the specimen, showing the principal stress in the specimen with Crack Pattern One, viewed at the back of the glass flange.

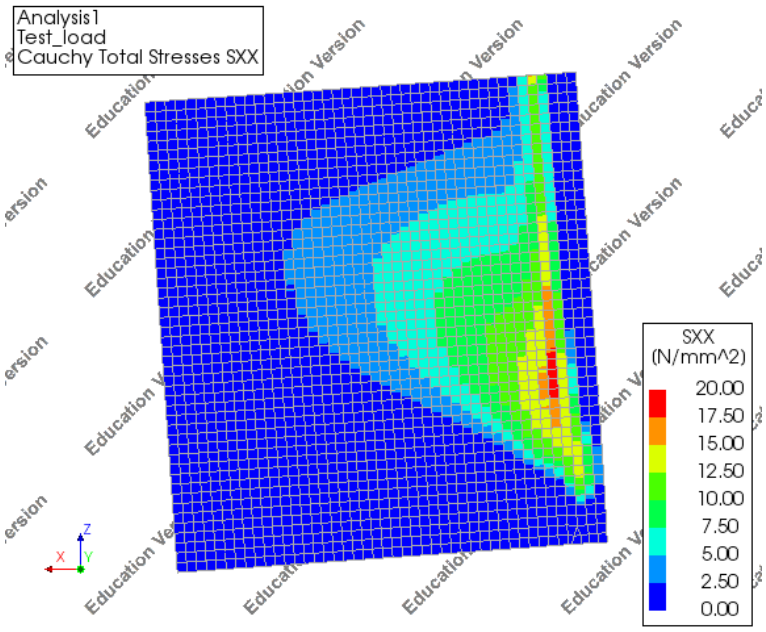

Figure G.6: Manually scaled (0 to 20 MPa) stress plot of the glass of the specimen, showing the stress parallel to horizontal web edge, in the specimen with Crack Pattern One, viewed at the symmetry plane. Support and flange are on the right side of the picture.

H Statistics behind Test Conclusions

In section 31, the test results are translated to a possible minimal capacity. To find this value, the minimum measured load or stress is divided by three. This factor seems arbitrary, but it is not. In this section, the statistics behind this factor is explained. The theory is based on the experience and explanation of Fred Veer, with whom the test has been designed, executed and interpreted.

Suppose the strength of annealed float glass follows a statistical normal distribution. This is not the case, some argue the asymmetric Weibul distribution should be applied, but this would overcomplicate the explanation.
The strength of annealed float glass is $40\ MPa$ on average, the one in 10.000 failure strength is $20\ MPa$. This means that the design strength is about 50% of the average measured value. This percentage is an indication for the width of the distribution. Because the distribution is symmetric, there is a one in 10.000 probability that the capcity of glass is larger than $60\ MPa$ (Figure H.1). The relation between the statistically minimum capacity and statistically maximum capacity is a factor 3.

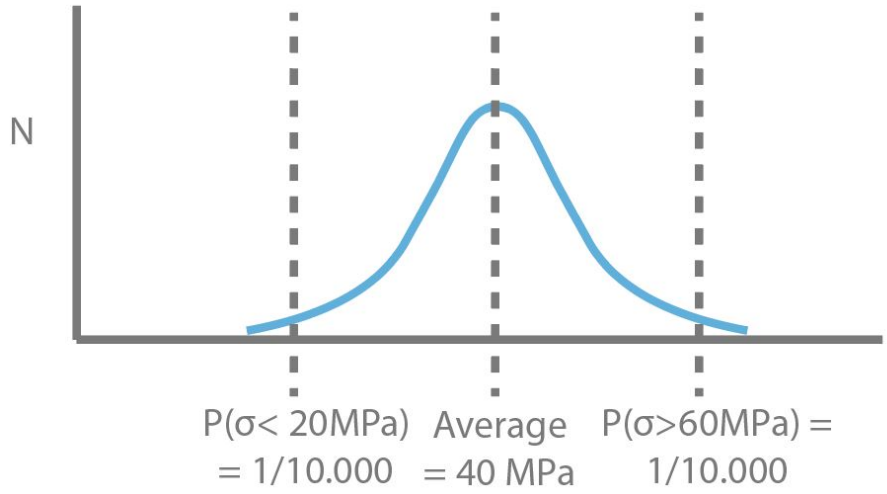

Figure H.1: Assumed normal distribution of glass strength

The tests were performed in series of three to five per connection type. This is too little to draw conclusions based on the mean and standard deviations of the test results. Therefore, the worst case scenario for an engineer is adopted.
This scenario, is that the measured data are all above an exceptionally high capacity. This would be if all measured data points are from the region above the one in 10.000 probability of a exceeding capacity (Figure H.2).

Because the connection is made of glass, it is most logical to assume that the width of the statistical distribution is similar. If the measured data is to be related to the $60\ MPa$ capacity and the predicted capacity can be related to the $20\ MPa$ capacity, the same factor, 3 can be applied.

Therefore, it is considered conservative to use one third of the minimum measured value as a probable statistical minimum.

This application of theory does not result in definitive conclusions. There is a probability that the

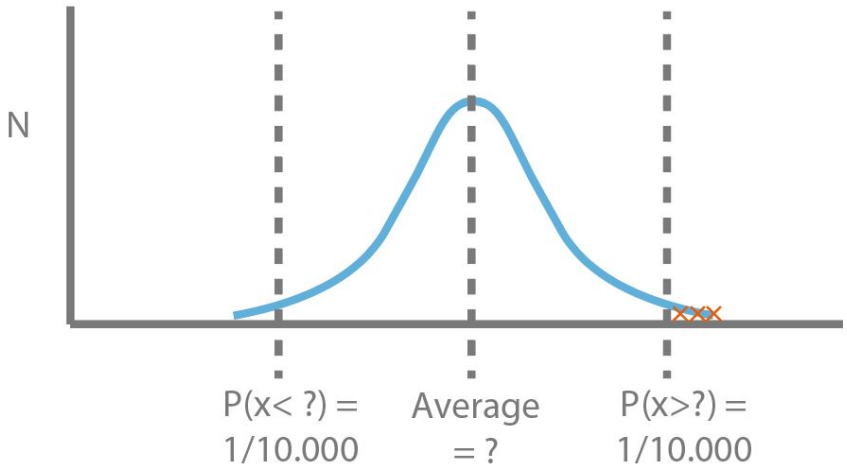

Figure H.2: Assumed normal distribution of glass connection capacity. Worst case scenario is when the red crosses are the measured test results.

minimum capacity is lower. This should be demonstrated by performing more tests wit larger series. The probable statistical minimum capacities mentioned in this thesis are only a way to interpret and visualize results for tests with small series. It is used to explain what the results indicate.

One could argue that this factor 3 does not hold for the adhesive connections, because these are not made of glass. It is an option to apply the distribution width of adhesive. However, in three out of five tests, the glass fractured. It cannot be excluded that failure originated in the glass. Therefore, the distribution width of glass is applied and the factor 3 is applied on the probable minimum capacity of the adhesive connection as well.